N° 2013 - 32 Année 2013

THESE

présentée devant

L'ECOLE CENTRALE DE LYON

pour obtenir le grade de DOCTEUR

Spécialité: Matériaux

par

Jiao YANG

Master Université Jiaotong du Sud-Ouest (Chine)

ON THE USE OF STATISTICAL ANALYSIS FOR TRIBOLOGICAL EVALUATION OF A SOLID LUBRICANT

À PROPOS DE L'UTILISATION DE METHODES STATISTIQUES POUR L'EVALUATION TRIBOLOGIQUE D'UN LUBRIFIANT SOLIDE

Soutenue le 9 Octobre 2013 devant la commission d'examen composée de

Cécile LANGLADE	Professeur, Université de Technologie de Belfort-Montbéliard	Rapporteur
Hamid ZAIDI	Professeur, Université de Poitiers	Rapporteur
Luc CARPENTIER	Docteur, Université de Franche-Comté	Membre
Jean-Yves PARIS	Docteur, Ecole Nationale d'Ingénieurs de Tarbes	Membre
Vincent FRIDRICI	Docteur, Ecole Centrale de Lyon	Co-directeur de thèse
Philippe KAPSA	Directeur de Recherche CNRS, Ecole Centrale de Lyon	Directeur de thèse

ACKNOWLEDGEMENTS

This thesis is written according to my three years' work in Laboratoire de Tribologie et Dynamique des Systèmes at Ecole Centrale de Lyon.

I express my sincere gratitude to Prof. Philippe KAPSA, my supervisor of the thesis, for giving me basics of research and supporting me during the whole thesis work. He also enlightens me on the research methods.

I address my special appreciation to Dr. Vincent FRIDRICI, my co-supervisor of the thesis. During my three years of thesis, he gave me uncountable suggestions to my work, and he also patiently and critically proofread the manuscript.

I would like to express my thanks to all the colleagues in the laboratory for their generous help. In particular, I address my thanks to Maha MESSAADI for her great help in my French and doing the experiments. Besides, I would like to thank Gérard MEILLE for his training in SEM/EDX, Gaëtan BOUVARD for his help in addressing the machine-related problems and teaching French, Imen LAHOUIJ, Sophie LOEHLE, Christine MATTA, Sophie PAVAN, Ousseïni MAROU ALZOUMA, Sandrine BEC, Olga GORBATCHEV, Marine BERNARD, Jean-Christophe ABRY, Julien FONTAINE, Jean-Luc LOUBET… for their generous help.

I am so grateful to Prof. Minhao ZHU and Zhongrong ZHOU, professors of Tribology Research Institute at Southwest Jiaotong University, for being my supervisors in China. They brought me into the tribology world and recommended me to study in LTDS.

I wish to thank China Scholarship Council and le Groupe des Ecoles Centrales. Due to their financial support, the thesis became possible.

At the end, I must appreciate my parents for their supporting on my overseas study.

CONTENTS

INTRODUCTION

The objectives of this thesis are to discuss the friction and wear behavior of a solid lubricant, and then to compare the effect of test parameters on the friction coefficient and lifetime of the coating by statistical analysis, sequentially to propose some approaches to predict friction behavior of tribological coatings.

Background

Fretting is considered as a complex phenomenon related to interaction between two sliding bodies under very low displacement amplitude, which limits the lifetime of elements significantly. It includes fretting wear, fretting corrosion and fretting fatigue. In industrial applications, the use of a tribological coating has served as an effective and economical way to reduce friction and protect the surface of elements from fretting wear and to extend the service lifetime of machine elements. Therefore, it is necessary to study the friction and wear behavior of coatings to evaluate the coatings, thereby optimizing the quality of coatings. However, the coating system depends on many factors (such as coating properties, substrate, counterbody, interface adhesion and running conditions). There are no general rules to compare the effect of factors on the quality of coatings.

Objectives and research approaches

The objectives of this thesis are to discuss the friction and wear behavior of coatings under different running conditions, and then to analyze the effect of test parameters on the friction coefficient and lifetime of coatings, which can be effectively helpful for the evaluation of coatings.

Around the objectives, the following research approaches will be realized. Firstly, literature study will be carried out to investigate the coating development in the field and the tribological response of coatings. Secondly, the fretting experiment of coating under different running conditions will be performed to understand the relationship between tribological response of coating and test conditions. Finally, some statistical methods (such as analysis of variance, regression analysis and reliability analysis) will be used to compare the effect of test conditions on the tribological behavior of coatings and to evaluate the coatings.

Organization of the manuscript

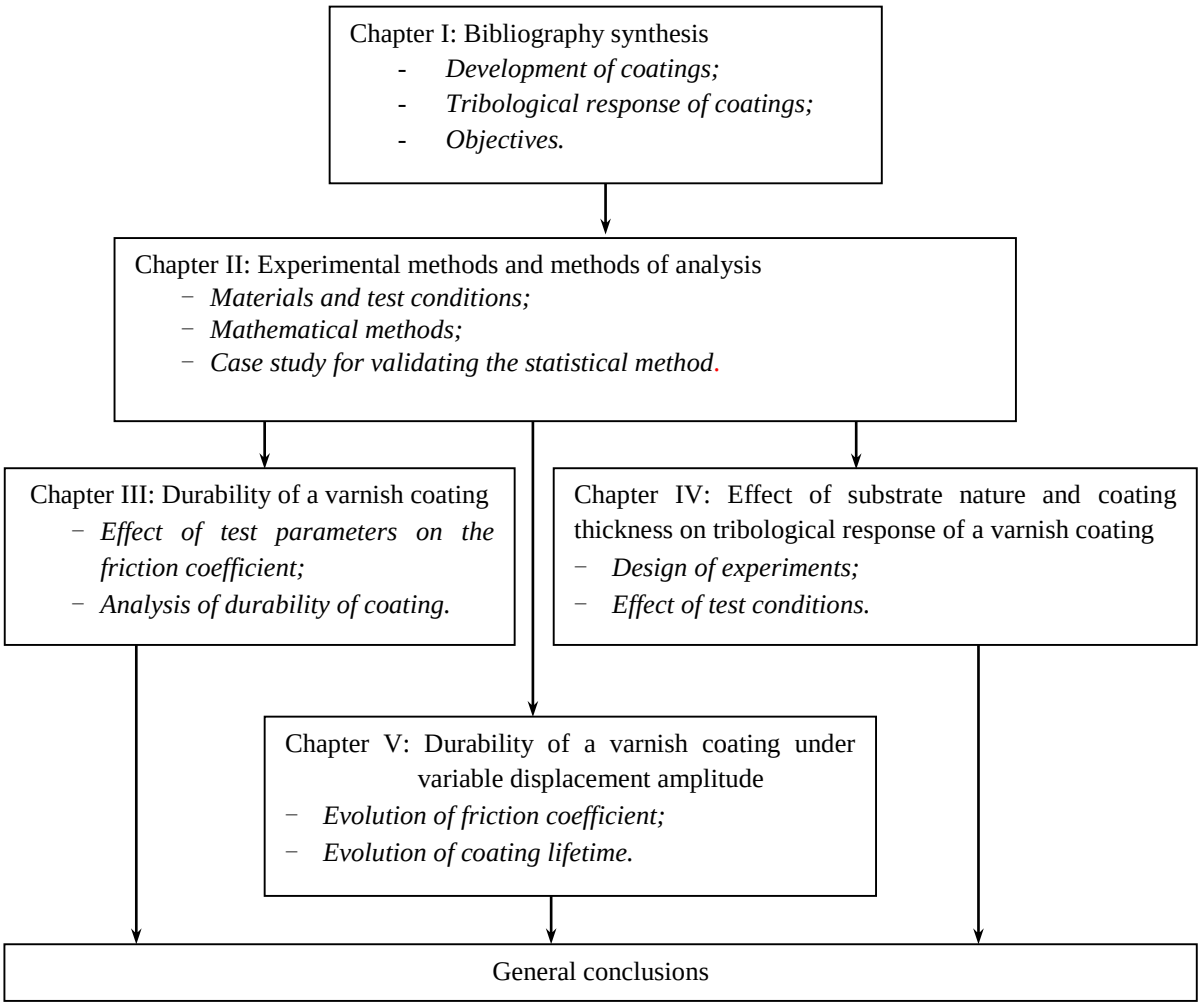

Figure 1: Organization of the manuscript.

The manuscript is organized as presented in Figure 1.

In Chapter I, literature survey will be summarized, including types of coatings, structures of coatings, coating deposition method, tribological response of coating, tribological evaluation of coatings, methods of mathematical statistics used to evaluate the coatings systems.

The test conditions and test rigs will be detailed in Chapter II. Fretting experiments will be performed to understand the tribological behavior of coatings under different tribological conditions. The statistical methods will be explained in details. A group of data from a previous study will be used to validate the availability of statistical methods.

Chapter III will discuss the different test conditions (such as contact force, displacement amplitude, contact configuration and coating positions) on the friction coefficient and lifetime of coatings. The statistical methods (like analysis of variance) will be used to compare the effect of test conditions. Regression analysis will be used to predict the value of friction coefficient and lifetime of coating under various test conditions.

In Chapter IV, the method of orthogonal design will be used to design the experiments. The effect of test conditions such as nature of substrate and thickness of coatings will be compared with other effects such as contact force, displacement amplitude, contact configuration and coating positions.

Chapter V describes the effect of variable displacement amplitude on the friction coefficient and lifetime of coatings. The lifetimes of variable displacement amplitude and constant displacement amplitude will be compared with aim to assess if a linear wear model can be used to predict the lifetime of coatings under variable displacement amplitude from the results of the experiments of constant displacement amplitude.

Finally, the annex gives a summary of nomenclatures used in the equations for this thesis. This annex can be used by the reader to better understand the standardized values of parameters used in Chapter III.

CHAPTER I

BIBLIOGRAPHY SYNTHESIS ON TRIBOLOGY OF COATINGS AND STATISTICAL METHODS

CHAPTER I: BIBLIOGRAPHY SYNTHESIS ON TRIBOLOGY OF COATINGS AND STATISTICAL METHODS

In this chapter, literature study is summarized to understand the research context, including the coating types, deposition methods, tribological response of different coatings and the related evaluation methods.

I.1 **Introduction**

Coatings are employed to improve the surface properties of a substrate, so that it has a good ability of resisting to wear, corrosion, extreme temperature and wettability. Based on these excellent properties, they have been used in different industrial fields such as automobile, aerospace and etc. In the field of aeronautics, the thermal barrier coating can protect the materials of motor from the high-temperature oxidation and corrosion and thus it prolongs the service life of turbine blade by two or three times [1]. In the automobile industry, the application of diamond-like coatings on the components in low-sulfur fuel can protect all components from massive wear, because low-sulfur oil guarantees their normal function [2]. MoS_2 based coating is used in the high vacuum environment such as aerospace to provide the lower friction coefficient, thereby ensuring the performance of all elements.

The function of tribological coating looks like the liquid lubrication that can reduce wear between two contactbodies and extend the service life of elements by interposing a third body between two contact surfaces. The interposed third body has a low shear resistance and thus prevents the contact surfaces from the serious surface damage. The third body is composed by various materials including adsorbed gases, reaction films, solid or liquid lubricants [3].

In 2007, a total of 37.2 million tons of lubricants was consumed worldwide (56% automotive oils, 35% industrial lubricants, and 10% process oils), as shown in Figure 2. Among the industrial lubricants, 37% were hydraulic oils, 7% industrial gear oils, 31% other industrial oils, 16% metal working fluids (such as temporary corrosion preventives), and 9% greases [4, 5]. Most part of the lubricants induces the pollution of the environment, either during or after use due to leaks, spillages, emissions, or other problems. According to the survey, approximately 2 – 2.5 million tons of used lubricants in Europe will ultimately pollute the environment every year [4]. In order to protect the environment, therefore, it is necessary to use some environment-friendly materials rather than the oil based lubricants.

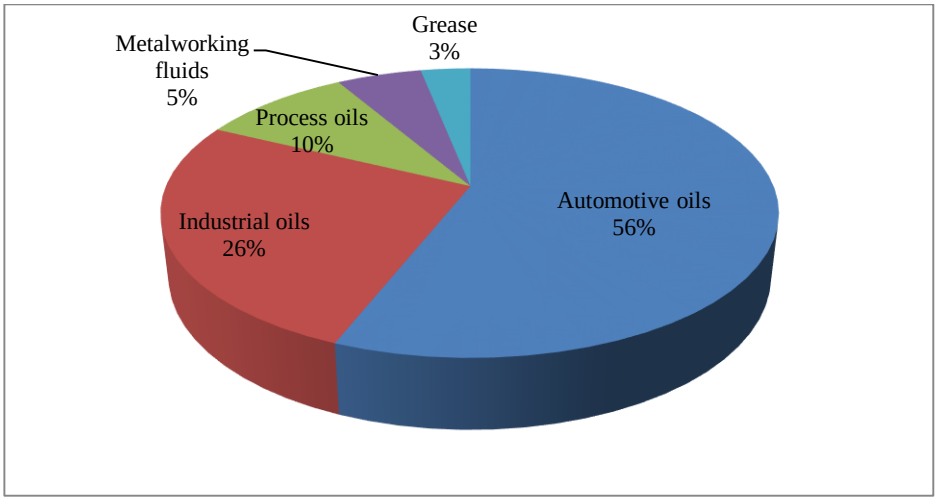

Figure 2: Segment break down of the global lubricant market in 2007 [4, 5].

Table 1: Application of solid lubricant: areas where fluid lubricants are undesirable [6].

Requirement	Applications
Avoid contamination product or environment	Food-processing machines Optical equipment Space telescopes Metal-working equipment Surface-mount equipment Tape records Microscopes and Cameras Textile equipment Paper-processing machines Business machines Automobiles Medical and dental equipment Spectroscopes
Maintain servicing or lubrication in inaccessible or unlikely area	Aircraft Space vehicles Satellites Aerospace mechanisms Nuclear reactors
Resist abrasion in dirt-laden environments	Aircraft Space vehicles (Rovers) Automobiles Agricultural and mining Equipment Off-road vehicles and equipment Construction equipment Textile equipment
Provide prolonged storage or stationary service	Aircraft equipment Railway equipment Missile Components Nuclear reactors Telescope mounts Heavy plants, buildings, and bridges Furnaces

Therefore, tribological coatings can be used, instead of oil based lubricants, in some places to reduce the friction coefficient and then reduce the energy consumption. Table 1 presents different situations including food and manufacturing industries where fluid lubrication has to

be eliminated. It displays several positive effects such as avoiding contamination product and maintaining lubrication in inaccessible or unlikely area where the oil lubricant cannot be used. It can decrease the friction like oil. Besides, it can reduce tendency to sticking and material pickup from the surface, which is very important to maintain the performance of forming tools and other sliding applications [7].

The application of solid lubricant has a very positive effect on the environment protection. At the same time, it can provide lubrication with the two contact parts, thereby maintaining the performance of tools. The objective of this thesis is to study one solid lubricant for the industrial applications.

I.2 **Type of coatings**

Generally speaking, coatings is generally divided into two types: soft coatings (hardness < 10 GPa) and hard coatings (hardness > 10 GPa) [8] (Figure 3).

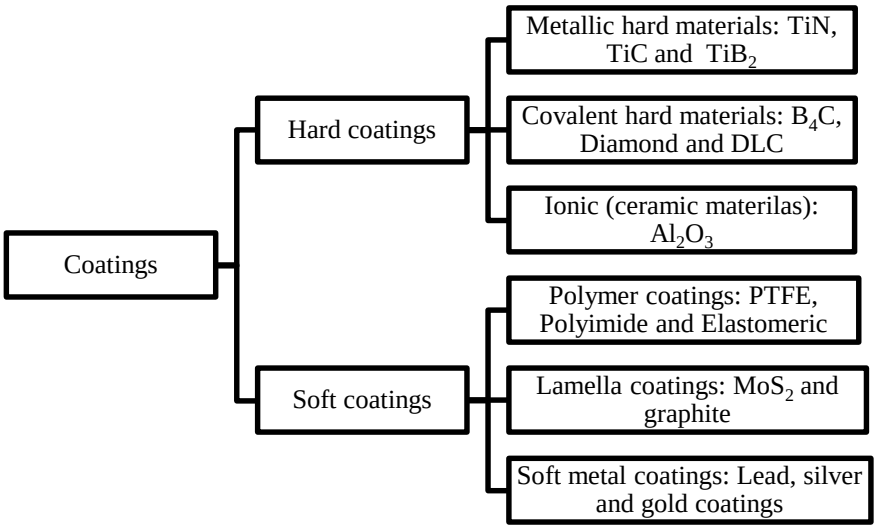

Figure 3: Types of coatings.

I.2.1 Hard coatings

Hard coating is a coating with high hardness (Table 2). High hardness represents the capability of resistance against permanent geometric deformation under mechanical loading. It is especially useful in application involving abrasive or erosive wear. When coating is harder than the abrasive particles, the conventional abrasive behavior is less possibility to be occurred. Hard coating is generally divided into three groups: metallic hard materials, covalent hard materials, and ionic materials (ceramic) according to their chemical bonding character [9].

Table 2:Properties of hard materials [9].

Minerals/synthetic materials	Formula	Density (g/cm^3)	Melting point (°C)	Hardness (HV)	*E* modulus (kN/mm^2)
Titanium nitride	TiN	5.40	2950	2100	590
Titanium carbide	TiC	4.93	3067	2800	470
Titanium diboride	TiB_2	4.50	3225	3000	560
Silicon carbide	SiC	3.22	2760	2600	480
Diamond	C	3.52	3800	8000	910
Boron carbide	B_4C	2.52	2450	4000	441
Aluminum nitride	AlN	3.26	2250	1230	350
Corundum	Al_2O_3	3.98	2047	2100	400
Titanium dioxide	TiO_2	4.25	1867	1100	205

I.2.1.1 Metallic hard materials

Metallic hard materials are able to form coherent or semi-coherent interfaces with metals or other metallic hard materials, leading to low energy interfaces with optimum adherence. It includes borides, carbides, and nitrides of the transitional metals [9]. Among these materials, borides, carbides, and nitrides of titanium are the most famous, which have been widely used in industry because of its high hardness, good adhesion to steel substrates, chemical stability and excellent resistance to wear, corrosion and high temperature.

- Titanium nitride

Titanium nitride (TiN) is the most widely used metallic hard coatings in industrial applications with the history of more than two decades ago [10]. TiN is obtained by reduction of titanium dioxide, as shown in Eq. (I-1):

$$2TiO_2 + N_2 + 4C = 2TiN + 4CO \qquad (I\text{-}1)$$

It is used on the surface of cutting tools to increase their lifetime (Table 3) and cutting speed as a result of its relatively high hardness, good adhesion to steel substrates and tough wear resistance. At the same time, the cost of production can be decreased by protecting tools from abrasive wear [11], because the abrasive particles cannot abrade the TiN layer or penetrate the coating by the deformation of substrate or collapse of the coating. In other words, abrasive failure may not occur [12]. Like most hard coatings, TiN layer is very sensitive to the humidity but it depends on the materials of counterbody. For the steel counterbody, the friction coefficient increases with increase of humidity. For the alumina counterbody, in contrast, the friction coefficient decreases with the increase of humidity from 2% RH to 25% RH due to the formation of aluminum–hydrated oxide. When the humidity is larger than 25% RH, the friction coefficient increases again [13].

Table 3: Life increase of TiN-coated tools [11].

Tool name	Substrate	Work piece	Life increase (%)
END MILL	M7	1022 STEEL	269
END MILL	M7	6061_T6 Al-alloy	804
END MILL	M3	7075T Al-alloy	489
GEAR HOB	M2	8620 Steel	100
BROACH	M3	303 Stainless steel	200
BROACH	M2	48% Nickel alloy	1600
BROACH	M2	410 Stainless steel	158-210
PIPE TAP	M2	Gray iron	200
TAP	M2	1040 Steel, RC30-33	917-1233
FORM TOOL	T15	303 Stainless steel	220

- Titanium carbide

Titanium carbide (TiC) is the most popular carbide coating for cutting tools and it can also be employed in pumps for transporting molten materials [14]. In vacuum environment, the application of TiC coating can increase the lifetime as many as 10 times under the pin-disc contact at speed of 200 rpm [15]. When it slides against steel, the humid environment can help to reduce the value of friction coefficient from 0.3 (in the dry and vacuum environment) to 0.2 (about 50% humidity), because a layer of TiO_2 formed in the humid air can decrease the value of friction coefficient [16].

- Titanium diboride

Titanium diboride (TiB_2) is especially useful for the continuous cutting operations due to its high hardness and temperature-resistance, while its friction coefficient is so high that it is not suitable for sliding components like bearings or piston ring *vs.* cylinder wall contacts [17]. For TiB_2, the humidity has also a positive effect on friction coefficient. The friction coefficient of TiB_2 can be decreased from 0.75 in vacuum to 0.65 in humid air [18].

- Summary

Although borides, carbides, and nitrides of titanium have been widely used in the industrial applications, they have one common weakness that limits their application in the high temperature and oxidation environment. It is because oxygen can be dissolved in the material until saturation of carbon or nitrogen vacancies with no changes in the f.c.c. crystal structure due to its defect structure [19]. To solve this problem, adding impurity element can serve as an effective way. Al can be added in the TiN so that the oxidation resistance can be increased from 600°C to 800°C [20]. In addition, impurities or metal binders can also improve the oxidation resistance of TiB_2 [19]. Adding TiC as an interlayer is a common method that it has been employed in the many wear-resistant parts like cutting tools, forming dies, or high-temperature structural components in heat engines or exchangers [21].

I.2.1.2 Covalent hard materials

Covalent hard materials can be obtained under high pressure or temperature. It includes borides, nitrides and carbides of Al, Si and B, as well as diamond.

- Boron carbide

Boron carbide (B_4C) is different from other covalent hard materials, because it can maintain its hardness even at high temperatures. At 1000°C, it still has a high microhardness (around 1500 kgf/mm^2), which is several times higher than the hardness of the hardest transition metal such as carbides and borides at this temperature. Therefore, it is used in the high-temperature wear-resistant applications (e.g., light weight armor plates, wheel dressing tools and blast nozzles) [22] [23]. Like other hard materials, it can also be used in the humid environment (Figure 4). Higher humidity can bring the lower friction coefficient and higher wear resistance, because chemical reaction in humid environment are involved in the oxidation of B_4C to B_2O_3 and the formation of boric acid (H_3BO_3) which is accompanied by an increase of graphite structure at the contact surface of coating, leading to a stable and low value of friction coefficient for boron carbide coating [24, 25].

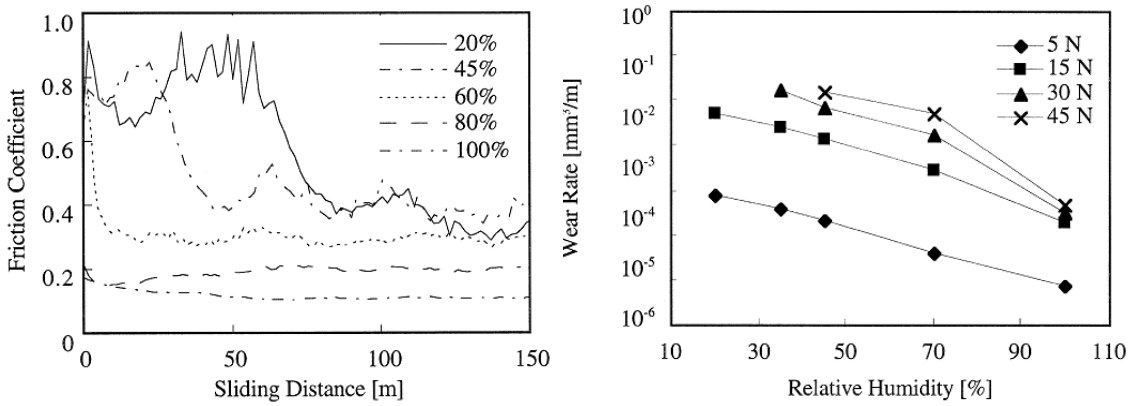

Figure 4: Pin-on-disc wear for B_4C coating vs. steel under different conditions: (a) friction coefficient as a function of sliding distance for different relative humidity (load is 15 N, sliding speed 1.0), (b) Wear rate as a function of the lowest relative humidity for different loads [25].

Although the B_4C based ceramics has attracted the technological interest, its industrial application is limited. Firstly, the sintering of pure B_4C components is very difficult, mainly due to the strong covalent bonding that leads to the low diffusion mobility [26]. Secondly, its low fracture toughness and low resistance to oxidation also limit the industrial application of B_4C.

- Diamond and diamond-like coatings

In recent years, diamond and diamond-like coatings (DLC) attract more attentions than other hard coatings as a result of its high hardness and excellent resistance to abrasion. They are widely applied on the surfaces of cutting tools.

There are some limits for diamond coatings although they have such good advantages. Firstly, it is not appropriate to use diamond coating at high temperature (around 1000°C), because it can react with iron. This reaction can cause a reversion to graphite and then leads to high wear rate [27]. Secondly, the adhesion between substrate and diamond coating is also a problem. Fortunately, diamond-like coatings (DLC) can overcome these disadvantages in some extent [28], but it depends on the substrate materials. If Si substrate is used, it will be impossible to remove DLC from Si except by several conditions such as O_2 plasma or heating in air, because

Si can offer the most remarkable adhesion force at all materials [29]. In contrast, if the soft substrate (Au, Cu, W, or on stainless steel containing Cu) is used, it will lead to the loss of substrate in competition with DLC deposition, because the soft substrate can be etched away by the H ions in the plasma. The application of intermediate can overcome this problem. He [28, 30] states that adding an intermediate layer, such as molybdenum or chromium, improves the adhesion force between DLC and substrate.

In addition to the industrial application, DLC is also one of the best materials for orthopedic applications due to its biocompatibilty. It can reduce the wear rate of the UHMWPE counterface and prevent itself from fracture of a brittle ceramic [31]. Besides, it also presents a low value of friction coefficient (typically ≤ 0.2) and excellent wear resistance (Figure 5), because it takes advantages of both polymer (elasticity, surface energy) and ceramic or metal (hardness, Young modulus) [32].

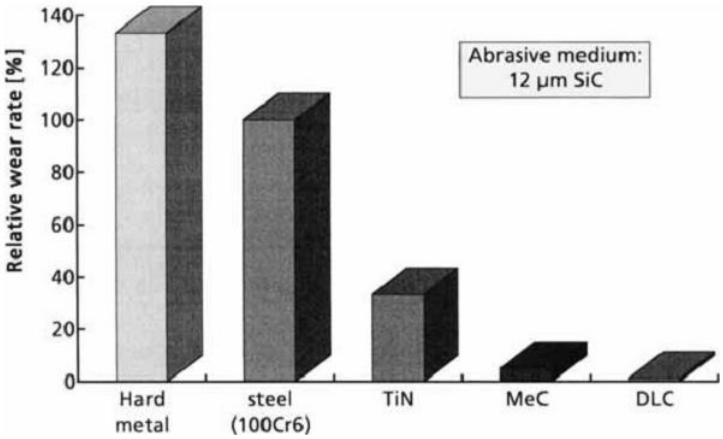

Figure 5: Abrasive wear of DLC coatings compared to other coating and substrate materials. As abrasive medium SiC with a particle dimension of 12 µm was used [32].

Field *et al.* [33] explained that its high hardness and wear-resistance was a result of the strong carbon-carbon bonding across the clean interface. It was formed between sliding diamonds mating surface. This strong bonding force resulted in high hardness and abrasion-resistance but it also resulted in rather high friction coefficient. Therefore, he concluded that the DLC was not used as friction-reducing materials. However, the rule can only work in the dry environment, because DLC shows a low friction coefficient in the moist environment. Liu stated [34] that the adsorbed water might reduce the shear strength of the contacting interface and increase true contact area, thereby reducing the contact pressure at the interface. In addition, the interface between diamond and a water layer is weak that shear is easy to be occurred due to a lower shear stress. It is expected that a low tangential force could maintain the relative motion between the mating surfaces.

I.2.1.3 Ionic (ceramic) materials

Ionic (ceramic) coatings refer to the oxides of Al, Zr, Ti and Be. For example, Al_2O_3 is employed to improve wear resistant properties of metal cutting tools. The wear loss of coated substrate is significantly lower than the uncoated substrate, as shown in Figure 6. Like other carbide coatings, it can be introduced as an intermediate layer in the multilayer arrangement to

increase the hardness and high temperature strength. At the same time, it does not influence on the adherence and toughness of the coating [35].

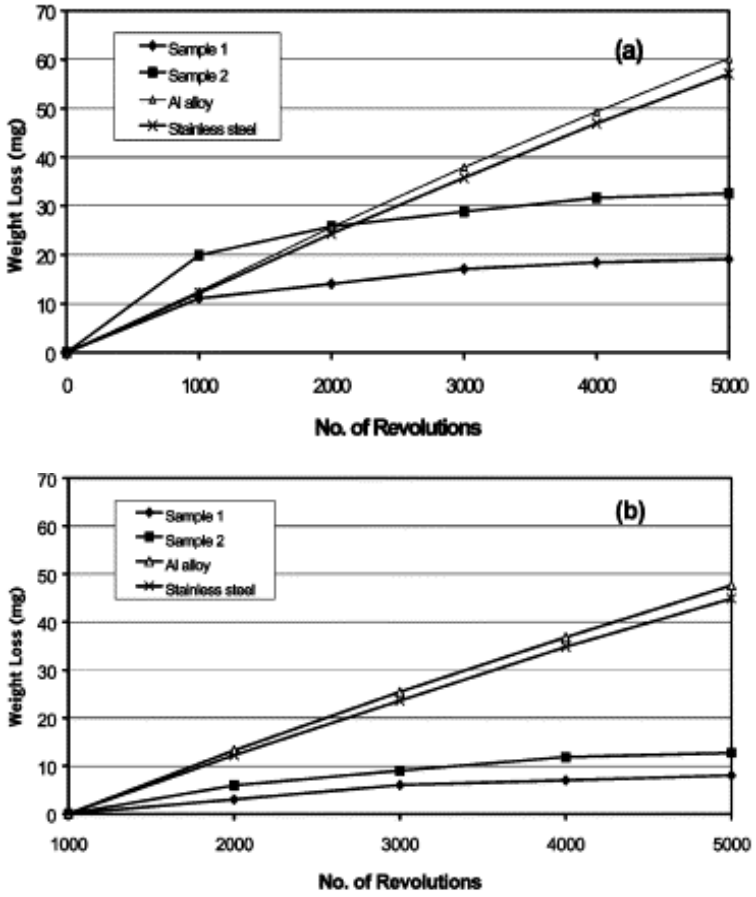

Figure 6: Weight loss data before (a) and after 'running-in' (b) for dry rubber wheel abrasive wear tests of the various samples (sample 1: 150 µm PEO alumina coating; sample 2: 250 µm PEO alumina coating) [36].

I.2.1.4 Summary of hard coatings

The properties of hard coatings have been summarized in Table 4. It can be seen that covalent coating has the highest hardness but lowest adherence to metallic substrate. For metallic coating, it has middle hardness and high adherence to metallic substrate, which can effectively avoid the delamination. Therefore, metallic coatings become the most widely used coatings among three candidates. Thanks to its good adherence to the metallic substrate, the hard coatings has high hardness and a better wear resistance to abrasive wear, but this good bonding between planes induces the high friction coefficient (above 0.5) in vacuum. The friction coefficient can be decreased as a function of humidity because the water can accelerate the formation of oxide layer for most hard coatings and thus provides a rather low friction coefficient. At the same time, the wear resistance is also improved.

Table 4: Properties and behavior of various groups of hard materials (M=Metallic, C=Covalent, I=ionic) [9, 37].

Level	Hardness	Brittleness	Melting point	Stability	Thermal Expansion coefficient	Adherence to metallic substrate	Interaction tendency	Multilayer suitability
High	C	I	M	I	I	M	M	M
Middle	M	C	C	M	M	I	C	I
Low	I	M	I	C	C	C	I	C

I.2.2 Soft coatings (MoS_2 coating)

As we know, the soft thin coating on a hard substrate offers the possibility to reduce sliding friction. It includes polymer coating, lamellar solid coating and soft metal coating.

I.2.2.1 Polymer coatings

Polymer coatings are one of the important categories in the soft coatings, because they have good self-lubricating properties (the value of friction coefficient sliding against steel is typically in the range of 0.1 to 0.5 which is lower than the typical value of 0.6 for non-lubricated steel against steel contacts), good resistance to wear and corrosion, and low noise emission. In addition to these advantages, they are cheap to produce [17]. The most common polymer coatings are polytetrafluoroethylene (PTFE), polyimides and elastomers. The wear behavior is dependent of a transfer film formed during the sliding against each other.

- PTFE

PTFE can be used as an additive in lubricating oils and greases due to its low surface energy. Adding PTFE can improve the adsorption phenomena of the lubricant and lower the contact angle, thereby increasing the adhesion between oil and substrate and at the same time preventing failure of the lubricant film, i.e., more load can be born without the lubricant film breaking down [38].

PTFE can also be used as a film, which can provide low friction coefficient (typically < 0.05) because the macromolecules of PTFE slip easily along each other. When rubbed against a smooth metal counterface, a very thin transfer film of PTFE can be immediately observed at the opposing surface due to the low activation energy of the slippage between crystalline slices in bands [39] and the molecules immediately in contact with one another become highly orientated with their major axes aligned in the direction of sliding, resulting in the low friction coefficient [40]. Therefore, the wear mechanism of PTFE is featured by a transfer film mechanism. It also means that its intermolecular strength is not very high, leading to the low yield strength and low load-carrying capacity [17].

Recently, a lot of efforts have been made in this field to improve its wear-resistance ability and to keep its lower friction coefficient by adding new particles or changing its structures such as glass fiber reinforced (GFR), bronze and graphite (Figure 7*)*, carbon nanotube, molybdenum and tungsten disulfide to get lower wear rate, because its load carrying ability has been improved [41].

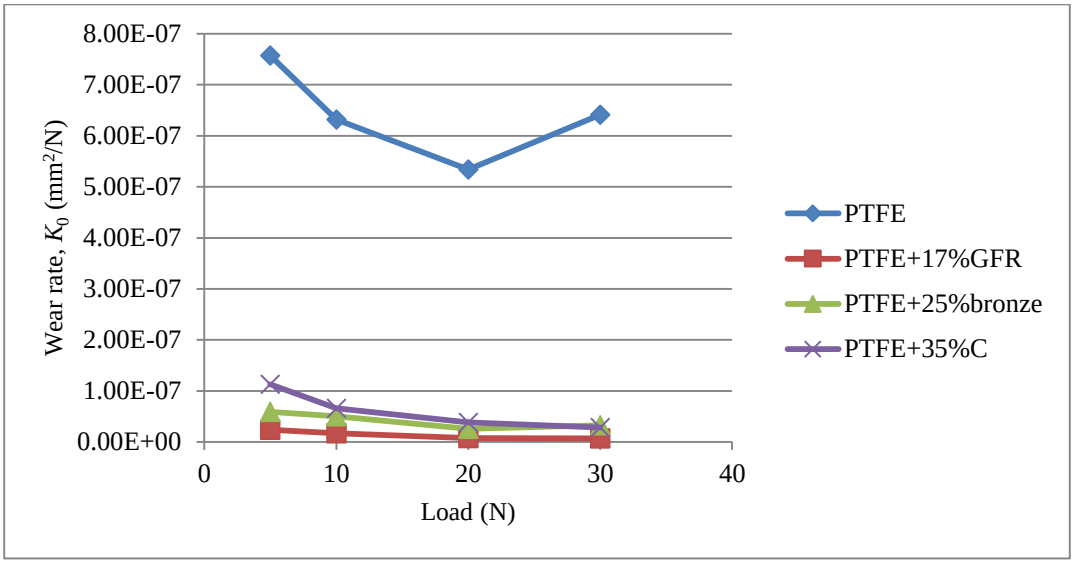

Figure 7: The wear rate as a function of load for different coatings [41].

- Polyimide

Polyimide is a polymer used in tribological applications such as bearings and seals [17]. Its friction coefficient is sensitive to the temperature and humidity while it is less sensitive to the sliding speed, because (1) it behaves in an essentially brittle way when the temperature is low, showing little elongation before fracture due to the existence of a degree of crystallinity, and it becomes amorphous and glassy when the temperature is above the glass transition temperature [40]; (2) the water molecular can be directly attached to the chain of polymer through hydrogen bonding, thereby limiting the flexibility of a molecule of polyimide. If the flexibility is limited, the stress causes fracture rather than plastic flow and the wear rate is increased [42]. Fusaro [43] found out that the wear process can be divided into two parts. At the beginning, the tips of films asperities bear the load and the lubricating mechanism is the shear of a thin surface layer (of the film) between the rider and bulk of the film. Then, after the bonded film has worn to the substrate, the shear of very thin lubricant film occurs between the rider and flat plateaus, generating on the metallic substrate asperities. The wear mechanism is dependent of the contact pressure. This conclusion is similar to other soft coating CuNiIn. There is a pressure threshold for wear mechanism. Below the pressure threshold, the conventional abrasive wear processes are activated, while the severe adhesive wear predominates when it is higher than the pressure threshold, because the contact pressure modifies the interface structure and the wear kinetics [44].

- Elastomeric coatings

The elastomeric coatings are usually used in the automotive pre-primed sheets to overcome severe conditions such as press, cutting and stamping process [45], because its low crosslink density, high molecular weight and content of flexible can make it recover from large deformation segments and thus the good resistance to erosive and abrasive wear can be obtained. At same time, however, this special structure also brings the high friction coefficient, because the hysteresis phenomena may deteriorate their friction behavior and stick-slip often occurs. It

is better to be used on the flat rather than ball, because the curved substrate may stop its continuous elastic deformation and recovery, as shown in Figure 8 [17].

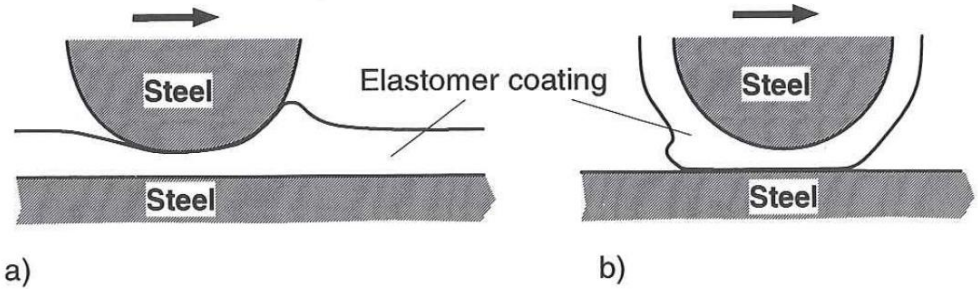

Figure 8: Hysteresis friction occurs (a) continuously when the plane surface is covered by an elastomeric coating and (b) only in the load and unload position when the ball is coated [17].

I.2.2.2 Lamellar coating

The most widely used lamellar coatings are graphite and molybdenum disulphide (MoS_2). The characteristic structure (Figure 9) is that the strength of the interatomic bonding between successive layers is very much weaker than that within the planes themselves [40]. Therefore, they can afford relatively heavy loads at right angle to the layers while still being able to slide easily parallel to the layers. Besides, an adherent part of the lubricant (a transfer film) form on the opposing surfaces. According to the above two functions, the low value of friction can be gained, which is nearly equal to the shear stress parallel to the layers divided by the yield stress or hardness perpendicular to the layers [46].

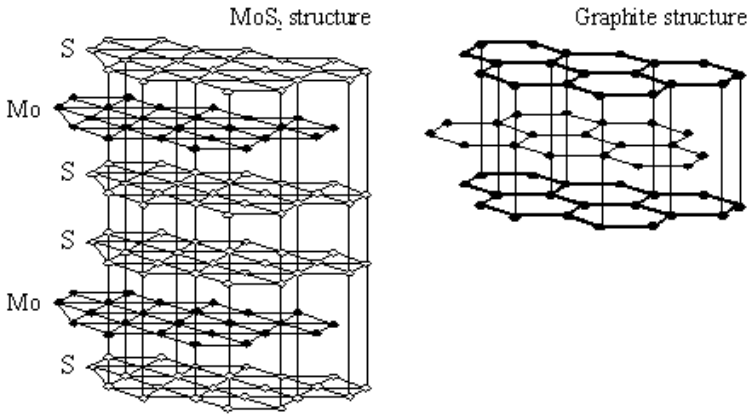

Figure 9: Structure of two commonly used solid lubricants: (a) molybdenum disulphide; and (b) graphite, showing the arrangement of parallel basal planes [47].

- Graphite

Graphite is one of the best lubrications in a normal atmosphere. Its reaction with gases like water vapor reduces the bonding energy between the hexagonal planes of the graphite to a lower level than the adhesion energy between a substrate and the graphite, leading to easy shear and transfer of the crystalline platelets on the contact surfaces [48]. Hence, it is not a suitable solid lubricant in the vacuum. In addition, it can be used as an additive in the oil to improve the thermal tolerance and in some materials to provide material with low wear rate, low friction, and excellent anti-seizing properties. Babic [49] shows that the increase of the graphite content

within the zinc–aluminum alloy results in increase in ductility, compressive strength, ultimate tensile stress, and corrosion resistance, but it leads to a decrease in hardness, as a result of a formation of the graphite-rich film on the tribo-surface that provides lubrication.

- Molybdenum disulphide

MoS_2 is a mined material found in the thin veins within granite and highly refined with aim to achieve purity suitable for lubricants [47]. It shows better performance than graphite in tribological applications. Firstly, the quality of MoS_2 is more rigidly controlled than graphite because graphite has various values due to different sources; secondly, the friction coefficient of MoS_2 is lower in vacuum than in air because it does not depend on adsorbed vapors; finally, the load-carrying capacity of MoS_2 is generally superior [50]. However, it is very sensitive to the humidity, because the water vapor can penetrate into porous MoS_2 coatings along edge sites which are parallel to the *c* axes of the crystals, resulting in growing rate of formation of MoO_3, which will deteriorate friction and wear [51]. Different from other soft materials, its wear mechanism can be separated into four groups [52]:

1) Platelet wear: It is the deformation and fraction of MoS_2 platelets that makes MoS_2 coatings as deposited. Spalvins [53] postulates that the basal planes, which are predominantly perpendicular to the substrate surface, becomes reoriented parallel to the surface during the initial stage of sliding. A large pressure increases basal plane reorientation [51]. The platelets can occur the simple deformation, leading to compaction of the porous coating, fracture and loosing particles [54].

2) Oxidative wear [54]: oxygen deteriorates MoS_2 coatings by three modes. Firstly, wiping of surface oxides: surface oxides can be 'wiped off' of the coating and transferred to the ball; secondly, degradation of cohesiveness: oxygen permeates the coating to form the mixtures of MoS_2 and MoO_3 and thereby losing its cohesion; thirdly, blistering of coating: different from the degradation of cohesiveness, oxygen permeate the coating to form MoO_3 and SO_2 and thereby forming spherical brittle void and causing consequent destruction.

3) Adhesive wear: some parts of coatings are observed to transfer to the counterbody and then become basally oriented along the sliding direction.

4) Plowing wear: hard particles like Fe_3O_4, embedded in a MoS_2 transfer film, behave as abrasive particle to scratch the coating [55].

I.2.2.3 Soft metal coating

Compared to the lamellar coating, fewer studies have been made on soft metal coatings like lead, silver, gold and indium. Soft metal coatings also have the crystal structures with multiple slip planes, similar to solid lubricant, providing the low shear ability that is also needed for good tribological properties of coated surfaces. Like other metals, the dislocation and point defects can occur during shear deformation, but they are rapidly nullified by the frictional heat produced by the friction between two contacts [56]. Therefore, their wear behavior is also influenced by the film thickness, adhesion force to the substrate, surface roughness, load and sliding speed. For example, a thin layer of a soft metal coated on a hard substrate can delay the

wear of the hard substrate by preventing plastic deformation and crack nucleation in the hard substrate. If the thickness of soft layer is more than a critical value, delamination can occur within this layer and form wear particles. The wear particles can in turn cause ploughing and further plastic deformation [57].

- Lead coatings

Lead (Pb) coatings were the first to be widely used in the space application instead of liquid lubricants [17] because of its good wear-resistance and low friction in aerospace. Pb-coated sheets are the primary material used in anti-corrosion automotive applications, especially in eastern Europe and Asia [58]. Recently, the focus of research changes from a single lead coating to a composite material because the adhesive bonding of coating-to-substrate is a critical factor determining the lifetime of coating [59], while the introduction of a copper interlayer and metal dopants copper, molybdenum and platinum substantially extends its lifetime [60].

- Silver coatings

Silver can behave as a solid lubricant that present as a thin layer between hard sliding surfaces due to its significantly marked ductility. This extreme ductility allows the silver film to plastically shear between the sliding surfaces and thus to provide lubrication [61]. It has also a very highest thermal and electrical conductivity and good oxidation resistance so that it has been used as electroplated coating on the retainer of rolling element bearings. However, it is very expensive. Generally, it is applied as an additive to improve the lubrication and load carrying capacity [62] of other materials.

- Gold coatings

Gold is a noble metal with excellent corrosion resistance and good electrical and thermal conductivities. So, it has been widely used in the electrical industry for electrical connectors and similar components [17]. It has the similar mechanical properties as Ag, but a higher friction coefficient [63].

I.2.2.4 Summary of soft coatings

Soft coatings can often bring lower friction coefficient than hard coating, because they are easy to shear and parts of them can be transferred to the counterbody to form the transfer film. The transfer film will accommodate the relative movement of two contact parts, thereby providing the low friction coefficient. Accordingly, the transfer film characterizes the wear mechanism of soft coating.

I.3 **Structures of coatings**

A comparison of properties of various hard coatings has been shown in Table 4. It can be seen that covalent coating has the highest hardness but lowest adherence to the metallic substrate. The metallic coating has better adherence to metallic substrate that can effectively avoid the delamination, but it has a lower hardness than the covalent coating, which indicates its force durability is lower than covalent coatings. There is no one group that has all the properties to the highest level, so it is interesting to have a composite coating which can combine the merits of various coatings to achieve optimum performance. To improve the tribological properties of

surface coatings, the structure of coating is changed from single component to multicomponent or multilayer (Figure 10) with aim to combine the advantages of each kind of coatings together.

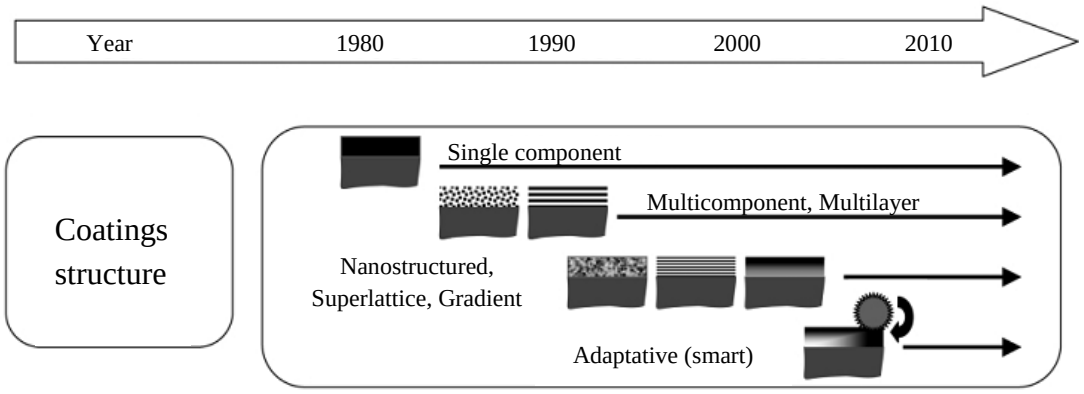

Figure 10: Historical development of tribological coatings [56].

I.3.1 Multicomponent and multilayer coatings

I.3.1.1 Multicomponent coatings

Multicomponent coatings are made up of two or more constituents in the form of particles, grains, or fibers. From the aspect of microstructure, it can be realized by adding non-metallic elements in the coating or substituting the metal lattice of compound phase with another compatible metal. For the former one, it is aimed to change the valence electron concentration (VEC) and thus to improve the mechanical and physical properties [17]. Figure 11 describes the relationship between VEC and hardness. Adding the nonmetal elements or changing the stoichiometry varies the value of VEC. When the value of VEC is about 8.4, maximum hardness occurs for the most components [9]. Sometimes, the added new element will not change the hardness but increase the ability to wear resistance. Cosemans [64] adds soft MoS*x* phase (±8 wt.%) in the TiN matrix without a decrease in hardness, but it significantly decreases the friction coefficient by a factor of 2 – 3 and increases the lifetime of coatings as many as 10 times.

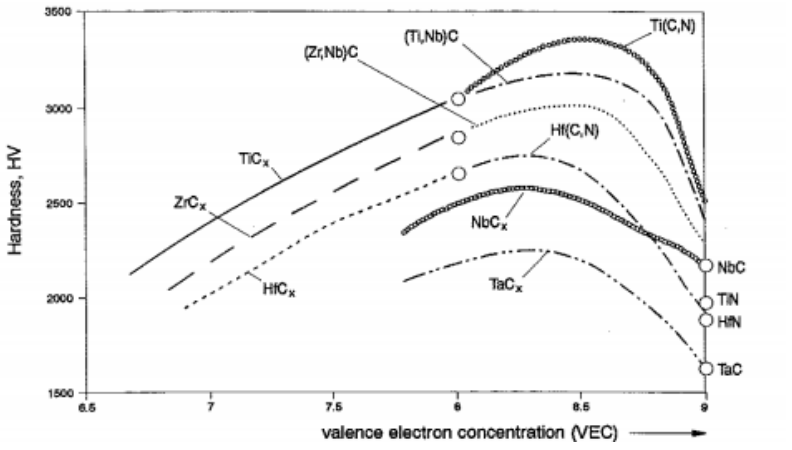

Figure 11: Microhardness of carbides, mixed carbides or carbonitrides as a function of valence electron concentration (VEC) [9].

For the latter one (substituting the metal lattice), it also improves the wear-resistance and temperature-resistance and thereby fulfilling special requirements such as high speed and dry cutting. In the TiN coatings, the lattice of Ti can be partly substituted by transition metals. For example, Y and Cr can greatly improve the resistance to oxidation; Zr and V improve the resistance to wear, because the stabilization effect of zirconium in the fcc TiN monocell and the formation of very thin zirconium oxide layer on top of the coating in the crater area can reduce diffusion wear [65]; Si can increase the hardness and chemical stability [20].

I.3.1.2 Multilayer coatings

Multilayer coatings are composed of a periodically repeated structure of lamellae of two or more materials (Figure 12), whose thickness is up to a few tens of micrometers [56] with aim to improve the adhesion force between coating and substrate or other physical and mechanical properties.

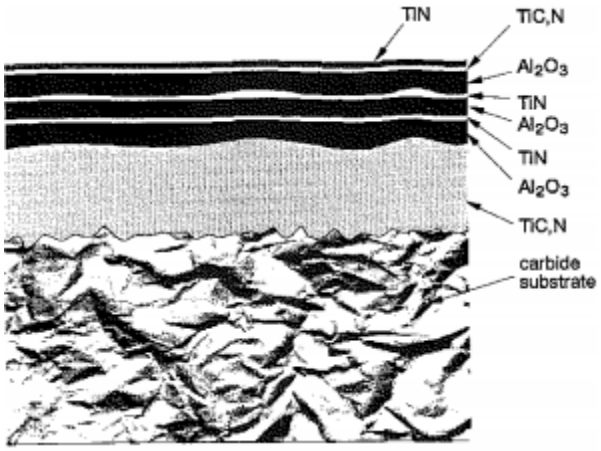

Figure 12: Schematic of a multilayer of coating architecture of Kennametal's KC990 grade cutting tool [37].

The presence of a lot of interfaces between individual layers of a multilayered structure increases drastically the hardness and strength. Hollect [35] gives the comparison for different combination of interlayers. The interlayer structure has improved the durability of single layer by about a factor of two, as shown in Figure 13, because interfaces in multi-layer coatings are sites of energy dissipation and crack deflection resulting in a toughening of the layer materials [35]. The cracks in multilayer composite coating cannot always propagate in a given direction because it lacks columnar crystals in the multilayer coating and its grains are finer, leading to a lower rate of crack propagation than the single layer, as shown in Figure 14. Therefore, its cracks are thinner and shorter, thus the possibility of severe wear can be retard [66].

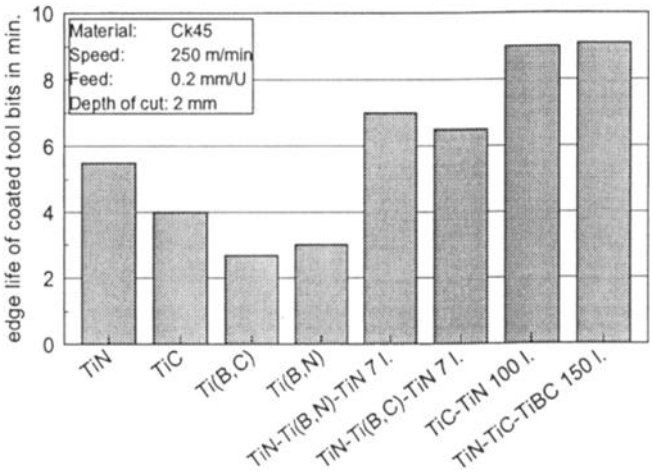

Figure 13: Edge life of cutting tool bits coated with single and multilayer metallic hard materials (edge life= first change of cutting conditions, TiN –Ti (B, N)-TiN 7 |.= 7 layer TiN-Ti(B,N)-TiN, TiN –Ti(B,C)-TiN 7 |. = 7 layer TiN-Ti(B,C)-TiN, TiC-TiN100 |= 100 layer TiC-TiN, TiN-TiC-TiBC 150|.=150 layer TiN-TiC-TiBC [35].

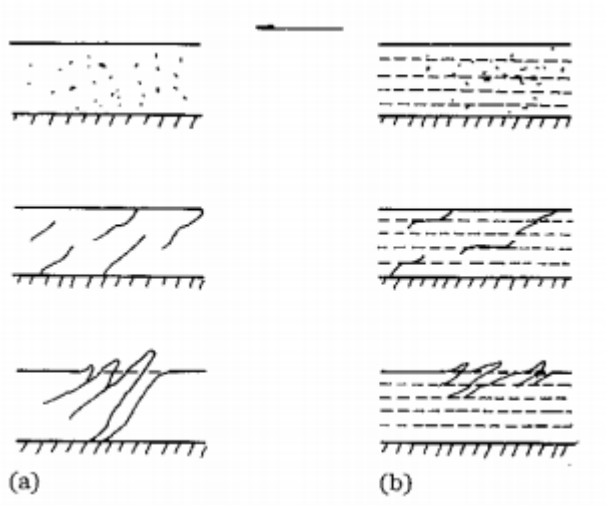

Figure 14: Comparison of wear mechanisms of coatings with (a) single layer; (b) multi-layer [66].

Therefore, the advantage of combining several structures and composition within one coating includes reduction of mismatch in chemical and mechanical properties between the substrate and coating, improvement of physical properties, control of the residual strain and the stress within the coatings, and the ability to stop cracks [56].

I.3.2 Gradient, superlattice and nano-structured coatings

The new development of coatings is based on the multicomponent or multilayer coatings. It controls the structure and composition of coatings at the nano-scale to get a significant increase in mechanical properties or wear-resistance.

I.3.2.1 Gradient coatings

Gradient coatings is a multicomponent coatings with a new structure where the microstructure and properties vary gradually from the surface to the interior of the material [67]. The formation of functionally gradient ternary systems with a different concentration of elements, both on

inside the coating and interphase boundary allows to reduce the internal compressive stresses of gradient systems and to increase adhesion [68].

I.3.2.2 Superlattice coatings

Superlattice is a periodic structure of layers of two (or more) materials. Typically, the thickness of one layer is several nanometers. Supperlattice coatings are one type of multilayer coatings, but its size is within the nano-scale. This kind of structure can help increase the hardness enhancement (Figure 15) and provide the high oxidation resistance [69]. These features are attractive for the practical wear-resistant applications.

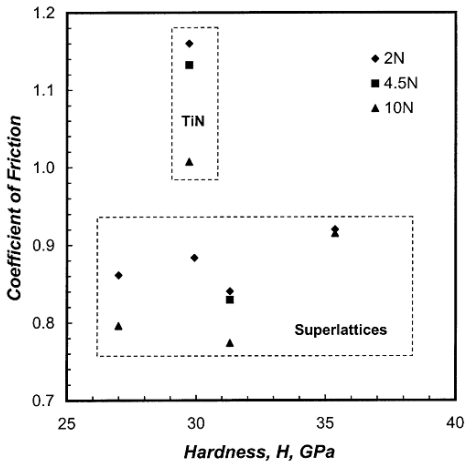

Figure 15: Coefficients of friction of TiN and superlattice coatings against the WC-Co counter-face as a function of hardness and applied normal load [69].

I.3.2.3 Nano-structured coatings

By decreasing the grain size, the hardness of coating can be increased through a high dislocation resistance. The nano-structured coatings have received more attentions, because this special structure can be used in both soft and hard coatings to improve their mechanical and friction properties. It is reported that thin films of fullerene-like MoS_2 nanoparticles, deposited by a localized high-pressure arc discharge method, can have an order of magnitude of friction coefficient lower than for sputtered MoS_2 thin films (Table 5), because inter-crystallite slip can still occur in fragmented nanoparticles and crystallites consist of irregularly shaped curved S±Mo±S planes, providing the lower friction coefficient. At the same time, the curvature of the hexagonal planes can buffer the Mo atom from oxidation by reducing the number of exposed dangling bonds at the edges of the planes [70]. In addition, it can be added in polymer nanocomposite, which transfers from the surface of the nanocomposite to the mated surface during the friction test, leading to a low friction and wear rate [71].

Table 5: Results of tribological test on MoS_2 film [70].

Film	μ	K ($mm^3N^{-1}mm^{-1}$)
Nanoparticle MoS_2	0.008-0.01	$\sim 1\times10^{-11}$
Sputter MoS_2	0.1-0.3	$\sim 3\times10^{-9}$

For hard coatings, the nanostructure can increase the hardness and at the same time decrease some defects such as pore, inter-lamellar and intra-lamellar cracks in the coating, leading to

reduced probability of adhesion-induced spalling and fracturing of lamellae and thus bringing the higher resistance to wear [72].

I.4 Coating deposition method

The quality of coating is not only dependent on the properties of coating, but also on the method of deposition. It can be classified as conduction and diffusion process, chemical process, wetting process, physical vapor process and spraying process.

I.4.1 Conduction and diffusion process

Anodization is one of representative process in conduction and diffusion. It is an electrochemical conversion process. Plasma anodization is a method used for depositing a much coherent oxide layer on the surface of silicon and some metal compounds [73].

I.4.2 Chemical process

The main generic coating sub-groups are Chemical Vapor Deposition (CVD) and Physical Vapor Deposition (PVD). Both CVD and PVD accounted for approximately 65% coatings for the metal-cutting tools in North America and Western Europe [74]. In other words, they are very effective for producing hard coatings.

Chemical Vapor Deposition (CVD) involves the vaporization of material by a chemical reaction occurring on or in the vicinity of a normally heated substrate surface [75]. Typical CVD deposited films for tribological applications, like titanium nitride (TiN), have large angle grain boundaries and grain sizes in a range of 0.5 - 5 µm [17]. TiN hard coating was first coated commercially on tools by the CVD method, as shown in Figure 16, following the gas phase reaction [76] as Eq. (I-2).

$$2TiCl_4 + H_2 + 2NH_3 = 2TiN + 8HCl \qquad (I\text{-}2)$$

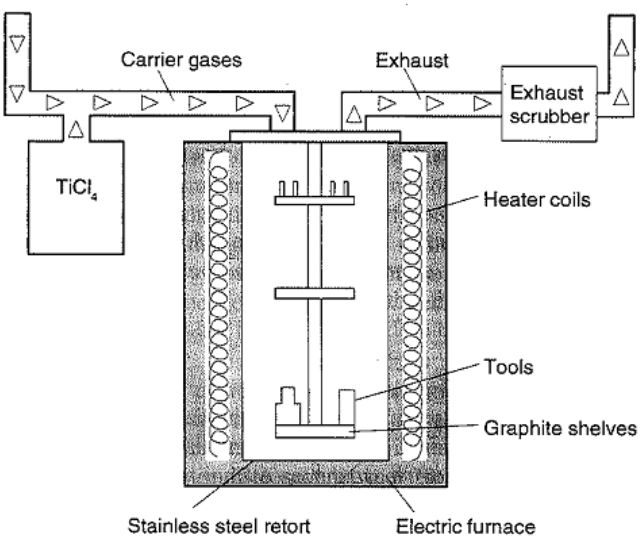

Figure 16: A typical CVD process layout [17].

It employs $TiCl_4$ as a precursor, with nitrogen or ammonia (carrier gas) as oxidants, because $TiCl_4$ is a fairly inexpensive and volatile liquid at room temperature, which can be easily

delivered as a vapor by direct liquid injection sources or bubbler. The liquid decomposes readily upon exposure to moisture or air, generating HCl vapor, but it does not lead to exploding or burning. At this time, the temperature is above 600°C to avoid forming a dusty yellow $TiCl_4$: NH3, which oxidizes readily upon exposure to air producing HCl and white TiO_2 dust. In addition, it is also helpful for the reasonable deposition rates and low Cl concentration in the deposited film [77].

However, this traditional method may not provide the good adhesion between substrate and coating. When this kind of coating is used in the cutting tools, it can delaminate or break off in a brittle manner, because the adhesion is poor due to a poor interfacial contact, low degree of chemical bonding, low fracture toughness or high internal stresses [17]. To solve this problem, the plasma assisted PVD process has been applied to improve the adhesion and then brings better tribological properties.

I.4.3 Wetting processes

Wetting processes can change the material form from liquid to solid by solvent evaporation, spinning, curing, baking, or cooling. It is a traditional way to brush the solid lubricant on the substrate. However, it is same as the traditional CVD method that it cannot guarantee the adherence between the coating and surface.

I.4.4 Physical vapor deposition

Physical vapor deposition (PVD) technology includes the techniques such as ion plating, evaporation and sputtering. Compared with the CVD, the toughness of PVD coatings is an order of magnitude lower than of CVD. In addition, it has a better adhesion between substrate and coating than CVD coating [78]. Thirdly, it is able to produce unusual microstructures and new crystallographic modifications, e.g. amorphous deposits and deposits with very high purity [79].

- Evaporation

In the evaporation process, vapors are produced from a material located in a source which is heated by direct resistance, eddy currents, e-beam, radiation, laser beam, or an arc discharge [79].

- Ion plating

In the ion-plating process, the material is vaporized in a manner similar to that in the evaporation process but passes through a gaseous glow discharge on its way to the substrate, thus ionizing some of the vaporized atoms (Figure 17).

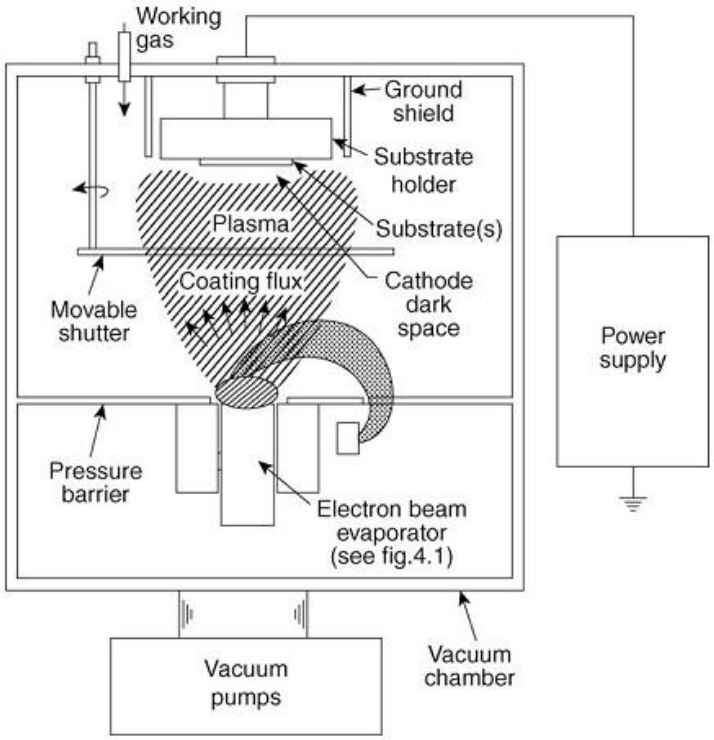

Figure 17: Iron plating process [79].

- Sputtering

The sputtering process is shown in Figure 18. Positive gas ions (usually argon ions) produced in a glow discharge (gas pressure 20-150 mtorr) bombard the target material (also called the cathode), dislodging groups of atoms which then pass into the phase and deposit onto the substrate [79]. In addition to depositing hard coating, it is especially useful for depositing soft coatings. Sputtered MoS_2 coating is the second-generation methods for deposition of MoS_2, which follows the early simple burnishing or rubbing, air-spraying resin-bonded or inorganically bonded coatings. By this method, the thickness of coating can be reduced from the typical range of 5-15 mm to 0.2 mm with good uniformity and reproducibility [51].

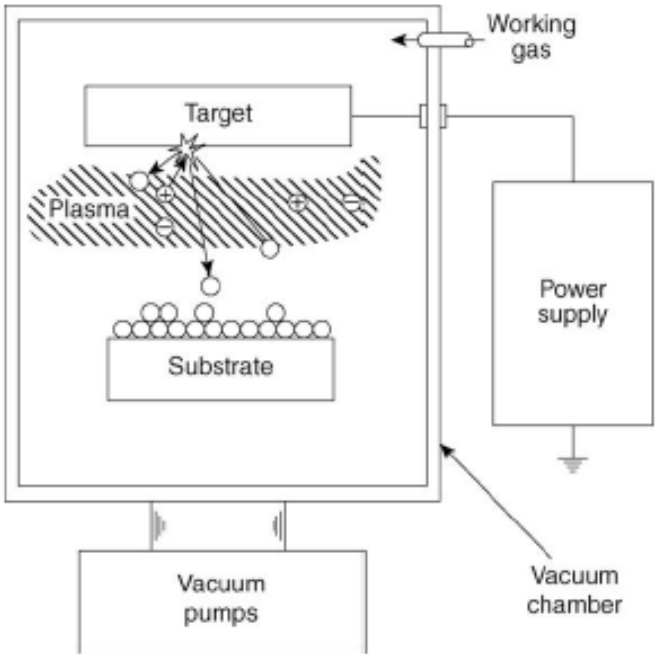

Figure 18: Basic sputtering process[79].

I.4.5 Spraying processes (varnish coating)

The spraying processes are usually divided into macroscopic and microscopic spraying depending on the size of sprayed particles. If the diameter of particle composed by many molecules is usually greater than 10 μm, it is called macroscopic spraying. If it is in contrast, it is called microscopic spraying. Among the spraying process, there is one called the air or airless spraying that is dependent of the spraying speed. When a liquid exceeds a certain critical velocity, it breaks up into droplets. The atomized droplets, by advantage of their velocity (acquired from high-pressure air or airless source), can be sprayed onto a substrate [80]. This method has been widely used in industrial applications to get a varnish coating that can prevent the surface from severe wear. The advantage of a lubricating varnish is its simple application in an immersion centrifuge or spray drum, both of which are time-tested procedures for the coating of mass-produced parts. Special areas of application for lubricating varnishes and sliding films include metric screws, thread-shaping screws, thread-cutting screws, all types of wood screws, screws made from plastic, thread-grooving screws, and screws made from aluminum alloys [81]. In order to have a low friction coefficient, the solid lubricant can be added into the varnish. Generally, a lubricating varnish contains 20–40 vol.% solid lubricant particles. The sprayed varnish can cover all ‘valleys’ and the surface asperities. During the sliding between two counterparts, the varnish can be released out of the ‘valleys’ and transferred between the two sliding counterparts, thereby providing a low friction coefficient and a good lubrication between two contacts [82].

I.4.6 Summary of deposition method

To get better mechanical and physical properties, the single layer is not the direction of development. Instead, more attentions have been put in the composite coatings. For the composite coatings, therefore, the combination of deposition method can get better tribological response. Take the multi-layer coating as an example. CVD deposited coating can be used as

the interlayer coating due to its high adherence strength. The diffusion, occurring at high temperature, can improve adhesion between the first coating and substrate. The subsequent PVD coating layer provides a fine grained microstructure with better resistance to wear and toughness [37] .

I.5 **Tribological response of coating**

As we know, the coating-substrate system (hard/soft coating on hard/soft substrate, thickness of coating and its roughness) also has a significant influence (Figure 19) on the tribological response of coating, except for the deposition method.

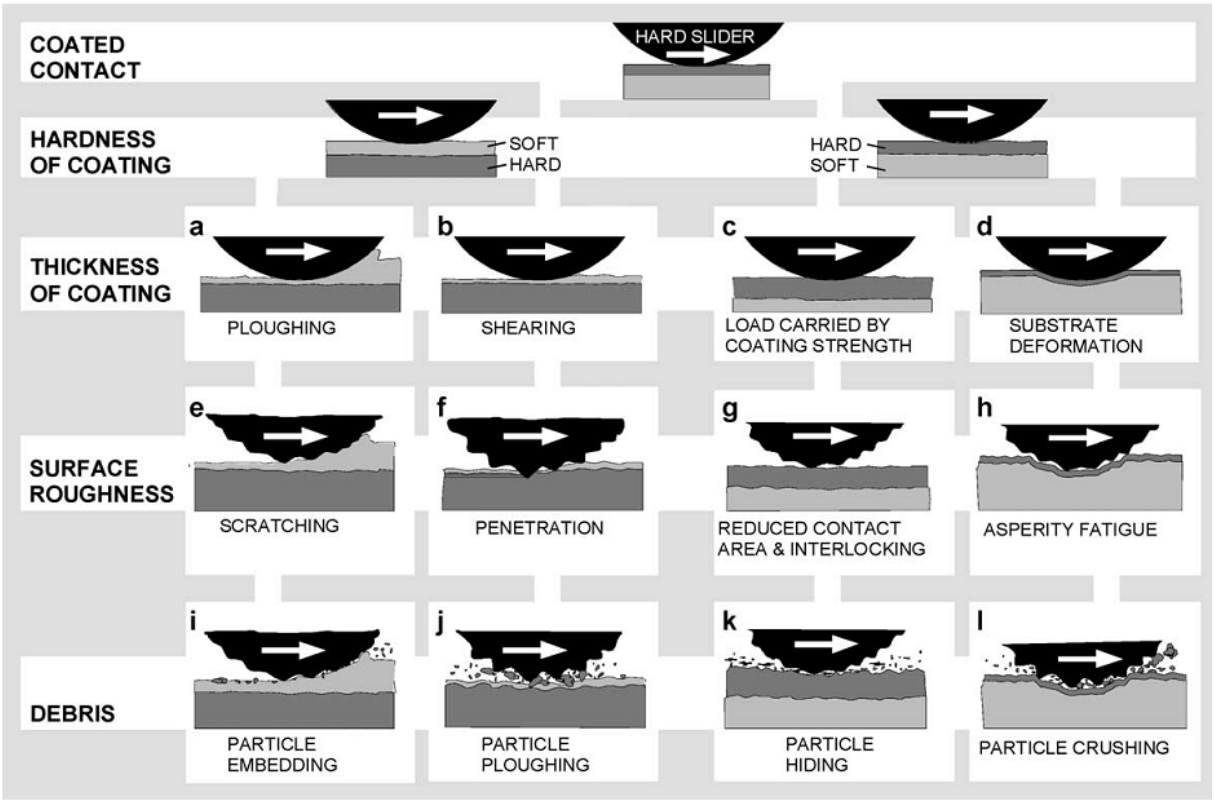

Figure 19: Macromechanical contact conditions for different mechanisms which influence friction when a hard spherical slider moves on a coated flat surface [83].

I.5.1 Hardness of coating

Hardness is a very important parameter for the tribological response of coatings. The different combination of hardness will affect the wear behavior and wear processes significantly.

I.5.1.1 Hard coating

In most cases, the hard coating is mostly deposited on the soft substrate because it prevents the coating system from the delamination. The substrate significantly deforms and the stress can be easily dispersed underneath, as shown in Figure 20 [84]. In contrast, a hard substrate can result in fracture in the scratch response [85].

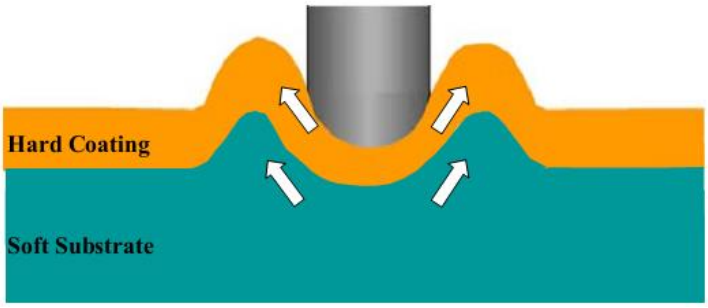

Figure 20: Illustration of the mechanical deformation of hard coating on the soft substrate [84].

I.5.1.2 Soft coating

Soft coating can work as a lubricant to reduce the friction coefficient and it is preferred to deposit on the hard substrate rather than soft substrate, because the soft coating on soft substrate can induce the significant plastic deformation and groove formation [85]. However, if the soft coating is deposited on the hard substrate, the soft coating will increase the contact area but decrease interfacial shear strength for hard substrate because only soft coating will suffer from the deformation, as shown in Figure 21. The white dash line that is the interface between the substrate and coating does not change since no significant deformation occurred on the steel substrate [84]. Therefore, it can well prevent the substrate from wear and provide the low friction coefficient and good lubrication between two contacts.

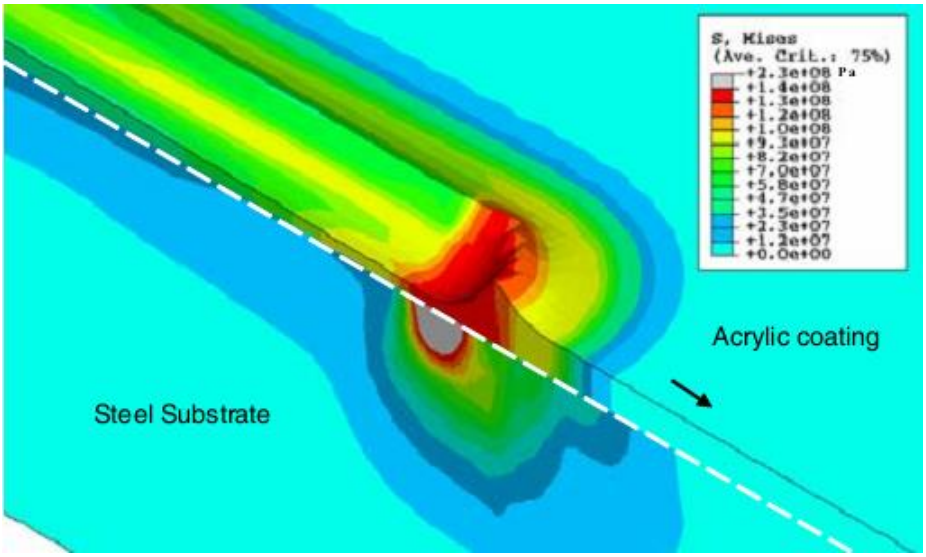

Figure 21: The von Mises stress field for the soft coating on the hard substrate [84].

I.5.2 Thickness of coating

I.5.2.1 Hard coatings

When hard coatings are thin, the friction coefficient is high, because the coating is so thin that it cannot afford the load and thus the soft substrate deforms accordingly (Figure 19). The deformation of soft substrate adds a ploughing or hysteresis effect to friction [17]. When it is thick, in other words, it can afford the load and avoid the deformation of substrate so that a low friction coefficient occurs.

I.5.2.2 Soft coatings

For the soft coatings, the thinner coating can lead to less ploughing of the film [17]. Then, the contact area and shear strength of the film determine the friction, which is related to the deformation properties of the substrate. The friction coefficient will decrease with the decrease of film thickness until the film is very thin [86]. When the thickness of coating is less 1 µm, the thickness of coating is inversely proportional to the friction coefficient, as shown in Figure 22.

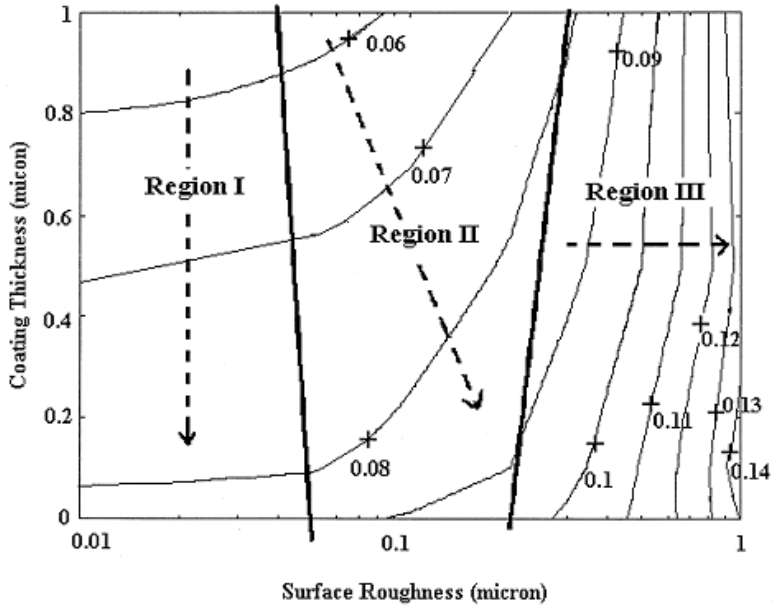

Figure 22: Map showing the effect of surface roughness and MoS_T coating thickness on friction coefficient contours are lines of equal friction coefficient [87].

I.5.3 Roughness

In the industrial applications, there is no entire smooth surface so that it is interesting to consider the effect of roughness on the frictional behavior.

I.5.3.1 Hard coating

For the thin hard coatings, roughness of substrate, coating or counterpart may affect significantly the friction behavior of two contact bodies. The roughness of substrate is proportional to the friction coefficient (Figure 23), while it is affectless to the thick coating [17]. Hayward [88] also points out that decrease of the roughness of coating and counterparts can reduce the friction coefficient because of decreasing the slope angle of the asperities according to the theory of Tabor [89] (Eq.(I-3)).

$$\mu_{av} = \frac{\mu_t(1+tan^2\theta)}{1-\mu_t^2 tan^2\theta} \qquad (I\text{-}3)$$

where μ_t refers to the true friction between smooth surfaces, θ is the slope angle of the asperities the stylus is traversing.

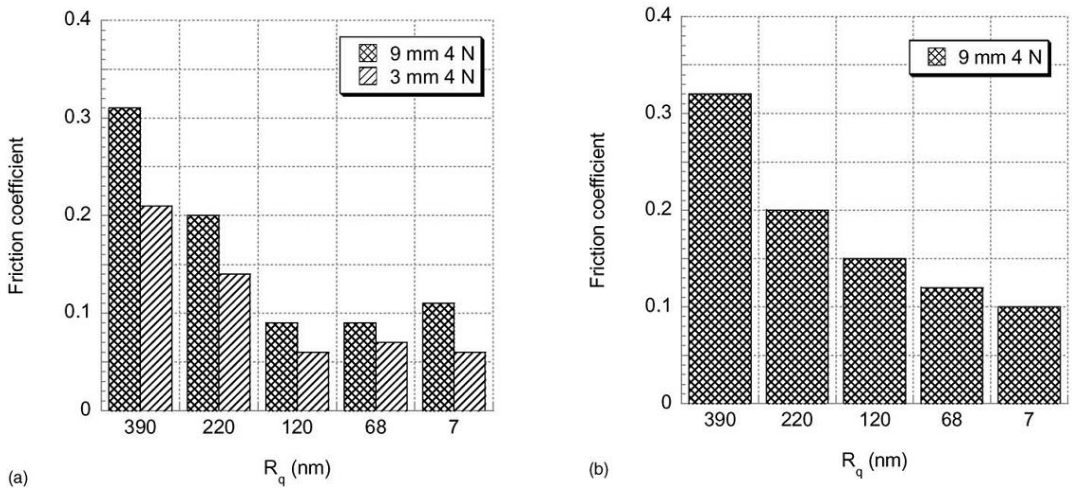

Figure 23: Friction coefficients in a ball-on-disc test of a-C:W coated specimen. Values after (a) 20 000 cycles and (b) 100 000 cycles; sliding speed: 0.07 m/s. The 9 mm ball and 36 N load are not included in (a) because of coating failure [90].

I.5.3.2 Soft coating

If the coating is thick enough, the influence of roughness of substrate can be ignored. However, its influence is significant for the thin coating, as shown in Figure 24, due to the reduction in true contact area. In addition, the penetration of asperities through the film is also a reason, which leads to the increase of shear resistance and ploughing of either the substrate or counterface and thus to an increase of friction coefficient.

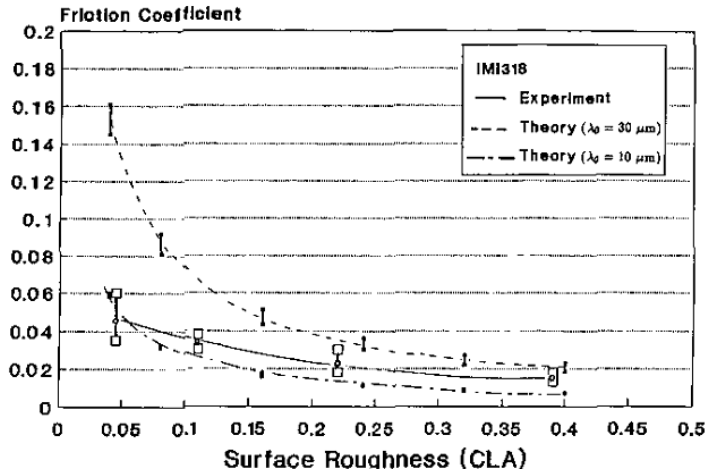

Figure 24: Variation in friction coefficient as a function of CLA roughness for 52100 steel substrate [91].

I.6 **Tribological evaluation of coatings**

The wear modes are generally classified by abrasive wear (like scratching), adhesive wear (like galling and scuffing), fretting or fretting corrosion, erosive wear, rolling contact fatigue (like spalling), delamination and tribo-corrosion, leading to the failure of elements. Therefore, it is necessary to know the wear resistance of one element for each wear mode before applying in the machine.

Characterization of coating includes many perspectives including the mechanical properties, physico-chemical properties and tribological properties. The mechanical properties can be realized by the nanoindentation test (for hardness and elastic properties), scratch and indentation tests (for adhesion force). Transmission electron microscopy (TEM), scanning electron microscopy (SEM), Auger electron spectroscopy (AES), X-ray diffraction analysis (XRD), Electron spectroscopy for chemical analysis (XPS), Rutherford backscattering spectroscopy (RBS) and secondary ion mass spectrometry (SIMS) are usually used to investigate physico-chemical properties. For the tribological properties, it includes sliding tests, abrasion testing and rolling contact fatigue tests.

I.6.1 Experimental methods

I.6.1.1 Sliding test

Various sliding tests (Figure 25) have been widely applied to test the wear rate and friction coefficient, of which the pin-on-disc is used mostly.

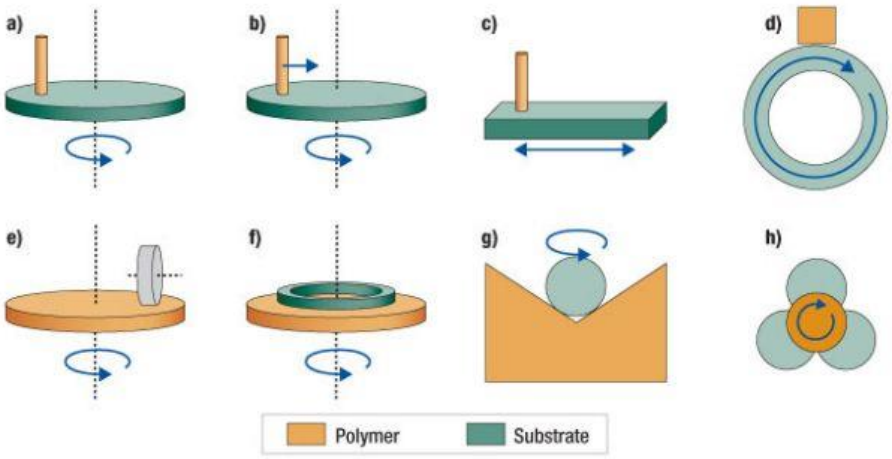

Figure 25: Common wear test geometries: (a) pin-on-disc with circular track (b) pin-on-disc with spiral track (c) reciprocating linear test (d) block-on-ring (e) disc-on-wheel (f) thrust washer (g) ball-on-prism (h) four ball. Pin-on-disc and pin-on-plate may be identified as ball-on-disc or ball-on-plate, respectively, if the pin has a hemispherical tip [92].

- Pin-on-disc

The pin-on-disc is employed to determine the wear rates and coefficient of friction at low loads. Due to the size of test, it can be put in different box to control the environment. Therefore, it is preferred to test the effect of environment such as humid air, oxidation, temperature or vacuum on the friction coefficient and wear rates. The layout of pin-on-disc is shown in Figure 25 (a-b). The sliding friction test occurs between a stationary pin stylus and a rotating disk. Rotational speed, normal load and wear track diameter can be different according to the design of experiment. Electronic sensors can be used to record wear and tangential friction force as a function of speed, load, or environmental conditions.

- Block-on-ring and hammer wear

Block-on-ring is often used to determine the abrasive and adhesive wear rate of materials. A steel ring is rotated against a stationary block. It can simulate the wear rate of line contact.

Hammer wear test is used to give information about the cohesion and adhesion qualities of coatings. For above two tests, they are not popular in the scientific research.

- Fretting test

Fretting is considered as a complex phenomenon related to interaction between two sliding bodies under a very low displacement amplitude [93], which limits the lifetime of elements significantly. It includes three modes of failure: fretting wear, fretting fatigue and fretting corrosion. Applying coating can reduce these problems in some degree, because it can increase surface elasticity and decrease the friction and thus reduce the crack initiation and propagation. It can also increase the surface inertness and reduce the unfavorable chemical reactions. Sometimes, it can build up favorable transfer of reaction layer between the contacting bodies so as to decrease the shear and friction [94]. Therefore, it is necessary to evaluate the fretting performance of a coating in different working conditions by fretting machine, which can provide some information such as wear rate and friction. For fretting, the contact counterbody can be changed to realize the research on the point-contact, line-contact and conformal-contact.

I.6.1.2 Abrasion testing

Good abrasive resistance ability is an important criterion for the tooling materials. Through the abrasion testing, the rack of materials in their resistance to abrasion under specified set conditions can be sure. Figure 26 shows the basic layout of abrasion testing. Different size of particles or water slurry can be put in hopper to test the influence of slurry on the friction and wear rate, thereby getting a tribological evaluation about the coating.

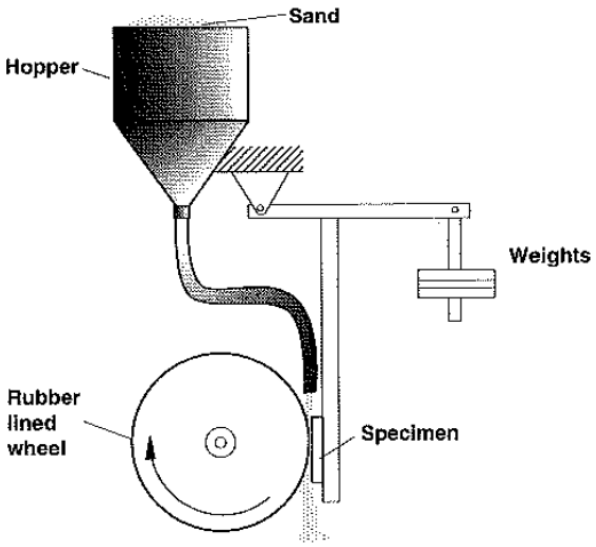

Figure 26: Layout of the dry sand rubber wheel abrasion test apparatus [95].

I.6.2 Modeling methods

According to the experimental results, different treatments of data can be applied so that the internal relationship between different parameters can be discovered, thereby better explaining the results and providing the data for industrial applications. It is generally divided into three aspects: wear models, friction models and mechanical models.

I.6.2.1 Wear Models

- Archard Model

Talking about the wear models, Archard model [96] is the most famous one with the history of more than 50 years. Based on it, many related models have been developed for the industrial applications. It describes the relationship between the wear rate and different parameters such as hardness, displacement amplitude and normal force (Eq. (I-4)).

$$W' = \frac{W}{S_L} = k \times \frac{P}{H} \qquad (I\text{-}4)$$

where W' refers to wear rate (material volume loss W for a given total sliding distance S_L). According to Archard's law, the wear rate W' is proportional to normal load P, inversely proportional to material hardness H and proportional to a constant k, the wear coefficient that is volume of material removed per unit load and sliding. k is strongly affected by the material properties and the test parameters. It can be used to predict component lifetimes if the tribo-system does not change wear modes.

- Dissipated energy models

Mohrbacher [97] presented the conception of cumulated dissipated energy in 1999. According to the fretting wear results, they stated that the wear of materials in fretting is proportional to the dissipated energy due to friction of contacting bodies. Due to the appearance of third body in the contact, the dissipated energy is decreased as a function of cycles (Figure 27). This is the very early discovery about the dissipated energy.

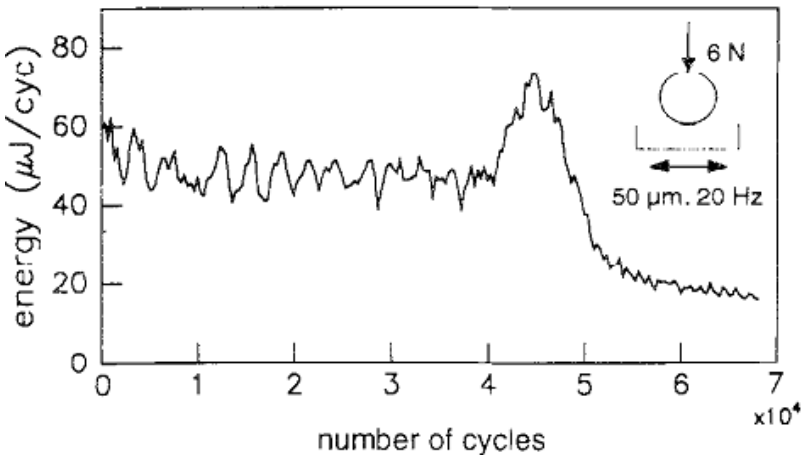

Figure 27: Evolution of mechanical contact response in contact TiN vs. corundum during displacement induced fretting (D=80 μm, F_n=2 N, F=10 Hz, T=23°C) [97].

In recent years, Fouvry [98] has done several studies to develop this theory. The dissipated energy is proportional to the wear volume, shown in Figure 28 as

$$V = \alpha \sum E_d + \beta \qquad (I\text{-}5)$$

where α is the wear energy coefficient (μm^3/J), β is the residual value (μm^3).

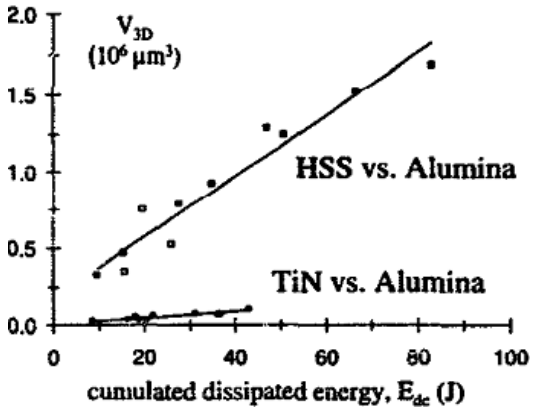

Figure 28: Evolution of TiN and HSS wear volume versus the accumulated dissipated energy [98].

For the application of coating, the durability of coating is more useful for industry. According to the theory of Fouvry, Fridrici [99] developed this theory to the prediction of coating lifetime (Eq. (I-6)), because lifetime has the linearly relationship with the maximum value of dissipated energy density ($Ed_{0\ \max ini}$) shown in Figure 29.

$$Ed_{0\,\max ini} = 4\mu_{ini}\delta_0 P_{max} \qquad (I\text{-}6)$$

$\mathrm{Ed}_{0\,\max ini} = 4\mu_{ini} \cdot \delta_0 \cdot \mathrm{P}_{max} Ed_{0\ \max ini}$ is the maximum value of dissipated energy density. It is located at the center of the contact in cylinder on plane contact, while it is located in the outer parts of the contact in the punch on plane contact. δ_0 is the sliding distance at the interface during an entire cycle and μ_{ini} is initial friction coefficient. P_{max} refers to the maximum contact pressure.

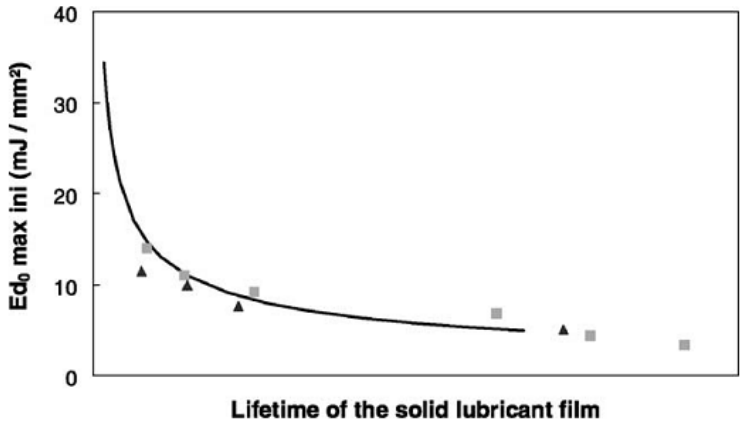

Figure 29: Relation between the lifetime of the solid lubricant and the initial maximal dissipated energy density for the punch on plane contact (■: P = 2000 N; ▲: P = 3000 N) and comparison with the predicted lifetime from the cylinder on plane contact (plain line) [99].

I.6.2.2 Models of friction coefficient

Except from the development of wear models, the friction coefficient models were deduced in 1990s by Singer [100]. The friction coefficient is inversely proportional to contact pressure for the MoS_2 coating. With the increase of contact pressure, the friction coefficient is decreased, as shown in Eq. (I-7).

$$\mu = \left(\frac{S_0}{P}\right) + \alpha \qquad (I\text{-}7)$$

S_0 and α represent material properties controlling friction. P is the mean Hertzian contact pressure so that it can be only used in the elastic deformation. Dvorak [101] proposed to divide the friction coefficient into two parts, shown in Eq.(I-8). One part (μ_{int}) depends on an interfacial shear strength (S_{int}), and other part μ_{shear} depends on a shearing term (S_{debris}), with aim to explain the effect of third body on the friction behavior. The former term (S_{int}) describes the interfacial shear strength between the debris and the track, and the latter one (S_{debris}) refers to the shear strength of the debris (not that of the coating)

$$\mu = \mu_{int} + \mu_{shear} \qquad (I\text{-}8)$$

Due to the high sensitivity of MoS_2 to humidity, it has a significant difference of value for the dry air and humid air. Therefore, it provides a good example to describe the shear strength of debris or between debris and track. S_{int} value is sensitive to relevant humidity, but S_{debris} does not, because it accounts for the time dependence in both the friction coefficient and the delayed shear/extrusion.

I.6.2.3 Mechanical model

Finite element analysis (FEM) is a numerical method that divides very complicated problems into partial different equations or integral equations so that it can model the mechanical evolution during the movement of contact bodies. It can be used with the coatings systems or no coating systems.

For the coating system, FEM helps explain the position of deformation and cracks. When coating is thin, the maximum shear stress occurs at the coating/substrate interface that accelerates the crack propagation, leading to the delamination, while the thick coating can avoid this problem (Figure 30). In addition, the stress discontinuity at the interface for thin coating is larger than that of thick coating, which accelerates the delamination wear.

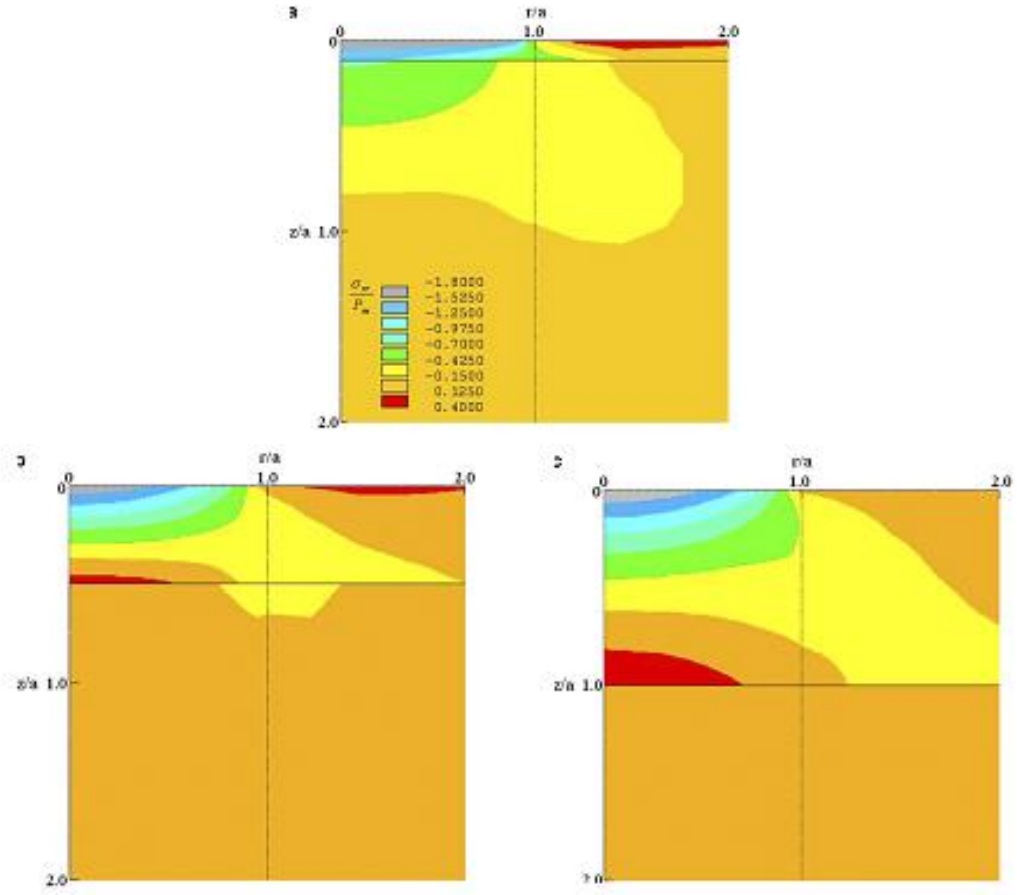

Figure 30: Counter plots of radial stress for the single-layer coatings with different thicknesses subjected to the same loading conditions, (a) t_c/a= 0.1 (b)t_c/a= 0.5 (c)t_c/a= 1.0 [38].

I.7 **Methods of mathematical statistics**

Statistics is the study of the collection, organization, analysis, interpretation and presentation of data. It is divided into two parts that are descriptive statistics and inferential statistics. The former one is used to organize, summarize and focus on the main features of the data, which includes the factorial analysis and regression analysis. The later one is focused on generalization or interference from the data to a larger set of data, based on probability theory, which includes the logistic regression and survival analysis. The results of tribological response such as friction coefficient and wear rate or coating lifetime are the continuous data, which are suitable for the analysis of mathematical statistics.

I.7.1 Descriptive statistics

In 1998, Mondal [102] used factorial analysis to make a comparison of effect of normal force and particle size on the wear rate, which cannot be realized by the traditional tribological analysis. By the factorial design, it builds a mathematical or quantitative description for the relation of different test parameters on the wear rates, as shown in Figure 31. When the point (one test parameter) is located in the right-up corner of normal probability distribution, it indicates that it is independent on the wear rates. In other words, no matter what kind of change of reinforcement will bring no effect on the tribological response of materials. In contrast, a little change of environment may bring a significant change of wear rates. It also provides an

evaluation rate for different test parameters. The parameters at the left down corner present more important than the parameters at a higher position. The importance of parameters of model can be well explained by the observation and chemical analysis of wear scar. In addition, it can give a final relationship between the tribological response and test parameters. Apart from the model of wear rate and friction coefficient, it can be used to evaluate the relationship among surface hardness, cutting speed, cutting force and tool life, which is difficult to describe by the existing models [103]. It is also a useful method in predicting the trends and building models in complex processes such as wear–corrosion interactions, because it can explain the interaction between erosion and corrosion with ease [104].

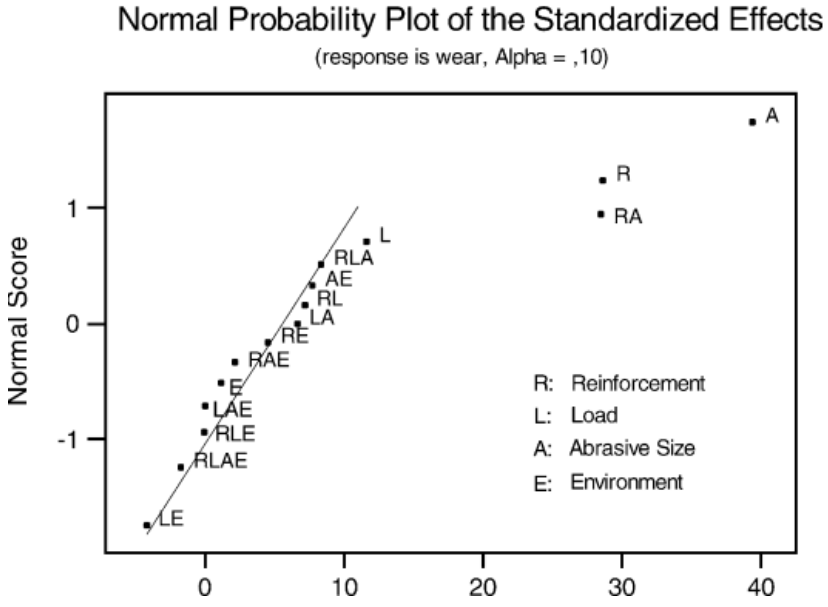

Figure 31: Normal probability of the effects of the factors and their interactions [105].

I.7.2 Inferential statistics

Life distribution is very important for lifetime data analysis, because it describes the statistical probability distribution of time to failure of a component, subassembly, assembly or system. Besides, it offers an appropriate model to estimate the life reliability [106]. It explores deterministic physical/chemical mathematical relationships between rate of failure mechanism and accelerating variables [107] like contact force, displacement amplitude and contact configuration. It is one general way to fit reliability distribution to failure data. By reliability analysis, an appropriate parametric distribution, such as exponential, normal, lognormal, Weibull or gamma, can be chosen to estimate the unknown parameters.

1) Exponential distribution

It is the most commonly used for components or system exhibiting a constant failure rate due to its simplicity. It can be defined by Eq. (I-9):

$$f(t) = \lambda e^{-\lambda(t-\gamma)}$$

where λ is the constant failure rate and γ is the location parameter.

2) Weibull distribution

It is generally used to model material strength, time-to-failure of electronic and mechanical components or systems. It can be defined by Eq. (I-10):

$$f(t) = \frac{\beta}{\eta}\left(\frac{t-\gamma}{\eta}\right)e^{-\left(\frac{t-\gamma}{\eta}\right)^{\beta}}$$

where β is a shape parameter, η is a scale parameters and γ is a locating parameter, as shown in Figure 32.

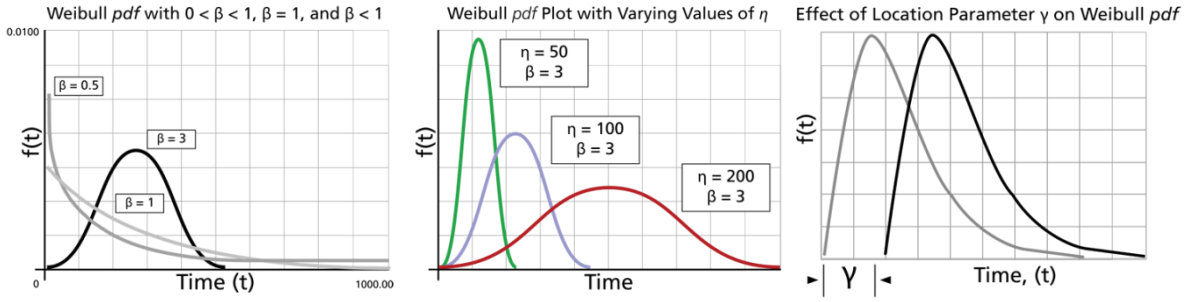

Figure 32: Effect of different parameters on Weibull probability density function (pdf) [108].

3) Normal distribution

Normal distribution is commonly used for simple electric and mechanical component, equipment. It can be expressed Eq. (I-11):

$$f(t) = \frac{1}{\sigma\sqrt{2\pi}}e^{-\frac{1}{2}\left(\frac{t-\mu}{\sigma}\right)}$$

where μ is the mean value of failure time and σ is the standard error of failure time.

4) Lognormal distribution

It is generally used for reliability analysis of materials design and loading variables. When the natural logarithms of time to failure are normally distributed, it means that the data follow the lognormal distribution.

$$f(t) = \frac{1}{t\sigma'\sqrt{2\pi}}e^{-\frac{1}{2}\left(\frac{t'-\mu'}{\sigma'}\right)^2}$$
$$f(t) \geq 0, t > 0, \sigma' > 0, t' = \ln(t)$$

where μ′ is the mean value of $\ln(t)$ and σ' is the standard deviation of $\ln(t)$.

At present, the Weibull distribution has been widely used in the material fatigue as an evaluation method. According to the Weibull distribution, an empirical cumulative distribution function (CDF) graph can be drawn to compare the fitted distributions for each treatment and estimate the percentile of failure [109], as shown in Figure 33. It can give a reference for the industrial application of this material.

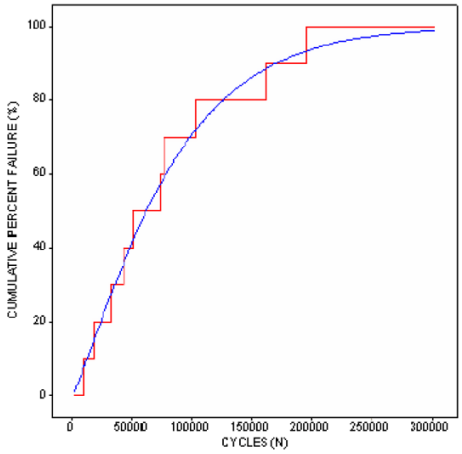

Figure 33: Empirical cumulative distribution function (CDF) to failure of as cast material [109].

Guseva and Evans [110, 111] employed an accelerated test to predict service life of aircraft coating under different temperature, UV and aerosols by the Weibull distribution. In the experiment of fatigue test, one of the most popular curves is called the *S*-*N* curve. This test describes the data as a plot of stress (*S*) against the number of cycles to failure (*N*), as shown in Figure 34. The *S*–*N* curves show four different safe levels (R= 0.99, R= 0.50, R= 0.368, R= 0.10) according to the Weibull distribution, which provide the possibility to predict reliable fatigue life needed to designer [112, 113].

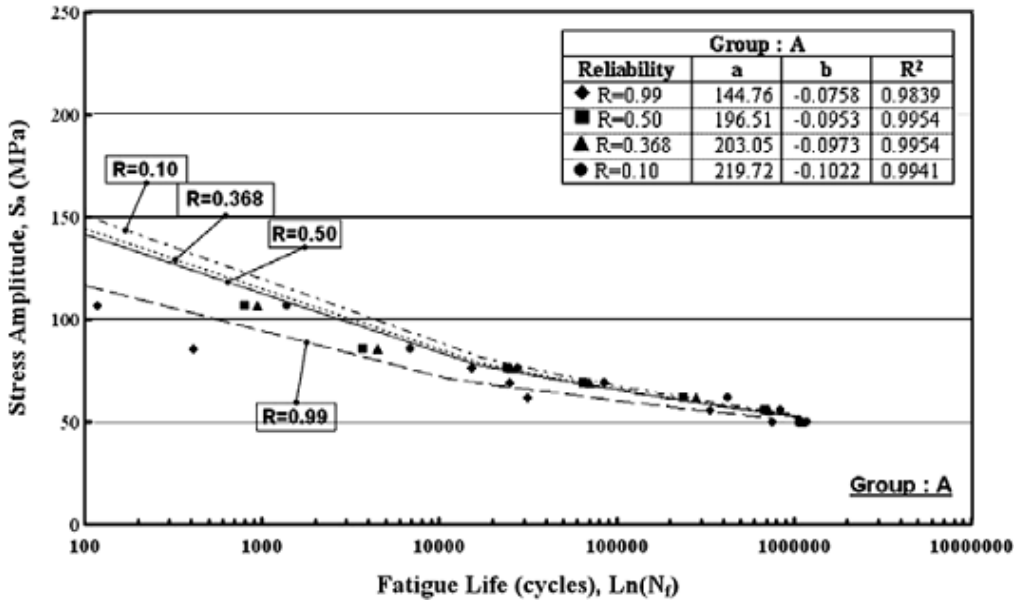

Figure 34: The S–N curves for different reliable levels [113].

Recently, some researchers find out that the distribution of 2-parameter Weilbull can serve as a tool to differentiate failure mechanisms. Generally speaking, a group of product will fail due to more than one failure mode, but one product can be failed one time due to one failure mode. A Weibull plot demonstrates the statistical percentage of a specimen for the failed event in fatigue tests. If the data points follow an *S*-shape on the probability plot, it may indicate that

more than one failure mode occur during the time. Based on the research, the shape value β is related to different failure modes as following [108]:

1) if β<1, it is induced by the early failure where the substandard components fail and are removed from the population, corresponding to a decreasing failure rate.

2) if β≈1, it is indicative of failure of component by chance alone and constant failure rate

3) if β>1, wear-out process occurs and more components are removed out, corresponding to increasing failure rate. This part is the focus in this study.

The plot in Figure 35 (a) shows that a simple Weibull model does not adequately fit the data, because the points do not scatter around a straight line [114]. In contrast, it clearly exhibits a bimodal distribution. This special distribution of the life data may reflect the difference in failure modes of the coatings under the same tribological condition of contact stress [115]. As the Weibull modulus becomes larger and the plot becomes steeper, the failure mode shifts from early E modes to D modes, as shown in Figure 35 (b). Therefore, the Weibull distribution reveals information about the failure mechanisms of the specimens [116].

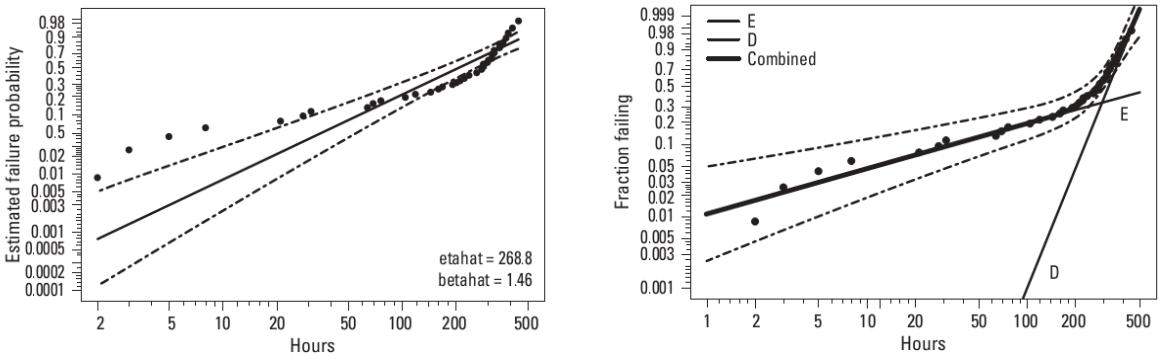

(a) Omnibus analysis (b) Combining separate failure mode analyses

Figure 35: Weibull Probability Plot for Voltage Endurance Data [114].

I.8 **Conclusions**

Coatings are effective coverings to reduce friction and palliate wear and protect contacting surfaces. Therefore, it is interesting to understand the application area of different coatings. In order to do this, in this chapter, bibliography synthesis was carried out from the following aspects:

- Coating types and structures linked to the friction and wear behavior,
- Deposition methods linked to adhesion force between coating and substrate,
- Tribological response of coating systems,
- Important parameters influencing the tribological response of coating systems,
- Wear and friction prediction of coatings,
- Theoretical analysis of depth.

The friction reducing function of coatings is dependent on the shear strength at the contact interface and the real contact area. The wear resistance of coatings is related to the hardness of

coatings. Therefore, the soft coatings have lower friction coefficient than hard coatings, but hard coatings have better wear resistance than soft coatings.

With the aim to combine their individual advantages, more coating structures and deposition methods have been developed in the past 20 years. In this study, a MoS_2 based varnish will be used to do the research, because the varnish with MoS_2 particle can have a low friction coefficient between sliding counterfaces. However, the tribological response of a coating system is complex, which is influenced by many parameters such as the counterpart, coating properties, interface, substrate and running conditions. The effects of parameters for friction reduction and wear resistance under different wear mechanisms are quite different.

In order to give a fair evaluation to the tribological response of coatings, some models like FEM and dissipated energy have been proposed. FEM is an effective way to describe the mechanical evolution of materials, while dissipated energy give a valid way to predict the wear volume in fretting test. Recently, the statistical method has been applied in the model to give an equation that describes the relation between various test parameters and tribological response.

According to the literature study, the following 4 aspects are very important, and they will be respectively discussed in the subsequent chapters:

- Explore the effect of test parameters on the tribological response of one coating,
- Give a simple wear and friction prediction model,
- Explain properly the relationship between the wear process and predicted model,
- Evaluate the relationships between tribological response and coating properties and running conditions.

CHAPTER II

EXPERIMENTAL METHODS AND METHODS OF ANALYSIS

CHAPTER II: EXPERIMENTAL METHODS AND METHODS OF ANALYSIS

This chapter introduces the materials under investigation, including the coatings, substrates and counterparts, the experimental tests and the analytical methods.

II.1 Introduction

In this study, the effects of normal force, displacement amplitude, contact configuration, coating position, thickness of coating and nature of substrate are studied to understand the application scope of the coatings. Some statistical methods are used to compare the effect of various test conditions. Factorial analysis is used to understand the competition of various test conditions on the friction coefficient and coating lifetime. Reliability or survival analysis is used to establish the relation between wear mechanism and reliability.

II.2 Materials

In this work, MoS_2 based varnish coating is used in the experiments. It is a product of ORAPI Company (MoS_2 dry lubricant MOLYSPRAY 700), which has been widely used in the treatment and pre-treatment of all machinery and parts to be assembled. The varnish is served as an effective bonding agent to help improve the adhesive and film-creating properties of MoS_2 coatings.

II.2.1 Substrate materials and pretreatment

Three substrates are used in these experiments, 304 stainless steel, AISI 52100 and AISI M2 steel whose chemical composition and mechanical properties are shown in Table 6 and Table 7, respectively. 304 stainless steel is one kind of stainless steel with a minimum of 10.5% chromium content by mass. This content of chromium can form a protective layer of chromium oxide on the steel surface. The 10% of nickel can improve general corrosion resistance. The lower carbon content lowers the possibility of formation of chromium carbides which can decrease the corrosion resistance [117]. M2 is one kind of high-speed steel with an addition of 11 % of tungsten-molybdenum, which can efficiently improve the hardness and toughness of steel and thereby leading to high wear resistance. Due to the technology of powder metallurgy, some porosity can be observed at the surface, as a result of low carbon content and undersintered [118]. In this study, the porosity percentage is about 20% of surface. Thanks to this special structure, it allows to do the study on the effect of porosity on the tribological behavior compared with the 304 stainless steel (without porosity). Three shapes of materials (ball, cylinder and flat) are used as shown in Figure 36. The purpose of different curvatures of substrate (flat or ball/cylinder) is to estimate the effect of curvature on the friction coefficient and coating lifetime during the relative movement. Before the deposition of MoS_2 coating, the surfaces of the flat substrates were polished with abrasive papers (grade 400, 800 and 1200),

corresponding to a final roughness R_a = 0.025 µm ± 0.01 µm. All substrates were cleaned 15 mn in an ultrasonic bath of acetone before tests.

Table 6: Chemical composition of the materials.

Material	C	Cr	Ni	Mn	Fe	Si	W	Mo	V
304 stainless steel	0.06	18	10	-	Balance	-	-	-	-
AISI 52100 steel	1.0	1.5	-	0.35	Balance	0.25	-	-	-
AISI M2 steel	0.9	4	-	0.3	Balance	0.3	6	5	2

Table 7: Mechanical properties of the materials (determined by nano-indentation tests).

Material	Elastic modulus (GPa)	Hardness (GPa)
304 stainless steel	200	3
AISI 52100 steel	207	6.8
M2 steel	210	7.7
Coating	1.5	0.015

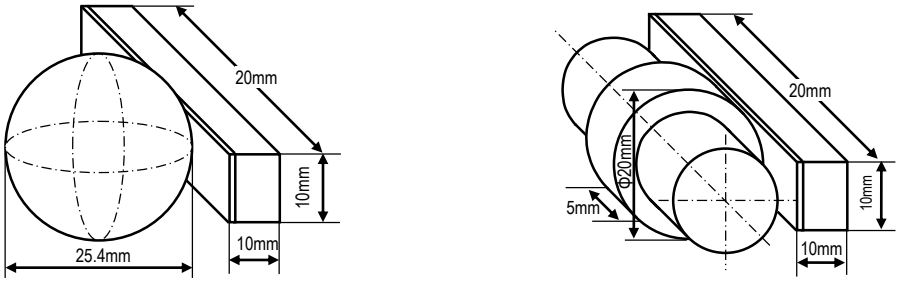

(a) ball-on-coated flat (b) cylinder-on-coated flat

Figure 36: Schematic outline of contact configuration.

II.2.2 Deposition process

The MoS_2 based varnish was sprayed from the aerosol spray can. The liquids contained in the can are hexane (50 <=x% < 100) and dimethoxymethane (25 <= x% <50). They are all colorless liquids at room temperature, with relatively low boiling points (50 – 70 °C). The additives are MoS_2 particles with the size of 700 nm. They are conserved in the can under pressure. When the container's valve is open, the liquid (made from hexane and dimethoxymethane) with some particles is forced out of a small hole and emerges as an aerosol, leaving the droplets on the surface of substrate. Finally, a film of varnish is formed on the surface. During the deposition, the distance between the aerosol and sample was about 25 cm. To gain a well-distributed coating on the ball or cylinder, its holder was rotated at a given constant speed. After deposition, sample was put in a dry box for 24 hours before experiments. The deposited coating on ball and cylinder can be seen in Figure 37. The SEM micrograph of the coating is shown in Figure 38. Prior to spraying, one part of the sample was covered by a paper band so that it was not coated and then comparing the profiles between coated part and uncoated part allowed us to estimate thickness of the coating. The thickness of coatings on flat substrate is 9.7 µm ± 1.6 µm (for one layer coating) and 19.8 µm ± 4.7 µm (for two layers coating). Thickness of one layer coating on the other substrates is 12.7 µm ± 4.7 µm (ball) and 12.1 ± 3.5 µm (cylinder), measured by a

profilometer. The values for two layers of coating are about 22.2 µm ± 1.0 µm (ball) and 23.8 µm ± 1.8 µm (cylinder). Stoichiometry of the MoS_2 particles is about 1:1.98 (determined by energy-dispersive X-ray spectroscopy).

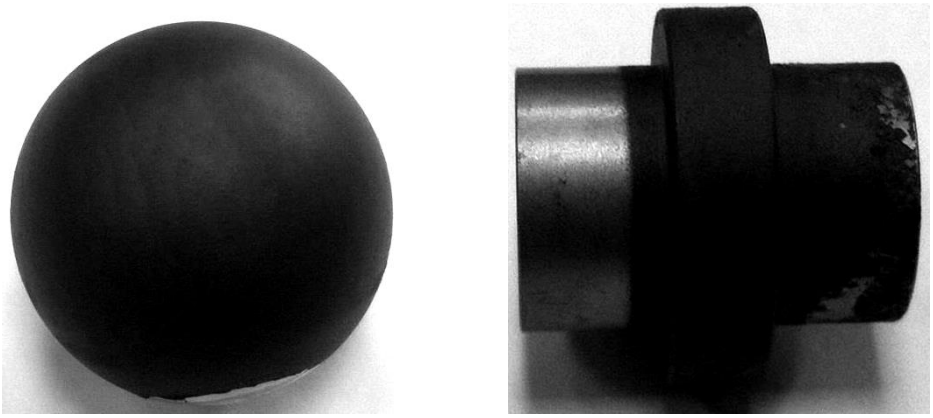

Figure 37: coating on ball and cylinder substrates.

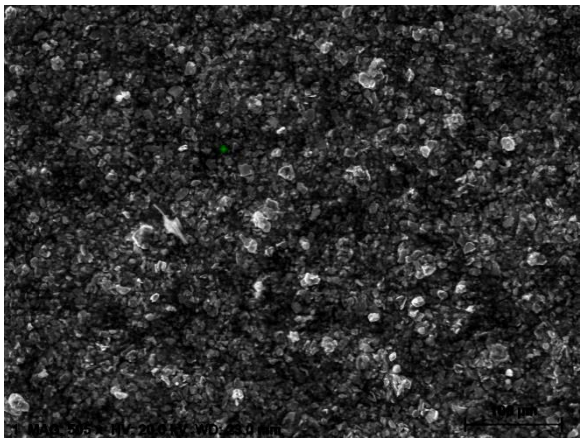

Figure 38: SEM micrograph of aerosol sprayed MoS_2 based varnish.

The mechanical properties of coating are determined by the nanoindentation tests. It was performed by the continuous stiffness measurement method with a Nanoindentation XP with a Berkovich diamond tip (three-side pyramid with an angle of 115.12° between edges). This method consists in superimposing a small displacement oscillation (3 nm, small enough to generate only an elastic strain) at a given frequency during the indentation test (32 Hz). Therefore, the sample endures small loading-unloading cycles. The mechanical properties of materials were calculated, following Bec and Loubet model [119]. The maximum load was 450 mN and the ratio between the load rate ($\dot{P}$) and the load (P) was kept constant, following the Eq. (II-1). Figure 39 shows the load-displacement indentation curve for coating on the flat substrate.

$$\frac{\dot{P}}{P} = 3 \times 10^{-2} s^{-1}$$

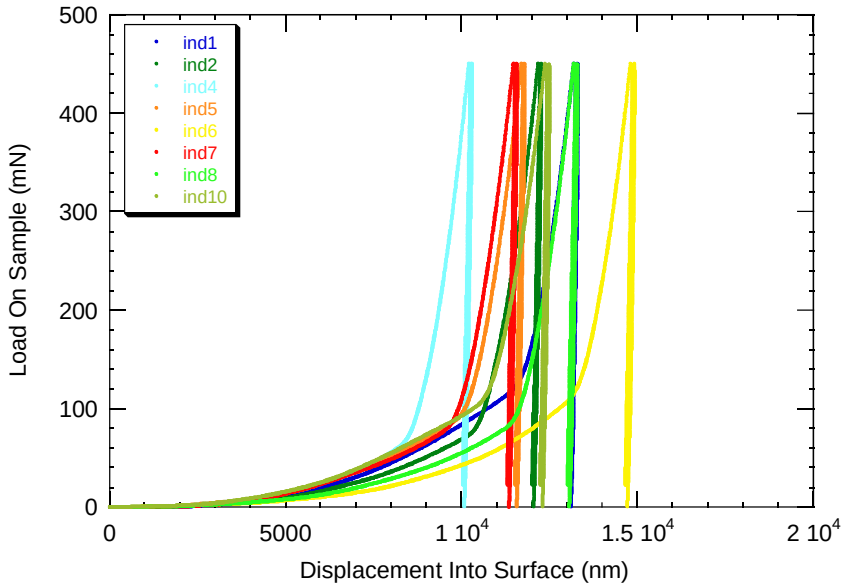

Figure 39: Load-displacement indentation curve.

II.3 Experiments

II.3.1 Fretting rig

The fretting tests were carried out on a fretting device developed in LTDS, which is based on a tension-compression hydraulic machine MTS®. The schematic outline of the test rig is shown in Figure 40 (a). Coated block specimen is mounted on a main shaft, which moves up and down. Displacement is controlled by the extensometer. The counterpart is fixed in the other side. For selected numbers of cycles during a fretting test, evolutions of the displacement amplitude δ^*, contact force F_n and tangential force F_t are recorded during one cycle. According to the captured data, the relationship between friction force and displacement can be drawn in Figure 40 (b). The area of the quadrangle is the frictional dissipated energy (E_d) in the cycle.

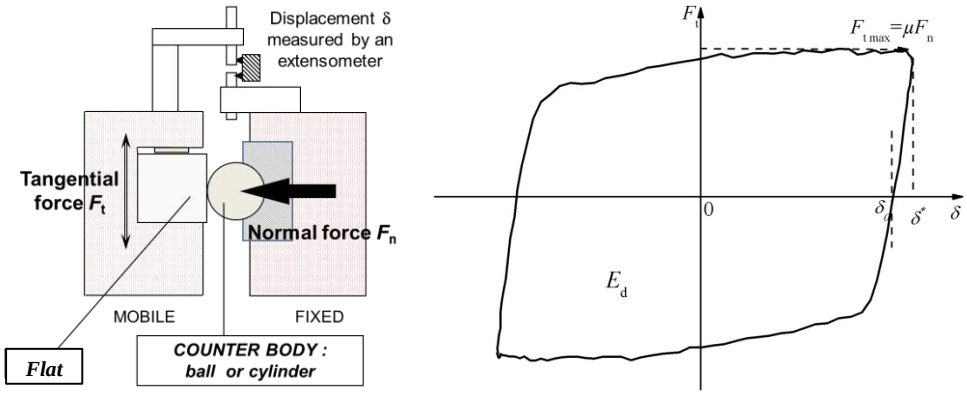

(a) (b)

Figure 40: Fretting test rig (a) and fretting loop F_t-δ curve (b).

II.3.2 Test conditions

Table 8 describes the test conditions for the soft coating. The fretting test of pressure sprayed MoS_2 based varnish was carried out under two contact configurations (i.e. ball-on-flat and cylinder-on-flat) (Figure 36). In addition, the coating is deposited on spherical or cylindrical

substrate to investigate effects of curvature of substrate on wear and friction behavior of the coating. Table 8 describes the coating position (flat, ball or cylinder and both). This is because of interesting observation of Descartes in 1995 [120] explained that coating on the sphere could lead to a long durability by reducing adherence of the moustaches, which is the ejected coating particles layered outside the contact area, thereby modifying the energy of the surface. Early investigations of bonded coating made exclusively on the flat substrate sample [121-124] so that it is necessary to do some research to discuss the effect of coating position on the friction coefficient and coating lifetime. In 2011, Mary *et al.* [44] concluded that the wear process was dependent on the wear pressure. Below a pressure threshold, conventional abrasive wear processes were activated, while the severe adhesive wear phenomena operated when it was higher than the pressure threshold. Therefore, it is necessary to do the experiment to explore the interaction between contact pressure and wear process for coatings. According to the Hertzian contact theory, the contact pressure is determined by the contact force and contact configuration. The chosen contact force is shown in Table 8. Displacement amplitude affects the third body flow, which is a very important wear process of soft coating. Three displacement amplitudes are chosen to understand the third body flow under certain working conditions. Coating thickness and different structures of substrates may influence the friction coefficient and lifetime of coating.

Table 8: Test parameters.

Test variable	Levels
Contact force	100 N, 400 N, 700 N
Displacement amplitude	± 10 µm, ± 25 µm, ± 40 µm
Frequency	5 Hz
Contact configuration	ball-on-flat, cylinder-on-flat
Coating position	coating on the flat, coating on ball or cylinder, coating on both counterparts
Thickness of coating	one layer coating, two layers coating
Substrate materials	304 stainless steel (flat), AISI M2 steel (flat), AISI52100 (ball and cylinder)

Calculations of Hertzian contact parameters are shown in Table 9 and Table 10. They were performed without taking into account the coating because of its relatively small thickness and low mechanical properties. In addition, the contact pressure by Hertzian theory has exceeded the critical stress of plastic deformation of the coating (=1.6Y=1.6H/3=5 MPa), so the result of Herzian theory cannot be used. The mean contact pressure can be calculated by the FEM model (with coating), which is discussed in next section.

Table 9: Hertzian contact parameters for ball-on-flat and cylinder-on-flat without coating (304 stainless steel flat).

Contact force F_n (N)	Contact configuration (304 stainless steel)			
	Ball-on-flat		Cylinder-on-flat	
	Contact radius (µm)	Maximum contact pressure (GPa)	Contact width (µm)	Maximum contact pressure (GPa)
100	204	1.144	96	0.266
400	324	1.816	191	0.533
700	391	2.189	253	0.705

Table 10: Hertzian contact parameters for ball-on-flat and cylinder-on-flat without coating (AISI M2 steel flat).

Contact force F_n (N)	Contact configuration (AISI M2 steel)			
	Ball-on-flat		Cylinder-on-flat	
	Contact radius (µm)	Maximum contact pressure (GPa)	Contact width (µm)	Maximum contact pressure (GPa)
100	200	1.195	92	0.275
400	317	1.896	185	0.551
700	382	2.285	245	0.728

II.4 Finite element analysis

The simulation methodology for determining stress distribution is based on a two-dimensional FE modeling approach using ABAQUS, a general purpose, linear, commercial code. Two basic models were chosen, because two contact configurations were employed in this study. Axisymmetric model was used to simulate the point contact (ball-on-flat) and 2D planar was chosen to simulate the line contact (cylinder-on-flat). As the tangential friction component was not the focus of this work, quarter symmetry was implemented into the model to reduce the computational effort. Hence, as depicted in Figure 41 (a), the model consisted of a 90° cylindrical or sphere section in contact with plate. The coating was modeled as a perfectly adhered, the thickness of layer, equal to 10 µm or 20 µm for coating on flat and 12 µm or 24 µm for coating on cylinder or ball on both contacting surfaces. The substrates were set to be linear-elastic and the polymer coating layer was modeled with an elasto-plastic behavior with isotropic strain hardening. Constrains were applied to the top and right hand side of the finite element model. The bottom of plate substrate was constrained in all 6 degrees of freedom to have it fixed throughout the whole simulation. The normal load was applied on the top surface of cylinder or ball.

The mesh is shown in Figure 41 (b). The substrate and coating layer were discretized by 4-node bilinear plane strain quadrilateral elements for contact configuration of cylinder-on-flat and by 4-node bilinear plain stress quadrilateral elements for contact configuration of ball-on-flat. The mesh size at the densest mesh area was about 0.5 µm. This gave a high degree of accuracy for the predicted stress field. Detailed mesh studies have been carried out to arrive at the mesh design (Figure 41 (b)), which includes a sharp transition from the fine mesh region to the coarser mesh (further from the contact) to minimize CPU times, on the one hand, whilst maintaining solution accuracy on the other. The contact pressure-overclosure relationship used in the FEM model is chosen as the "hard" contact model. Contact surface roughness was considered smooth throughout each simulation.

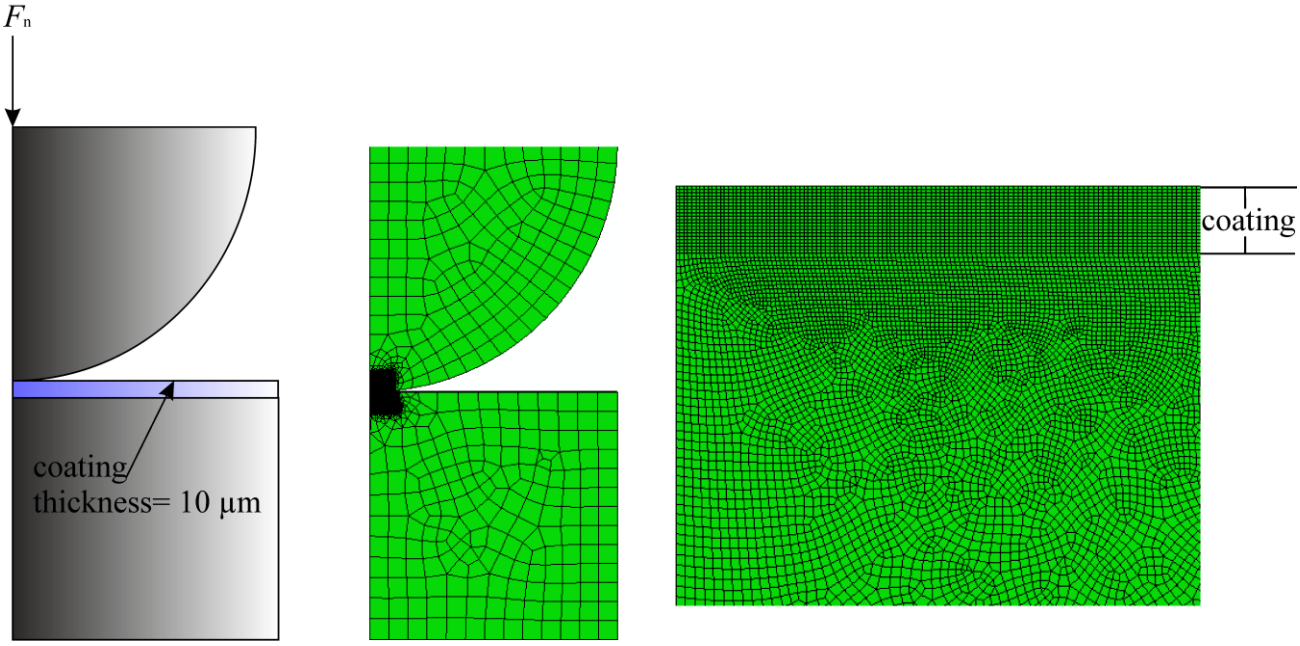

Figure 41: (a) Schematic view of the cylinder on flat coated substrate model; (b) full model mesh (c) contact region mesh detail.

II.5 Statistical method

In this thesis, some methods such as factorial design, orthogonal design, analysis of variance (ANOVA), reliability or survival analysis used in the tribological analysis have been employed. Firstly, factorial design and orthogonal design are the methods used to design the experiment with an aim to conduct experiments effectively; Secondly, analysis of variance is a method used to describe the effect of factors on the dependent values; Thirdly, the reliability analysis is served as an effective way to describe the survival rate of materials under certain running conditions.

II.5.1 Design of experiment

An experimental design is a plan for running experiments. Factors in design of experiment can have two or more fixed values (or called levels). Experiments are performed to study the effects of factor levels on the response variables.

II.5.1.1 Factorial design

Factorial design is generally divided into two parts that are full-factorial design and fractional-factorial design. Full-factorial design consists of all possible combinations of the levels of factors. Therefore, all main effects, two-interactions and high-order interactions are estimable and uncorrelated. However, it is not cost-effective, because it requires to carry out experiments for all combinations, of which some are not necessary [125]. For this reason, the fractional-factorial design is usually preferred, because it can reduce the numbers of tests and thus reduce the cost and time. A fraction is usually ½ or ¼ part of full factorial design. It reduces the number of runs and it keeps the balance property that every level of a factor appears the same number of times at every level of the other factor. However, the numbers of runs violates the efficiency of experimental design. If the number of tests is not enough, the main effect can be confounded

by the interaction effect between two factors. In this case, the efficiency of experimental design is violated. Therefore, the design of fractional-factorial design should consider the resolution property. The property of resolution is the ability to separate main effects and low-order interactions from one to another, which is very important to the fractional-factorial design.

II.5.1.2 Orthogonal design

Orthogonal design is a special type of fractional-factorial design, in which all estimable effects are uncorrelated, as shown in Table 11. Dr. Genichi Taguchi proposed it at the end of 1940s. Actually, orthogonal design is the design according to the orthogonal tables. The columns (factors) in table have the orthogonality, which means the levels of all factors are uncorrelated [125] and every factor can be independently estimated from every other factor, because it is orthogonal to every other column. In addition, the sum of one column is zero. This orthogonality guarantees that the effect of one factor or interaction is estimated out of any influence due to any other factor or interaction. Figure 42 describes the distribution of experimental parameters in the orthogonal design, which reduces 2/3 the numbers of runs and effectively saves time and cost. In each line of orthogonal design, there is only one experimental point, indicating that the experimental distribution is homo-disperse. A perfect design includes the property of both balance and orthogonality. Therefore, the number of test cannot be determined optionally. It has some specific number of runs (e.g. 16, 18, 20, 24, 27, and 28) for specific numbers of factors with two or three levels.

Table 11: Orthogonal table.

Number of runs	Column (factor)		
	1	2	3
1	-1	-1	-1
2	-1	0	1
3	-1	1	0
4	0	-1	1
5	0	0	0
6	0	1	-1
7	1	-1	0
8	1	0	-1
9	1	1	1

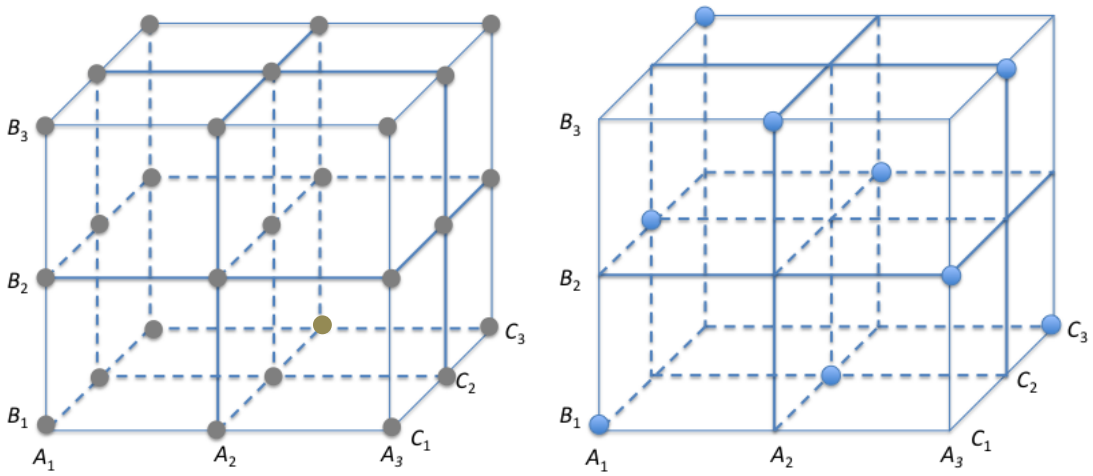

(a) Full factorial design (b) orthogonal design

Figure 42: The distribution of experimental parameters in the full factorial design (a) and orthogonal design (b).

II.5.1.3 Uniform design

In addition to the factorial design and orthogonal design, the uniform design has been widely used in the industrial applications. Different from the orthogonal design, the uniform design only considers the uniform distribution in the experiment, ignoring the homodisperse. It can reduce the runs of experiments in some degree. It is suitable for more levels of one factor.

II.5.1.4 Summary of design of experiments

According to the above description of design of experiments, the advantage and disadvantages are concluded in Table 12. In this study, the orthogonal design will be employed to design of experiment, because the order of effect of various factors is a very important parameter for the study.

Table 12: Comparison of three experimental designs.

Design of experiment	Advantages	Disadvantages
Full factorial design	all effects (two-effect interactions or high-order interaction can be estimated)	high cost, longer time
Orthogonal design	middle cost, middle time	not applicable for the high-order interactions; less levels are better
Uniform design	low cost, less time, applicable for more levels	not be used for the ANOVA

II.5.2 Analysis of variance (ANOVA)

Factorial analysis technique enables designers to determine simultaneously individual and interactive effects of many factors that can affect output results in any design [126]. It helps to point out sensitive parts and areas in designs that cause problems in experimental results by the method of analysis of variance (ANOVA). It is a statistical technique that used to compare the means of two or more groups of observation. For example, assume the response data measured in k levels of one factor, where y_{ij} represents the value of i^{th} observation ($i=1,2,\ldots,n_j$) on the j^{th} factor level (j=1,2…k). The relation between y_{ij} and i_j can be expressed as Eq. (II-2):

$$y_{ij} = u + i_j + \varepsilon_{ij},\ j = 1,2,\ldots,k, i = 1,2,\ldots\ n_j \qquad \textit{(II-2)}$$

Before the analysis, it proposed a hypothesis that different levels have equal variances, which is commonly called homogeneity of variance. According to the assumption of ANOVA, the means of different levels are same (Figure 43(a)), expressed as Eq. (II-3):

$$H_0: \mu = \mu_1 = \mu_2 = \cdots = \mu_k \qquad (II\text{-}3)$$

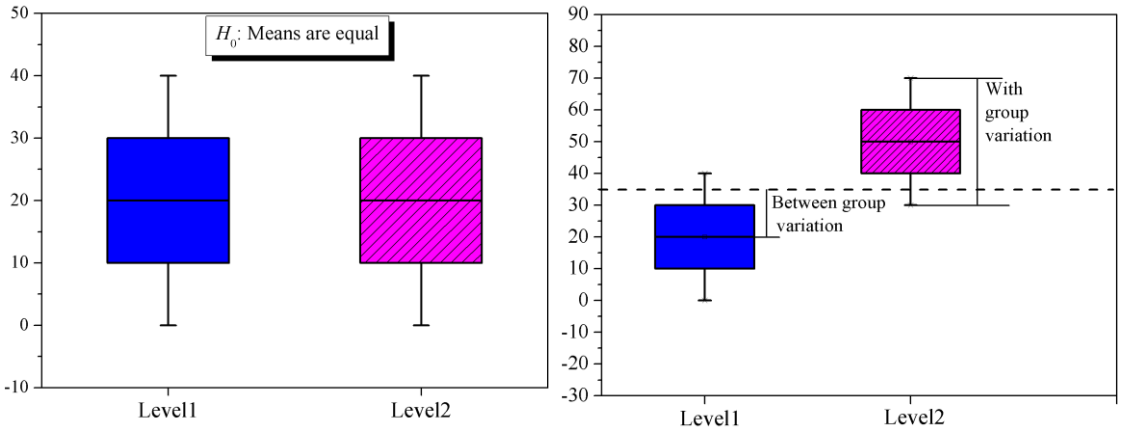

(a) (b)

Figure 43: The explanation of ANOVA assumption.

When the assumption of H_0 is true, the mean of Level1 and Level 2 is same. In other words, the change of value for this factor (x) does not bring the change of response value (y). There is no relationship between dependent value (y) and independent value (x). The response value (y) is independent from the factor (x). In contrast, the value change of factor (x) (from value of level 1 to level 2) can lead to significant change of response value (y) (Figure 43 (b)). The assumption (H_0) is violated. It indicates that the response value (y) is dependent on the factor (x). This comparison can be also realized by Table 13. The sum of square between groups is called model sum of square (SSM), and the sum of square with group variation is called Error sum of square (SSE). The total sum of square is the sum of SSM and SSE. F is the value of difference of between group variation and within group variation. If it equals to or less than 1, it indicates that there is no effect of factor (x) on the response value (y). As the value of F increases above 1, the change of levels for factor brings increasing variance between mean values of two levels. Generally, if $F \geqslant F_{\text{critical}}$, the y is dependent on x. F_{critical} is the critical value $F_{(k-1,\, n-k,\, \alpha)}$, which is the tabular value of the F distribution with k-1 and n-k degrees of freedom at level α. In contrast, if $F \leqslant F_{\text{critical}}$, the change of value for factor produces same result. *Prob>F* is the probability of a value of F greater than or equal to F_{critical}. For example, the statistical significance level of a equals to 0.05. If *Prob>F* equals to 0.001 (less than 0.05), then the null hypothesis (y is independent on x) is rejected. In other words, the response value (y) is dependent on the factor (x).

Table 13: One-way Anova table
(k=number of levels, n=number of total tests).

Source of variation	Degrees of Freedom (DF)	Sum of Squares (SS)	Mean Square (MS)	*F* Value	*Prob>F*
Model (Factor)	*k*-1	SSM	MSM	MSE/MSE	$P\{F \geq F_{(k-1,n-k,a)}\}$
Error	*n-k*	SSE	MSE		
Total	*n*-1				

II.5.3 Regression analysis

Regression analysis is a statistical technique for estimating the relationships among dependent variables and response variables. Eq. (II-4) is a simple regression model according to Eq. (II-5). According to the relationship, an estimation of the change of response variables can be made. Therefore, it is widely used for prediction and forecasting. This is also one goal of the present work.

$$y = a_0 + a_1 x_1 + a_2 x_2 + \cdots a_n x_n \qquad \textit{(II-4)}$$

$$\begin{cases} E(\varepsilon_i) = 0, i = 1, 2, \cdots n \\ \operatorname{cov}(\varepsilon_i, \varepsilon_j) = \begin{cases} \sigma^2, i = j \\ 0, i \neq j \end{cases} (i, j = 1, 2, \cdots n) \end{cases} \qquad \textit{(II-5)}$$

This assumption indicates that the quantitative model follows i) linearity between dependent and independent variables; (ii) independence of the errors (no serial correlation); (iii) homoscedasticity (constant variance) of the errors (a) versus time and (b) versus the predictions (or versus any independent variable); (iv) normality of the error distribution.

To describe fitting quality of a model equation, R^2 is preferred in most cases. An R^2 of 1.0 indicates that regression line perfectly fits the data. However, *Adjusted* R^2 is preferred when considering the effect of each explanatory term on the model, because *Adjusted* R^2 is a modification of R^2 that adjusts for number of explanatory variables in the model. Unlike R^2, *Adjusted* R^2 increases only if added explanatory term improves the model more than that can be expected by chance.

II.5.4 Survival analysis

Based on the lifetime of the coating, survival analysis or reliability under different levels of variables can be obtained. Firstly, the Kaplan–Meier curve (a non-parametric analysis) is used to describe the evolution of survival rate *S*(t) under different levels of variables. *S*(t) gives the probability that random variable *T* exceeds specified time *t*. Secondly, a parametric analysis is introduced to extrapolate a time-to-failure from failure data obtained at various levels. These models describe the degradation path of the life characteristics from one parameter level to another. A life characteristic can be expressed as a function of various working conditions [112]. Results such as mean life or median life can be obtained from this analysis.

Since Weibull distribution provides a closer approximation to probability of many natural phenomena [112, 113], it is used as the underlying life distribution. The Weibull distribution function can be expressed mathematically as Eq. (I-10).

According to the PDF (probability density function) equation, survival function (S(t)) in is obtained from Eq. (II-6):

$$S(t) = \exp(-(\frac{t}{\alpha})^{\beta})$$

Prior to employing the Weibull distribution, following assumptions were made:

1. Underlying life distribution has a common shape parameter across different stress level, which means coating will fail in the same manner or with same failure mode across different stress levels [112, 113];
2. Initial life parameters are constant over the life of the product;
3. Material property is isotropic and homogeneous.

II.6 Case study for validating statistical method

The results of thesis of Vincent Fridrici [127] are used in this part to prove the validity of statistical methods in friction and wear analysis. In this research, the full-factorial design is used to design the experiments due to the limited number of factors (3 factors with two or three levels). The experimental details are shown in Table 14. According to the theory of full-factorial design, the number of experiments will be 18 ($2^1 \times 3^2$). The number of experiments is so small that it is not necessary to use other design of experiments such as orthogonal design or uniform design. Then, the method of analysis of variance will be used to describe the effect of factors (contact force, displacement amplitude and interlayer) on the friction coefficient and lifetime of coatings. Reliability analysis will be used to describe the survival rate under certain running conditions.

Table 14: Test parameters for coatings with interlayer.

Test variable	Levels
Contact force	400 N, 1000 N
Displacement amplitude	± 15 µm, ± 50 µm, ± 75 µm
Contact configuration	Cylinder-on-flat
Coating position	Coating on the flat
Interlayer	Roughness interlayer, none interlayer, smooth interlayer

II.6.1 Effect of test parameters on friction coefficient of coatings

Analysis of variance is one method used to statistically distinct the effect of each factor on the dependent value. Before doing the analysis, it should make sure that each treatment (a group combination of test parameters) has the same variance. In addition, the data should be normally distributed for each treatment. In this study, only one test is carried out so that these two assumptions are complemented. Some scholars proposed that the analysis of variance should be complemented with 1) a run sequence plot of the residuals; 2) a normal probability plot of the residuals; 3) a scatter plot of the predicted values against the residuals [128]. According to this requirement, the normal test of residuals is made, as shown in Figure 44. It can be seen the distribution of residuals is normal and residuals are scarred randomly around the center line, which arrives the requirement for the ANOVA.

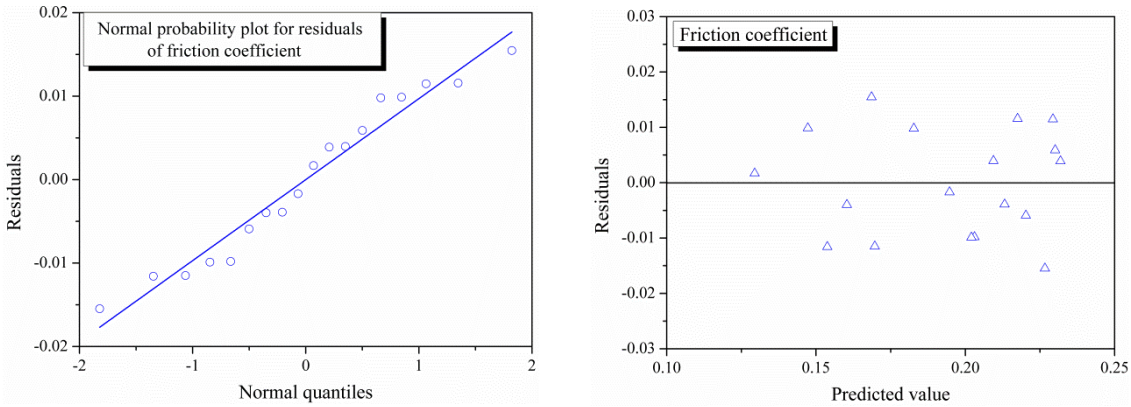

(a) (b)

Figure 44: The diagnostics for residuals of friction coefficient: (a) the normal probability plot for residuals of friction coefficient; (b) the residuals of friction coefficient vs. the predicted value.

According to the analysis of variance (Table 15), it can be seen that the most significant factors are contact force and interlayer, because its value of *P*r > *F* is significantly less than 0.05. With the increase of contact force, the friction coefficient is decreased significantly (column 1 and line 1 of Figure 45). The smooth interlayer can have the lower friction coefficient compared with rough interlayer and none of interlayer (line 3 and column 3 of Figure 45). This is because the contact pressure may change a little with the interlayer. The rough layer may increase the shear strength of coating so that the friction coefficient is increased.

Table 15: Analysis of variance for friction coefficient.

Source	DF	Sum Square	Mean Square	*F* Value	*F* critical	*P*r > *F*
Contact force	1	2.57E-01	2.57E-01	25.52	4.45	0.01
Displacement amplitude	2	2.62E-02	1.31E-02	1.3	3.59	0.37
Contact force × Displacement amplitude	2	3.48E-03	1.74E-03	0.17	3.59	0.85
Interlayer	2	1.45E-01	7.23E-02	7.17	3.59	0.05
Contact force × Interlayer	2	6.53E-02	3.26E-02	3.24	3.59	0.15
Displacement amplitude × Interlayer	4	2.65E-02	6.63E-03	0.66	2.96	0.65
Error	4	4.03E-02	1.01E-02			
Corrected Total	17	5.64E-01				

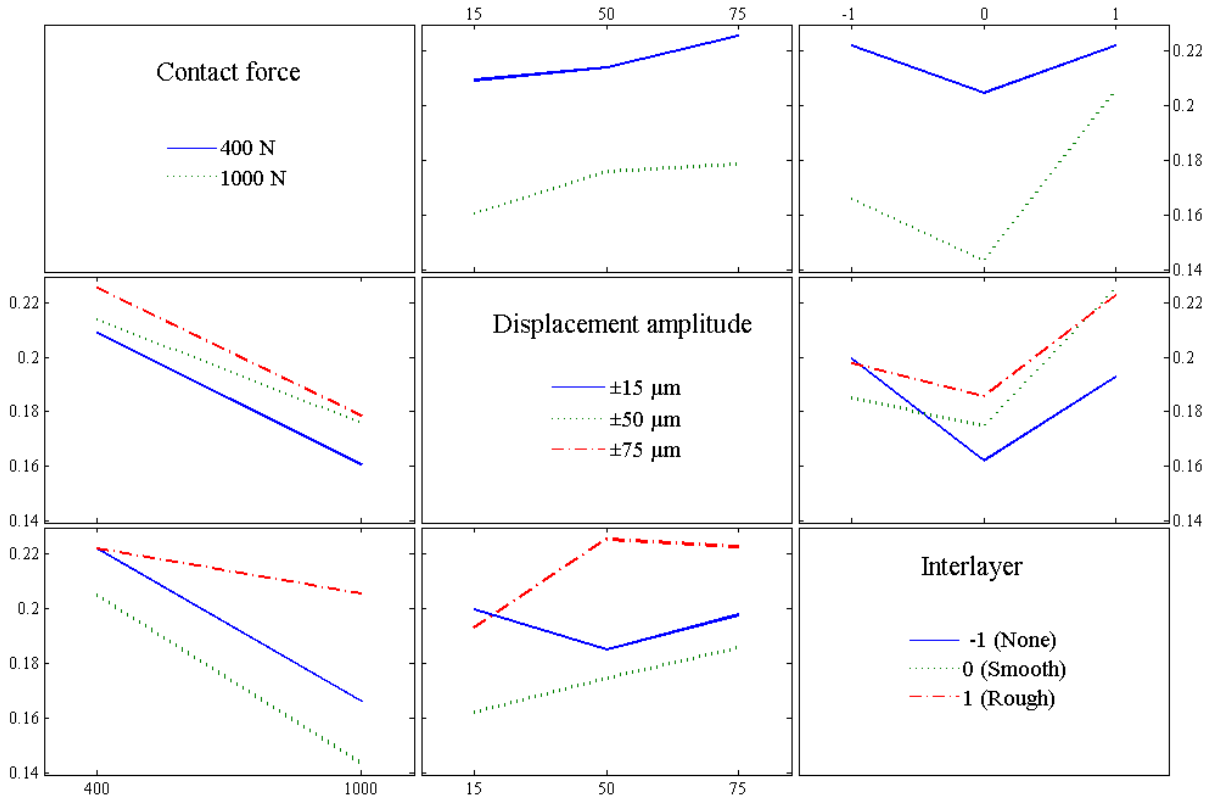

Figure 45: Interactive map of friction coefficient.

II.6.2 Effect of test parameters on coating lifetime of coatings

Before analyzing the variance, the normal test is made for the data of lifetime. It can be seen that the residuals of lifetime are not distributed randomly (Figure 46) so that it is necessary to do the transformation of lifetime. According to the theory of Box-cox, the lifetime is changed to the *ln*(lifetime) to achieve the requirement. Figure 47 describes the residuals of transformed lifetime that is distributed randomly around the center line.

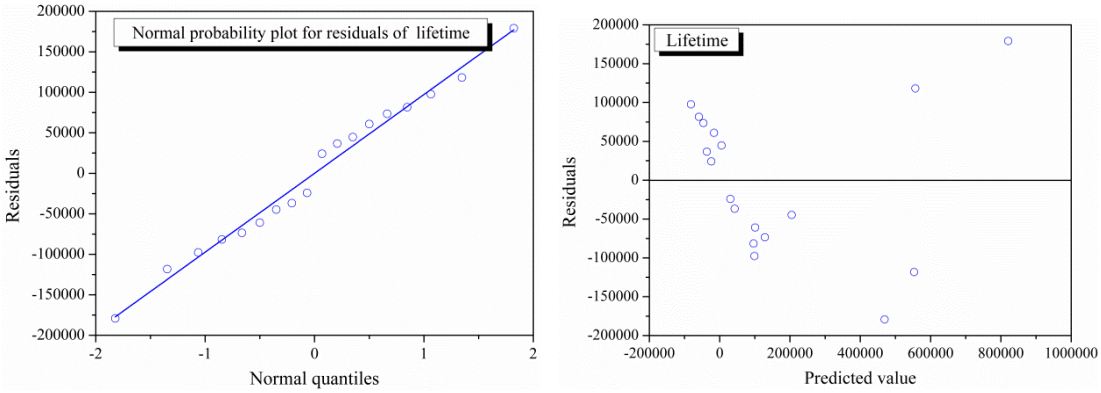

(a) (b)

Figure 46: The diagnostics for residuals of coating lifetime: (a) the normal probability plot for residuals of lifetime; (b) the residuals vs. predicted value.

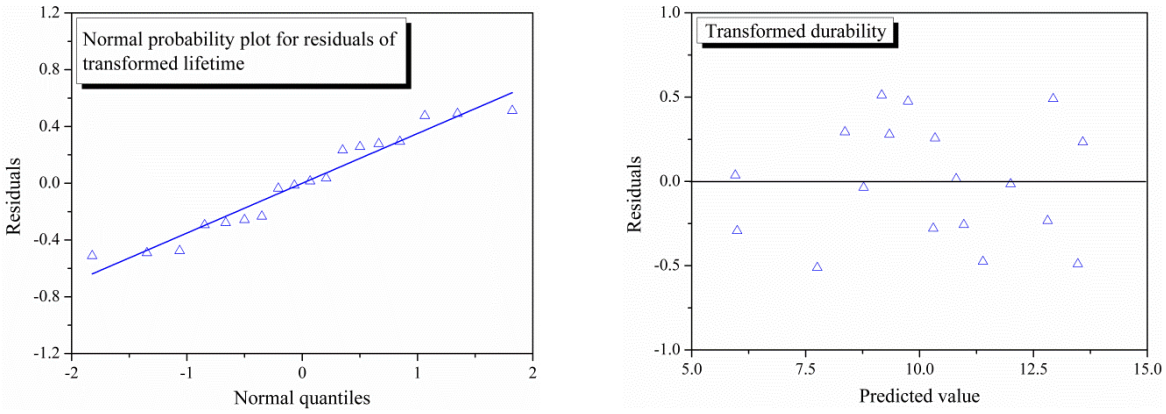

(a) (b)

Figure 47: The diagnostics for residuals of transformed lifetime (ln (Nc)): (a) normal probability plot for the residuals of ln(Nc) (b) the residuals of ln(Nc) vs. predicted value.

Different from the friction coefficient, the lifetime is firstly dependent on displacement amplitude, secondly dependent on interlayer (Table 16). With the interlayer, it can increase the adhesion force between substrate and coating, leading to better coating lifetime (line 3 and column 3 of Figure 48). Rough interlayer can have longer durability than smooth interlayer, because the rough substrate surface can help hold the coating during fretting movement.

Table 16: Analysis of variance for ln(Nc).

Source	DF	Sum Square	Mean Square	*F* Value	*F* critical	Pr > *F*
Contact force	1	5.24E+00	5.24E+00	10.35	4.45	0.03
Displacement amplitude	2	4.28E+01	2.14E+01	42.22	3.59	0.00
Contact force × Displacement amplitude	2	3.99E+00	2.00E+00	3.94	3.59	0.11
Interlayer	2	3.39E+01	1.69E+01	33.44	3.59	0.00
Contact force × Interlayer	2	1.70E+00	8.50E-01	1.68	3.59	0.30
Displacement amplitude × Interlayer	4	3.53E+00	8.83E-01	1.74	2.96	0.30
Error	4	2.03E+00	5.07E-01			
Corrected Total	17	9.32E+01				

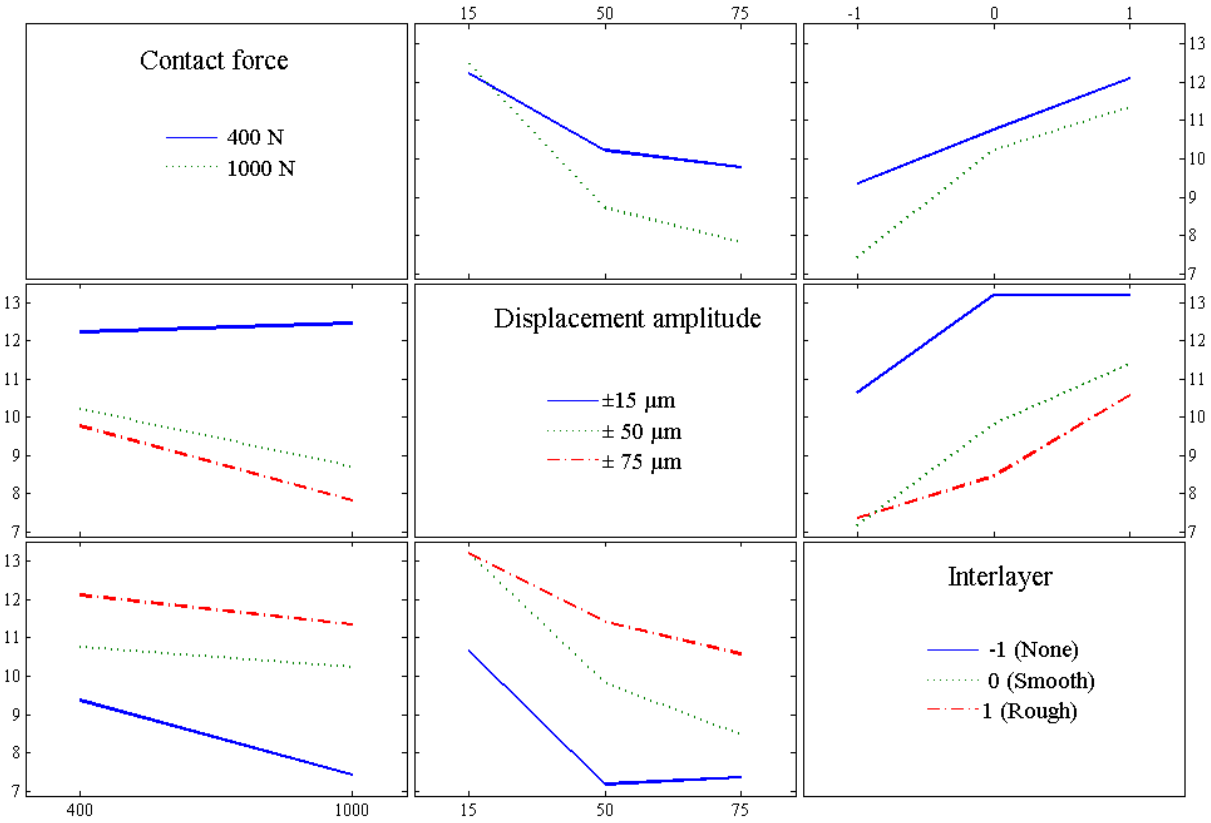

Figure 48: Interactive map of ln(lifetime) (a transformed value of 7 means a coating lifetime of 1096 cycles; a transformed value of 13 means a coating lifetime of 442413 cycles).

II.6.3 Regression analysis

V. Fridrici [127] has shown that the initial maximum dissipated energy has a relationship with the lifetime of coatings (Figure 49). It can be used as an effective method in the industry to predict the durability of coating by a lower cost. The long lifetime is related with the low initial maximum dissipated energy density.

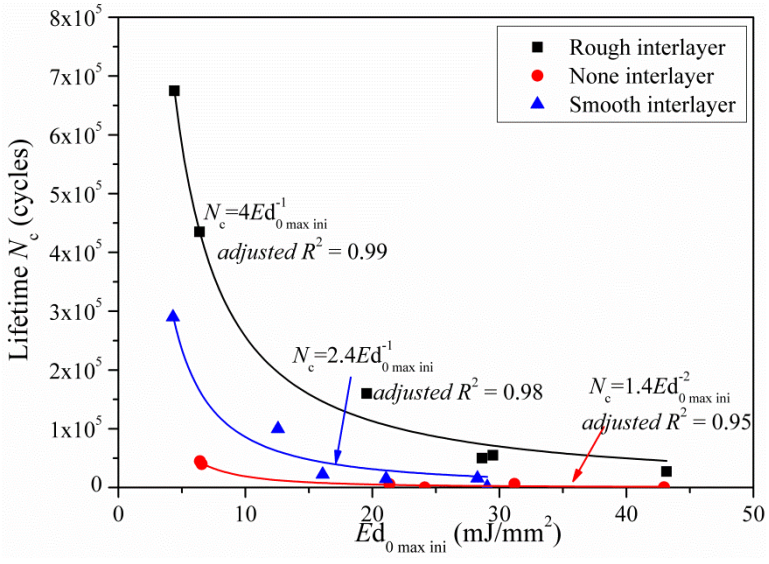

Figure 49: Relation between the lifetime of the solid lubricant and the initial maximal dissipated energy density [127].

Based on the significant factors in analysis of variance, a regression analysis can draw an equation to describe the relationship between independent variables and dependent variable, as shown in Eq. (II-7):

$$Nc = \exp(8.39 - 1.37F_n - 2.18\delta^* + 2.09 \times INTER1 + 3.32INTER2 - 1.12F_n \times \delta^* + 0.66\delta^{*^2} + 0.99F_n \times INTER1 + 0.83F_n \times INTER2 - 1.24\delta^* \times INTER1) \quad \textit{(II-7)}$$

adjusted R^2= 0.91

here, the value of each variable is normalized value of coded value. Firstly, coding can reduce range of each factor to a common scale regardless of its relative magnitude and scaling establishes factor levels that can be orthogonal (or nearly). Secondly, normalized values allow the comparison of corresponding normalized values for different datasets in a way that eliminates the effects of certain gross influences. To get the value of contact configuration and coatings position, dummy values can be used because they are categorical values. Dummy coding uses only one and zero to convey all of the necessary information on group membership, as shown in Table 17. The value of displacement amplitude is not chosen with the same interval so that its coding method is complicated. According to [129], the normalized value for displacement amplitude is shown in Table 18. The quadratic part should be considered because the evolution of lifetime as a function of displacement amplitude is not linear (Figure 48). In addition, the 400 N of contact force is normalized as $F_n = -1/\sqrt{2}$ and 1000 N of contact force is $F_n = 1/\sqrt{2}$.

Table 17: Dummy values of interlayer.

Interlayer	*Inter1*	*Inter2*
None	0	0
Smooth	1	0
Rough	0	1

Table 18: Normalized value for displacement amplitude.

Displacement amplitude	Linear part	Quadratic part
± 15 µm	$-19/\sqrt{654}$	$5/\sqrt{218}$
± 50 µm	$2/\sqrt{654}$	$-12/\sqrt{218}$
± 75 µm	$17/\sqrt{654}$	$7/\sqrt{218}$

According to this equation, it can be seen that the increase of contact force has a negative effect on the friction coefficient. Increase of displacement amplitude can lead significant decrease of coating lifetime because its coefficient is a large negative value. Rough interlayer may increase more lifetime than smooth interlayer because the coefficient of roughness is larger than the coefficient of smooth.

This method has a lower value of *adjusted* R^2 than the method of maximum initial energy so that its fitting result is not so good as the latter one. However, the latter one should recalculate the equation according to the different interlayer. The regression method can predict the lifetime of all working conditions by adding or deleting a variable. The comparison between model and experimental results has been shown in Figure 50. Several points are failed to be fitted. For example, the predicted value of point 4 (400 N, ± 15 µm, rough interlayer) is higher than the

experimental value. Generally, high normal force will lead to the lower coating lifetime (Figure 48). Therefore, the lifetime of 400 N should be much higher than 1000 N. However, in this experiment, the value of (400 N, 15 µm, rough interlayer) is lower than (1000 N, 15 µm, rough interlayer) so that the equation gives a higher prediction. To solve this problem, more experiments should be done to assure the reliability of experiments.

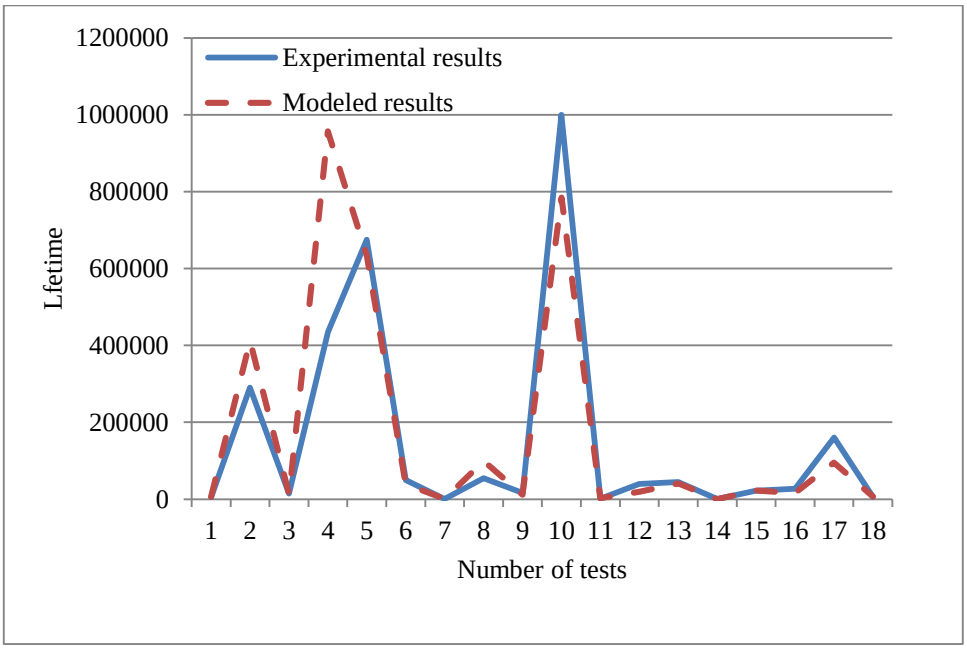

Figure 50: Comparison of experimental results and modeled results for coating lifetime.

The regression analysis can also be done for the friction coefficient, as shown in Eq. (II-8):

$$\mu = 0.19 - 0.04F_n - 0.02INTER1 + 0.019INTER2 + 0.03F_n \times INTER2 + 0.02\delta^* \times INTER1 + 0.02\ \delta^* \times INTER2 \quad \textit{(II-8)}$$

adjusted R^2= 0.82

The values used are also normalized value (Table 17 and Table 18). The equation (II-8) describes the relationship between variables and friction coefficient. The coefficient associated with factors can be used to describe the change of dependent value as a function of variables, because the normalizing can reduce range of each factor to a common scale regardless of its relative magnitude. With the increase of contact force, the decrease of friction coefficient is the most significant, because the absolute value of coefficient associated with F_n is largest, reaching an agreement with the analysis of variance. The smooth layer can have a low value of friction coefficient than none interlayer, because the coefficient is a negative value. Rough interlayer can lead to increase of friction coefficient.

Figure 50 compares the results of friction coefficient between experimental and modeled one. It can be observed that the modeled ones are almost near to the experimental results. It is due to the limited number of results. For the regression analysis, more results can give more stability of regression.

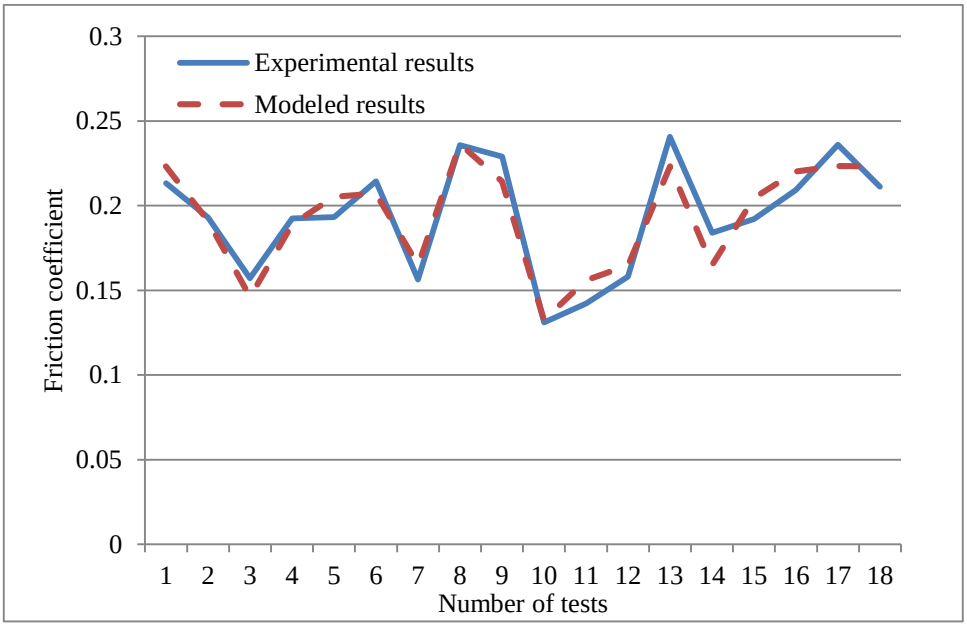

Figure 51: Comparison of experimental results and modeled results for friction coefficient.

II.6.4 Survival analysis

Kaplan-Meier analysis is one of survival analysis methods that often used to biostatistics to describe the death rate due to different factors. It can also be used in the failure analysis to compare the failure rate of different factors. Figure 52 to Figure 54 show the comparison of survival probability of the coating under different test conditions. Log-rank test and the Wilcoxon test give the test of whether the survival probabilities are same for different treatments (different level of one factor). Therefore, there is an assumption for Log-rank test and Wilcoxon test that the survival probabilities are same for different treatments. The value of *P*r >chi-square is a test whether the probability of the assumption is accepted. If the probability of chi-square is less than 0.05, it means that the assumption (the means of different levels for one factor are same) is rejected and the treatment leads to the change of survival probability. Sometimes, the values of *P*r > chi-square for Log-rank and Wilcoxon test are different. If Log-ranks test rejects assumption but Wilcoxon test accepts the assumption, it indicates that the difference between the levels of factor occurs in later failure events in time ant no difference between the levels of treatment occurs in earlier failure events in time, since the Wilcoxon test gives more weight to early times than to late times and it is less sensitive than log-rank test to the difference occurred at later events in time. If both values are less than 0.05, their individual value chi-square can be employed distinct the deviance degree between earlier survival rate and later survival rate. The likelihood-ratio tests the assumption that the event time has an exponential distribution. If the value of *P*r > chi-square is more the 0.05, the assumption is accepted.

Generally, the results of KM seem to agree with the main effect plot of lifetime, but it gives some information in detail. Figure 52 describes the survival probability for coating under different contact force. It can be seen that curves are most overlapped. In other words, the change of contact force does not bring significant influence on the survival probability of coatings. The survival probability is significantly influenced by the displacement amplitude

(Figure 53). The survival probability of ± 15 µm is significant higher than that of ± 50 µm and ± 75 µm. Its mean that lifetime of ± 15 µm is about 10 times as many as ± 50 µm. It is because that the displacement can affect the third body flow (flow of wear debris). With the increase of displacement amplitude, the third body flow between contact bodies is accelerated. More wear debris can be delaminated at earlier time, leading to the decrease of survival probability. When the running cycle arrives 200 000, all of the coatings running under ± 50 µm and ± 75 µm fail, but coating running under ± 15 µm still has one half probability of normal working. Figure 54 shows the survival probability of coating for different interlayer. With the interlayer, the survival probability is significant higher. After 50 000 cycles, all of coatings without interlayer have failed, but the coating with interlayer still has 40% survival probability. When comparing the lifetime for rough and smooth interlayer, it can be observed that the curves are farthest apart in the early part in time before becoming closer later. It indicates that the roughness of interlayer can lead to the significant difference in early time, but the difference is reduced with the increase of time. This is because the trapped coating in the rough interface shows fatigue after suffering from long time of relative movement. Some coatings begin to be removed from the rough interface. With the increase of cycles, the survival probability for rough and smooth interlayer arrives similar.

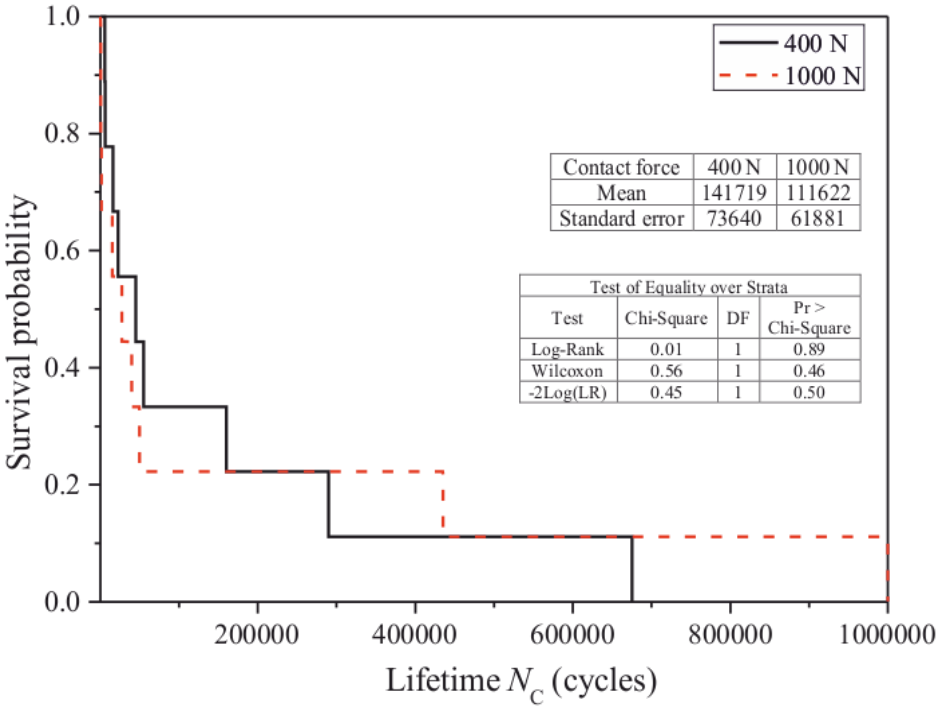

Figure 52: KM test for different contact force.

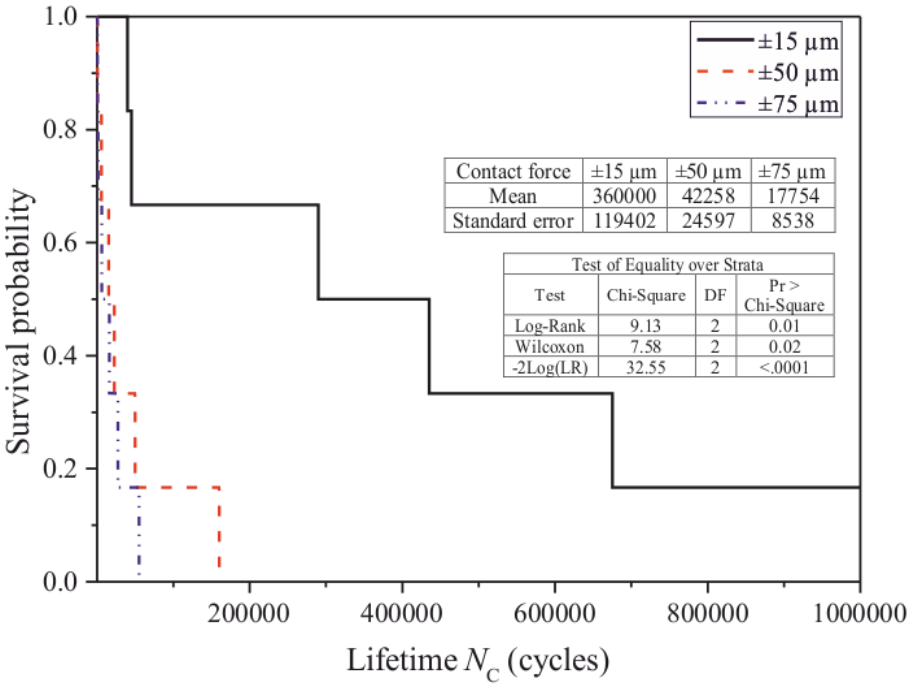

Contact force	±15 µm	±50 µm	±75 µm
Mean	360000	42258	17754
Standard error	119402	24597	8538

Test of Equality over Strata

Test	Chi-Square	DF	Pr > Chi-Square
Log-Rank	9.13	2	0.01
Wilcoxon	7.58	2	0.02
-2Log(LR)	32.55	2	<.0001

Figure 53: KM test for different displacement amplitude.

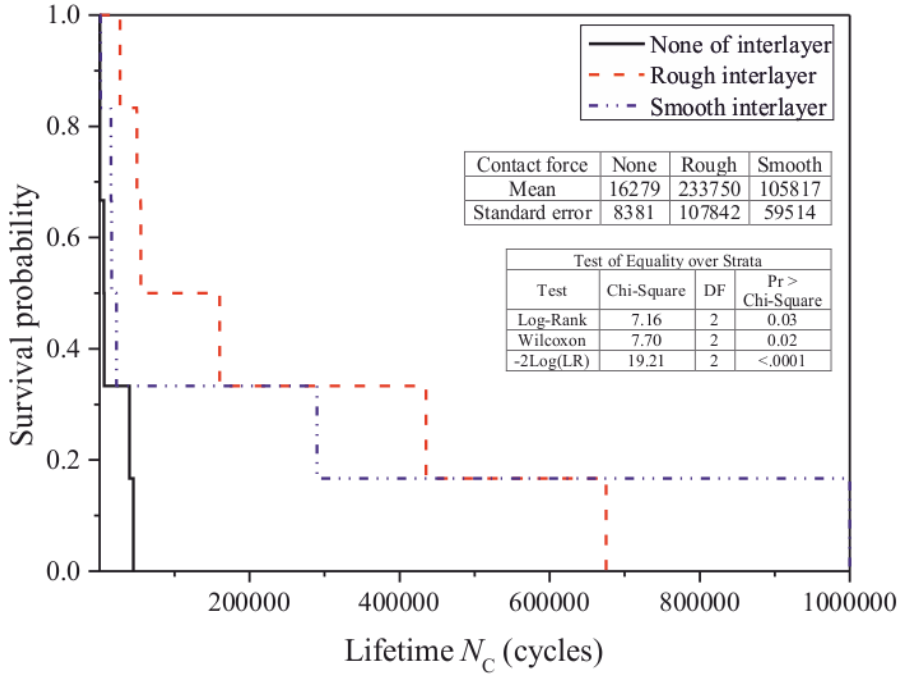

Contact force	None	Rough	Smooth
Mean	16279	233750	105817
Standard error	8381	107842	59514

Test of Equality over Strata

Test	Chi-Square	DF	Pr > Chi-Square
Log-Rank	7.16	2	0.03
Wilcoxon	7.70	2	0.02
-2Log(LR)	19.21	2	<.0001

Figure 54: KM test for different interlayer.

II.6.5 Summary

Statistical method such as analysis of variance can effectively distinct the important factors on friction coefficient and lifetime of coatings. During the competition of various factors, the contact force and interlayer are most important variables on friction coefficient. For the lifetime, the most important factors are displacement amplitude and interlayer. With rough interlayer can significantly improve the durability of coatings, because it can provide the good adhesion force than smooth coating.

II.7 Conclusions

In this chapter, the test parameters are confirmed, including the contact force, displacement amplitude, contact configuration, coating positions, thickness and substrate. It is expected to describe the evolution of wear as a function of various test parameters to explain the potential problems related to the application of coatings.

Some statistical methods such as ANOVA, regression analysis and survival analysis are used to describe the relationship between independent variables (test parameters) and dependent values (friction coefficient and lifetime of coating). According to the analysis of data from Dr. Fridrici, it is proved that these statistical methods can explain well the relationship between different variables. It is interesting to use these statistical methods to describe the wear behavior of coating under different test parameters.

CHAPTER III

DURABILITY OF A VARNISH COATING

CHAPTER III: DURABILITY OF A VARNISH COATING

This chapter investigates the effects of factors like contact force, displacement amplitude, contact configuration and coating positions on friction coefficient and lifetime of the coating. The wear evolution as a function of different parameters is also discussed. Two predictive equations are used to predict the friction coefficient and durability.

III.1 Introduction

Fretting is a complex phenomenon related to interaction between two sliding bodies under a very low displacement amplitude [93], which limits the lifetime of elements significantly. To protect the element from the fretting wear, it is necessary to deposit the coating on the surface. Therefore, it is interesting to carry out research on the fretting wear of coating to improve the coating quality by understanding the wear mechanism of coatings. The tests in different conditions were performed and compared with modeled results from the statistical model. The thickness of coating was one layer and the flat substrate used was 304 stainless steel.

III.2 Tribological behavior

III.2.1 Evolution of friction coefficient

Generally, the evolution of friction coefficient as a function of cycles allows to define three typical conditions (partial slip, mixed slip and gross slip regimes) depending on various test parameters. Partial slip condition is as a result of elastic deformation between contact bodies. It is defined as a quasi-linear shape as a function of friction coefficient and displacement amplitude, as shown in Figure 55. The contact area is divided into two parts including stick area at the contact center and sliding area. To describe the friction behavior of partial slip regime, it is better to use friction force ratio rather than friction coefficient, because the discontinuity of friction force occurs during the partial slip regime. This discontinuity is associated to a maximum value of the tangential force amplitude. In this case, it is not appropriate to apply the friction coefficient to describe the friction behavior. Instead, the ratio of friction force and contact normal force is a good representative of the friction coefficient operating under partial slip regime. Gross slip is characterized by open or quasi – rectangular cycles. Sliding occurs at the entire contact [93]. Mixed slip is complicated, because it is composed by the two regimes (i.e. partial slip and gross slip regimes). It can be divided into two situations: firstly, the gross slip is transformed to partial sip after a period of running. It is characterized by the elliptic shape of F_t/F_n - δ after some cycles of gross slip, because the partial slip at this time is accompanied by plastic deformation in the upper layer of the stick area of contact center. Secondly, it is characterized by the alternative transformation between gross slip and partial slip.

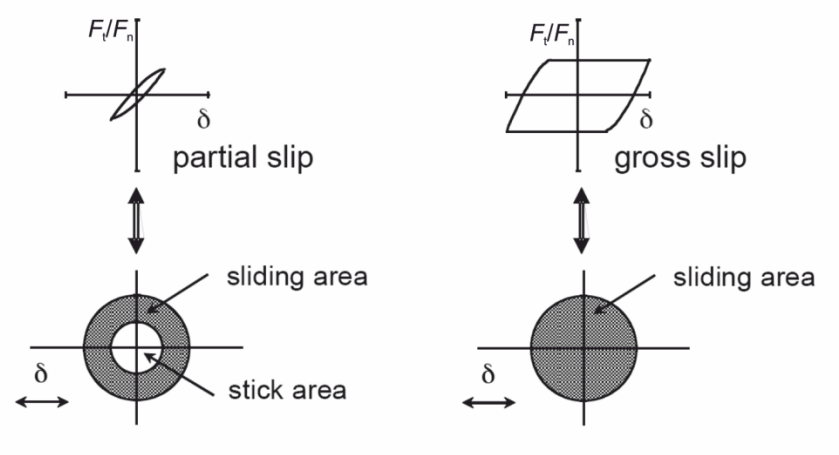

Figure 55: Three types of running regimes [93].

III.2.1.1 Fretting properties of uncoated substrate

In order to determine the friction-reducing capability of MoS_2 based varnish coating, fretting behavior of substrate (304 stainless steel) versus counterbody (AISI52100) has been tested. The evolution of friction coefficient as a function of cycles has been shown in three typical conditions depending on various test parameters.

- **Ball-on-flat**

Three types of running regimes are found out under the contact configuration of ball-on-flat as a function of normal force. When the normal force is large, the fretting is running in the partial slip regime. With the decrease of normal force, the fretting running regime is transformed from partial slip to mixed slip regime and then to gross slip regime.

1) Partial slip regime

For the small amplitude (δ^* = ± 10 µm) and large contact force (F_n = 700 N), the fretting loops are gradually transformed from the quadrangle shape to linear shape within 20 cycles and it keeps to the end of test (Figure 56). It indicates that the fretting is running in the partial slip regime. The initial quadrangle shape is a result of an adsorption film or contamination film on the surface.

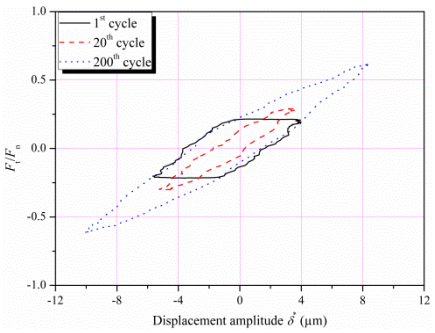

(a) Fretting loops

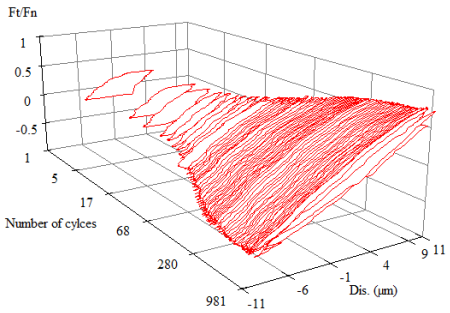

(b) Fretting log

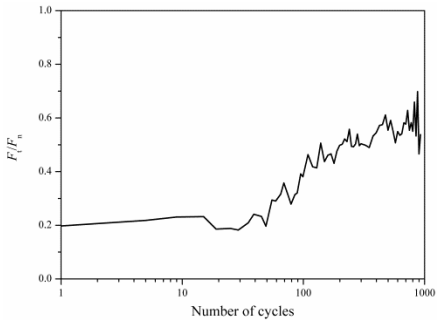

(c) Friction force ratio as a function of cycles

Figure 56 : Fretting loops (a), fretting logs (b) and the evolution of friction force ratio (c) under ± 10 µm, 700 N.

2) Mixed-slip regime

When the contact normal force is reduced to 400 N, the running regime reaches mixed slip regime: fretting loops are transformed from quadrangle to linear, and then to ellipse shape, as shown in Figure 57.

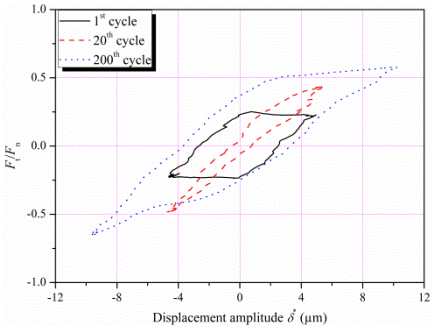

(a) Fretting loops

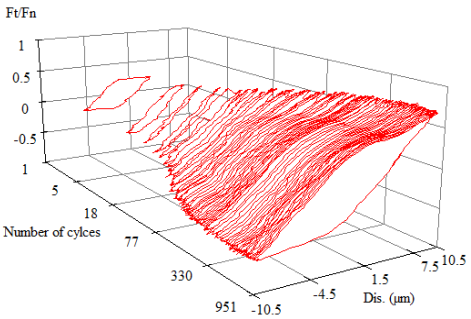

(b) Fretting log

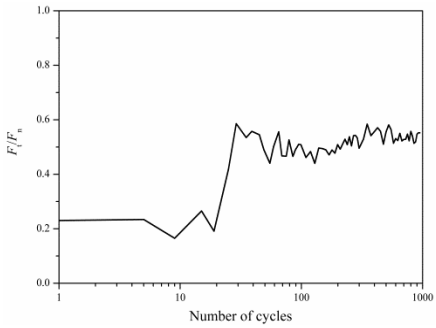

(c) Friction force ratio as a function of cycles

Figure 57: Fretting loops (a), fretting logs (b) and the evolution of friction force ratio (c) under ± 10 µm, 400 N.

3) Gross slip regime

When the normal force is 100 N, fretting loops keep quadrangle shapes during the whole test duration (Figure 58). In the first cycles, the friction force ratio is rather low due to the protection film like contamination film that protects the surface from wear. With the increase of cycles, the two bodies become to contact directly, leading to the increase of friction force ratio. As a function of cycles, some wear particles appear in the contact area, resulting in the increase of friction force ratio. When the ejection rate of wear particles is larger than formation rate, the friction force ratio is decreased. When the formation rate equals to ejection rate, the friction force is decreased to a rather low value and keeps this value to the end of test.

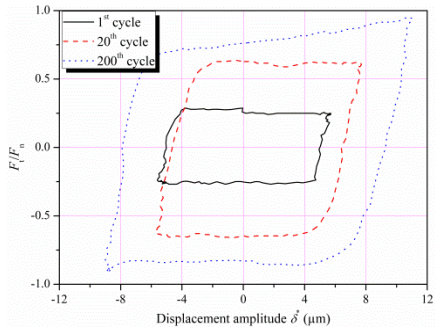

(a) Fretting loops

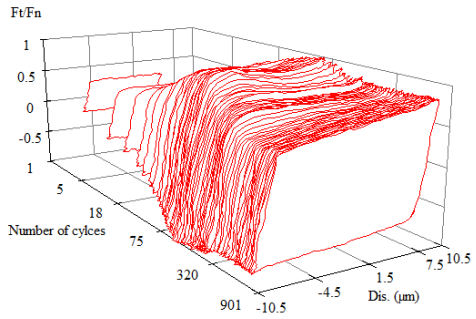

(b) Fretting log

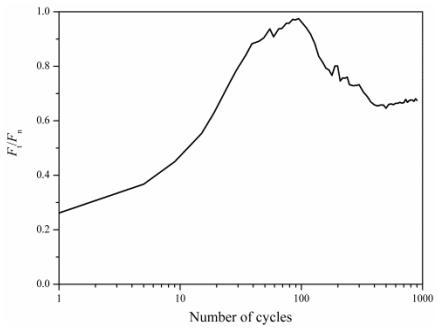

c) Friction force ratio as a function of cycles

Figure 58: Fretting loops and the evolution of friction force ratio under ± 10 µm, 100 N.

- **Cylinder-on-flat**

Different from the situation of ball-on-flat, two running regimes (including mixed-slip and gross slip regimes) are found out under the contact configuration of cylinder-on-flat (Figure 59). Compared with gross slip, the curve of mixed slip is unstable due to the stick-slip effect. In addition, the initial friction coefficient of cylinder-on-flat is higher than that of ball-on-flat.

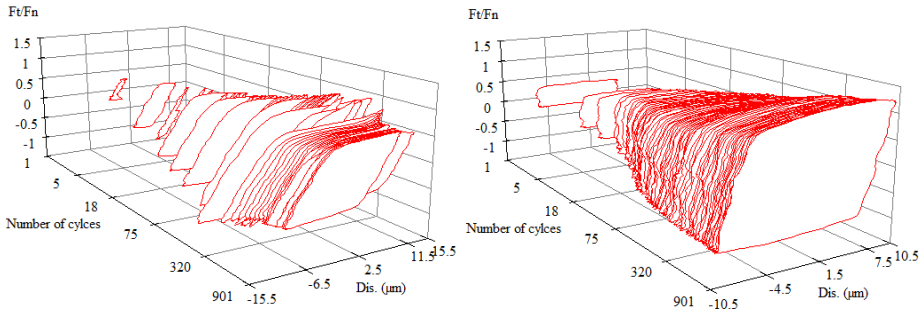

(a) Mixed slip regime, F_n = 700 N (b) Gross slip regime F_n = 100 N

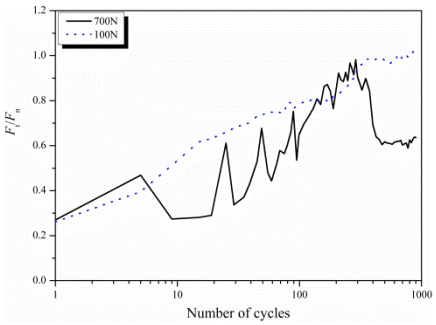

(c) Evolution of friction coefficient

Figure 59: Fretting loops and the evolution of friction force ratio under ± 10 µm.

- **Summary**

Three running regimes are observed for the contact of two substrates. With the decrease of normal force and increase of displacement amplitude, the running regime is changed from partial slip, to mixed slip and then to gross slip. However, only mixed slip and gross slip are observed under the contact configuration of cylinder-on-flat due to the limit of test parameters.

III.2.1.2 Fretting properties of MoS_2 coating

Under the same test parameters, the fretting test of MoS_2 based varnish coating show gross-slip and mixed slip regimes due to the lubricating function of coatings.

- **Ball-on-flat**

Figure 60 describes the evolution of friction force ratio as a function of cycles. The uncoated substrate suffers from the increase of friction force ratio after 10 cycles due to the removal of contamination layer. For the coated substrate, the coating can protect the substrate from high friction force ratio and it can also decrease the friction force ratio from around 0.7 to 0.18, thereby prolonging the lifetime of elements. This decrease of friction force ratio is called lubrication and it can last for about 1000 cycles. After phase I (friction reduction of coating), the coating begins to be removed and the friction process enters into phase II (degradation process of coating). At phase II, friction force increases. When it arrives a stable value (around 0.9), which is near to the value of direct contact of two substrates, it enters the last phase (direct contact of two substrates).

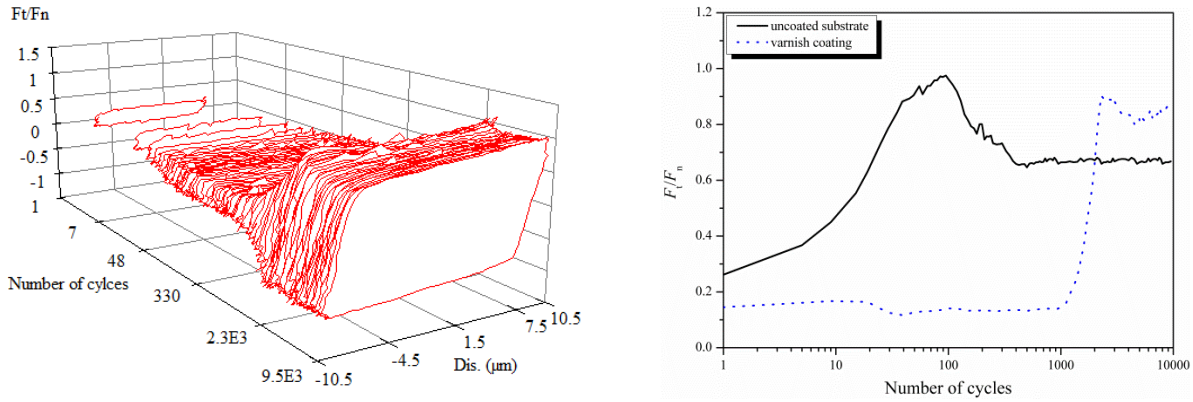

(a) (b)

Figure 60: Fretting loops and evolution of friction force under 100 N, ± 10 µm: (a) fretting log of coating, (b) comparison of friction force ratio between coating and substrate.

- **Cylinder-on-flat**

The value of friction force ratio is 0.12, which is lower than uncoated substrate, indicating that coating effectively reduces friction force between two contact bodies. With the increase of cycles, coating is gradually removed from two contact bodies, resulting in increase of friction force. At the same time, the curve of coating is transformed to the shape of uncoated substrate (Figure 61). At the same time, the fretting enters into the mixed slip regime. The coating loses its function.

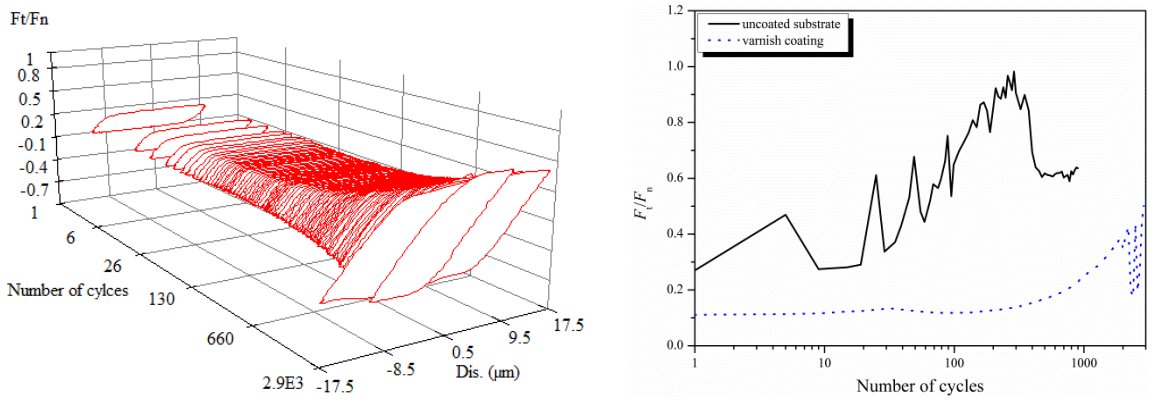

(a) (b)

Figure 61: Fretting loops and evolution of friction coefficient under 700 N, ± 10 µm: (a) fretting log of coating, (b) comparison of friction force ratio between coating and substrate.

- **Summary**

Generally, the friction behavior for coating is divided into three phrases: the friction reduction of coating, the degradation process of coating and direct contact of two substrates. The details of each phase such as the value of friction force ratio and number of cycles in each phase depend on the test parameters.

III.2.2 Coating lifetime and wear phenomena of the coating and substrate

III.2.2.1 Definition of coating lifetime

Coating lifetime refers to failure of the coating. In other words, the coating loses its lubricating function and leads to an increase of friction coefficient. According to Langlade *et al.* [130], lifetime of the coating can be defined as the number of cycles for which the friction coefficient is equal to half sum of μ_a and μ_b (where μ_a is the friction coefficient of the coating and μ_b is the friction coefficient of the substrate, after removal of the coating), as shown in Figure 62.

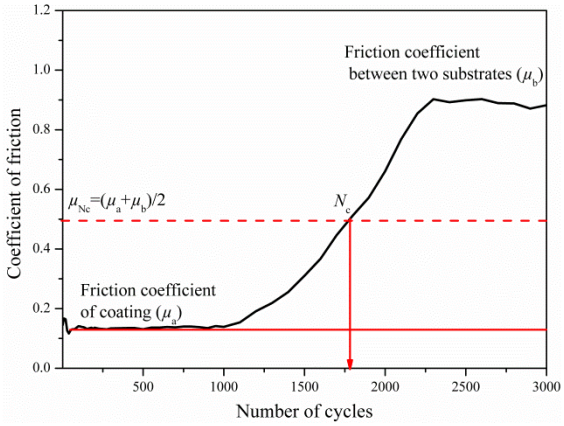

Figure 62 : Evolution of the coefficient of friction vs. the number of cycles (N_c = coating lifetime).

III.2.2.2 Summary of wear phenomena occurring before and after lifetime of the coating

- **Ball-on-flat**

Deposition of coating on the substrate can effectively protect substrate from wear and provide a low friction coefficient for the friction system (Figure 63 (a)). Due to the significant stress discontinuity between the coating and the substrate, it is easy for debonding and fracture to occur at the interface between the coating and the substrate (Figure 64). Some coating is pushed to the outer part of contact area. Other parts of coatings are transferred to the counterbody, as shown in Figure 63 (b) and (c). It is a character of adhesive wear. At this moment, the contact at contact center is between coating and transferred coating. In addition, some island of coating around contact area (Figure 63 (b)) can also be recirculated into the contact center due to the movement of two contact bodies. Thanks to the lubricating properties of coating, the friction coefficient keeps a low value (Figure 63 (a)). As a function of cycles, the coating and transferred coating are gradually ejected from the contact center. Then, no coating is observed at the contact center, as shown in Figure 63 (d) and (e). When the third layer of steel debris occurs, the friction coefficient reaches a stable and high level.

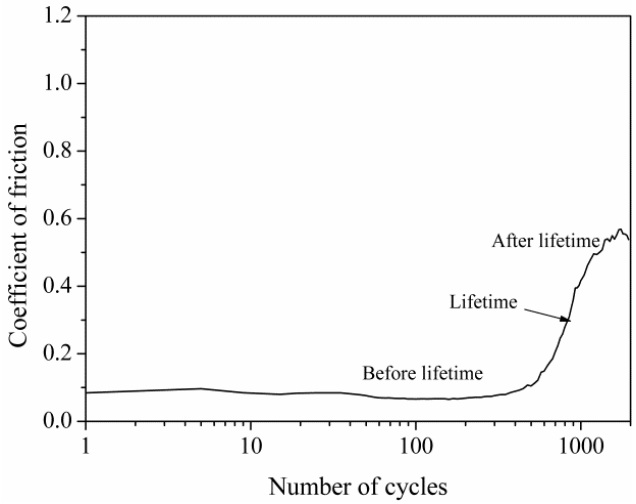

(a) Evolution of friction coefficient

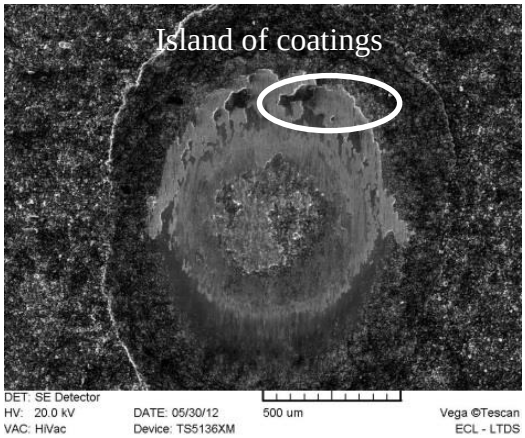

(b) Coated flat before lifetime

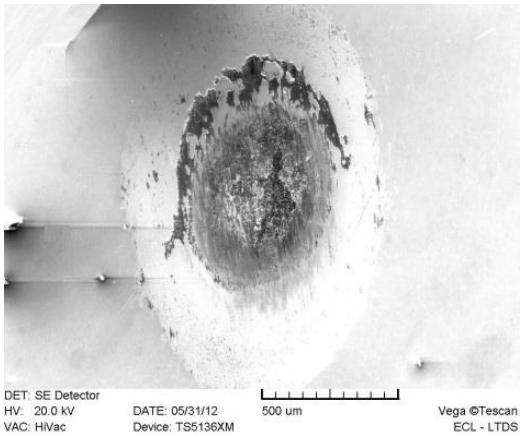

(c) Uncoated ball before lifetime

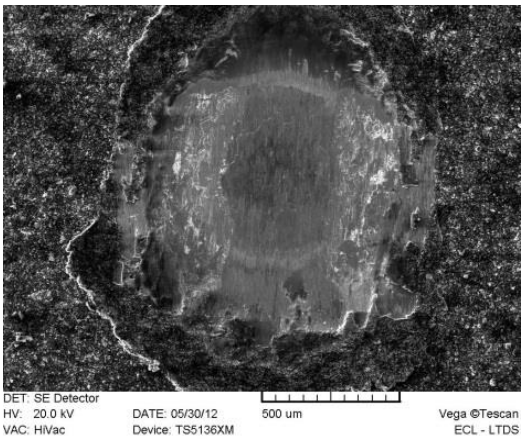

(d) Coated flat after lifetime

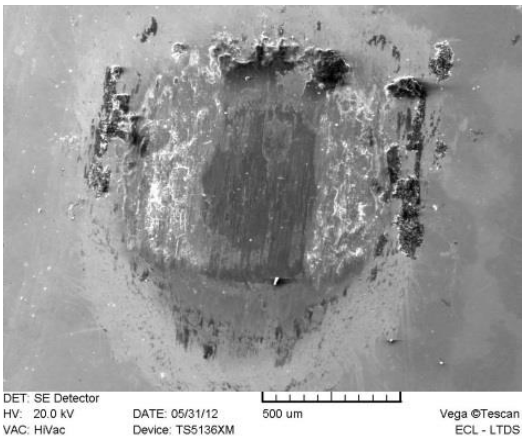

(e) Uncoated ball after lifetime

Figure 63: Evolution of friction coefficient and SEM micrograph of wear scar for ball-on-flat (F_n = 400 N, δ^* = ± 25 µm).

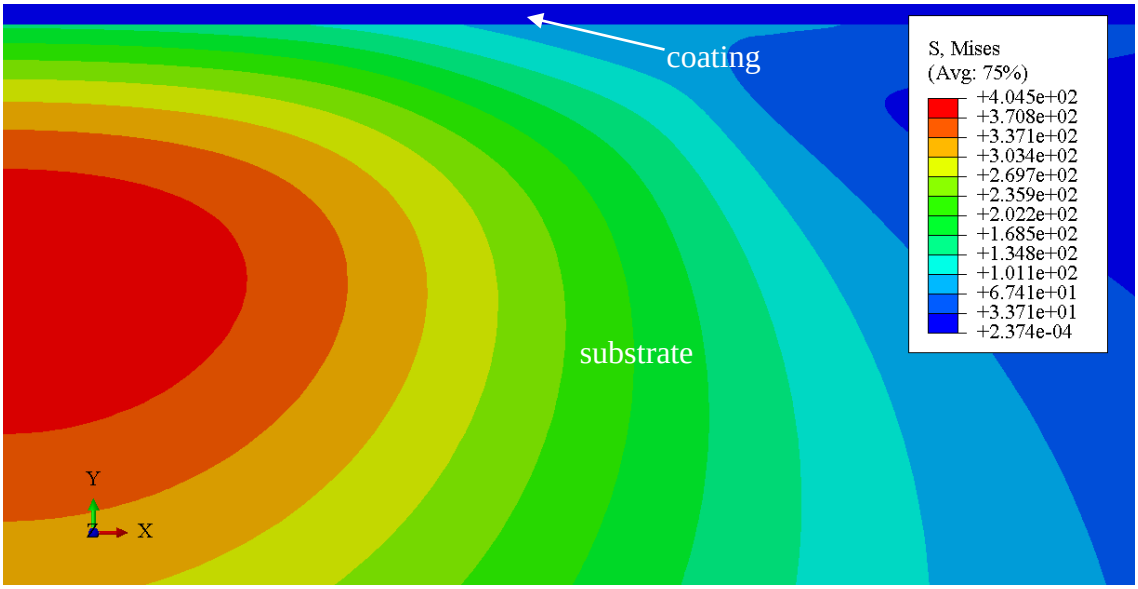

(a)

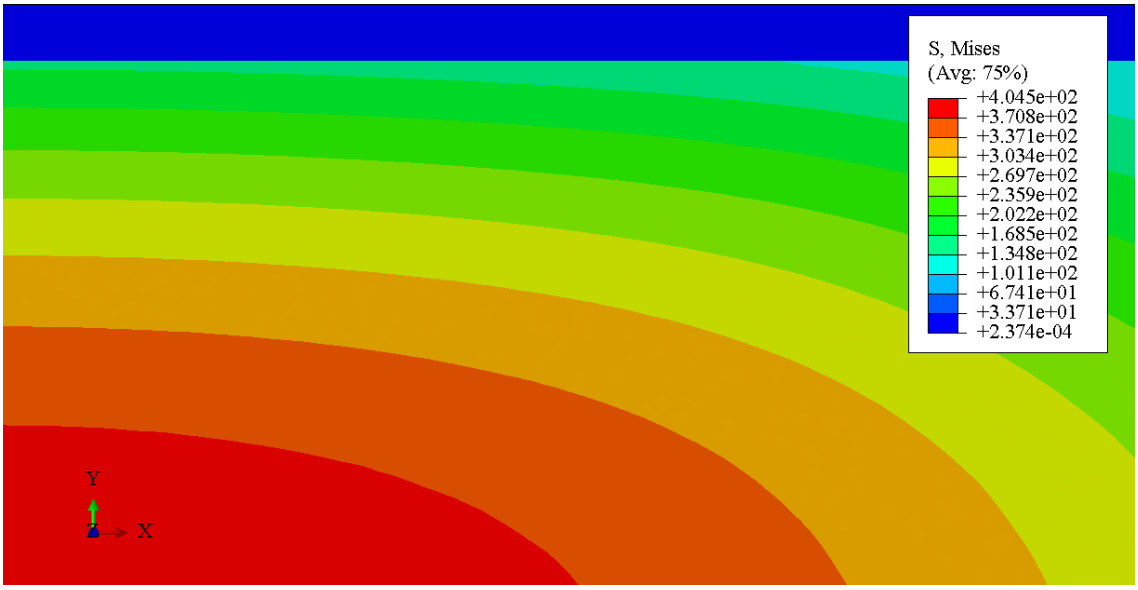

(b)

Figure 64: Stress distribution for coating on the substrate under ball-on-flat (F_n = 100 N) (a) and (b) zoomed part of stress distribution for coating on the substrate under ball-on-flat.

- **Cylinder-on-flat**

Many abrasive grooves are observed on the surface and many fine particles are at the slip end, as shown in Figure 65 (a) and (b). Due to the stress discontinuity between coating and substrate, debonding and fracture of coating can occur (Figure 66). In addition, different hardness of the two contact bodies makes it easier for abrasive wear to occur, and asperities of hard body push the soft material out. Some strips debris of coatings are observed in both counterbodies before the failure of coating. With the movement of two contact bodies, these strip debris may recirculate into contact center, thereby maintaining the friction coefficient at a stable value. In addition, some abrasive particles are observed around the contact area. As a function of cycles,

some wear begins to appear on two substrates (Figure 65 (c) and (d)), the coating loses its function of providing a low friction coefficient.

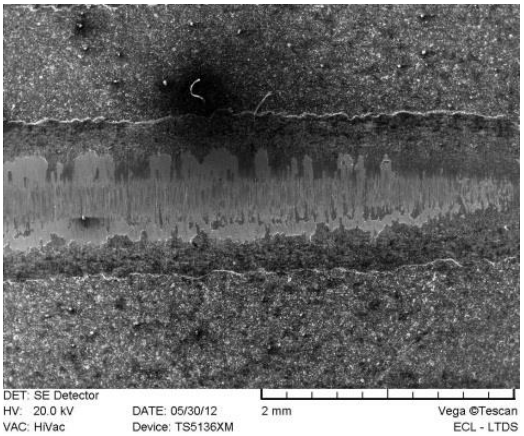

(a) Coated flat before lifetime

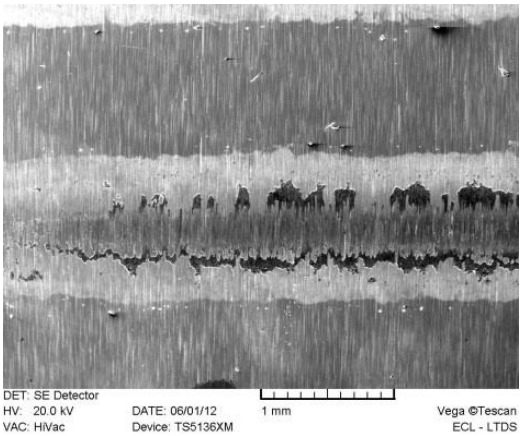

(b) Uncoated cylinder before lifetime

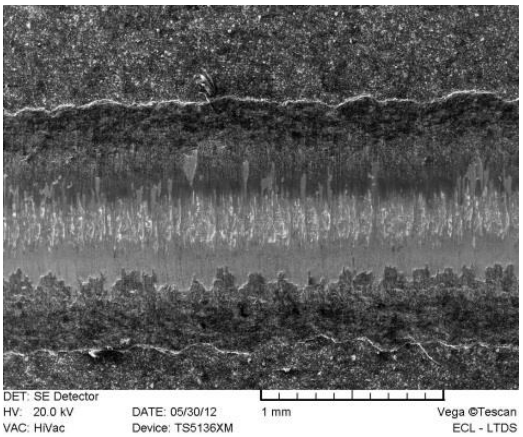

(c) Coated flat after lifetime

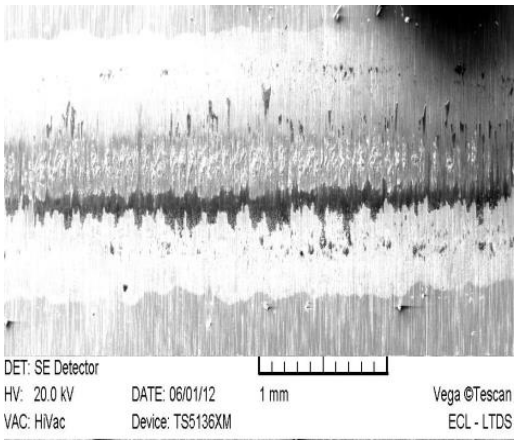

(d) Uncoated cylinder after lifetime

Figure 65: SEM micrograph of wear scar for cylinder-on-flat (F_n = 400 N, δ^* = ± 25 µm).

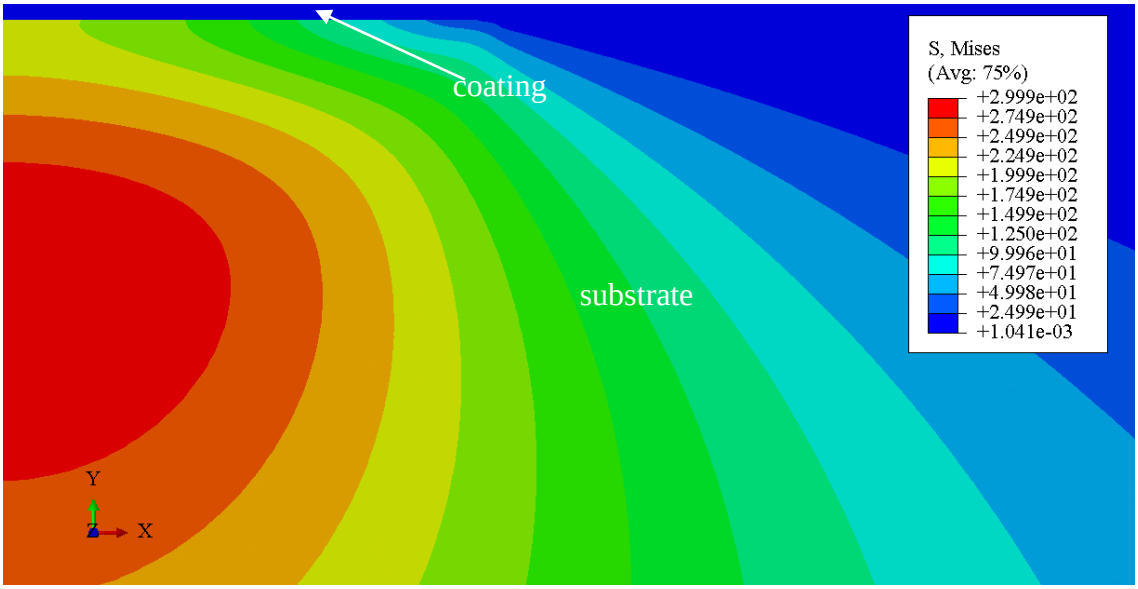

(a)

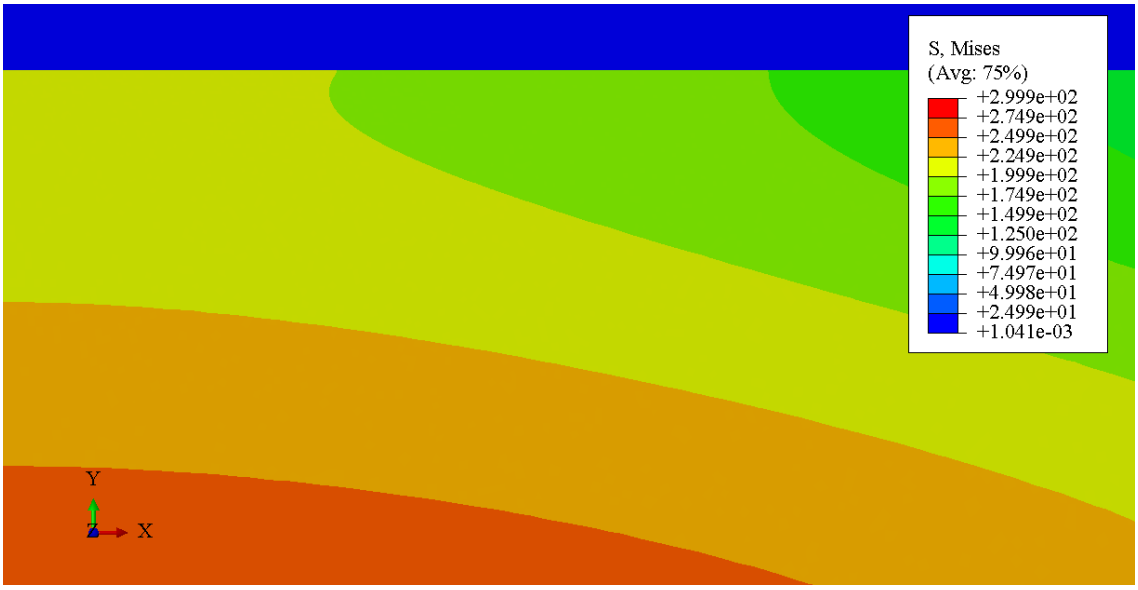

(b)

Figure 66: Stress distribution for coating on the substrate under cylinder-on-flat (F_n = 100 N) (a) and (b) zoomed stress distribution for coating on the substrate under cylinder-on-flat.

- **Summary**

In this study, the contact configuration is related to different wear mechanism. For ball-on-flat, it is dominated by the adhesive wear, accompanied by the recirculation of coating debris. The fretting process of cylinder-on-flat configuration is dominated by the abrasive wear, accompanied by the recirculation of coating debris. The failure of coating can be divided into two phase: firstly, the third-body flow and debris circuit of coating provide a good protection for the substrate. Secondly, as a function of cycles, the coating is removed and direct contact between two substrates and finally the coating fails.

III.3 Effect of test parameters on friction coefficient

Friction coefficient can be influenced by many factors such as contact force, contact configuration, displacement amplitude and coating position. Therefore, there is a need for a statistical method to describe the competition of these factors in order to determine which one is more important for increase or decrease of friction coefficient. Each test condition is repeated at least three times. Analysis of variance is a statistical method used to compare the effect of each factor on the response value.

Prior to analysis of variance, two assumptions should be complemented. One is the normal distribution of data for each treatment (the combination of one group of test parameters) and the other is the homogeneity of variance across the treatment. Due to the fact that only two tests have been performed for each condition, these two assumptions can be complemented automatically. Some scholars suggested doing other assumptions prior to analysis of variance: 1) a run sequence plot of the residuals; 2) a normal probability plot of the residuals; 3) a scatter plot of the predicted values against the residuals [128].

Due to the fact that the experiments are done by the random sequence, it is not necessary to test the relationship between sequence of experiments and residuals. Figure 67 describes the distribution of residuals. It follows line distribution in the normal probability plot except for one point. This test parameter for this point is 100 N, ± 40 µm and coating on cylinder, leading to a rather large value of friction coefficient (>0.4). The coating loses its function at very beginning. Actually, one distinct point will not change the dispersion of residual value so that the dispersion of residuals is normal. The residuals are distributed around the centerline as a function of predicted value. Therefore, the value of friction coefficient can be used directly in the study.

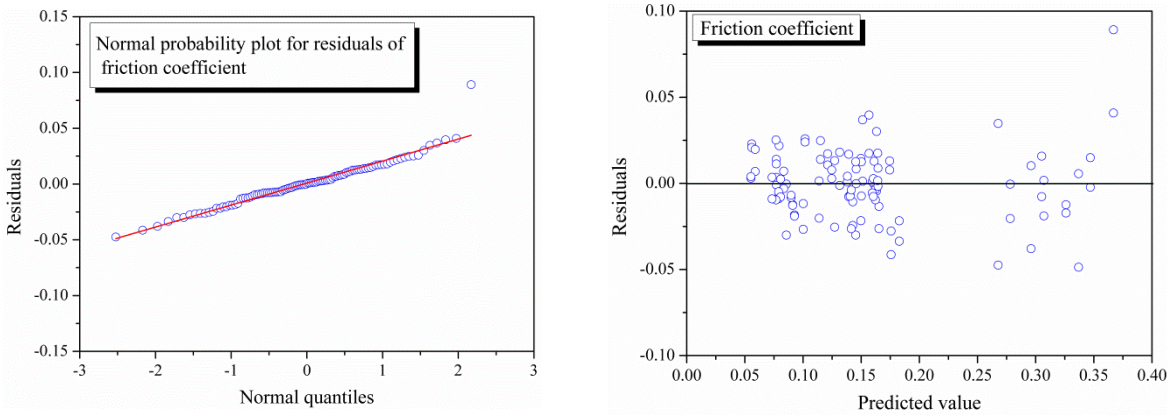

(a) (b)

Figure 67: The diagnostics for residuals of untransformed and transformed friction coefficient: (a) normal probability plot for residuals of friction coefficient and (b) the residuals of friction coefficient vs. predicted value.

In order to determine the effects of the test parameters (contact configuration, displacement amplitude, coating position and contact force) on friction coefficient, we will use Figure 68 to give a description for the evolution of friction coefficient of the coating *vs.* different test parameters: for instance, 3 curves of the graph of the second row and first column of Figure 68

are curves of evolution of friction coefficient of the coating *vs.* contact force (from 100 N to 700 N) for 3 different displacement amplitudes applied (± 10 µm (solid line), ± 25 µm (dash line) and ± 40 µm (dash dot line)); and 3 curves of the graph of the first row and second column of Figure 68 are those of evolution of friction coefficient *vs.* displacement amplitude (from ± 10 µm to ± 40 µm) for 3 different normal forces (100 N (solid line), 400 N (dash line) and 700 N (dash dot line)).

Table 19 gives a corresponding quantitative description. The number of degrees of freedom is the number of values that are free to vary. Sum of square describes the variance of average value of each level for a factor and the average value for one factor. *F* value is used for comparing the factors of the total deviation. If the value of *F* is less or equal 1, it means that the factor has no effect on the friction coefficient of coating. If the *F* value is larger than $F_{critical}$, it indicates that the factor has a significant effect on the friction coefficient of coating. *P*r *>F* describes the probability of a value of *F* is greater than or equal to the critical value. Generally, the significance level (α) is 0.05. If value of (*P*r *>F)* < 0.05, it indicates the factor has a significant effect on the evolution of friction coefficient. The last column PC (%), values for each factor in the table of analysis of variance. PC (%) is the relative contribution of sum of squares minus the variance due to error for each factor or error to total variance [131].

From Figure 68 and Table 19, it can be seen that the contact force and contact configuration are the most significant variables, totally contributing to 82% for the change of friction coefficient. The friction coefficient of cylinder-on-flat configuration is significantly higher than that of the ball-on-flat configuration (line 3 or column 3 of Figure 68). Higher contact force has lower friction coefficient (line 1 or column 1 of Figure 68). In addition, there is a significant interaction between contact force and contact configuration, accounting for 7.02% of the variation of friction coefficient. It can be explained by the fact that the difference of friction coefficient between cylinder-on-flat and ball-on-flat configurations is decreased when the contact force is increased (line 3 and column 1 of Figure 68). Besides, some contributions such as interaction between contact force and coating disposition and interaction between displacement amplitude and coating position are less than 0. It indicates that they have no effect on the variation of friction coefficient. The error contribution is a little large with the value of 7.63%. The error contribution is not only the pure error (due to the deviance of experiments in the same conditions) but it includes also the contribution of interaction of between three or four variables. To improve the efficiency of analysis, the variance of interaction of three or four variables is contained in the error contribution. In this study, we focus on the most important variables so that the error contribution is not important. Several negative contributions of variables have been observed because it is not significant compared with the other variables.

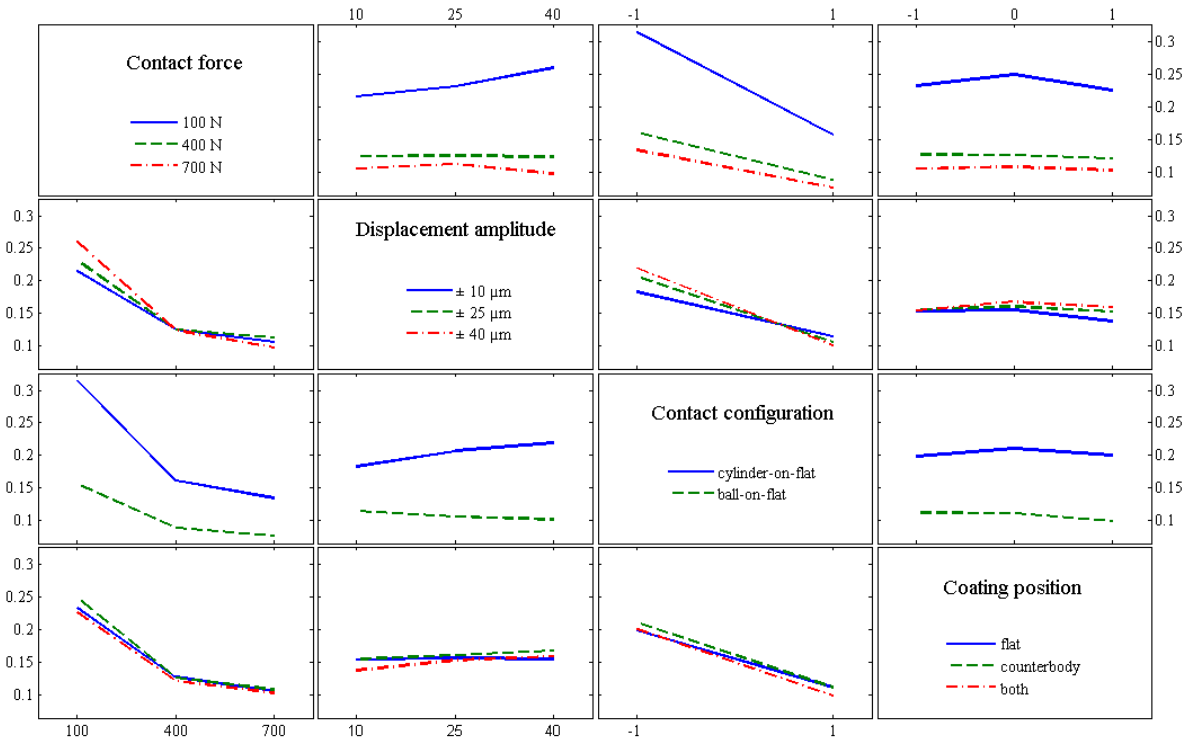

Figure 68: Interaction map of friction coefficient of the coating.

Table 19: Analysis of variance (ANOVA) for friction coefficient.

Source	DF	Sum Square	Mean Square	*F* Value	*F* critical	Pr > *F*	PC
Contact force	2	3.59E-01	1.79E-01	341.49	3.11	<0.0001	48.58%
Displacement amplitude	2	2.57E-03	1.28E-03	2.44	3.11	0.09	0.21%
Contact force × Displacement amplitude	4	1.10E-02	2.75E-03	5.24	2.48	0.0008	1.21%
Contact configuration	1	2.50E-01	2.50E-01	475.85	3.96	<0.0001	33.88%
Contact force × Contact configuration	2	5.27E-02	2.64E-02	50.19	3.11	<0.0001	7.02%
Displacement amplitude × Contact configuration	2	1.17E-02	5.86E-03	11.16	3.11	<0.0001	1.45%
Coating position	2	2.25E-03	1.13E-03	2.14	3.11	0.12	0.16%
Contact force × coating position	4	1.66E-03	4.15E-04	0.79	2.48	0.53	-0.06%
Displacement amplitude × coating position	4	1.38E-03	3.45E-04	0.66	2.48	0.62	-0.10%
Configuration × coating position	2	1.16E-03	5.80E-04	1.10	3.11	0.33	0.01%
Error	82	4.31E-02	5.25E-04				7.63%
Total	107	7.36E-01					100%

III.3.1 Contact configuration and contact force

Contact force and contact configuration are the most important factors on friction coefficient (Table 19). For contact force, it accounts for 48.58% of change of friction coefficient, followed by the contribution of contact configuration whose value is 33.88%. This is in an agreement with theory of Singer [100] (Eq. I-7, Page 35). The evolution of friction coefficient is inversely proportional to the contact pressure. According to the Hertzian contact theory, the contact pressure is proportional to $F_n^{-1/3}$ for ball-on-flat and it is proportional to $F_n^{-1/2}$ for cylinder-on-flat. Therefore, a fitting curve can be drawn in Figure 69 to describe the evolution of friction coefficient as a function of contact force. With the increase of contact force, the friction

coefficient is decreased. The friction coefficient of contact configuration cylinder-on-flat is higher than that of ball-on-flat. The coefficient (S_0) in the case of cylinder-on-flat is always higher than that of ball-on-flat. According to the analysis in III.2.2.2, it can be explained as a parameters (S_0) controlled by the ploughing effect, because the fretting movement of cylinder-on-flat is dominated by the abrasive wear and the ball-on-flat is dominated by the adhesive wear.

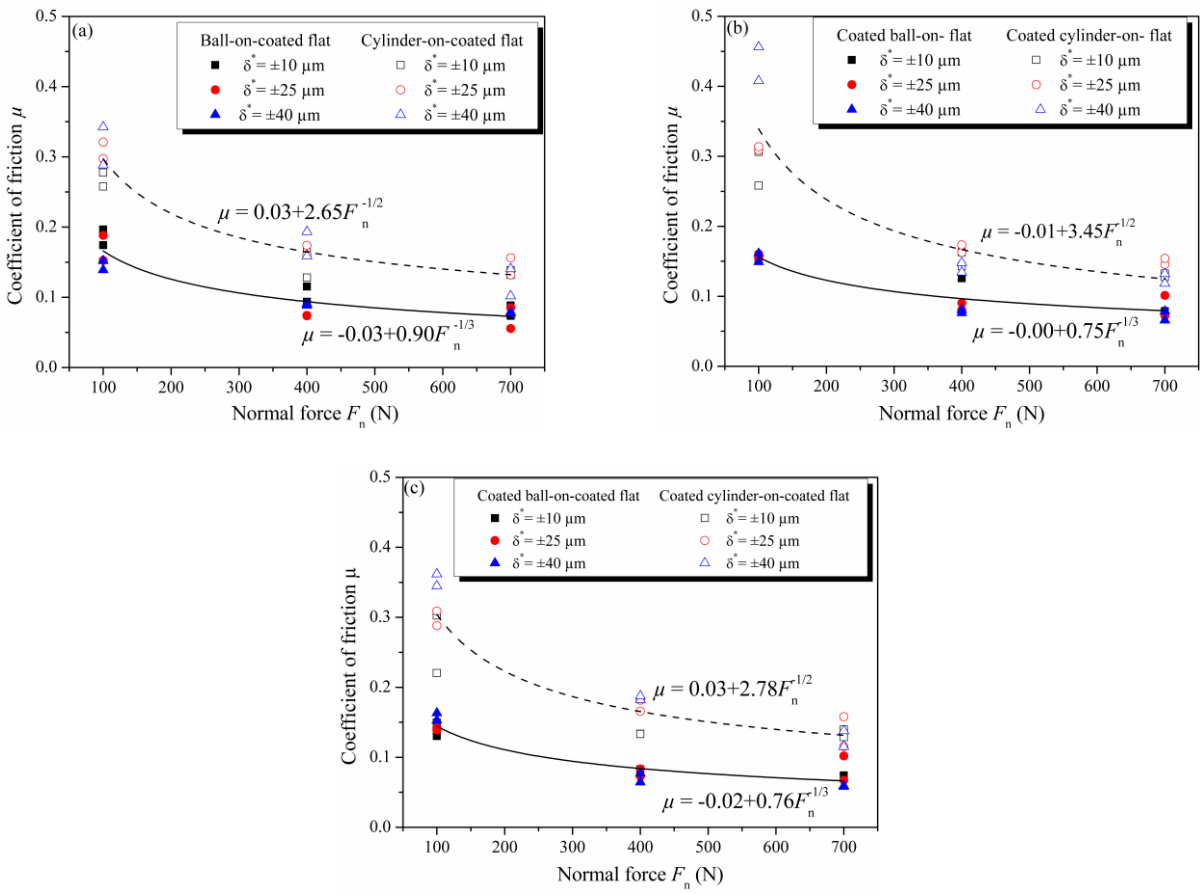

Figure 69: Evolution of friction coefficient as a function of normal force: (a) coating on flat, (b) coating on counterbody (ball or cylinder) and (c) coating on both counterbodies.

For the competition between contact force and contact configuration, the *F* and *PC* values give different conclusions. In the terms of *F* value, the contact configuration is more important than the contact force, while the conclusion is in contrast for *PC* value. This is due to the different degrees of freedom. Contact force has 2 *DF*s, but contact configuration has only 1*DF* so that it leads to different conclusions according to two comparing methods. For *F* value, it is calculated according to mean square. If degree of freedom is large, it may have a low *F* value. For *PC*, it is calculated according to sum of square and it is independent of *DF* so that it is possible to have different conclusions with *F* value for the ranks of importance of factor. When contact force is increased from 100 N to 400 N (Figure 68), the decrease of friction coefficient is more significant (about 0.18) than contact configuration (0.15). When the contact force increases from 400 N to 700 N, the decrease of friction coefficient is less than contact configuration.

III.3.2 Displacement amplitude

Displacement amplitude seems to have no effect on the friction coefficient, because friction coefficient barely shares the same evolution versus displacement amplitude, for the other test

parameters. However, the interaction between displacement amplitude and contact configuration is quite significant. In other words, friction coefficient with ± 10 µm is higher than that with ± 40 µm under ball-on-flat configuration, but it is the opposite under cylinder-on-flat configuration. It may be due to the difference of the ratio between displacement amplitude and radius of contact between the two configurations. Nevertheless, this effect is quite small compared to that of other parameters.

III.3.3 Coating position

Coating position has no effect on the friction coefficient. Under the cylinder-on-flat configuration, coating position is independent of friction coefficient. Under ball-on-flat, coating on both counterbodies will decrease the friction coefficient a little. It is because real friction pair for three different coating positions is indeed similar (friction between coating and transfer film). The coating transfer film adheres to the uncoated counterbody, thereby achieving similar friction coefficient as the coated-coated contact.

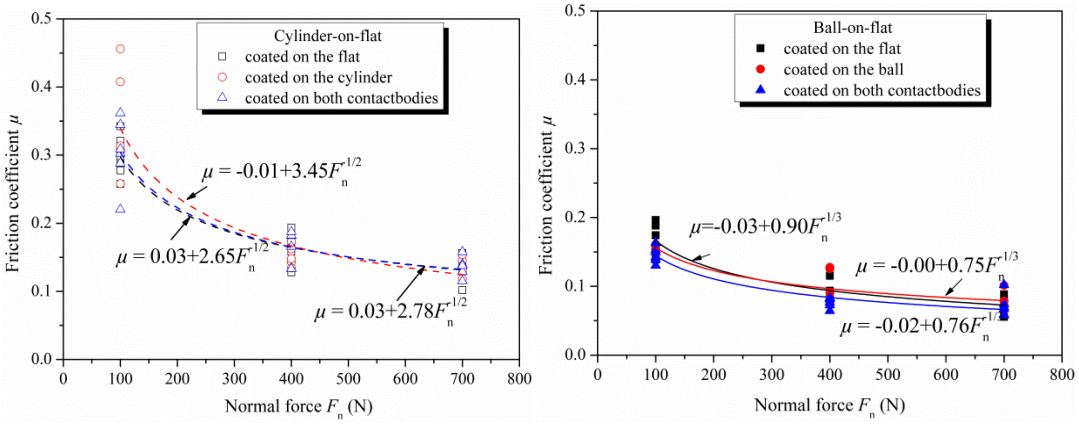

Figure 70: Evolution of friction coefficient as a function of normal force under different contact configurations.

III.3.4 Summary and prediction of friction coefficient of the coating

One of purpose of this research is to predict the friction coefficient for various test conditions. Regression analysis is applied to reach this purpose. The value of each variable is coded value, because coding can reduce range of each factor to a common scale regardless of its relative magnitude and scaling establishes factor levels that can be orthogonal (or nearly). Generally, the coded value for numeric value can be calculated according to Eq. (III-1). In this study, the evolution of friction coefficient as a function of normal force is not linear so that it should consider the quadratic part for coded value. The array of linear part and quadratic should be orthogonal (Table 20). The calculation of linear part is completed according to Eq.(III-1).

$$coded\ value = \frac{x_i - \frac{x_n + x_1}{2}}{\frac{x_n - x_1}{2}} \quad i = 1, 2, \cdots n \qquad (III\text{-}1)$$

Table 20: Coded value for contact force and displacement amplitude.

	Real value	Coded value	
		linear part	quadratic part
Contact force	100 N	-1	1
	400 N	0	-2
	700 N	1	1
	Real value	Coded value	
		linear part	quadratic part
Displacement amplitude	± 10 µm	-1	1
	± 25 µm	0	-2
	± 40 µm	1	1

To get the value of contact configuration and coatings position, dummy values can be used because they are categorical values. Dummy coding uses only one and zero to convey all of the necessary information on group membership, as shown in Table 21.

Table 21: Dummy values of coating position.

Coating position	C_1	C_2
Coating on the flat	0	0
Coating on the ball or cylinder	1	0
Coating on both counterbodies	0	1

In addition, the ball-on-flat configuration is coded as $CON = 1$ and cylinder-on-flat configuration is $CON = 0$. Finally, to compare the coefficient associated with each variable, the coded value should be normalized. Then, the normalization can be calculated according to the coded value is divided by the square root of summer of square of coded value for each factor. Finally, standardization is done to complete the regression analysis (Table 34 of the Annex).

According to ANOVA, correlation between the factors (normal force, displacement amplitude, contact configuration and coating position) and measured friction coefficient of the coating are expressed in Eq.(III-2). To describe fitting quality of a model equation, R^2 is preferred in most cases. An R^2 of 1.0 indicates that regression line perfectly fits the data. However, *Adjusted* R^2 is preferred when considering the effect of each explanatory term on the model, because *Adjusted* R^2 is a modification of R^2 that adjusts for number of explanatory variables in the model. Unlike R^2, *Adjusted* R^2 increases only if added explanatory term improves the model more than that can be expected by chance. Here, *Adjusted* R^2=0.92 is highest one among all kinds of combination of explanatory variables. It indicates that the best combination of explanatory variables have been found to get the best fit of model.

$$\mu = 0.20 - 0.13F_n + 0.04F_n^2 - 0.09CON + 0.07F_n \times CON + 0.02\delta^* - 0.04\delta^* \times CON - 0.01CON \times C_2 \quad \textit{(III-2)}$$

Adjusted $R^2 = 0.90$

Concerning Eq.(III-2), it is found that the configuration and contact force have higher coefficients, leading to the same conclusions as ANOVA. For coating position, only C_2 is added in this equation without C_1, indicating that the coating on flat or coating on counterbody (ball or cylinder) does not change the friction coefficient, but coating on both counterbodies under

the ball-on-flat configuration will slightly change the friction coefficient, reaching an agreement with Part 2.3.

Figure 71 shows comparison between the modeled and experimental average results for repeated experiments. Results show that the regression (Eq.(III-2)) is in agreement with experimental results with the average deviance of 0.78%. However, the maximum deviance is very large (34%) due to point 16 (F_n = 100 N, δ^* = ± 40 µm, cylinder-on-flat, coating on the cylinder). This may be related to the high value of friction coefficient for this combination of conditions.

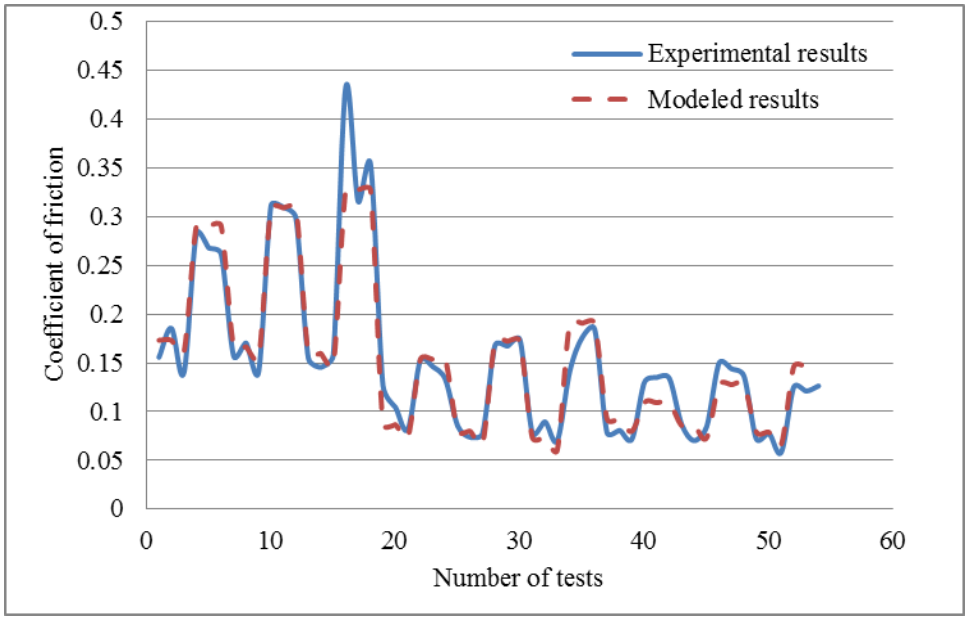

Figure 71: Comparison between experiment and model for friction coefficient of the coating.

According to the analysis of variance and regression analysis, it can be seen that contact force and contact configuration are the most important variables for friction coefficient. Coating on ball, cylinder or flat substrate do not change friction coefficient significantly.

III.4 Analysis of durability of coating

One of the purposes of this study is to study the influence of coating position on the coating lifetime. In this part, the comparison of coating position and other test parameters is made by the analysis of variance.

III.4.1 Statistical analysis of durability

Like the analysis of friction coefficient, the analysis of variance should be complemented with 1) a run sequence plot of the residuals; 2) a normal probability plot of the residuals; 3) a scatter plot of the predicted values against the residuals [128]. Figure 72 describes the distribution of residuals between untransformed and transformed data of lifetime. The equation of transformation is shown in Eq. (III-3) according to the Box-cox transformation.

$$Trans(Nc) = \ln(Nc) \qquad (III\text{-}3)$$

Prior to transformation, the residuals are almost distributed normally, because most residuals are distributed around the reference line except from some points (Figure 72), but several points do not change the dispersion of residuals. However, with increase of coating lifetime, the residuals are also increased. Therefore, it is necessary to do the transformation to lifetime to reach the assumptions. After transformation, the residuals of lifetime can be distributed around the centerline instead of linear relationship between predicted value and transformed lifetime.

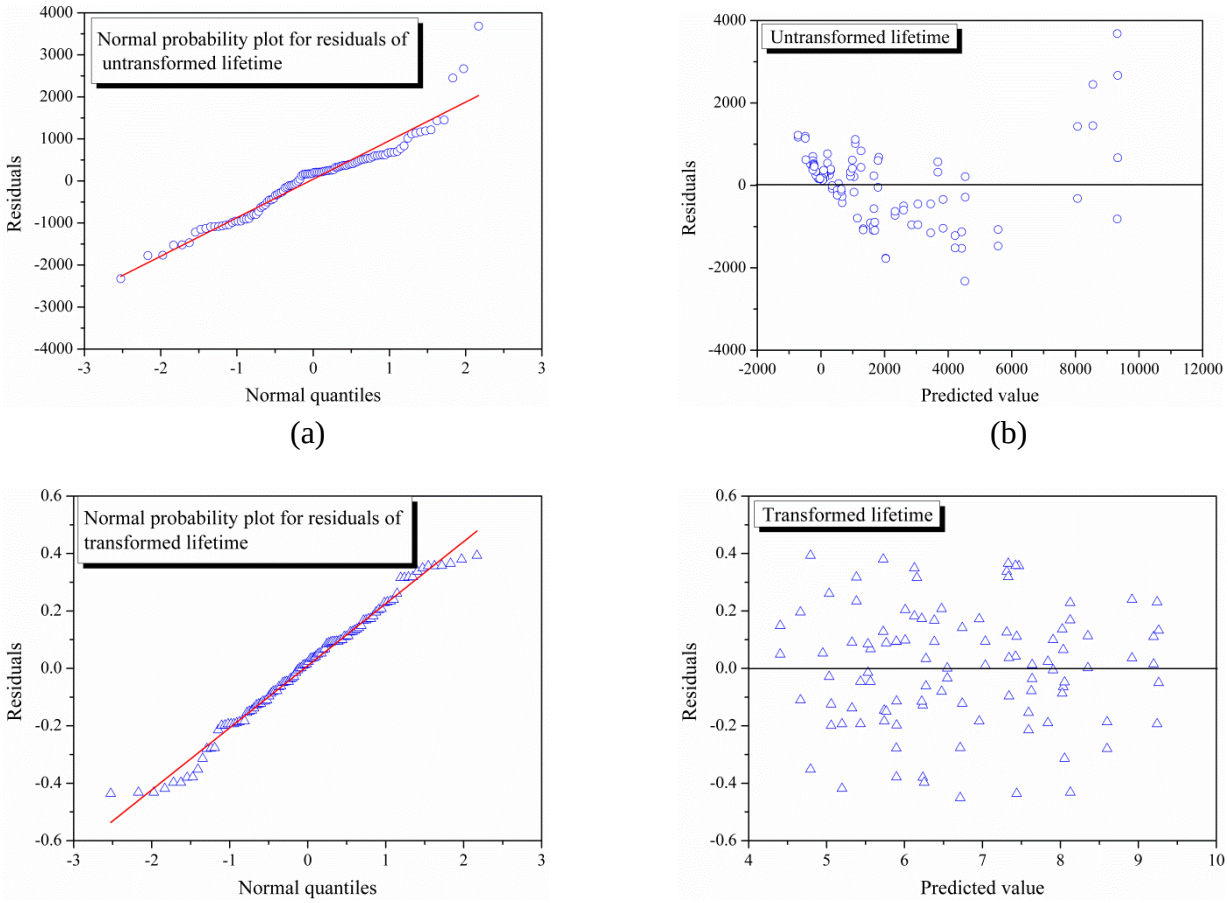

Figure 72: The diagnostics for residuals of untransformed and transformed durability: (a) the normal probabilities plot for residuals of real lifetime; (b) the residuals vs. predicted value of real lifetime; (c) the normal probabilities plot for residuals of transformed lifetime; (d) the residuals vs. predicted value of transformed lifetime.

In order to determine the effects of the test parameters (contact configuration, displacement amplitude, coating position and contact force) on coating lifetime, we will useFigure 73 to give a description for the evolution of coating lifetime *vs.* different test parameters: for instance, 3 curves of the graph of the second row and first column of Figure 73 are curves of evolutions of coating lifetime *vs.* normal force (from 100 N to 700 N) for 3 different displacement amplitudes applied (± 10 µm, ± 25 µm and ± 40 µm); and 3 curves of the graph of the first row and second column of Figure 73 are those of evolution of coating lifetime *vs.* displacement amplitude (from ± 10 µm to ± 40 µm) for 3 different normal forces (100 N, 400 N and 700 N). The lifetime in theFigure 73 is not real lifetime but the transformed lifetime to reach the assumption of ANOVA. Table 22 gives a corresponding quantitative description. Generally, with the increase of contact force, the lifetime is increased (line 1 and column 1 of Figure 73). However, this

variation of contact force only accounts for 0.47% of total variation of lifetime. In other words, the change of contact force can induce some change of lifetime of coating, but it is not so significant. In addition, when the coating is working under 100 N and cylinder-on-flat, its lifetime is longer than that of 400 N and 700 N. This is as a result of higher friction coefficient of coating for 100 N (> 0.3) than that of 400 N and 700 N (< 0.15). According to the calculation of lifetime, the lifetime is corresponding to the half sum of friction coefficient of coating and friction coefficient of two contacts. If the friction coefficient of coating is high, the value of half sum between friction coefficient of coating and friction coefficient between two substrates will be large so that lifetime will be longer. Actually, the lifetime of coating under 100 N is low. With the increase of displacement amplitude, the decrease of lifetime is very significant, which accounts for 11% of total variation of coating lifetime. In addition, the decrease of lifetime from ± 10 µm to ± 25 µm is more significant than the decrease from ± 25 µm and ± 40 µm. Contact configuration is the most important variable for the variation of lifetime, accounting for 71%. This is why the lifetime of cylinder-on-flat is lower than that of ball-on-flat. In addition, the change of coating position has also some effect on the coating lifetime, which accounts for 6%. Coatings on both bodies and counter body have longer durability than coating on flat (line 4 and column 4 of Figure 73).

In addition to the significant contribution of variables, it is also observed that interaction between the variables is significant. For example, interaction between contact force and contact configuration accounts for 4.74% of change of the durability. When the contact force is 100 N, the durability of cylinder-on-flat is larger than 400 N and 700 N, while the value of 100 N for ball-on-flat is always lower than 400 N and 700 N. In the analysis of lifetime, the error contributions including the pure error, interaction between three variables or four variables are lower (about 3.56%).

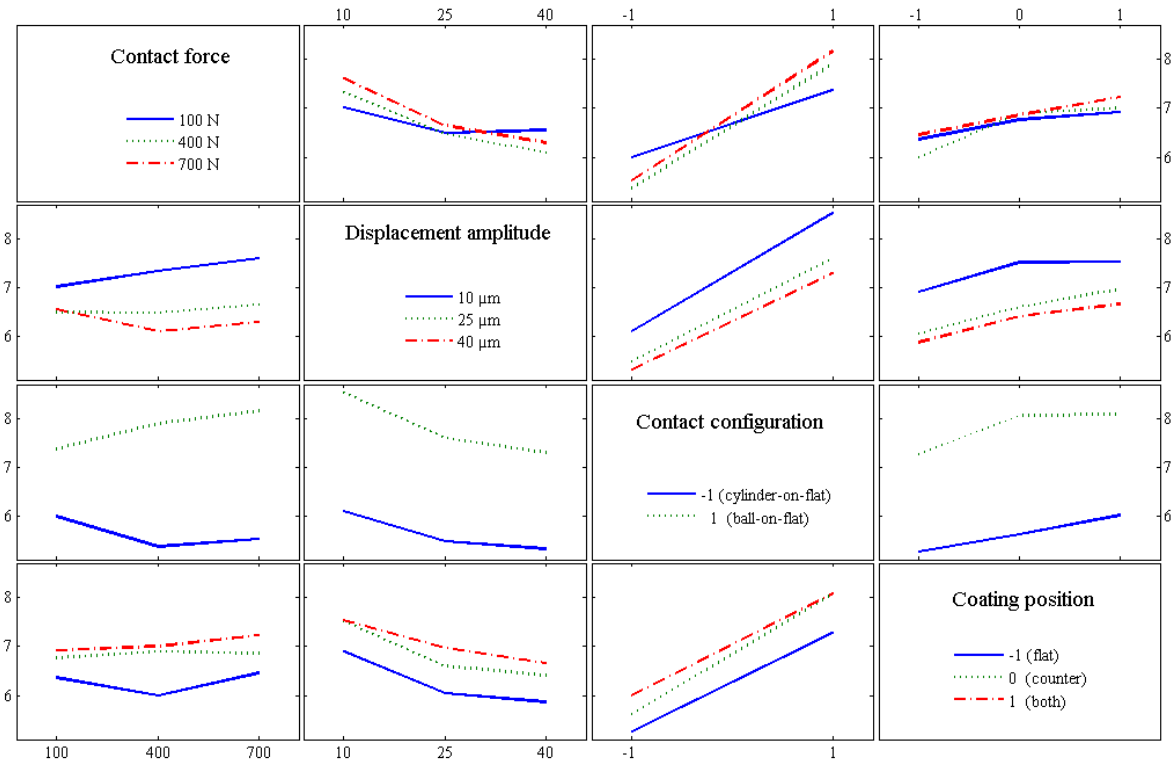

Figure 73: Interaction map of transformed lifetime (ln(Nc)) of the coating (a transformed value of 6 means a coating lifetime of 403 cycles; a transformed value of 8 means a coating lifetime of 2980 cycles).

Table 22: Analysis of variance (ANOVA) for transformed lifetime of the coating

Source	DF	Sum Square	Mean Square	*F* Value	*F* critical	Pr > *F*	PC
Contact force	2	0.87	0.44	7.34	3.11	0.0012	0.42%
Displacement amplitude	2	19.79	9.90	166.92	3.11	<0.0001	11.04%
Contact force × Displacement amplitude	4	2.59	0.65	10.91	2.48	<0.0001	1.32%
Contact configuration	1	126.50	126.50	2133.62	3.96	<0.0001	70.94%
Contact force × Contact configuration	2	8.57	4.29	72.31	3.11	<0.0001	4.74%
Displacement amplitude × Contact configuration	2	0.98	0.49	8.28	3.11	0.0005	0.48%
Coating position	2	11.47	5.73	96.71	3.11	<0.0001	6.37%
Contact force × coating position	4	1.20	0.30	5.07	2.48	<0.0011	0.54%
Displacement amplitude × coating position	4	0.43	0.11	1.79	2.48	0.138	0.11%
Contact configuration × coating position	2	0.99	0.49	8.32	3.11	0.0005	0.49%
Error	82	0.87	0.44	7.34			3.56%
Total	107	19.79	9.90	166.92			100%

III.4.2 Survival analysis

In addition to analysis of variance, survival analysis (also called reliability analysis) is also employed in this study to learn the ratio of lifetime under different test parameters. The Weibull distribution is also used to predict the distribution of survival rate.

III.4.2.1 Non-parametric survival analysis

Kaplan–Meier (KM) survival curve is used to describe probabilities of survival at given survival time and failure status information on a sample of subjects. It is one of the best options used to measure the fraction of subjects living for a certain amount of time after treatment. Generally, it has been widely used in biostatistics to calculate the survival probability after treatment. It is calculated according to the Eq.(III-4):

$$\hat{S}(t) = \prod_{t_i<t} \frac{n_i - d_i}{n_i}$$

n_i is just the number of survivors just prior to time t_i and d_i is the number of failed coatings at time t_i.

It involves computing of probabilities of occurrence of event at a certain point of time and multiplying these successive probabilities by any earlier computed probabilities to get the final estimate. The survival curve can be created assuming various situations [132]. Figure 74 shows the comparison of survival probability of the coating under different test conditions. Log-rank test and Wilcoxon test give the test of whether the survival probabilities are same for different treatments. If the probability of chi-square is less than 0.05, it means that the assumption (the survival probabilities are same for different treatments) is rejected and the treatment induces the change of survival probability. If Log-ranks test rejects assumption but Wilcoxon test accepts the assumption, it can explain that the difference between the levels of treatment occurs in later failure events in time and no difference between the levels of treatment occurs in earlier failure events in time, since the Wilcoxon test gives more weight to early times than to late times and it is less sensitive than log-rank test to the difference occurred at later events in time. If both values are less than 0.05, their individual value chi-square can be employed distinct the deviance degree between earlier survival rate and later survival rate. The likelihood-ratio tests the assumption that the event time has an exponential distribution. If the value of *P*r > chi-square is less the 0.05, the assumption is rejected.

Figure 74 (a) describes the survival probability of two contact configurations. The mean survival time of ball-on-flat is about 10 times as many as that cylinder-on-flat. Before 1000 cycles, the survival probability of cylinder-on-flat has reduced to 0. It reaches same conclusion as ANOVA that the contact configuration is the most important factor on the evolution of coating lifetime. Coating lifetime under cylinder-on-flat configuration is significantly lower than that of ball-on-flat. Two curves of 400 N and 700 N are almost the same before about 500th cycle, and both of them have lower survival probability than the 100 N (Figure 74 (b)). When lifetime exceeds 500th cycle, higher contact pressure leads to better survival probability (Figure 74 (b)), because failure before 500th cycle is attributed to abrasive wear and failure after 500th cycles is attributed to adhesive wear, which will be discussed in the next section. Moreover, it does not appear to be a meaningful difference between 400 N and 700 N. The logrank test (p=0.18) is not significant at 0.05 level, because change of the survival ability induced by the change of contact pressure is not so significant when it is compared with effect of other factors. Figure 74 (c) indicates that lower displacement amplitude always shows a better survival rate. Mean lifetime of ± 10 µm is 3 and 4 times as many as that of ± 25 µm and ± 40 µm, respectively. It appears that the difference between the coating on two bodies or ball/cylinder and coating on

flat is small before 500th cycle of follow-up but diverges after 500 cycles of follow-up (Figure 74 (d)). Moreover, the coatings on ball/cylinder or two sides always have better survival probability than coatings on the flat.

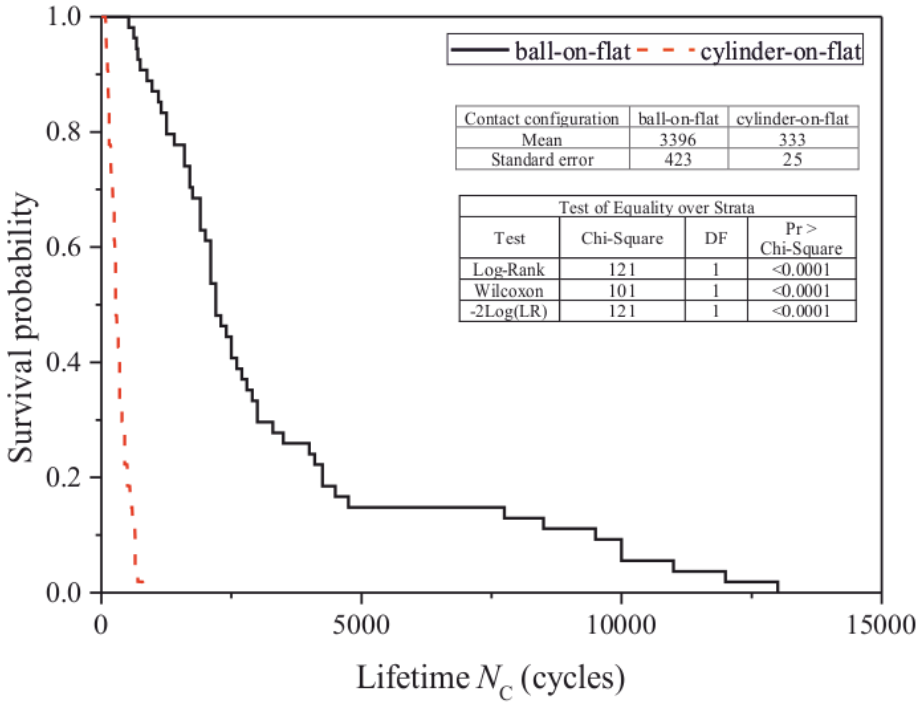

Contact configuration	ball-on-flat	cylinder-on-flat
Mean	3396	333
Standard error	423	25

Test of Equality over Strata			
Test	Chi-Square	DF	Pr > Chi-Square
Log-Rank	121	1	<0.0001
Wilcoxon	101	1	<0.0001
-2Log(LR)	121	1	<0.0001

(a) Comparison of different contact configurations

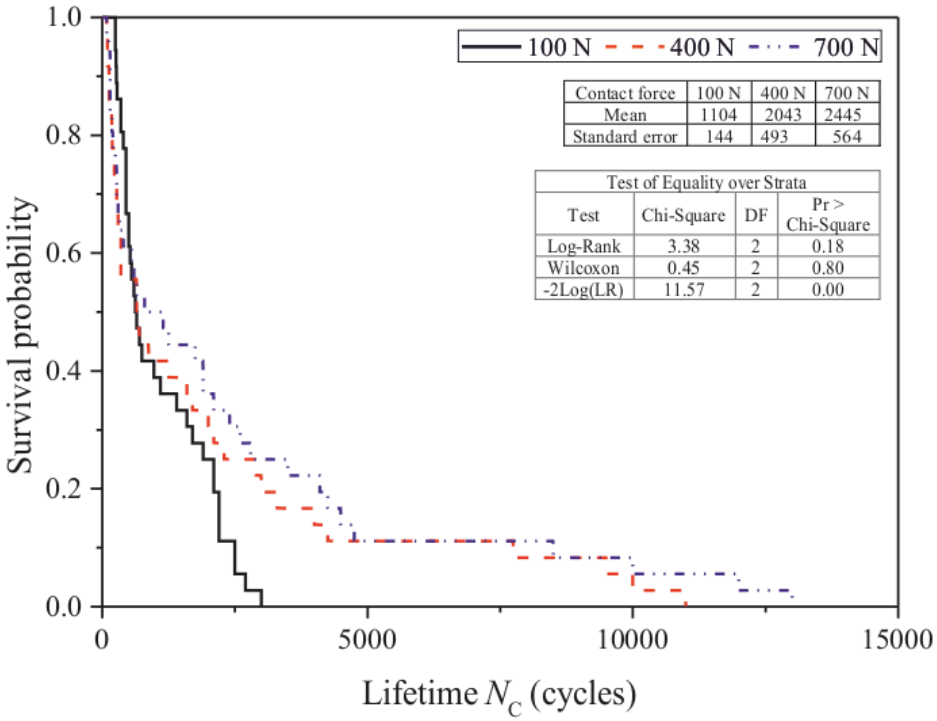

Contact force	100 N	400 N	700 N
Mean	1104	2043	2445
Standard error	144	493	564

Test of Equality over Strata			
Test	Chi-Square	DF	Pr > Chi-Square
Log-Rank	3.38	2	0.18
Wilcoxon	0.45	2	0.80
-2Log(LR)	11.57	2	0.00

(b) Comparison of different contact forces

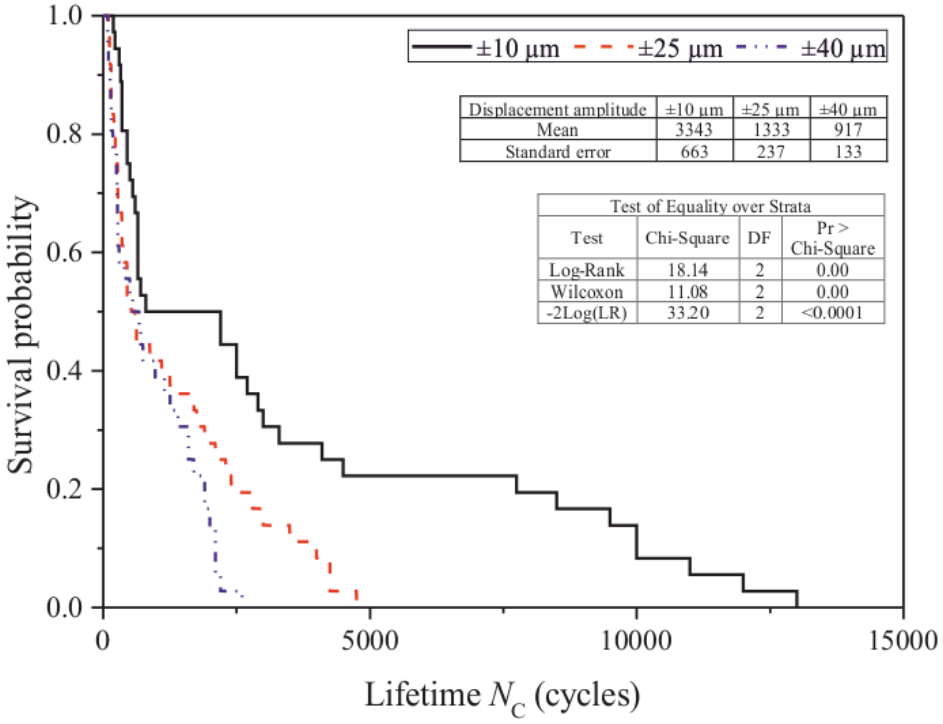

Displacement amplitude	±10 µm	±25 µm	±40 µm
Mean	3343	1333	917
Standard error	663	237	133

Test of Equality over Strata			
Test	Chi-Square	DF	Pr > Chi-Square
Log-Rank	18.14	2	0.00
Wilcoxon	11.08	2	0.00
-2Log(LR)	33.20	2	<0.0001

(c) Comparison of different displacement amplitudes

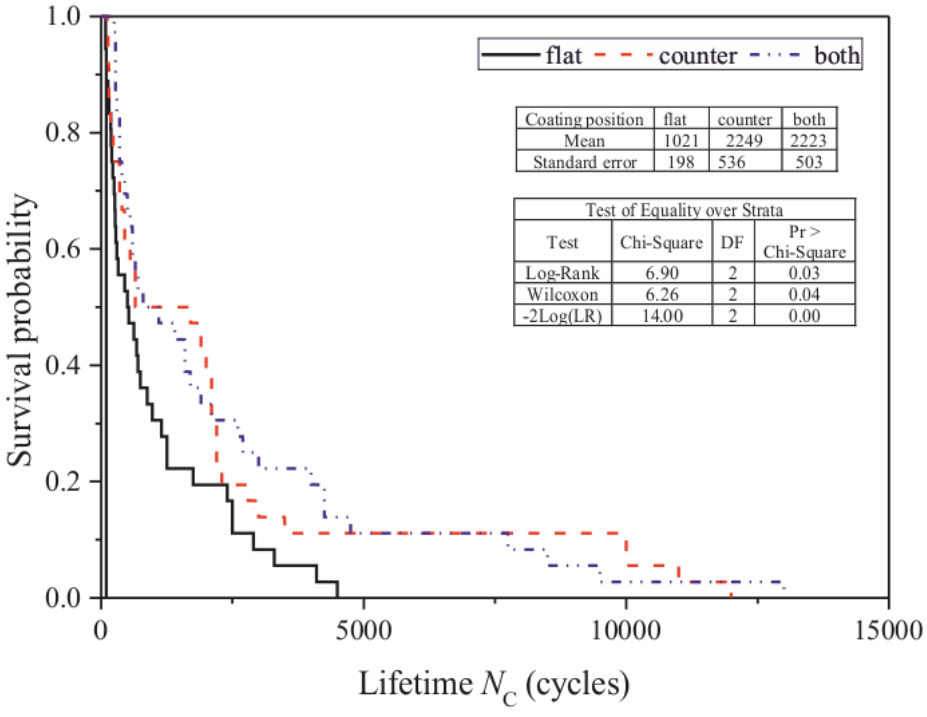

Coating position	flat	counter	both
Mean	1021	2249	2223
Standard error	198	536	503

Test of Equality over Strata			
Test	Chi-Square	DF	Pr > Chi-Square
Log-Rank	6.90	2	0.03
Wilcoxon	6.26	2	0.04
-2Log(LR)	14.00	2	0.00

(d) Comparison of different coating positions

Figure 74: The Kaplan–Meier (KM) survival curve under different working conditions (counter = coatings on the ball or cylinder substrate, flat = coating on the flat substrate, both = coating on both counterbodies).

III.4.2.2 Parametric survival analysis

The obtained times to coating failure for different applied stress parameters were used to construct the Weibull probability failure plot, along with approximate pointwise 95% confidence limits, as shown in Figure 75 (a). However, the plot shows that a simple Weibull model does not adequately fit the data because points do not scatter around a straight line and

a curvature occurs at around 32nd percentile of lifetime. In addition, the shape factor is less than 1. If the value of shape factor is less than 1, it is the failure induced by defects of components, corresponding to a decreasing failure rate [108]. In this study, the failure rate is increased as a function of cycles so that the Weibull model is not correct due to the failure modes are combined [114]. Prior to do the Weibull analysis, the failure point should be grouped according to their individual failure mode. The failure of coating under cylinder-on-flat is controlled by abrasive wear and the failure of coating under ball-on-flat is dominated by adhesive wear. Below 500th cycle, this curve is essentially the same as the expanded Weibull probability plot of cylinder-on-flat (in Figure 75(b)) and its latter part is similar to that of ball-on-flat (in Figure 75 (c)). Therefore, the failure point should be grouped according to the contact configuration. At this moment, both shape factors are larger than 1, corresponding to the wear-induced failure. Only several points do not scatter around a straight line. Combining with results of the interaction map (seeFigure 73), it can be observed that less than 500 cycles is under the cylinder-on-flat conditions, related to abrasive wear, while more than 500 cycles is under the ball-on-flat, dominated by the adhesive wear. Competitive failure modes are well distinguished by the Weibull distribution. In other words, Weibull can be used not only for different failure modes but also for different wear modes. For different wear modes, they share the same feature of shape factor that is more than 1, but they have different scale factor. Longer durability induce larger scale factor.

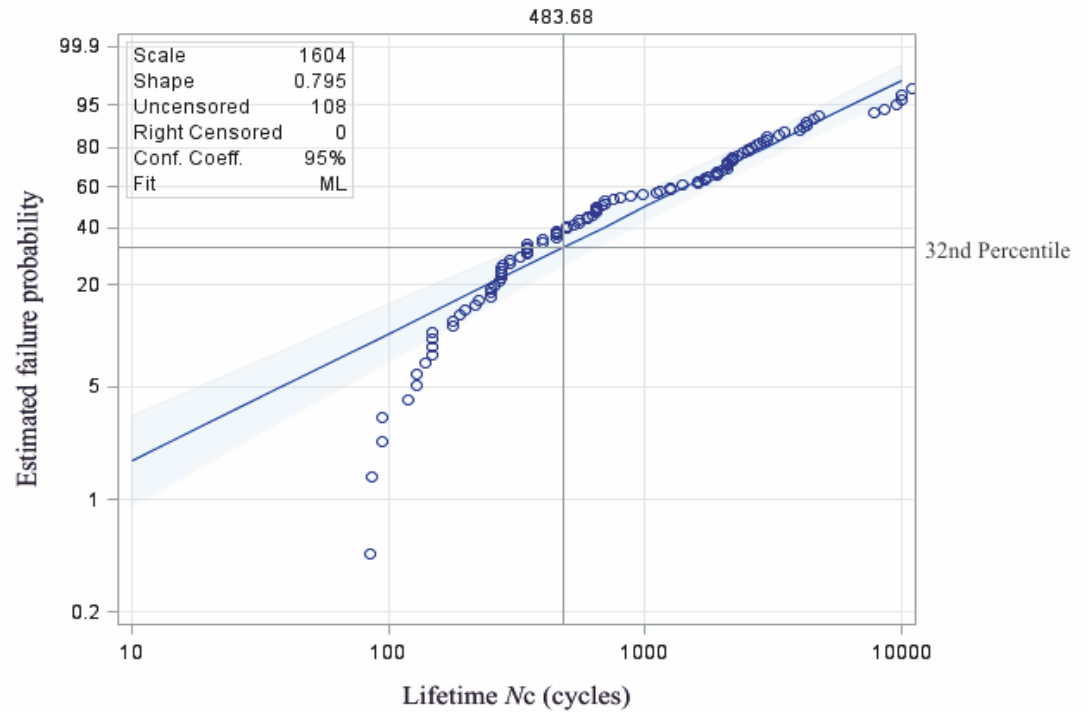

(a) Weibull probability plot for coating lifetime data: Omnibus analysis

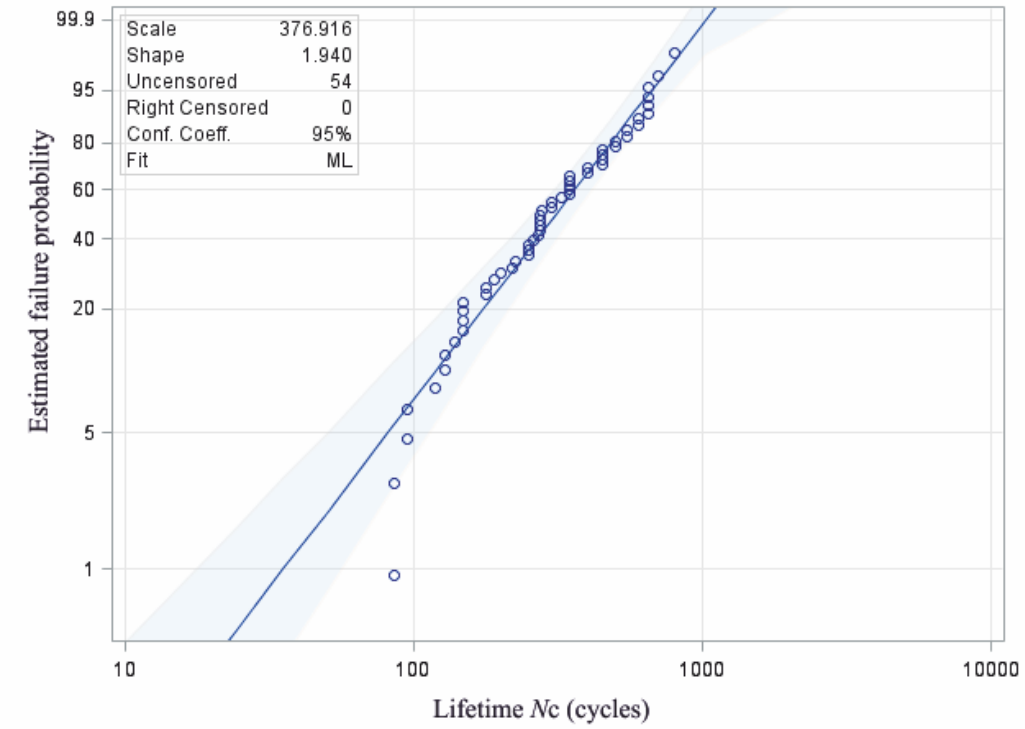

(b) Expanded Weibull probability plot and fit for cylinder-on-flat for coating lifetime

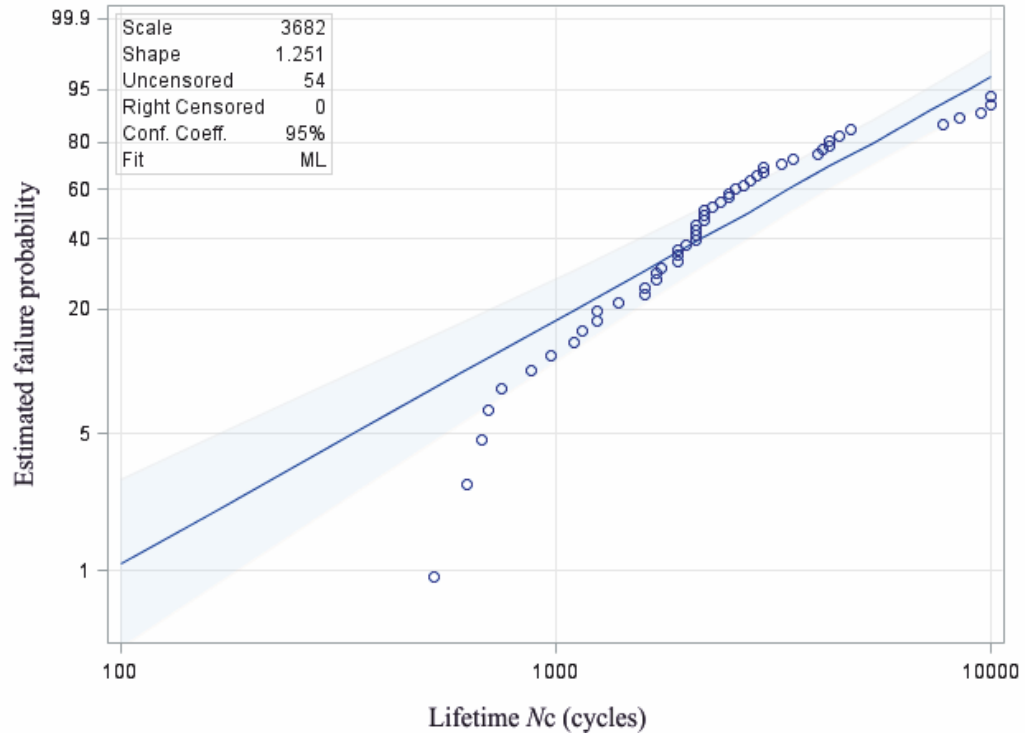

(c) Expanded Weibull probability plot and fit for ball-on-flat for coating lifetime

Figure 75: Weibull probability plot and fit for coating lifetime data: omnibus and separate failure mode analysis (the blue points are the distribution of lifetime, the blue line is referred to the reference line for Weibull distribution, the blue shadow is the 95% confidence limits).

III.4.3 Effect of various factors

Based on the statistical analysis of relation between coating lifetime and various test conditions, the wear mechanism should be used to explain their relationship.

III.4.3.1 Contact configuration

Contact configuration is a factor with biggest effect on durability, as shown inFigure 73. According to analysis in section III.2.2.2, the cylinder-on-flat configuration is related to the abrasive wear, where many abrasive grooves are observed on the surface and many fine particles are at the slip end (Figure 76 (a)). The ball-on-flat is dominated by the adhesive wear where overall transfer is discovered for the ball-on-flat (Figure 76 (b)). In both contact configurations, the coating begins to be delaminated from outer-part of contact within decades of cycles (Figure 76). It can be explained as following: the varnish, made of polymer, can absorb moisture, and absorbed moisture presumably reduces bonding strength between the coating and substrate [133]. In addition, ambient environment can provide opportunity for oxide or water molecule to contaminate the MoS_2 particles. Some water may directly attach to the chain through the hydrogen chain. Since the temperature involved in the fretting is far below the T_g, these attached water could behave as 'antiplasticizers' [133] so that the coating becomes brittle and it is easier to be pushed on the end of slip. Then, the delaminated debris will recirculate in the fretting or be ejected from contact area as a function of relative movement. Compared with ball-on-flat, the contact configuration of cylinder-on-flat provides larger opportunity to contact ambient environment. More coatings are ejected from contact center earlier than ball-on-flat, resulting in lower coating durability.

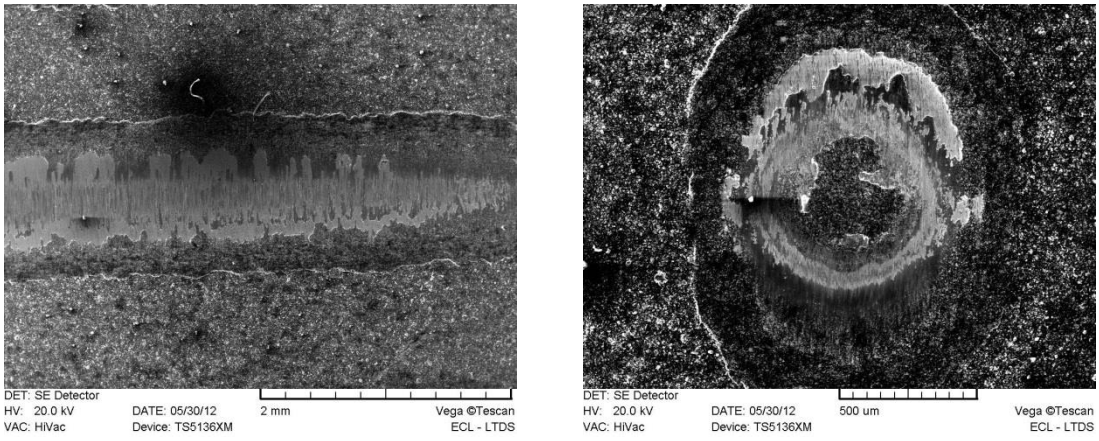

(a) (b)

Figure 76: SEM image of worn surface of coating before its lifetime under different contact configurations, 400 N, ± 25 µm, 50th cycle: cylinder-on-flat (b) coated flat, ball-on-flat, (a) coated flat.

III.4.3.2 Displacement amplitude

Displacement amplitude is a controlling factor for the coating lifetime, as shown in Table 22. The increase in displacement amplitude can increase wear and reduce lifetime of the coating by facilitating ejection of the wear debris, because the debris flow through interface was critically controlled by the imposed sliding amplitude. Relative displacement during a fretting cycle of debris trapped below surface will be longer by increasing the displacement amplitude and thus the debris kinetics and ejected third body flow should increase [134]. Moreover, It is observed that a significant interaction between the contact configuration and displacement amplitude.

When the contact configuration changes from the line contact (cylinder-on-flat) to point contact (ball-on-flat), the gap between different amplitudes is more significant, as shown in Figure 73. This is because a large contact (induced by ball-on-flat, as shown in Table 9 and Table 10) and small displacement amplitude can make it difficult for debris to eject [134]. In other words, the contact configuration of ball-on-flat is more sensitive to the change of displacement amplitude than that of cylinder-on-flat, because the contact length in the sliding direction for cylinder-on-flat configuration is small and the debris is not so difficult to be ejected as that of ball-on-flat. When the displacement amplitude is increased to a certain value (around ± 25 µm) for the contact configuration of cylinder-on-flat, the increase of displacement has no significant effect on the lifetime of coating (Figure 74 (c)). In Figure 74 (c), the earlier failure events (before 500 cycles) are mainly due to the abrasive wear under cylinder-on-flat configuration. However, the survival probability for ball-on-flat (after 500 cycles in Figure 74 (c)) shows the significant difference for different displacement amplitudes. Therefore, a significant interaction between contact configuration and displacement amplitude can be discovered, as a result that the discrepancy of survival rates of different displacement amplitude for ball-on-flat is not same as the case of cylinder-on-flat.

III.4.3.3 Coating position

There is almost no difference in coating lifetime between the coated ball (or cylinder) and both coated counterbodies. They have higher lifetime than that of coated flat substrate (line 4 and columnFigure 73). This is because the flat substrate is more sensitive to plastic deformation. In other words, the flat will be subjected to more serious plastic deformation compared to ball or cylinder so that more coatings has been pushed to the end of the contact due to plastic deformation. Therefore, less coating will form transfer film between two counterbodies, leading to a low durability. Moreover, another assumption is that coating on the sphere reduces the adherence of compacted wear particles at both sides of slip end and by consequence, external flow of the third body, track width and presence of cluster responsible for fretting wear [120].

Figure 77 compares the evolution of wear process for different coating positions under ball-on-flat configuration. At the first contact (stage I), there is a little deformation of the coating on the ball. As a function of cycles, some coating debris have been ejected to the outside of contact and some coating debris stayed on the wear track or are transferred to the flat (Figure 77 (stage 2)). As the movement of fretting continues, the coating that stayed on the wear track can recirculate into contact center. In addition, some new coating at out-edge of contact area can recirculate into the contact center due to the radius of ball. Different from the coating on flat, therefore, coating on ball provides a higher possibility for coating debris to rejoin the contact center due to its special geometry. If we assume that the formation and ejection rate of coating debris is constant, less coating debris will be formed and re-circulated after certain numbers of cycles because more coating has been ejected. At this moment, the friction coefficient begins to increase and thus the contact changes to the two-body contact between two substrates. Finally, all of the coating has been ejected from the contact and TTS structure [135] is formed on the contact center (Figure 77 (stage 3)). Around the contact center, the oxide particles could be formed around the contact area and it could be ejected outside to cover around coating. The

two-coated parts only increase the volume of transfer film, but its value is limited between two contact bodies so that it has no significant difference compared to one side coated contact case.

For the contact configuration of cylinder-on-flat, the wear process is dominated by the abrasive wear so that more debris have been pushed outside of the contact center compared with adhesive wear of ball-on-flat configuration. Therefore, the durability of low friction coefficient depends on the recirculation of coating debris. The curved substrate of cylinder also can provide a higher possibility for coating debris to rejoin the contact center due to its special geometry.

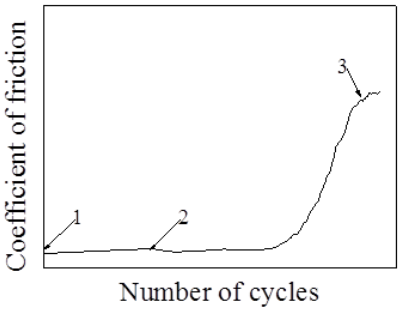

(a) Evolution of friction coefficient

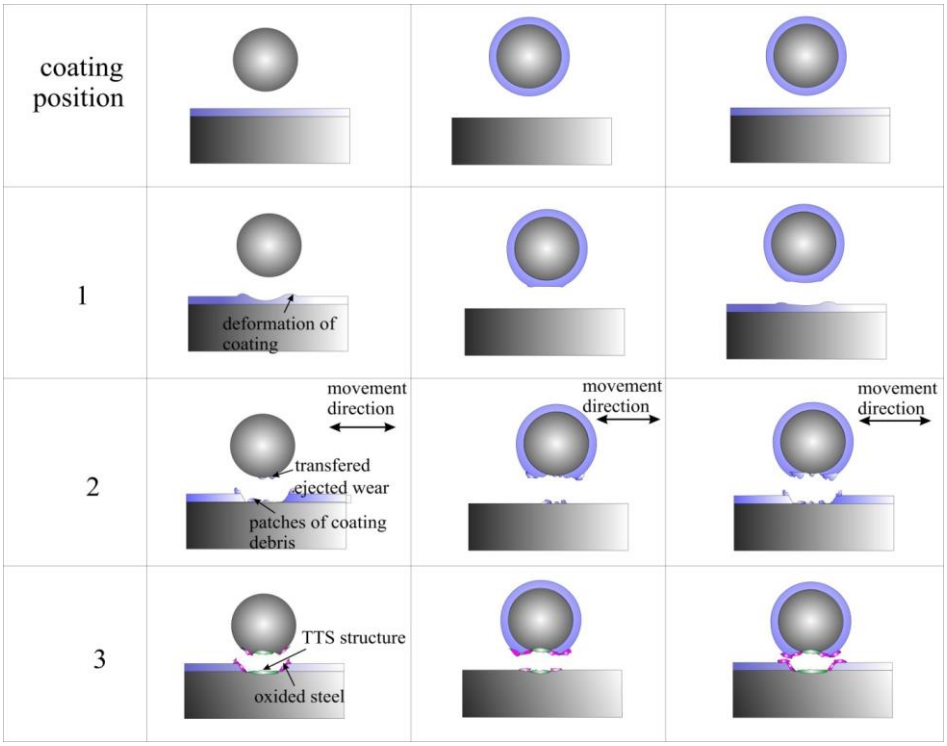

(b) Schematic drawing of wear process

Figure 77: The evolution of friction coefficient as a function of cycles (a) and corresponding schematic drawing of the wear process (b).

III.4.3.4 Contact force

A large pressure may also improve the formation of transfer films on the counterface and may shorten the time required to form an equilibrium particle size of MoS_2 [51] so that the lower friction coefficient occurs on high contact pressure. At the same time, the more third body of

coating debris may help improve the lifetime of coatings, because it can accommodate the fretting movement between two contact bodies. In addition, High contact pressure induces serious plastic deformation of tribological system that will offer small reservoir for the debris, thereby prolonging its period of lubrication and survival ability. Therefore, high contact force leads to high lifetime, as shown in Figure 73.

III.4.4 Prediction of coating lifetime

According to the results above, regression equation based on significant parameters can be determined as follows:

$$N_c = \exp(5.6 - 0.32F_n - 0.71\delta^* + 1.63CON + 0.22\delta^{*2} + 0.88F_n \times CON + 0.78CON \times C_1 + 0.80CON \times C_2) \quad \textit{(III-5)}$$

Adjusted R^2 = 0.89

Here, the value of each variable is the standardized value (Table 34 of the Annex). According to the equation, the lifetime of coating decreases with increase of contact force when the coating is running under contact configuration of cylinder-on-flat (*CON* = 0), because the coefficient associated with contact force is less than 0. When the coating is running under the contact configuration of ball-on-flat (*CON* = 1), the lifetime of coating increases with increase of contact force. This is because, for *CON* = 1, the very significant interaction between F_n and *Con* should be taken into consideration. Therefore, the coefficient associated with contact force is more than 0 (= 0.56), for ball-on-flat configuration. This leads to the same conclusion as the analysis of variance. The decrease of lifetime with the increase of contact force under cylinder-on-flat can be explained by the definition of coating lifetime. The friction coefficient is high under 100 N, thereby leading to higher average value between the friction coefficient of the coating and of two substrates and longer coating lifetime.

In addition, the contact configuration has also a significant interaction with the coating position, but the coefficients associated with coating on counterbodies and coating on both counterbodies is very close. It indicates that coating on counterbodies and both counterbodies can have significant improvement on coating lifetime compared to the coating on flat substrate, but these two coating positions have similar results on the coating lifetime, reaching an agreement with the ANOVA. Finally, with the increase of displacement amplitude, coating lifetime is decreased. Here, the quadratic part of displacement amplitude is considered because the evolution of coating lifetime as a function of displacement is not linear.

Based on Eq. (III-5), Figure 78 shows the difference between experimental and modeled results. Several points like samples 20, 21, 38 and 39 present a significant difference between model and experiment. This is because, in these conditions, the fretting tests are running in mixed slip regime, where the coating lifetime will be largely prolonged. It is very difficult for regression analysis to produce correct values in the mixed slip regime based on results that are mostly ranging in the gross slip regime.

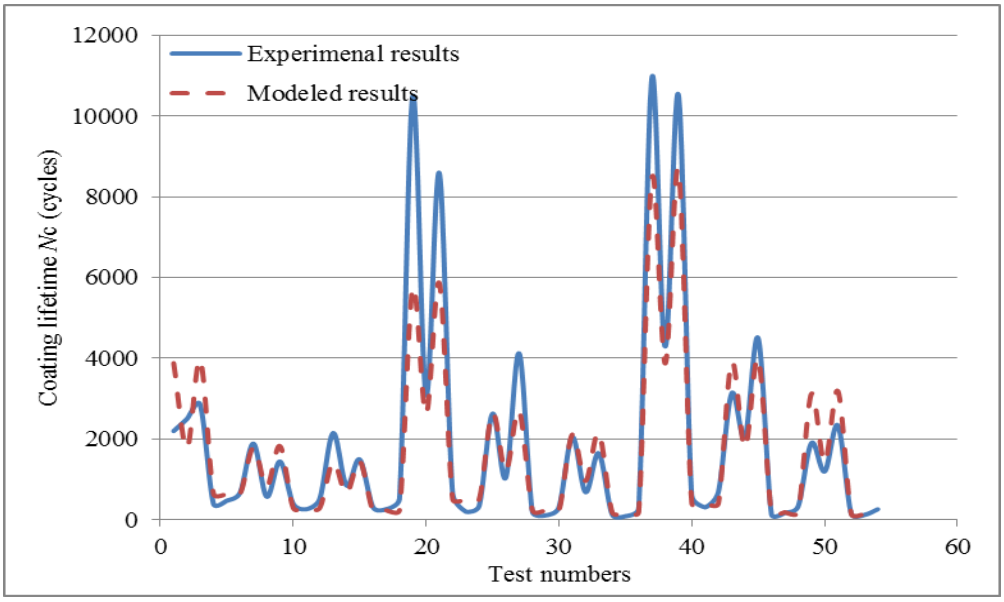

Figure 78 : Comparison between experiment and model for lifetime of the coating.

III.5 Conclusions

In this chapter, the effects of factors such as contact force, displacement amplitude, contact configuration and coating positions on the friction coefficient and lifetime of coating have been investigated.

Based on the analysis, contact configuration is the most important effect on both coating lifetime and friction coefficient, because it is related to different wear mechanisms. Contact force is the second significant factor on friction coefficient, while displacement amplitude is the second significant factor on coating lifetime.

Two predictive equations have been made by regression analysis to describe the relationship between test parameters and friction coefficient or lifetime.

Survival or reliability analysis can serve as an effective way to distinct the wear modes by different scaling factors.

CHAPTER IV

EFFECT OF SUBSTRATE NATURE AND COATING THICKNESS ON TRIBOLOGICAL BEHAVIOR OF A VARNISH COATING

CHAPTER IV: EFFECT OF SUBSTRATE NATURE AND COATING THICKNESS ON TRIBOLOGICAL BEHAVIOR OF A VARNISH COATING

In this chapter, orthogonal design is used to study the effect of contact force, displacement amplitude, contact configuration, coating position, thickness of coating and nature of the substrate.

IV.1 Introduction

Thickness of coatings can influence the distribution of contact pressure, thereby influencing the friction coefficient and lifetime of coating. Different substrates can affect the adhesion force between coating and substrate and then the coating lifetime. Concerning the variation of friction coefficient and lifetime of coating, the competition whether the two factors (thickness of the coating and nature of substrate) are more important than contact force, displacement amplitude, contact configuration and coating positions is a very interesting object to do research. To realize this object, orthogonal design is chosen to do experiments with aim to save cost of experiments.

IV.2 Design of experiment

IV.2.1 Full-factorial design

A full factorial design of experiments of type p^n was used in previous chapter where n corresponds to the number of factors and p represents the number of levels [102]. It consists of all possible combinations of the levels for all the factors and thus it can estimate all main effects, all two-factor interactions, and all higher-order interactions such as interaction between three factors or more [136]. Generally, the nature of the substrate affects the adhesion of the coating and thus the coating durability or friction coefficient. Besides, thickness is also a very important factor that affects the coating properties such as resistance to plastic deformation. Based on the previous study, therefore, two new factors (thickness of coatings and substrate nature) with two levels will be added in the study so that the number of factors will be extended to 6 (Table 23). According to the requirement of full-factorial analysis, there will be at least 216 tests. The deposition method is explained in Chapter II.

Table 23: Test parameters.

Factor	Level 1	Level2	Level3
Normal force	100 N	400 N	700N
Displacement amplitude	± 10 µm	± 25 µm	± 40 µm
Contact configuration	Ball-on-flat	Cylinder-on-flat	-
Coating positions	Flat	Cylinder or ball	Both
Substrate	SS 304	M2 steel	-
Thickness	1 layer (10 µm)	2 layer (20 µm)	-

IV.2.2 Orthogonal design

Although a full factorial design can be used to test all possible combinations of factors, it is not a practical way to carry out so huge numbers of experiments because it is a low cost-effective way to do experiments. In this study, one of the purposes is to rank the importance of variables so that it is not necessary to carry out full-factorial design. Instead, the orthogonal design is used due to its feature of balance and orthogonal. When each level occurs equally often within each factor, the design is balanced. A design is orthogonal when frequencies for level pairs are proportional or equal [136]. Therefore, this feature can give a fair evaluation on the ranks of importance of variables. The aim of orthogonal design is to reach operation within one of its components without creating side-effects to other components [68]. Deming and Morgan [137] have proven it to be an effective and efficient optimization strategy with widespread application in many research fields.

To be sure of the balance and orthogonal of design, the design should be a multiple of 36 runs for variables having two or three levels, since 36 runs can be divided by 2 × 3, 2 × 2 and 3 × 3. According to the theory of orthogonal table, the number of runs should be larger than the freedom of factors. If we only consider the main effect without the interaction of factors, the runs will be at least 36 (> 3 (factors) × 2 (degree of freedom) + 3 (factor) × 1 (degree of freedom)). However, the interaction effect should be considered in the study, as it is proved by Chapter III, where the significant interaction between contact configuration and displacement amplitude is found for the evolution of coating durability and interaction between contact configuration and contact force takes some responsibility for the evolution of friction coefficient. Therefore, the numbers of runs should be 72 (> 3 (factors) × 2 (degree of freedom) + 3 (factor) × 1 (degree of freedom) +interaction 9 (one three-level factor × one two-level factors) × 2 (degree of freedom) + interaction 3 (one three-level factor × one three-level factors) × 4 (degree of freedom) + interaction 3 (one two-level factor × one two-level factors) × 1 (degree of freedom)). The orthogonal design is shown in Table 24. By using the orthogonal design, it saves 2/3 cost and time of experiments. Each experiment is done two times. The order of experiment is random.

Table 24: Orthogonal design of 6 factors (SS 304: 304 stainless steel; M2: M2 steel).

No	Substrate	Contact-configuration	Thick-ness	Contact force	Displacement amplitude	Coating positions
1	SS 304	ball-on-flat	1	100 N	± 10 µm	both (ball and flat)
2	SS 304	ball-on-flat	1	100 N	± 25 µm	counter (ball)
3	SS 304	ball-on-flat	1	100 N	± 40 µm	flat
4	SS 304	ball-on-flat	1	400 N	± 10 µm	flat
5	SS 304	ball-on-flat	1	400 N	± 25 µm	both (ball and flat)
6	SS 304	ball-on-flat	1	400 N	± 40 µm	counter (ball)
7	SS 304	ball-on-flat	1	700 N	± 10 µm	counter (ball)
8	SS 304	ball-on-flat	1	700 N	± 25 µm	flat
9	SS 304	ball-on-flat	1	700 N	± 40 µm	both (ball and flat)
10	SS 304	ball-on-flat	2	100 N	± 10 µm	flat
11	SS 304	ball-on-flat	2	100 N	± 25 µm	both (ball and flat)
12	SS 304	ball-on-flat	2	100 N	± 40 µm	counter (ball)

13	SS 304	ball-on-flat	2	400 N	± 10 µm	counter (ball)
14	SS 304	ball-on-flat	2	400 N	± 25 µm	flat
15	SS 304	ball-on-flat	2	400 N	± 40 µm	both (ball and flat)
16	SS 304	ball-on-flat	2	700 N	± 10 µm	both (ball and flat)
17	SS 304	ball-on-flat	2	700 N	± 25 µm	counter (ball)
18	SS 304	ball-on-flat	2	700 N	± 40 µm	flat
19	SS 304	cylinder-on-flat	1	100 N	± 10 µm	counter (cylinder)
20	SS 304	cylinder-on-flat	1	100 N	± 25 µm	flat
21	SS 304	cylinder-on-flat	1	100 N	± 40 µm	both (cylinder and flat)
22	SS 304	cylinder-on-flat	1	400 N	± 10 µm	both (cylinder and flat)
23	SS 304	cylinder-on-flat	1	400 N	± 25 µm	counter (cylinder)
24	SS 304	cylinder-on-flat	1	400 N	± 40 µm	flat
25	SS 304	cylinder-on-flat	1	700 N	± 10 µm	flat
26	SS 304	cylinder-on-flat	1	700 N	± 25 µm	both (cylinder and flat)
27	SS 304	cylinder-on-flat	1	700 N	± 40 µm	counter (cylinder)
28	SS 304	cylinder-on-flat	2	100 N	± 10 µm	counter (cylinder)
29	SS 304	cylinder-on-flat	2	100 N	± 25 µm	both (cylinder and flat)
30	SS 304	cylinder-on-flat	2	100 N	± 40 µm	flat
31	SS 304	cylinder-on-flat	2	400 N	± 10 µm	flat
32	SS 304	cylinder-on-flat	2	400 N	± 25 µm	counter (cylinder)
33	SS 304	cylinder-on-flat	2	400 N	± 40 µm	both (cylinder and flat)
34	SS 304	cylinder-on-flat	2	700 N	± 10 µm	both (cylinder and flat)
35	SS 304	cylinder-on-flat	2	700 N	± 25 µm	flat
36	SS 304	cylinder-on-flat	2	700 N	± 40 µm	counter (cylinder)
37	M2	ball-on-flat	1	100 N	± 10 µm	counter (ball)
38	M2	ball-on-flat	1	100 N	± 25 µm	both (ball and flat)
39	M2	ball-on-flat	1	100 N	± 40 µm	flat
40	M2	ball-on-flat	1	400 N	± 10 µm	Flat
41	M2	ball-on-flat	1	400 N	± 25 µm	counter (ball)
42	M2	ball-on-flat	1	400 N	± 40 µm	both (ball and flat)
43	M2	ball-on-flat	1	700 N	± 10 µm	both (ball and flat)
44	M2	ball-on-flat	1	700 N	± 25 µm	flat
45	M2	ball-on-flat	1	700 N	± 40 µm	counter (ball)
46	M2	ball-on-flat	2	100 N	± 10 µm	counter (ball)
47	M2	ball-on-flat	2	100 N	± 25 µm	flat
48	M2	ball-on-flat	2	100 N	± 40 µm	both (ball and flat)
49	M2	ball-on-flat	2	400 N	± 10 µm	both (ball and flat)
50	M2	ball-on-flat	2	400 N	± 25 µm	counter (ball)
51	M2	ball-on-flat	2	400 N	± 40 µm	flat
52	M2	ball-on-flat	2	700 N	± 10 µm	flat
53	M2	ball-on-flat	2	700 N	± 25 µm	both (ball and flat)
54	M2	ball-on-flat	2	700 N	± 40 µm	counter (ball)
55	M2	cylinder-on-flat	1	100 N	± 10 µm	Flat
56	M2	cylinder-on-flat	1	100 N	± 25 µm	both (cylinder and flat)
57	M2	cylinder-on-flat	1	100 N	± 40 µm	counter (cylinder)
58	M2	cylinder-on-flat	1	400 N	± 10 µm	counter (cylinder)
59	M2	cylinder-on-flat	1	400 N	± 25 µm	flat

60	M2	cylinder-on-flat	1	400 N	± 40 µm	both (cylinder and flat)
61	M2	cylinder-on-flat	1	700 N	± 10 µm	both (cylinder and flat)
62	M2	cylinder-on-flat	1	700 N	± 25 µm	counter (cylinder)
63	M2	cylinder-on-flat	1	700 N	± 40 µm	Flat
64	M2	cylinder-on-flat	2	100 N	± 10 µm	both (cylinder and flat)
65	M2	cylinder-on-flat	2	100 N	± 25 µm	counter (cylinder)
66	M2	cylinder-on-flat	2	100 N	± 40 µm	Flat
67	M2	cylinder-on-flat	2	400 N	± 10 µm	Flat
68	M2	cylinder-on-flat	2	400 N	± 25 µm	both (cylinder and flat)
69	M2	cylinder-on-flat	2	400 N	± 40 µm	counter (cylinder)
70	M2	cylinder-on-flat	2	700 N	± 10 µm	counter (cylinder)
71	M2	cylinder-on-flat	2	700 N	± 25 µm	Flat
72	M2	cylinder-on-flat	2	700 N	± 40 µm	both (cylinder and flat)

To estimate the effects of factors, after carrying out the mixed-level orthogonal array, the analysis of variance (ANOVA) is changed a little bit, because the orthogonal array cannot guarantee the data distribution is obeyed with homoscedasticity. Therefore, a parameter of purified sum of square, SS', will be used to calculate percentage contribution, PC (%), values for each factor in the table of ANOVA. SS' is the sum of squares minus the variance due to error and PC (%) is the relative contribution of SS' for each factor or error to total variance [131]. In this study, PC (%) will be used instead of *P*r > *F* to evaluate the significance of factor. When PC (%) is less than 0, it indicates this factor has no effect of the dependent value.

IV.3 Friction coefficient

IV.3.1 Evolution of friction coefficient

IV.3.1.1 Fretting tests of uncoated substrate

In order to compare the friction-reducing capability of MoS_2-based varnish coating, fretting behavior of substrate (AISI M2 steel with porosity at the surface due to undersintering process) versus counterbody (AISI 52100) has been determined. The evolution of friction coefficient as a function of cycles has been shown in three typical modes depending on various test parameters. Two types of running regime are found out under the contact configuration of cylinder-on-flat as a function of normal force.

1) Mixed slip regime

When the normal force is large, the fretting is running in the partial slip regime after 20 cycles. However, within the first 100 cycles, the fretting loops are changed between elliptical and quadrangular shapes due to its special structure of porosity (Figure 79). This special structure may lead some contamination layer including oxide layer, adsorbed layer and contaminant layer (about 15 nm [17]) to be trapped in the porosity (depth = 15 µm) (Figure 80). With the increase of cycles, this trapped contamination layer may go out and provide the surface with lubrication and make the elliptical shape transform to quadrangular shape. It may not stop transforming between two shapes until the entire contamination layer has been squeezed from the porosity. At this time, the shape of ellipse can be kept until the end of the test.

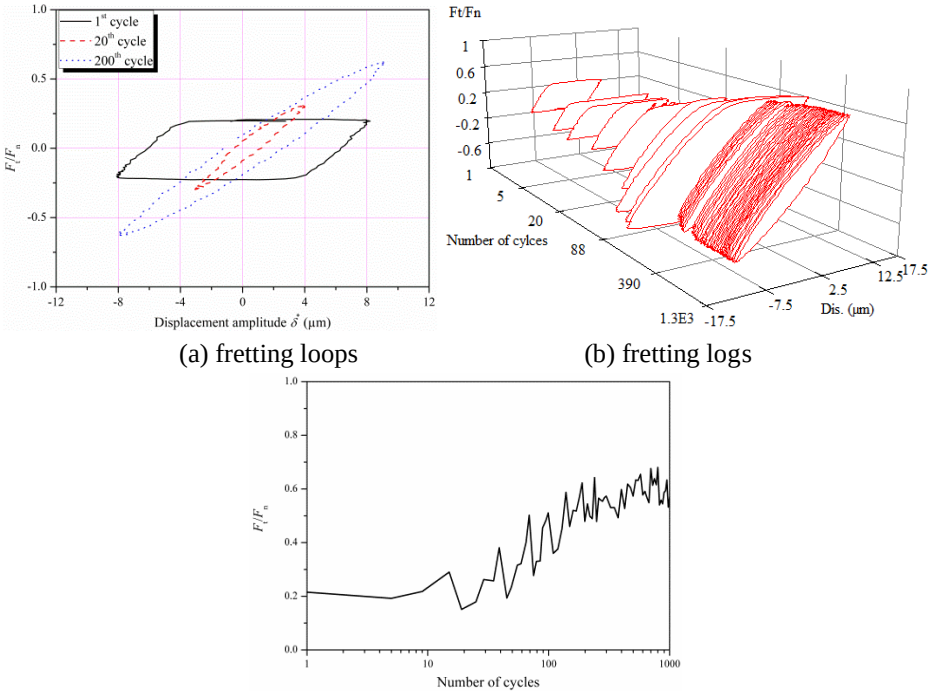

(a) fretting loops (b) fretting logs

(c) evolution of friction force

Figure 79: Fretting loops (a), fretting logs (b) and the evolution of friction force ratio (c) under ± 10 µm, 700 N, cylinder-on-flat.

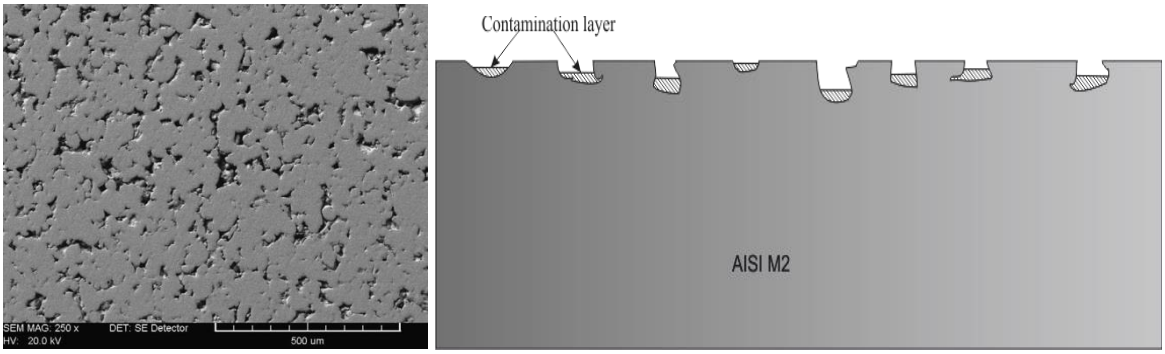

(a) SEM top-view of M2 (b) Cross-section view of M2

Figure 80: Schematics for AISI M2 in air: (a) SEM top-view of M2 and (b) cross-section view of M2.

2) Gross slip regime

When the normal force is 100 N, fretting loops keep quadrangular shapes during the whole test duration (Figure 81). In the first several cycles, the coefficient of friction is rather low (about 0.2) due to the protection film like contamination film which protects the surface from wear. With the increase of cycles, the two counterbodies become to contact directly, leading to the increase friction coefficient. As a function of cycles, some wear particles appear at the contact area, resulting in the increase of friction coefficient and then reaching a stable value (about 1.0).

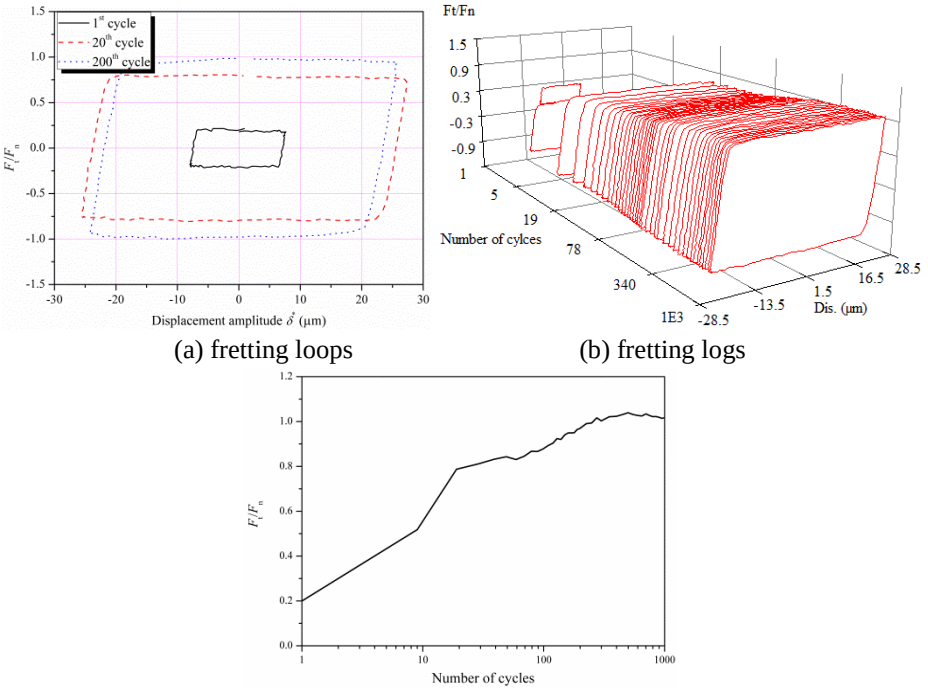

(a) fretting loops (b) fretting logs

(c) evolution of friction force

Figure 81: Fretting loops (a), fretting logs (b) and the evolution of friction force ratio (c) under ± 25 µm, 700 N, cylinder-on-flat.

IV.3.1.2 Fretting tests of MoS_2 coating

Under the same test parameters, the fretting tests of MoS_2 based varnish coating only show gross-slip regime due to the lubricating function of coatings. Thanks to the lubricating function of coatings, the friction coefficient is lowered. Similar to the results of FE modeling for SS 304, a significant stress discontinuity is also found in the case of M2 substrate (Figure 82). It indicates that debonding and fracture of coatings can occur at the interface of coating and substrate.

Similar as the SS 304, the wear mechanism includes abrasive wear and adhesive wear. Two types of curves of friction coefficient as a function of cycles have been observed (Figure 83 and Figure 85).

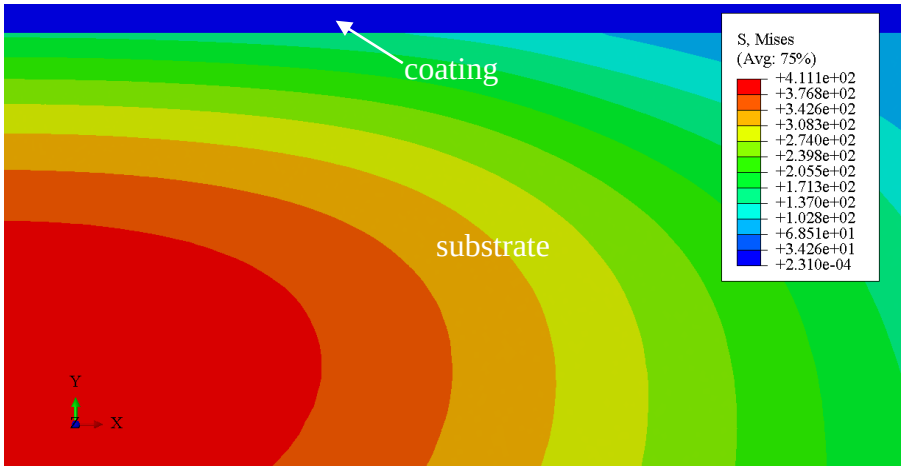

Figure 82: von Mises stress contour map of coating on the M2 substrate for ball-on-flat under 100 N, one layer.

- **Abrasive wear**

Similar to the tribological analysis of coated SS 304, the tribological process also involves abrasive wear and adhesive wear. However, it shows some different features from the coated SS 304.

Figure 83 describes the tribological process when the lifetime of the coating is more than 20 000 cycles. It is a result of the special structure of M2. With the increase of cycles, the coating is gradually removed from the contact area due to abrasive wear (Figure 83(b)). At the stage I, there are some coatings still on the surface of substrate (Figure 83(c)). The profile of Figure 83(h) shows that the thickness of the coating on the flat substrate is decreased. Some coatings around the contact area may transfer to the cylinder (Figure 83 (j)). As the movement of fretting occurs, some coating debris may recirculate in the fretting area, providing low friction coefficient. When it reaches stage II, most of the coating has been removed from the contact area (Figure 83(i)). However, some coating trapped in the porosity during the deposition (Figure 83(g) and Figure 84) is difficult to be squeezed under the lower contact pressure and small amplitude and coating is transferred on the counterpart (Figure 83(k) and (m)), so that friction coefficient can maintain a low value for a long time.

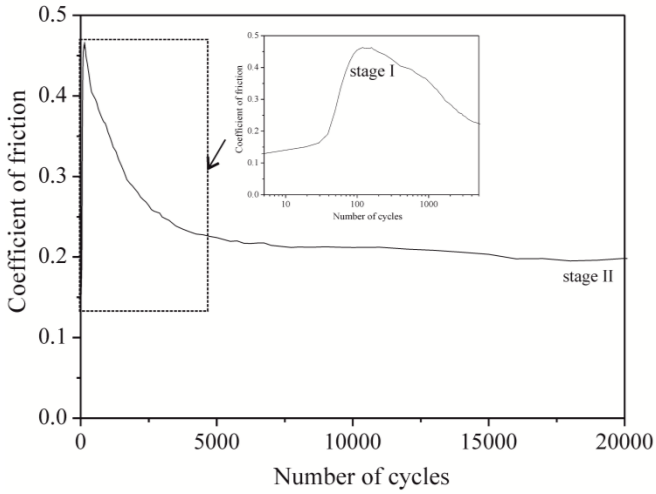

(a) Evolution of friction coefficient

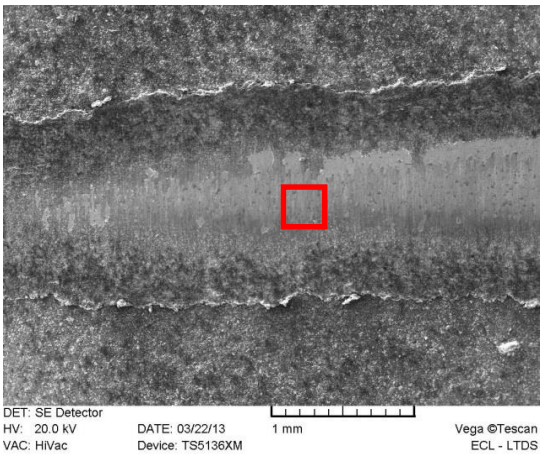

(b) Coated M2 substrate at Stage I

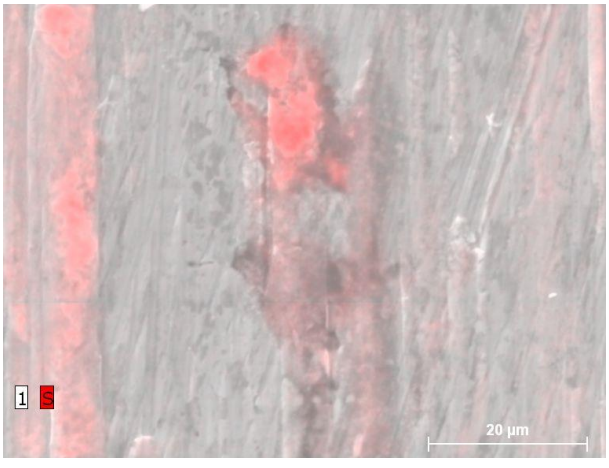

(c) EDX results for part in (b)

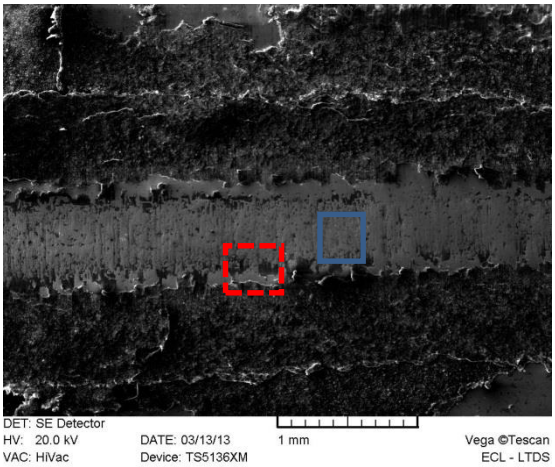

(d) Coated M2 substrate at Stage II

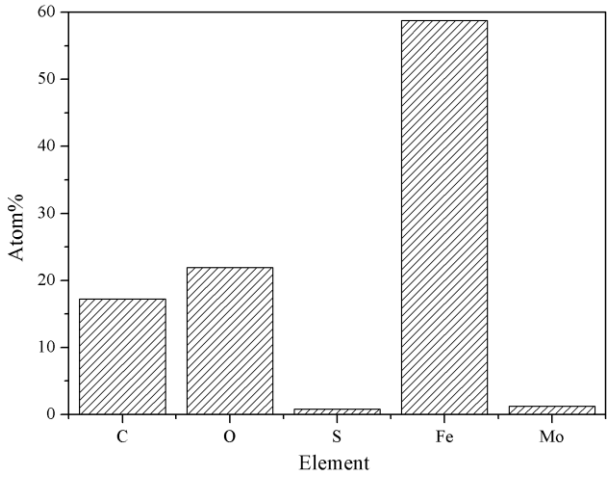

(f) EDX results for contact center in (d)

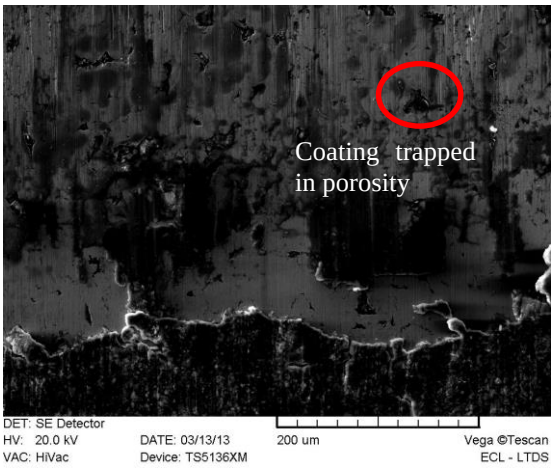

(g) SEM wear scar at the contact center in (d)

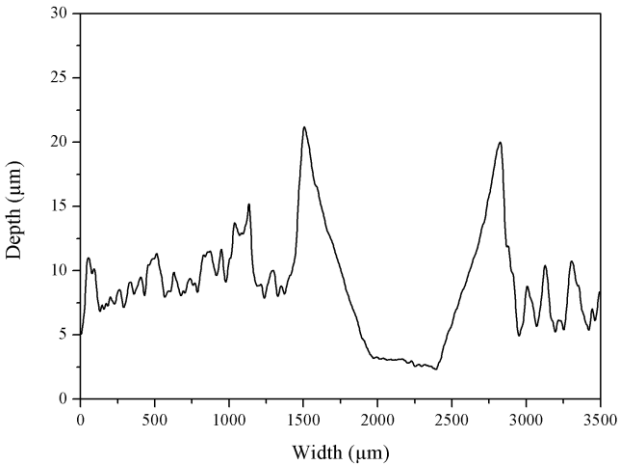

(h) Profile for coated M2 substrate at Stage I

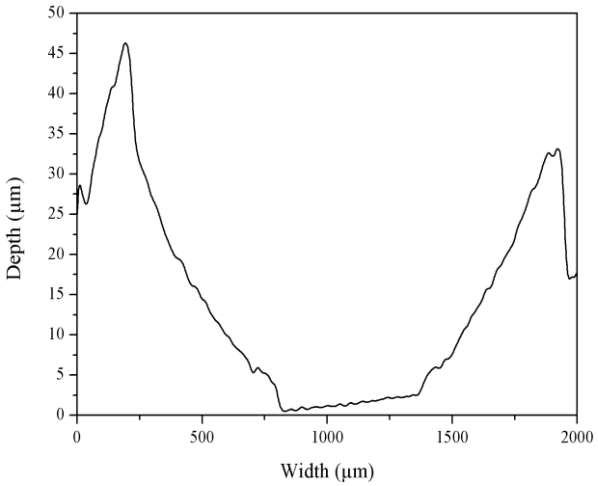

(i) Profile coated M2 substrate at Stage II

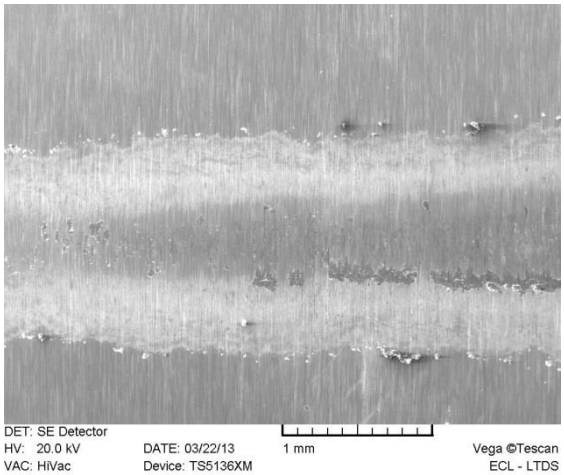

(j) Uncoated cylinder at stage I

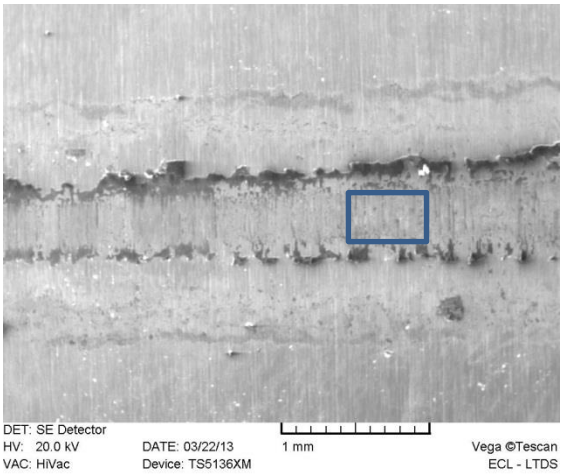

(k) Uncoated cylinder at stage II

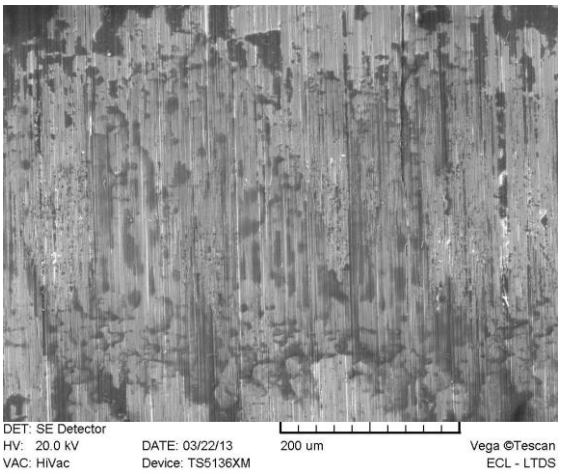

(m) Wear scar at the contact center of (j)

Figure 83: Evolution of friction coefficient and wear scars for 400 N, ± 10 µm, coated substrate = M2, 1 layer.

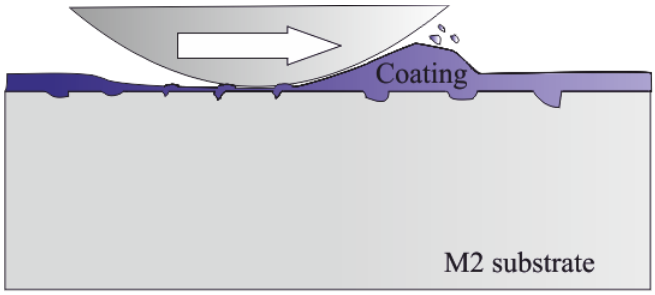

Figure 84: Wear of M2 substrate.

- **Adhesive wear**

Siginificant materials transfers are also observed for the M2 steel (Figure 85 (b) and (f)). With the increase of cycles, the coating and transferred coating are gradually ejected from the contact center (Figure 85 (d) and (e)), but the trapped coating is very difficult to be removed so that it will stay at the contact center (Figure 85 (c)) to provide low friction coefficient. At the same time, some coating near to the contact center can also recirculate in fretting process to accommodate the fretting movement of two contact bodies, leading to a slow growth of friction coefficient (Figure 85 (a)). When trapped coating is removed and no island coating appears at the contact area, some steel debris begins to appear. At this time, the coating totally loses its function. When third layer of steel debris appears, the friction coefficient reaches a stable high level.

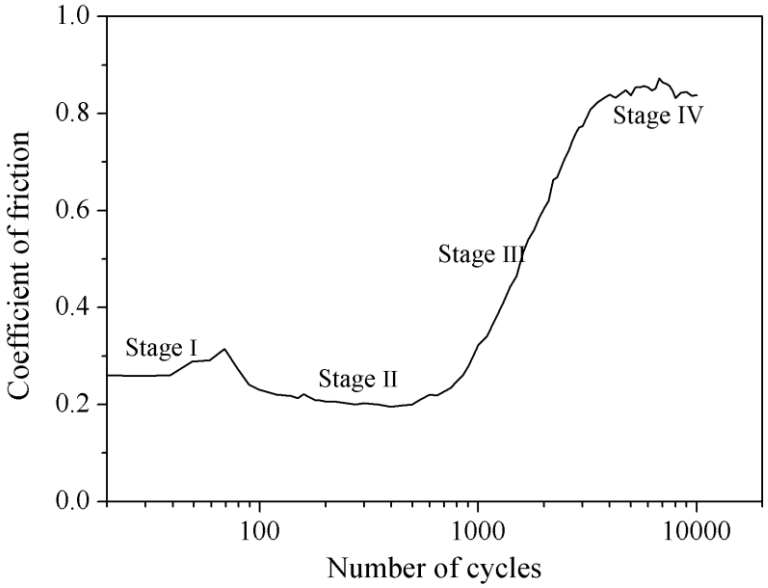

(a) evolution of friction coefficient

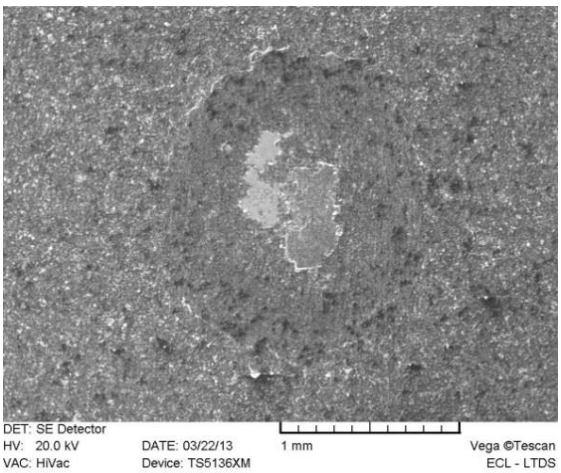

(b) coated M2 substrate at Stage I

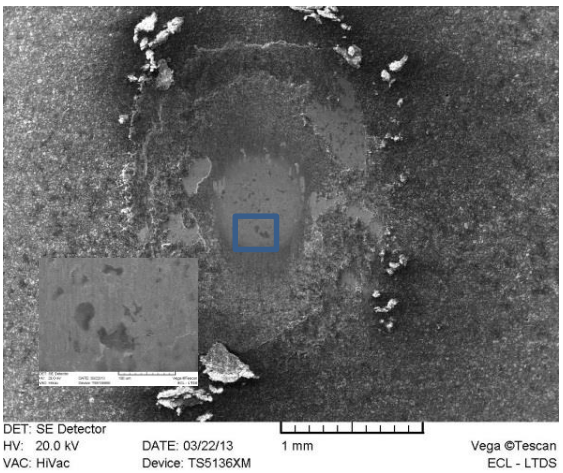

(c) coated M2 substrate at Stage II

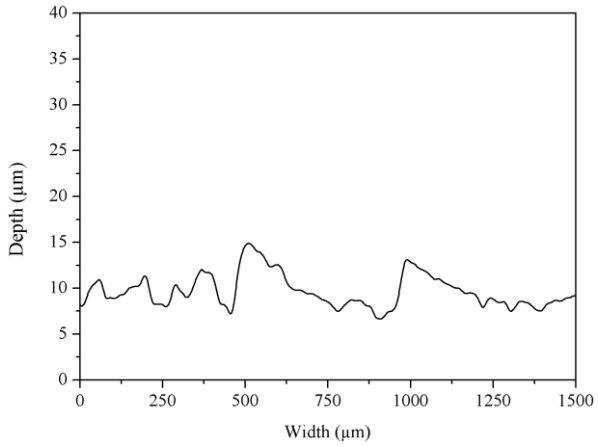

(d) profile for coated M2 substrate at Stage I

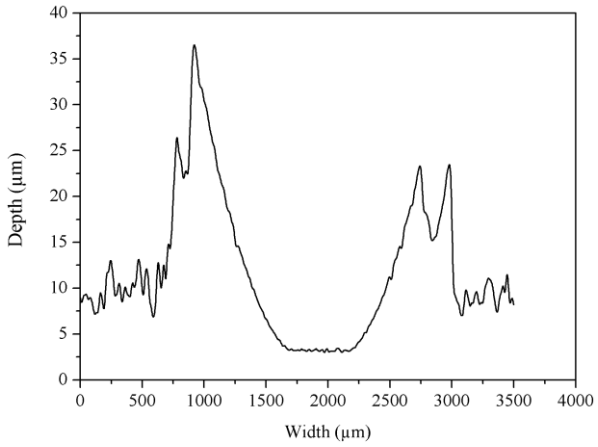

(e) profile coated M2 substrate at Stage II

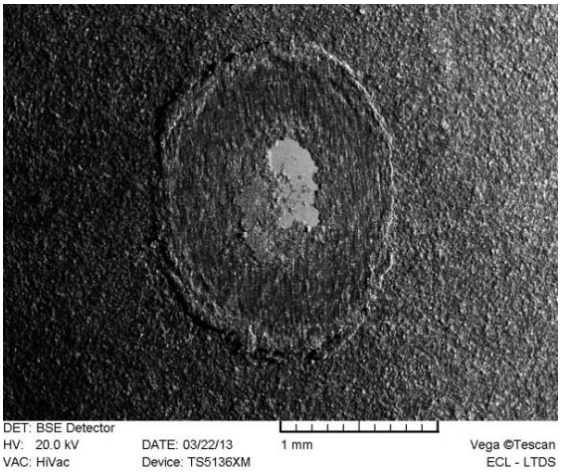

(f) coated ball at stage I

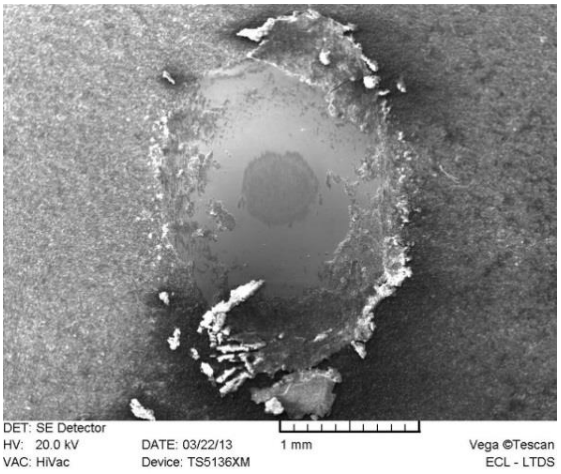

(g) coated ball at stage II

Figure 85: Evolution of friction coefficient and wear scars as a function of cycles for 400 N, ± 25 µm, 1 layer coating, coated both substrate, M2 flat substrate.

IV.3.1.3 Summary of wear mechanism of coating deposited M2 substrate

Comparing the wear mechanism between SS 304 and M2 steel substrates, it can be seen that the trapped coating in the porosity of M2 steel helps maintain the low friction coefficient and it is difficult to be ejected from the contact center, because its ejection includes two steps that is to be squeezed out from the porosity and then to be ejected from the contact center. Similar to SS304, the wear mechanism of cylinder-on-flat is related to abrasive wear and ball-on-flat is related to adhesive wear. The transformation from abrasive to adhesive depends on the contact pressure [44]. When contact pressure is low, it is not possible to form the transfer layer.

IV.3.2 Effect of factors on the friction coefficient

In addition to the requirements of homogeneity of variance across the treatment (combination of different factors), the analysis should be complemented with 1) a run sequence plot of the residuals; 2) a normal probability plot of the residuals; 3) a scatter plot of the predicted values against the residuals [128]. Due to the factor that the experiments are done in a random sequence, it is not necessary to test the relationship between sequence of experiments and residuals. Figure 86(a) and (b) describe its normal distribution and its predicted value with residuals. For its normality, it can be seen that it almost reaches an agreement with the definition of normality that the residuals is scared around the reference line, but several points are little far from the reference line (Figure 86 (a)). Concerning the value of skewness and kurtosis, they shows that the data are little skewed right and a "peak" distributed (Table 25). Skewness is a measure of whether the data are symmetrically distributed. When the value is zero, the data are totally symmetrical. Kurtosis is a measure of whether the data are peaked or flat relative to a normal distribution. If it is larger than 0, the data are peaked and the data are flat when the value is less than 0. Accordingly, the residuals are normally distributed. However, its values of residuals are little smaller when the predicted values are lower than that of when the predicted values are larger. Therefore, it is better to do a transformation to improve the scatter plot of the predicted values against the residuals.

A transformation is used according to the Box-Cox transformation theory. The equation of transformation is shown in Eq. (IV-1) :

$$Trans(\mu) = (\mu^{-0.5} - 1)/(-0.5) \qquad (IV\text{-}1)$$

The comparison of transformed and untransformed results is plotted in Figure 86 when considering all main effects and interactions between two variables. For the normality, the residuals of transformed friction coefficient are better than untransformed one. The points on Figure 86(a) form a nearly linear pattern, which indicates that the normal distribution is a good model for this data set, but some points still vary from this line. Generally, the further the points vary from the reference line, the greater the indication of departures from normality. In this aspect, the transformed data has better normality than untransformed data. Similarly, the distribution of residuals of transformed friction coefficient is more scarred around the centerline.

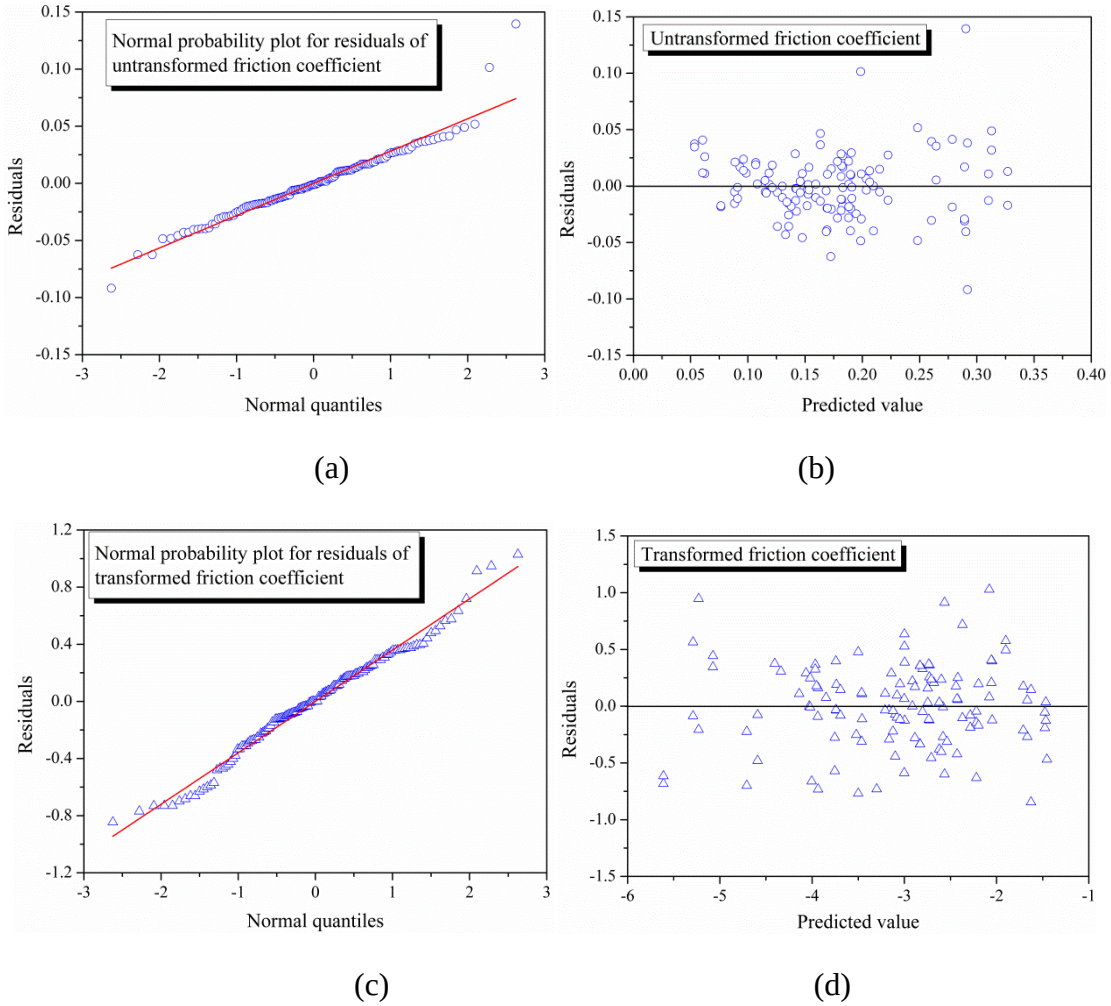

Figure 86: The diagnostics for residuals of untransformed and transformed friction coefficient (a) normal distribution plot for residuals for real value of friction coefficient, (b) the distribution of residuals vs. predicted value for real friction coefficient, (c) normal distribution plot for residuals for transformed value of friction coefficient, (d) the distribution of residuals vs. predicted value for transformed value of friction coefficient.

Table 25: Values of skewness and kurtosis.

	Mean	Skewness	Kurtosis
Residuals of μ	0	0.46	1.42
Residuals of trans (μ)	0	-0.11	-0.19

IV.3.2.1 Comparison of the results with results from Chapter III

Table 26 describes the results of analysis of variance for friction coefficient with two new variables that are thickness and substrate. However, adding two variables does not change prominence of variable. Contact configuration is the most important (percentage contribution is 38.27%) and contact force is following (PC = 29.65%). This is similar to the results in Chapter III. It indicates that the adding two new variables do not affect the friction coefficient significantly. However the prominence of interaction effects is changed a little. The interaction effect between contact force and contact configuration is less than the interaction effect between substrate and thickness and the interaction effect between contact force and substrate.

Table 26: ANOVA for transformed friction coefficient.

Source	DF	SS	MS	*F*	*F* critical	*PC*
Contact force	2	44.34	22.17	124.77	3.07	29.65%
Displacement amplitude	2	0.85	0.43	2.4	3.07	0.34%
Contact configuration	1	56.95	56.95	320.52	3.92	38.27%
Coating position	2	0.95	0.47	2.66	3.07	0.40%
Thickness	1	1.70	1.70	9.59	3.92	1.03%
Substrate	1	0.75	0.75	4.25	3.92	0.39%
Contact force × Contact configuration	2	2.69	1.35	7.58	3.07	1.58%
Contact force × thickness	2	2.23	1.11	6.27	3.07	1.26%
Contact force × substrate	2	3.71	1.85	10.43	3.07	2.26%
Displacement amplitude × contact configuration	2	1.37	0.69	3.86	3.07	0.69%
Displacement amplitude × thickness	2	1.16	0.58	3.26	3.07	0.54%
Displacement amplitude × substrate	2	1.92	0.96	5.39	3.07	1.05%
Contact configuration × thickness	1	1.09	1.09	6.12	3.92	0.61%
Contact configuration × substrate	1	1.58	1.58	8.9	3.92	0.95%
Substrate × thickness	1	5.91	5.91	33.25	3.92	3.86%
Error	119	21.14	0.18			17.13%
Corrected Total	143	148.34				100.00%

IV.3.2.2 Effect of coating thickness

The main effect plot is preferably used to analyze the effect of each variable, because it is appropriate for analyzing data from a designed experiment, where the factors are at two or more levels. Thickness of the coating (from one layer to two layers) changes a little friction coefficient, whose effect on friction coefficient is much less than the effect of contact configuration and contact force (Figure 87).

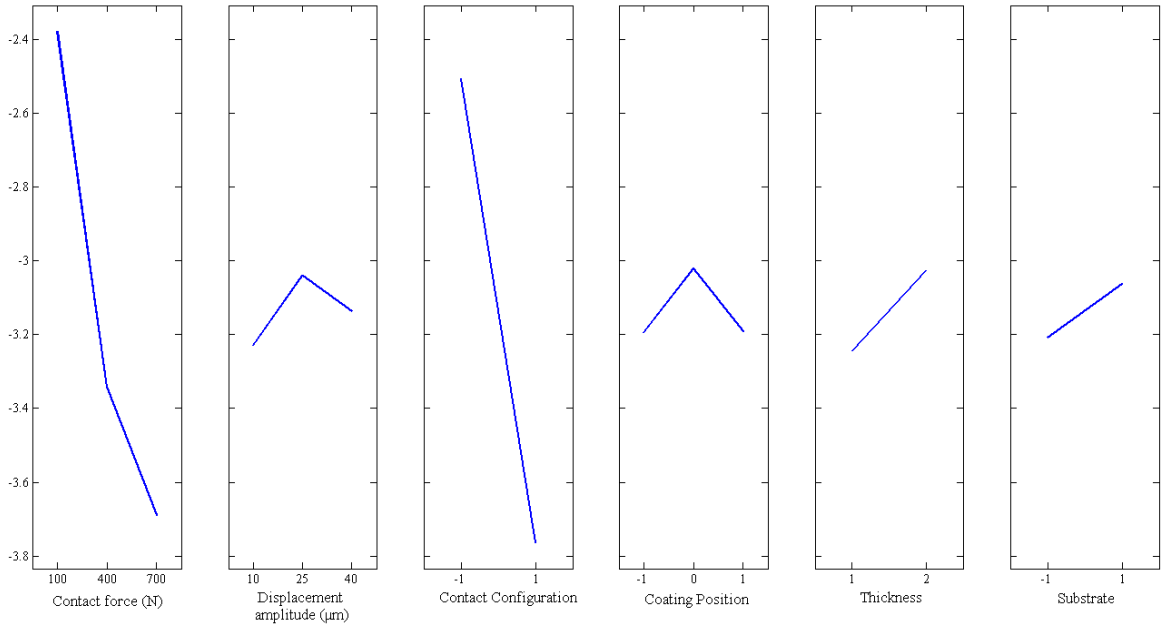

Figure 87: The main effect plot for transformed friction coefficient (contact configuration: -1 for cylinder-on-flat configuration and 1 for ball-on-flat configuration; coating position: -1 for coating on flat, 0 for coating on counterbody and 1 for coating on both flat and counterbody; thickness: 1 for 10 µm and 2 for 20 µm; substrate: -1 for 304 stainless steel, 1 for M2 steel; a transformed value of -3.8 corresponds to a friction coefficient of 0.12 and a transformed value of -2.4 to 0.21).

The friction coefficient in average increases with the increase of thickness (column 5 of Figure 87). Singer [100] states that the friction coefficient is inversely proportional to the mean contact pressure, but the value of contact pressure for different thickness is very similar (Table 27) then it can have rare effect on the friction coefficient. In addition, ploughing is one component of friction coefficient. Generally, thin soft coating leads to less ploughing effect of the film so that friction coefficient decreases with decrease of thickness, but the decrease is not so significant as the effect of contact force and contact configuration.

Table 27: Mean contact pressure obtained by FEM (F_n=100 N, substrate= SS 304).

Contact configuration	Thickness	Maximum contact pressure (MPa)	Contact radius (µm)	Mean contact pressure (MPa)
Ball-on-flat	1 layer (10 µm)	670.8	329.7	447.2
	2 layers (20 µm)	671.0	331.8	447.3
Cylinder-on-flat	1 layer (10 µm)	501.0	293.7	393.3
	2 layers (20 µm)	508.3	297.0	399.0

IV.3.2.3 Effect of substrate nature

According to column 6 of Figure 87, substrate can also affect the friction coefficient a little bit. Due to the fact that elastic modulus of M2 is a litter bit higher than that of SS 304, the mean contact pressure is higher with M2 steel substrate than that of 304 stainless steel substrate (Figure 88), but the difference is not significant. Therefore, the increase of friction coefficient of M2 can be explained by the product of shear strength of interface and the real contact area, which is related to the deformation properties of the substrate [17]. If the coating is thick enough, the influence of roughness of substrate can be ignored. However, its influence is significant for the thin coating, due to the reduction of true contact area. In addition, the penetration of

asperities through the film is also a reason, which leads to the increase of shear resistance and ploughing of either the substrate or counterface and thus to an increase of friction coefficient [17]. Due to the porosity at the surface of M2, the roughness of M2 substrate is higher than that of SS 304 even with same polishing process (as shown in Table 28 and Figure 89).

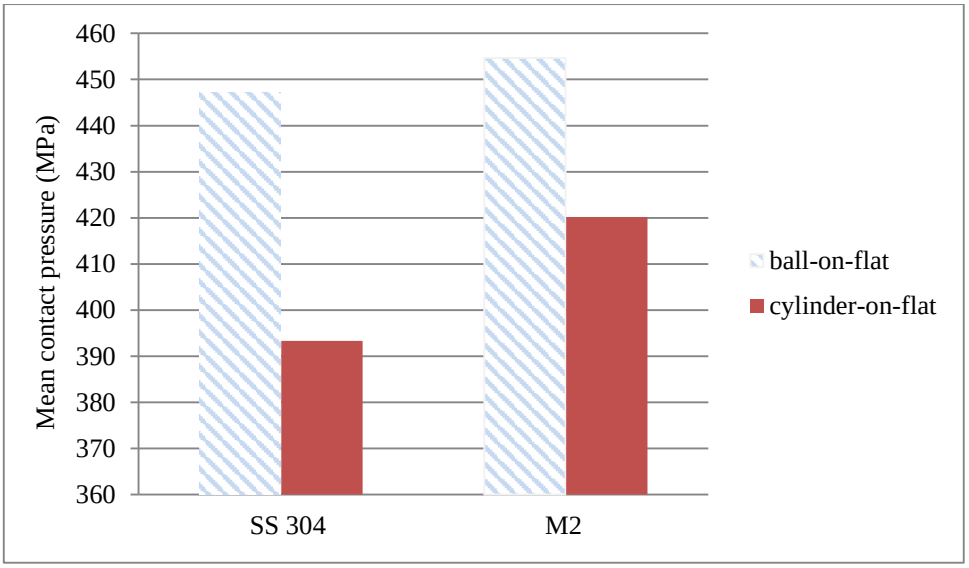

Figure 88: Mean contact pressure for one layer of coating on different substrates.

Table 28: Roughness of coating (R_a) for different thicknesses and substrates.

Substrate	no coating (µm)	1 layer (µm)	2 layers (µm)
SS 304	0.025 ± 0.01	0.47±0.04	1.29±0.14
M2	0.1 ± 0.0	1.08±0.08	0.9± 0.05

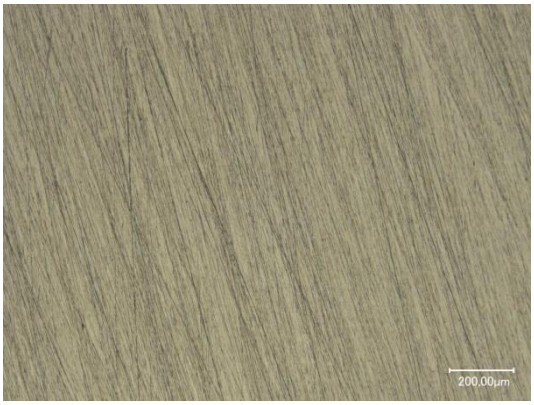

(a) SS 304 steel flat

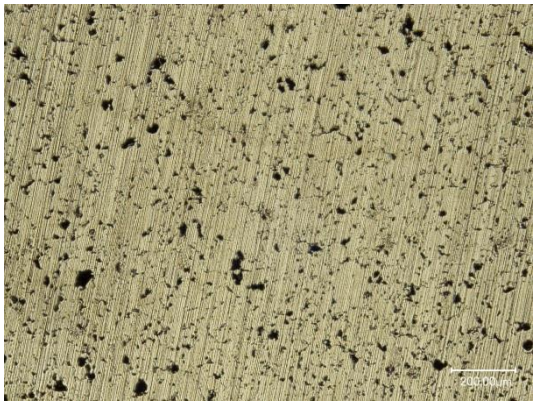

(b) M2 steel flat

(c) AISI 52100 cylinder

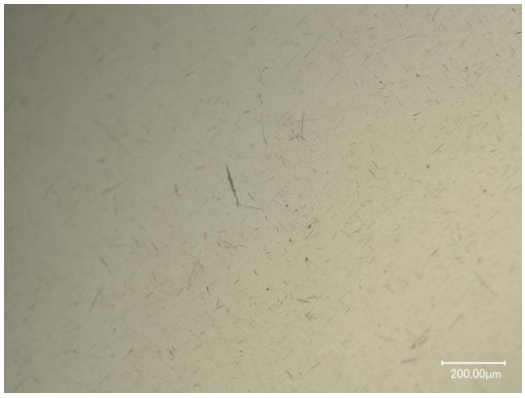

(d) AISI 52100 ball

Figure 89: Optical image of substrates: (a) SS 304 substrate, (b) M2 steel flat; (c) AISI 52100 steel cylinder; (d) AISI 52100 steel ball.

IV.3.2.4 Effect of coating position

In this study, coating the counterbody (ball or cylinder) can induce a little bit higher friction coefficient compared with other two coating positions (coating the flat substrate or coating both counterbodies), as shown in column 4 in Figure 87. This is due to different surface textures (Figure 89). SS 304 flat substrate and AISI52100 cylinder present unidirectional grinding marks with a roughness value of 0.07 ± 0.02 while M2 does present unidirectional grinding marks with some porosity. The ball has an isotropic roughness with a value of 0.04 ± 0.01. If the coating can slide across the unidirectional-grinding, the coating should flow over the asperities, inducing higher levels of stress and a more pronounced plane strain conditions. If coated ball or cylinder can slide parallel to the unidirectional-grinding, the coating may flow along the valleys of steel plate and thereby leading to low shear stress. For friction occurring with isotropic surface, the shear stress required is lower than across the unidirectional-grinding [138]. According to Figure 89 (a) and (b), it can be seen that the flat substrate may induce rather high shear stress, because the coated ball slides across the unidirectional-grinding with an angle. Generally, the coated ball or cylinder may have a little higher friction coefficient than coated flat. However, the contribution of effect of coating position for friction coefficient is as small as 0.4% (Table 26), whose value is a little higher than the value in Chapter III (Table 19). This may be explained by the higher friction coefficient of M2 steel at ±10 µm (line 2, column 4 of

Figure 90) when the coating is on the counterbody, which increases the average value of friction coefficient for all experiments in this chapter.

IV.3.2.5 Interaction between variables

In addition to the main effect plot, the interactive plot can also serve as an effective method to do the analysis for designed experiment, with aim to describe the interaction relationship with different variables (Figure 90). Three curves of the graph of the second row and first column of Figure 90 are curves of evolution of transformed friction coefficient *vs.* normal force (from 100 N to 700 N) for 3 different displacement amplitudes (± 10 µm, ± 25 µm and ± 40 µm); and 3 curves of the graph of the first row and second column of Figure 90 are those of evolution of transformed friction coefficient *vs.* displacement amplitude (from ± 10 µm to ± 40 µm) for 3 different normal forces (100 N, 400 N and 700 N).

According to the analysis of variance, it can be seen that the interaction between substrate and thickness and between substrate and contact force are significant.

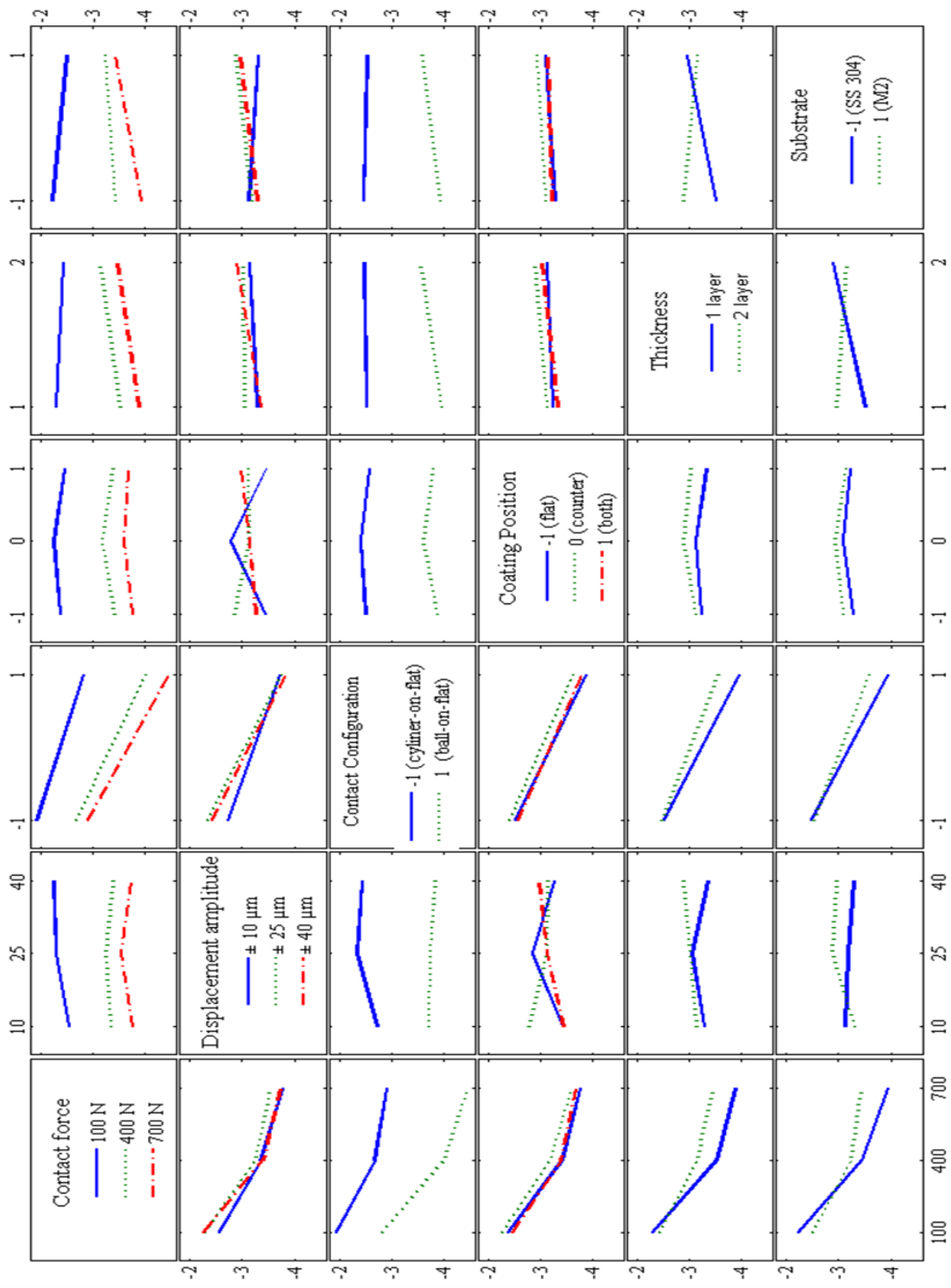

Figure 90: Interactive map of transformed friction coefficient under different test parameters (contact configuration: -1 for cylinder-on-flat configuration and 1 for ball-on-flat configuration; coating position: -1 for coating on flat, 0 for coating on counterbody and 1 for coating on both flat and counterbody; thickness: 1 for 10 µm and 2 for 20 µm; substrate: -1 for 304 stainless steel, 1 for M2 steel; a transformed value of -3.8 corresponds to a friction coefficient of 0.12 and a transformed value of -2.4 to 0.21).

■ **Interaction between thickness and substrate**

Considering its interaction effect with other variables, it can be seen that the substrate has a significant interaction with thickness. When the substrate is SS 304, the increase of thickness leads to an increase of friction coefficient, but the increase of thickness barely changes the friction coefficient when the substrate is M2 (line 6, column 5 of Figure 90). Therefore, it induces a significant effect of this interaction.

For M2 substrate, it almost shares the same friction coefficient for different thicknesses (Figure 91), because the difference of roughness for various thicknesses of M2 is very small (Table 28) so that increase of thickness affectless to the friction coefficient. In the case of SS 304 substrate, the increase of thickness also increases the roughness significantly. Therefore, it significantly increases the slop angle of asperities, leading to the increase of friction coefficient [89].

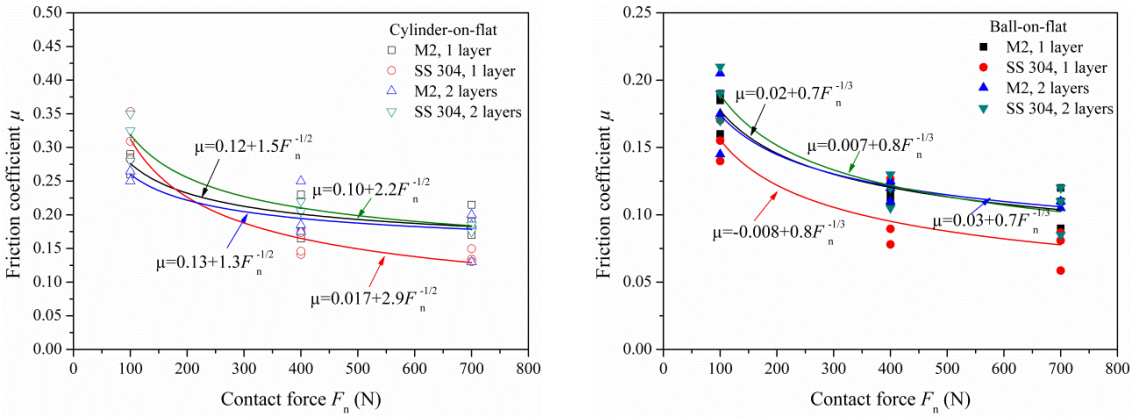

Figure 91: Evolution of friction coefficient as a function of contact force under different contact configurations (data for all coating positions).

■ **Interaction between contact force and substrate**

In addition, there is a significant interaction between substrate and contact force on the friction coefficient. When contact force is low (100 N), the friction coefficient of coating on SS 304 is higher than that on M2 (line 6, column 1 of Figure 90). Figure 91 describes the evolution of friction coefficient as a function of contact force in details. According to the equations in Figure 91, it can be seen that the decrease rate of friction coefficient of coating deposited on SS 304 as a function of contact force is faster than that of M2, leading to a significant interaction between contact force and substrate. For coating on the M2 under cylinder-on-flat, it is a combination of wear mechanisms of both abrasive wear and fatigue wear of trapped coating. Fatigue wear is the main mechanism, so the decrease of friction coefficient is less dependent on the wear mechanism transformation from abrasive wear to adhesive wear due to increase of contact pressure. Therefore, the decrease rate of friction coefficient is less than that of SS 304, which only consists of abrasive wear and adhesive wear.

IV.3.3 Summary of analysis of friction coefficient of the coating

Friction coefficient is mainly influenced by the contact configuration and the contact force. The effect of two factors, substrate and thickness, seem to be less than the effect of the previous two factors on the evolution of friction coefficient. It is because the friction coefficient is inversely

proportional to the contact pressure and the contact pressure is only dependent on the contact force and contact configuration. The porosity in substrate can induce increase of shear stress, leading to a little increase of friction coefficient. High thickness can increase ploughing effect in the friction coefficient, but it does not change the contact pressure significantly.

IV.4 Lifetime of the coating

One of the purposes of this study is to study the influence of substrates and thickness on the coating lifetime. In this part, the comparison of coating position and other test parameters is made by the analysis of variance and survival analysis.

Figure 92 describes the distribution of residuals of coating lifetime. It can be seen the distribution of lifetime is deviant from the reference line (Figure 93 (a)). In addition, the residuals increase with increased lifetime of coatings (Figure 92(b)). Due to the non-normal distribution of residuals of coating lifetime and the linear relationship between the predicted value and residuals, it is necessary to do a transformation according to the Box-Cox transformation. The equation of transformation is shown in Eq. (IV-2):

$$Trans(Nc) = (Nc^{-0.25} - 1)/(-0.25) \qquad \textit{(IV-2)}$$

The values of residuals after transformation on Figure 92 (c) form a nearly linear pattern, which indicates that the normal distribution is a good model for the transformed durability. After transformation, the residuals is scattered around the reference line instead of linear relationship (Figure 92 (d)).

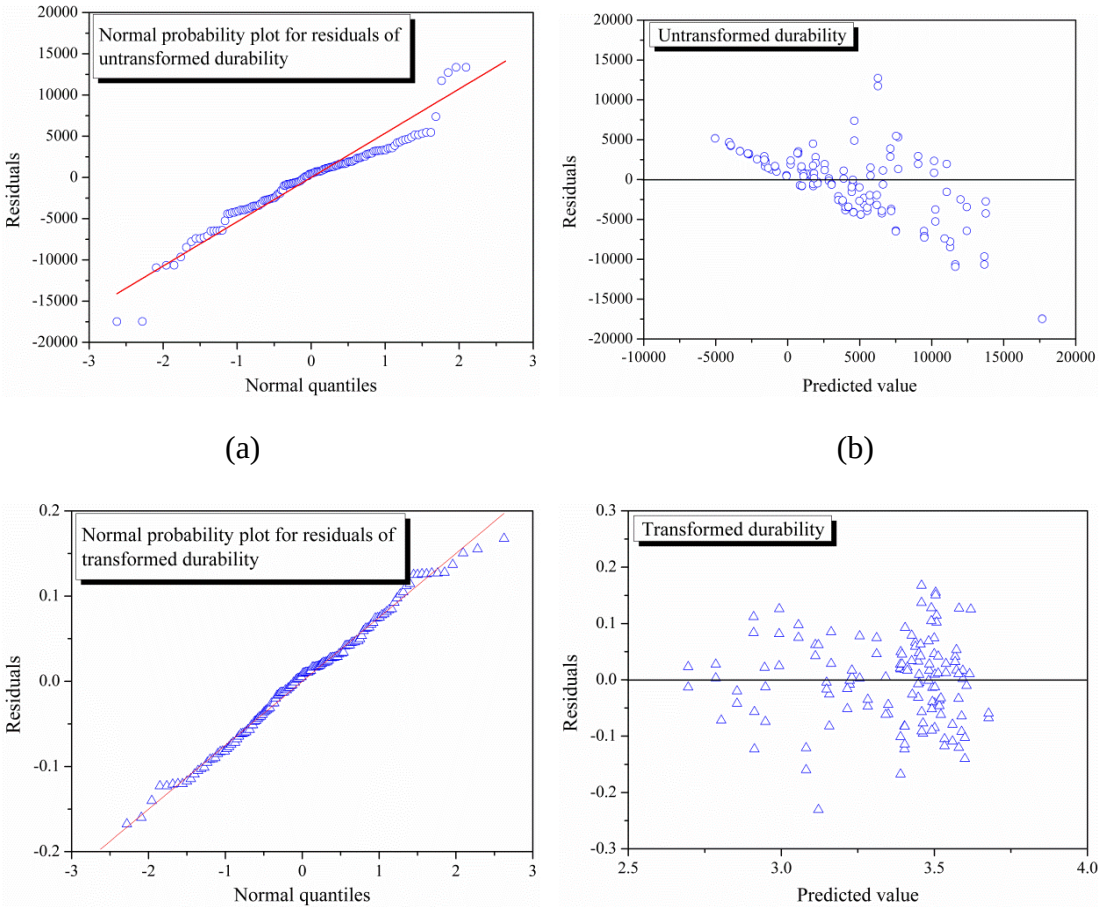

Figure 92: The diagnostics for residuals of untransformed and transformed durability (a) normal distribution plot for residuals for real value of coating lifetime, (b) the distribution of residuals vs. predicted value for real coating lifetime, (c) normal distribution plot for residuals for transformed value of coating lifetime, (d) the distribution of residuals vs. predicted value for transformed value of coating lifetime.

Table 29: Values of skewness and kurtosis.

Residuals	Mean	Skewness	Kurtosis
Residuals of N_c	0	1.09	6.70
Residuals of trans (N_c)	0	-0.14	-0.13

IV.4.1 Effect of substrate nature and coating thickness on the coating lifetime

IV.4.1.1 Comparison the results with results of Chapter III

Contrary to the analysis of friction coefficient the prominence of variables of coating lifetime is changed a lot when the two new variables, substrate nature and coating thickness, are considered (Table 30).

Table 30: Analysis of variance for transformed coating durability.

Source	DF	SS	MS	*F*	$F_{critcal}$	PC
Contact force	2	0.01	0.01	0.57	3.07	-0.11%
Displacement amplitude	2	0.42	0.21	21.40	3.07	4.56%
Contact configuration	1	2.21	2.21	224.91	3.92	25.09%
Coating position	2	0.08	0.04	4.13	3.07	0.69%
Thickness	1	0.00	0.00	0.16	3.92	-0.10%
Substrate	1	2.63	2.63	268.24	3.92	29.94%
Contact force × Configuration	2	0.36	0.18	18.35	3.07	3.88%
Contact force × Amplitude	4	0.08	0.02	1.95	2.43	0.40%
Displacement amplitude × Contact configuration	2	0.07	0.03	3.44	3.07	0.53%
Displacement amplitude × Coating position	4	0.08	0.02	2.16	2.43	0.49%
Displacement amplitude × substrate	2	0.12	0.06	6.32	3.07	1.18%
Contact configuration × Coating position	2	0.09	0.05	4.83	3.07	0.85%
Contact configuration × Substrate	1	1.37	1.37	139.18	3.92	15.48%
Substrate × Thickness	1	0.03	0.03	2.56	3.92	0.17%
Error	116	1.21	0.01			16.96%
Corrected Total	143	8.76				100.00%

It can be seen that some percentage contribution (PC%) is less than 0, indicating this variable is not significant. Contact force and thickness have the ignorable effect on the coating lifetime. In contrast, substrate, contact configuration and displacement amplitude have the most significant effect on the coating lifetime. This reaches an agreement with Chapter III, in some extent, that the contact configuration can bring a significant effect on lifetime, followed by displacement. This is because the contact configuration is related to different wear mechanisms. When the contact pressure is low, the wear mechanism is dominated by abrasive wear. With increasing contact pressure, the amount of transfer layer increases and the wear mechanism changes to adhesive wear. Wear mechanism is responsible for the durability of coating. In this study, the transfer layer made of coating can lubricate the mating parts and provide the interface with lower friction coefficient. Generally, the contact configuration of cylinder-on-flat (dominated by abrasive wear) has rather lower durability than ball-on-flat (dominated by adhesive wear). Displacement amplitude controls the ejection rate of wear particles so that its prominence should be lower than contact configuration.

IV.4.1.2 Effect of coating thickness

The main effect plot in Figure 93 describes the evolution of durability as a function of various parameters. Increasing thickness bring an ignorable increase of coating lifetime when it is compared with the effect of other variables. The real value of coating lifetime is corresponding to the transformed value of coating lifetime.

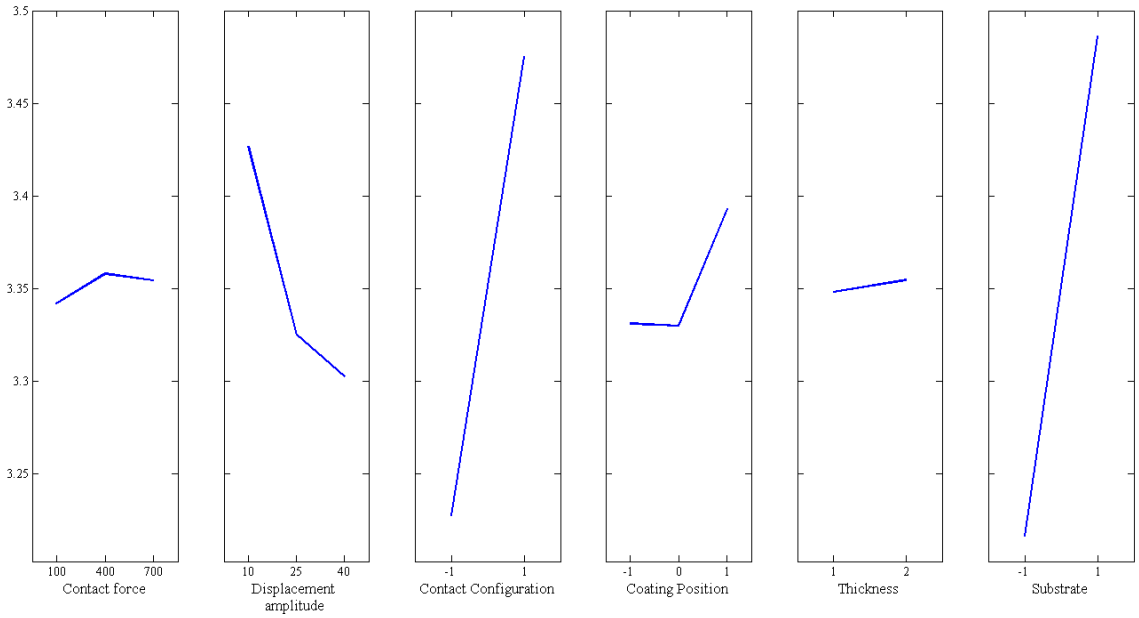

Figure 93: Main effect plot for transformed durability (contact configuration -1=cylinder-on-flat, 1= ball-on-flat; coating position -1= flat, 0=counterbody, 1=both; thickness 1=10 µm, 2= 20 µm; substrate -1=SS 304, 1= M2; a transformed value of 3.25 means a coating lifetime of 809 cycles, a transformed value of 3.5 means a coating lifetime of 4096 cycles).

Generally, increase of wear depth is attributed to three factors i.e. elastic deformation, plastic deformation and material removal. Large plastic deformation may induce the breakage or wear of coating. FEM predicts the maximum plastic equivalent strain for different thicknesses, which is related to degree of plastic deformation [139]. A small value of plastic equivalent strain means a less plastic deformation. According to the analysis of FEM, the thicker coating demonstrates a similar plastic deformation resistance as the thinner coating (Figure 94) with the similar PEEQ (equivalent plastic strain) value of around 0.5. If the value PEEQ is larger than 0, it indicates the plastic deformation occurs. This result is different from the modeling of Wang *et al.* [139] that the thicker soft coating (PEEK) can have better resistance to plastic deformation. This is because the PEEK materials have higher hardness than the MoS_2-based varnish coating. Therefore, the increase of thickness has less influence on the very soft coatings. However, in this study, the plastic deformation only accounts for a very small fraction of wear depth, because a large normal pressure has made the total plastic deformation to occur in most cases. Accordingly, materials loss accounts for a very large fraction of wear depth or coating lifetime. Materials loss is dominated by the wear mechanism and different thicknesses have the same wear mechanism so that various thicknesses may have no effect on lifetime. However, it is observed from Figure 93 that the increase of thickness induces a little increase of durability. It is because that two layers coating may give more low friction materials to be worn than one layer coating.

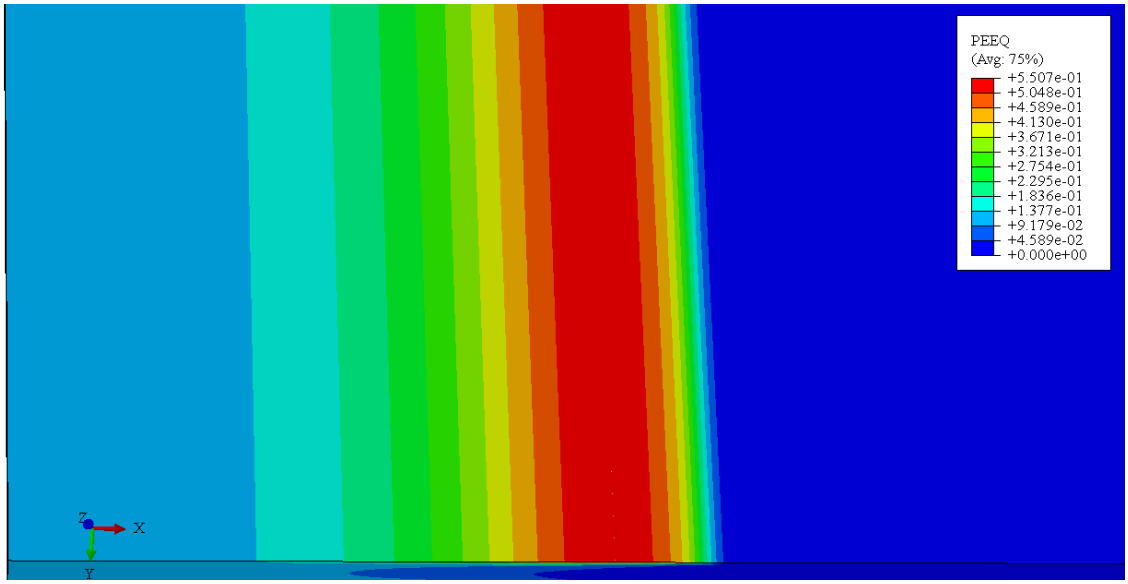

(a) one layer

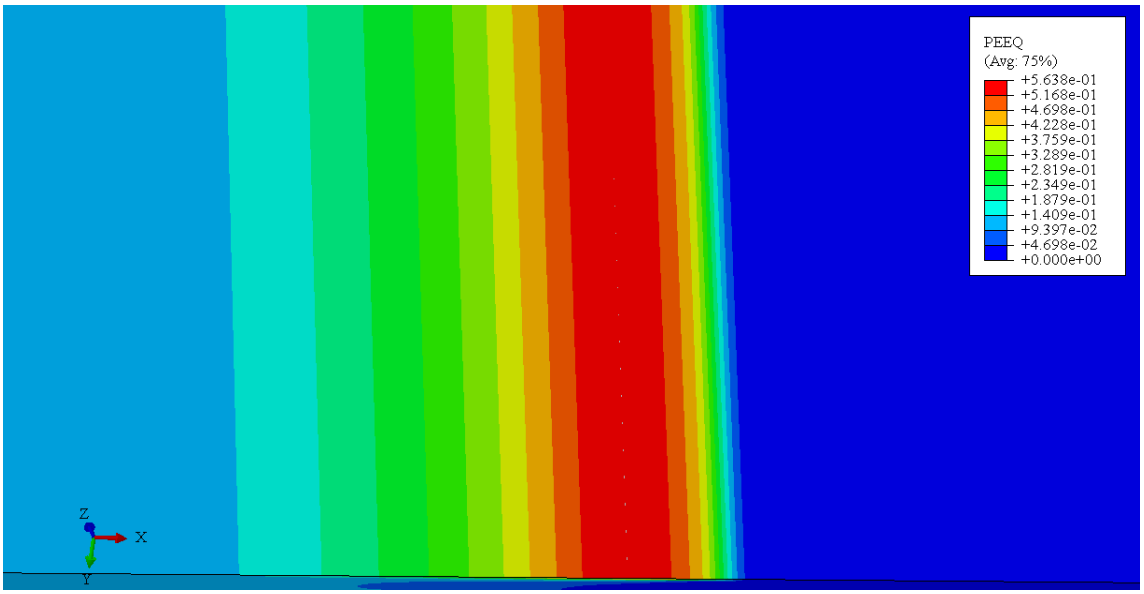

(b) two layers

Figure 94: Predicted strain distribution of coated M2 sample for one layer coating (a) and two layers coating (b) under cylinder-on-flat configuration (100 N, top-view of coating at the interface of coating and substrate).

IV.4.1.3 Effect of substrate nature

Generally, the wear behavior of coating can be influenced by substrate from several aspects such as hardness, elastic modulus and substrate surface structure. For example, hardness of substrate can affect the distribution of contact stress. In other words, the high hardness will delay the plastic deformation of substrate and micro-cracking of coatings as well as the size of the plastically deformed zone [140]. Finally, high hardness can delay the delamination, coating damage and material loss. High elastic modulus of substrate can affect the stress distribution in the coatings if the coating thickness is far lower than the contact radius. In this study, the mechanical properties of the two flat substrates are similar so that hardness and elastic modulus are not prominent reasons for lifetime. Instead, the surface structure of the substrate significantly affect the coating durability, because different structures of substrate can improve

or weaken the adhesion between coating and substrate, and the flow of coating debris [141]. For the substrate with porosity, the porosity can hold some varnish under the fretting movement, thereby providing longer lifetime (Figure 95). Compared with the SS 304 substrate, it is very difficult to eject the coating from porosity so that it can accommodate the wear process and maintain the low friction coefficient.

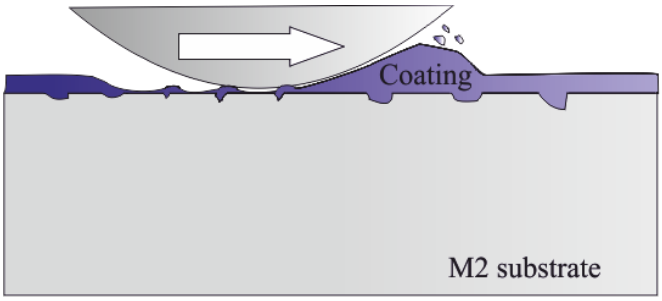

(a) wear for coating on M2 steel substrate

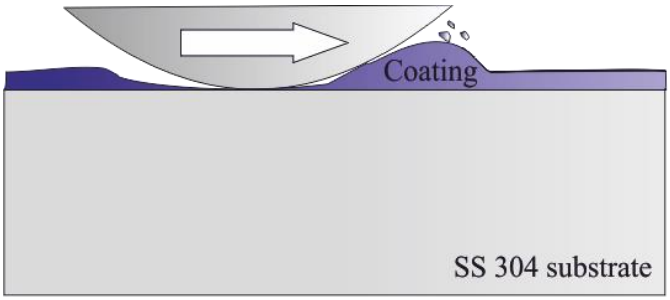

(b) wear for coating 304 stainless steel

Figure 95: Schematic of wear process: (a) wear for coating on M2 substrate; (b) wear for coating SS 304 substrate.

IV.4.1.4 Interaction effect between two variables

Figure 96 describes the interaction effects between two variables. It can be seen that the interaction between coating positions and thickness, the interaction between substrate and coating position and interaction between substrate and contact configuration are significant.

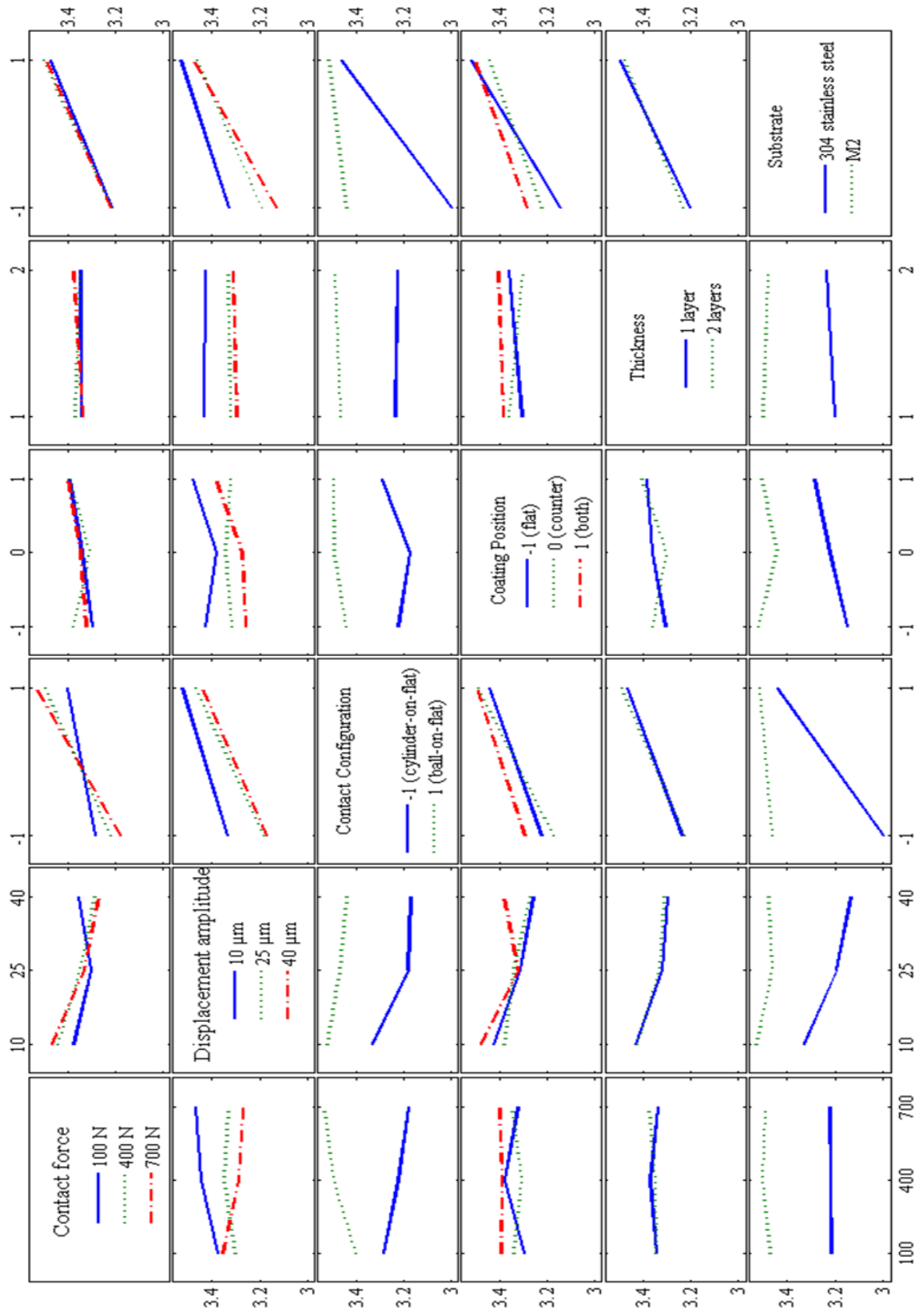

Figure 96: Interactive plot for transformed durability (contact configuration -1=cylinder-on-flat, 1= ball-on-flat; coating position -1= flat, 0=counterbody, 1=both; thickness 1=10 µm, 2= 20 µm; substrate -1=SS 304, 1= M2; a transformed value of 3 means a coating lifetime of 256 cycles, a transformed value of 3.4 means a coating lifetime of 1975 cycles).

■ **Interaction effect between coating position and thickness**

In Chapter III, we stated that coating the ball or cylinder and both counterbodies leads to longer durability than coating the flat. Figure 96 (line 4, column 5) shows that this conclusion is still available for one layer, but it does not work for two layers. In the case of two layers, coating both counterbodies leads to longer durability, followed by coating the flat and coating on counterbody. This is induced by two layers coating on the M2 steel substrate, as shown in Figure 97. For two layers of coating, it has lower coating lifetime when coating is deposited on the counterface AISI 52100 than coatings deposited on M2 substrate.

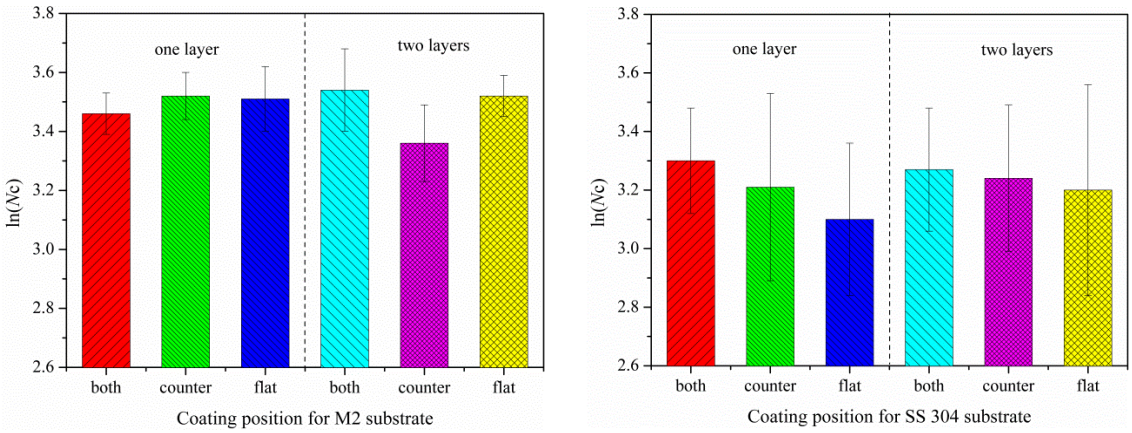

Figure 97: Comparison of coating lifetime under different coating positions, thicknesses and substrates (a transformed value of 2.6 means a coating lifetime of 67cycles, a transformed value of 3.2 means a coating lifetime of 625 cycles, a transformed value of 3.8 means a coating lifetime of 160000 cycles).

■ **Interaction between substrate and coating position**

Generally, it is considered that coating the flat has longer durability than coating the counterbody (line 6, column 4 in Figure 96). When considering the effect of thickness, the results are a little bit different. Figure 97 describes the lifetime of coating on M2 substrate under different thicknesses for different coating positions. It can be seen that the lifetime of one layer coating for different coating positions is similar, but the lifetime of two layers coating on the counterbody is significantly lower than that on the two other coating positions. It may be explained by that the function of substrate with curvature is decreased. When the layer is one, the coating on substrate with curvature can maintain more coating debris on the contact area, thereby prolonging the coating lifetime. This can be proved by the case of SS 304 steel substrate in Figure 97. However, with the increase of thickness of coating, the advantage of curvature is decreased. The difference of coating lifetime for SS 304 substrate among three coating positions is not so significant as the one of one layer coating, because the total volume of coating debris is increased due to the increase of coating thickness. However, the volume of coating debris is limited between two contact bodies so that there is no significant difference between three coating positions. For the case of M2 substrate, it is the same case. The volume of coating is increased as a function of thickness of coating and the advantage of coating on substrate with curvature is decreased. At the same time, the coating debris can be trapped in the porosity in M2 substrate. However, this kind of trapped coating debris is easy to be squeezed out from the porosity because it does not form an adhesive force between coating and substrate during the

deposition. Therefore, there is a lower coating lifetime on the counter body for M2 substrate with two layers coating than that of the other two coating positions.

- **Interaction between substrate and contact configuration**

If the fretting movements occur on the SS 304 substrate, the change of contact configuration leads to a significant change of durability, because the cylinder-on-flat configuration is dominated by the abrasive wear and ball-on-flat configuration is dominated by adhesive wear. A difference in the wear mechanism is the most important factor for materials loss so that it effect greatly determines the lifetime of coatings.

However, the change of durability induced by different contact configurations for M2 is small, because of the competition between lubricating function of embedded coatings and abrasive wear. Under cylinder-on-flat configuration, the contact pressure may be large enough to make the coating deform plastically, but it is not enough to squeeze the trapped coating from the M2 substrate. Instead, the squeezing process of embedded coating may result from the cyclic loading or fatigue so that it will not stay in the porosity and lubricate the contact area until fatigue occurs. Therefore, the case of M2 has significant longer durability than that of 304 stainless steel.

IV.4.2 Survival analysis

Survival analysis (also called reliability analysis) is also employed in this study to compare the survival probability under different test parameters such as contact force, displacement amplitude, contact configuration, coating position, thickness of coating and substrate nature. The Weibull distribution is also used to predict the distribution of survival probability.

IV.4.2.1 Non-parametric survival analysis

Kaplan–Meier (KM) survival curve is used to describe probabilities of survival at given survival time and failure status information on a sample of subjects. Figure 98 to Figure 105 show the comparison of survival probability of the coating under different test conditions. Log-rank test and the Wilcoxon test give the test of whether the survival probabilities are same for different treatment. If the value of probability > chi-square is less than 0.05, it means that the assumption (the survival probabilities are same for different treatment) is rejected and the treatment induces the change of survival probability. Log-ranks test rejects assumption, while Wilcoxon test accepts the assumption. It can explain that the difference between the levels of treatment occurs in later failure events in time ant no difference between the levels of treatment occurs in earlier failure events in time, since the Wilcoxon test gives more weight to early times than to late times and it is less sensitive than log-rank test to the difference occurring at later events in time. If both values are less than 0.05, their individual value chi-square can be employed to distinct the deviance degree between earlier survival rate and later survival rate. The likelihood-ratio tests the assumption that the event time has an exponential distribution. If the value of Pr > chi-square is more the 0.05, the assumption is rejected.

Generally, the results of KM seem to be in agreement with the main effect plot of lifetime, but it gives some information in detail.

■ Effect of substrate

M2 substrate presents better survival ability than SS 304 substrate (Figure 98). At the same cycle, the failure events in the group of M2 substrate are less than in the group of SS 304. The mean lifetime of M2 give the value 3 times as many as mean lifetime of SS 304 (Figure 98). In addition, the Wilcoxon test yields a higher chi-square value than the log rank test for the performance of two substrates. The curves of M2 and SS 304 are further apart in the early part in time before becoming closer later. This can also be due to the porosity in M2 substrate, which significantly improves the survival rates in the cylinder-on-flat (Figure 99). Due to the trapped coating that accommodates the fretting movement and maintains the low friction for cylinder-on-flat, the survival probability of cylinder-on-flat is greatly improved in the case of M2, similar to the survival probability of ball-on-flat for the case of SS 304.

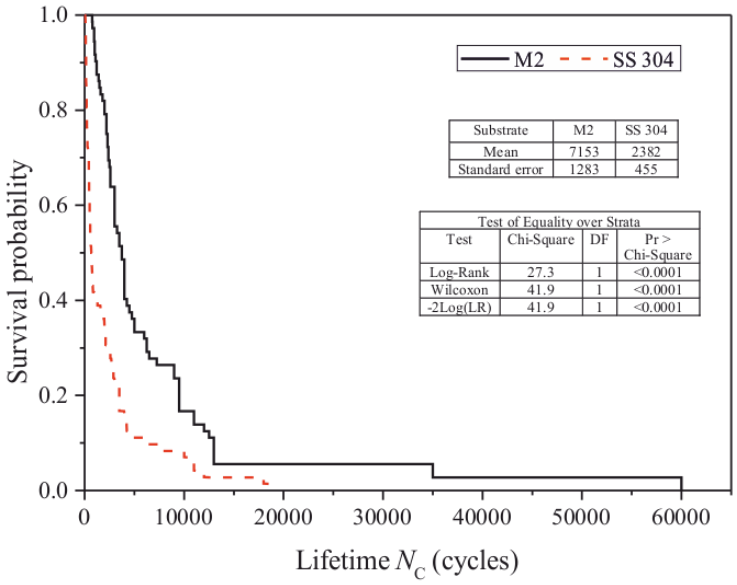

Substrate	M2	SS 304
Mean	7153	2382
Standard error	1283	455

Test of Equality over Strata			
Test	Chi-Square	DF	Pr > Chi-Square
Log-Rank	27.3	1	<0.0001
Wilcoxon	41.9	1	<0.0001
-2Log(LR)	41.9	1	<0.0001

Figure 98: Kaplan-Meier survival curves for different substrates.

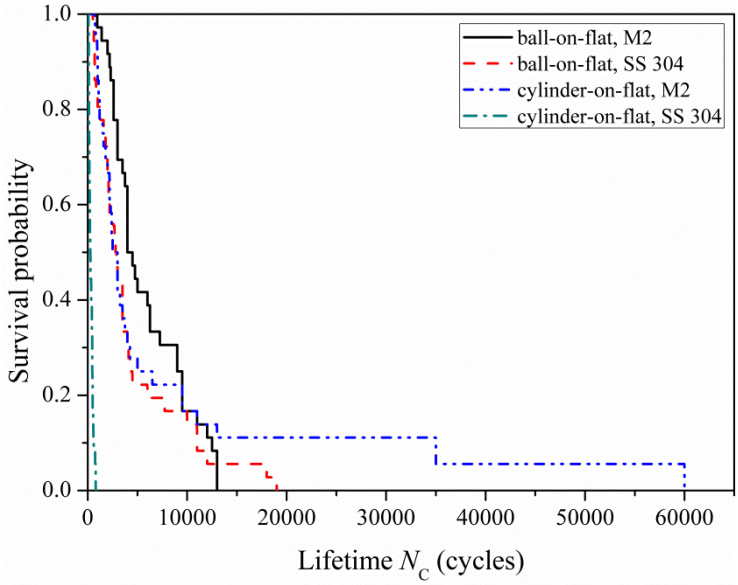

Figure 99: Kaplan-Meier survival curves for different substrate and contact configurations.

■ Effect of contact configuration

Figure 100 describes the survival distribution under different contact configurations. All the tests of coatings under ball-on-flat configuration also has better survival rate than that cylinder-on-flat due to the different wear mechanisms, except for two points (it will be explained later). Comparing the values of Wilcoxon test and log-rank test, it shows that the difference in early part in time is larger than in the later time.

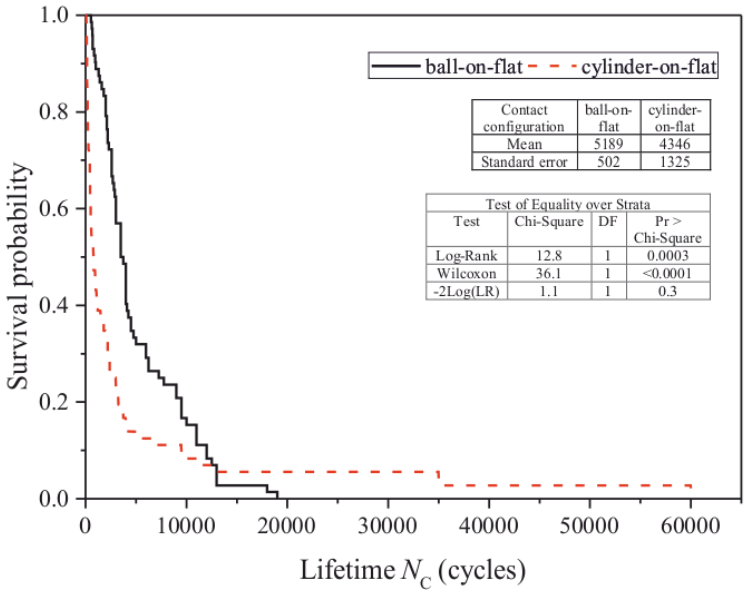

Contact configuration	ball-on-flat	cylinder-on-flat
Mean	5189	4346
Standard error	502	1325

Test of Equality over Strata

Test	Chi-Square	DF	Pr > Chi-Square
Log-Rank	12.8	1	0.0003
Wilcoxon	36.1	1	<0.0001
-2Log(LR)	1.1	1	0.3

Figure 100: Kaplan-Meier survival curves for different contact configurations.

■ Effect of displacement amplitude

Displacement amplitude of ± 10 µm leads to a higher survival rate than the other two displacement amplitudes (Figure 101), because increased displacement amplitude can facilitate the ejection of wear particles. In the early part in time, the displacement amplitude seems to have no effect on the survival rate because three curves are closer to each other before 500 cycles. The most failure events before 500 cycles are induced by the cylinder-on-flat configuration for SS 304 substrate. It indicates that the change of displacement amplitude cannot do a great contribution to the durability when ploughing effect is prevailing, because the wear particles are easy to be ejected in this case. Concerning later part of three curves, the survival rate of ± 25 µm is almost similar to ± 40 µm. It indicates that the ejection rate is increased when the displacement is increased from ± 10 µm to ± 25 µm, but it arrives to the maximum ejection rate at displacement amplitude of ± 25 µm. In other words, the survival rate will be barely changed with increase of displacement amplitude when the displacement amplitude is more than ± 25 µm.

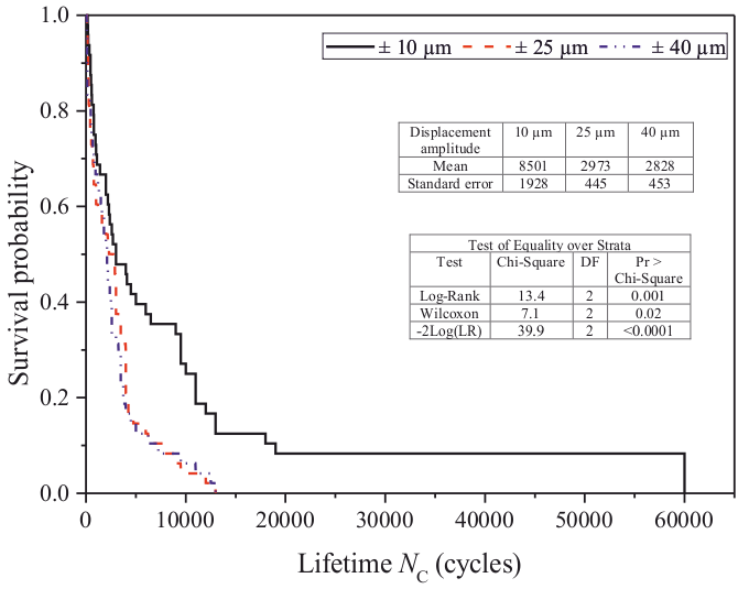

Displacement amplitude	10 µm	25 µm	40 µm
Mean	8501	2973	2828
Standard error	1928	445	453

Test of Equality over Strata			
Test	Chi-Square	DF	Pr > Chi-Square
Log-Rank	13.4	2	0.001
Wilcoxon	7.1	2	0.02
-2Log(LR)	39.9	2	<0.0001

Figure 101: Kaplan-Meier survival curves for different displacement amplitudes.

■ Effect of thickness

The difference between different thicknesses is not so significant, because the equation probability for different thicknesses is larger than 0.05 (Figure 102). Log-rank test yields a higher chi-square value than Wilcoxon test. The two curves being compared are closer before 5000 cycles and then become apart after 5000 cycles.

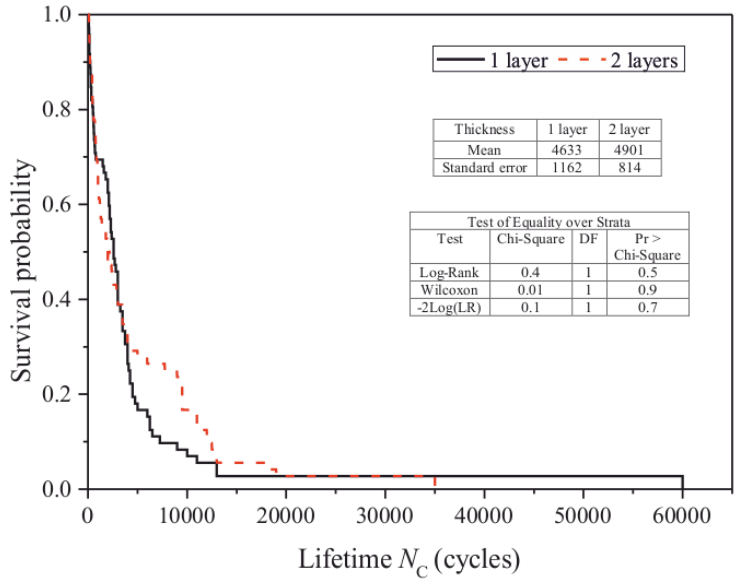

Thickness	1 layer	2 layer
Mean	4633	4901
Standard error	1162	814

Test of Equality over Strata			
Test	Chi-Square	DF	Pr > Chi-Square
Log-Rank	0.4	1	0.5
Wilcoxon	0.01	1	0.9
-2Log(LR)	0.1	1	0.7

Figure 102: Kaplan-Meier survival curves for different thicknesses.

■ Effect of contact force

Although the contact force is not a significant factor when it is compared with substrate and displacement amplitude, Figure 103 proves that it still can make a very small contribution to the lifetime. The decline rate of survival probability for 100 N is a little faster than 400 N and 700 N.

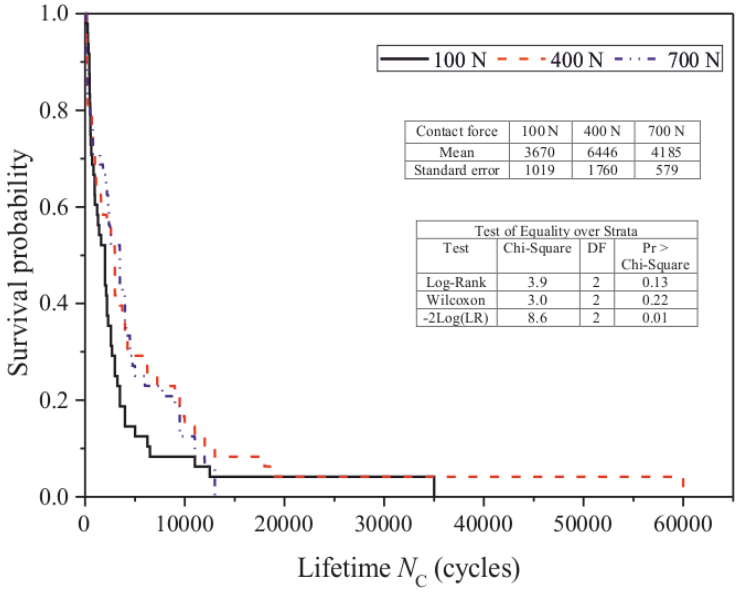

Contact force	100 N	400 N	700 N
Mean	3670	6446	4185
Standard error	1019	1760	579

Test of Equality over Strata			
Test	Chi-Square	DF	Pr > Chi-Square
Log-Rank	3.9	2	0.13
Wilcoxon	3.0	2	0.22
-2Log(LR)	8.6	2	0.01

Figure 103: Kaplan-Meier survival curves for different contact forces.

■ **Effect of coating position**

Although there is no significant difference between the three curves for the three different of coating positions (coating on flat, coating on counterbody, coating on both flat and counterbody), the value of Log-rank and Wilcoxon tests are different. Figure 104 shows the difference between three curves after 5000 cycles is larger than before 5000 cycles. In Chapter III, we have stated that the coating position has significant effect on the durability so that it is necessary to do the analysis for different coating positions when considering the substrates. Figure 105 describes the KM survival curves for different coating position when considering the substrates of M2. It can be observed that difference of coating positions becomes significant when considering M2 substrate, because the *P*r > chi-square is less than 0.05. The coating on the counterbody induces less deviance of durability between M2 and SS 304 substrate than coating on the flat or ball or cylinder (Figure 106). It is as a result of embedded coating. As the movement of flat, some coating is delaminated coating from ball or cylinder that can trap into the porosity in the M2 substrate, but this trapped coating does not have same adhesion force as that embedded coating during the deposition process. It is easy for this trapped coating to be ejected from the porosity so that the increase of durability on the counterbody is less than the coating on the flat or both counterbodies when it makes comparison of durability between M2 and SS304 substrates.

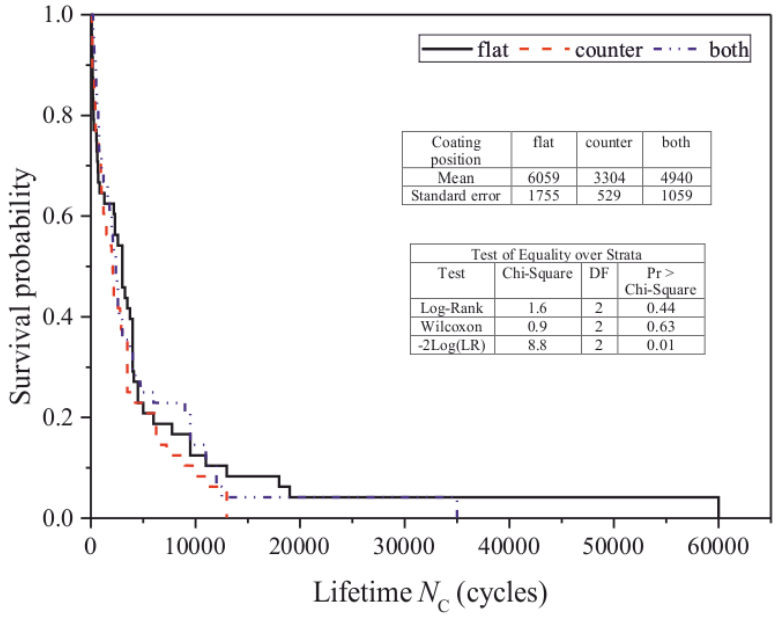

Coating position	flat	counter	both
Mean	6059	3304	4940
Standard error	1755	529	1059

Test of Equality over Strata			
Test	Chi-Square	DF	Pr > Chi-Square
Log-Rank	1.6	2	0.44
Wilcoxon	0.9	2	0.63
-2Log(LR)	8.8	2	0.01

Figure 104: Kaplan–Meier (KM) survival curve for different coating positions.

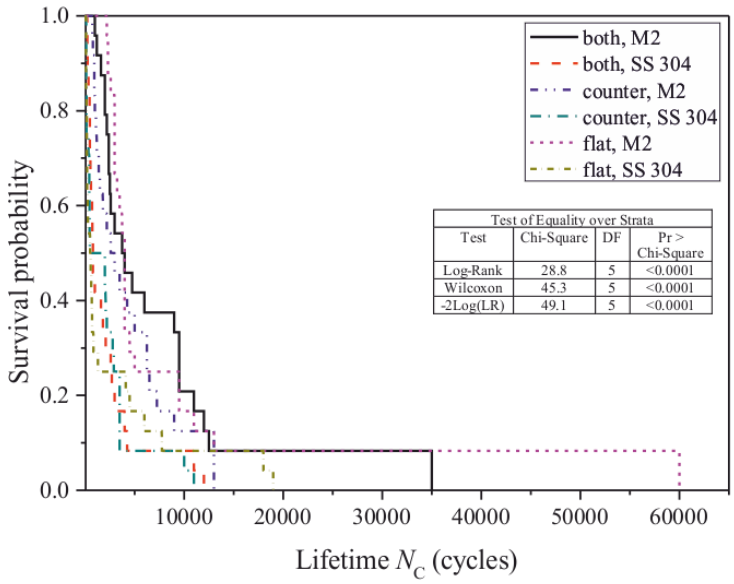

Test of Equality over Strata			
Test	Chi-Square	DF	Pr > Chi-Square
Log-Rank	28.8	5	<0.0001
Wilcoxon	45.3	5	<0.0001
-2Log(LR)	49.1	5	<0.0001

Figure 105: Kaplan–Meier (KM) survival curve for different coating positions and substrates.

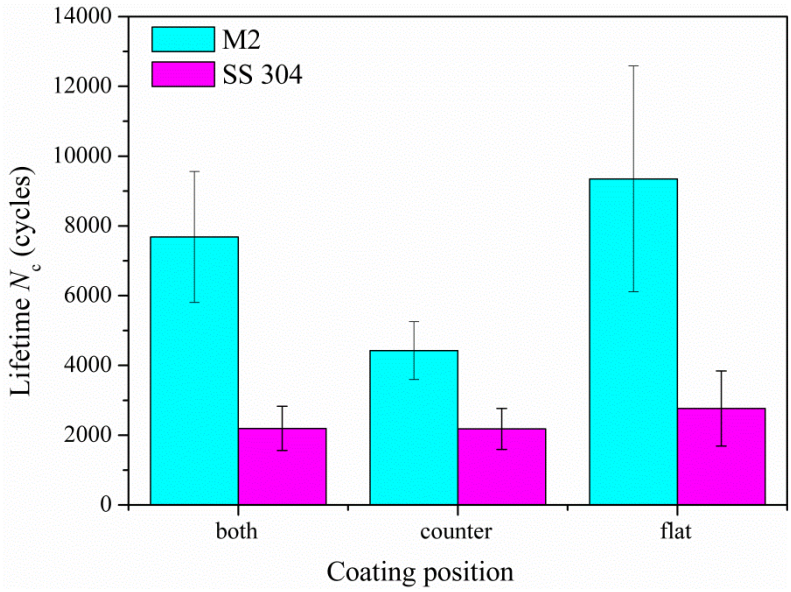

Figure 106: Comparison of mean lifetime for different coating positions and substrates.

- **Summary**

According to the above analysis, it can be observed that coatings on flat or both counterbodies under the cylinder-on-flat configuration for substrate M2 have an abnormal large value (Table 31), which extended the lifetime of coatings under lower survival probability.

Table 31: Two extreme longer durability points.

Normal force	Displacement amplitude	Thickness	Contact configuration	Substrate	Coating positions	Durability
400 N	± 10 µm	1 layer	Cylinder-on-flat	M2	flat	59999 cycles
100 N	± 10 µm	2 layers	Cylinder-on-flat	M2	both	39999 cycles

It can be seen that the lowest displacement amplitude and coatings on flat are in common. It may be explained by the special structure of substrates. The dimension of porosity is about 10 -30 µm in length (Figure 107). When the contact pressure is low and displacement amplitude is very low (less than ± 15 µm), it is impossible to squeeze the embedded coating in porosity in very short time so that it will also stay in porosity and accommodate the fretting process (Figure 108).

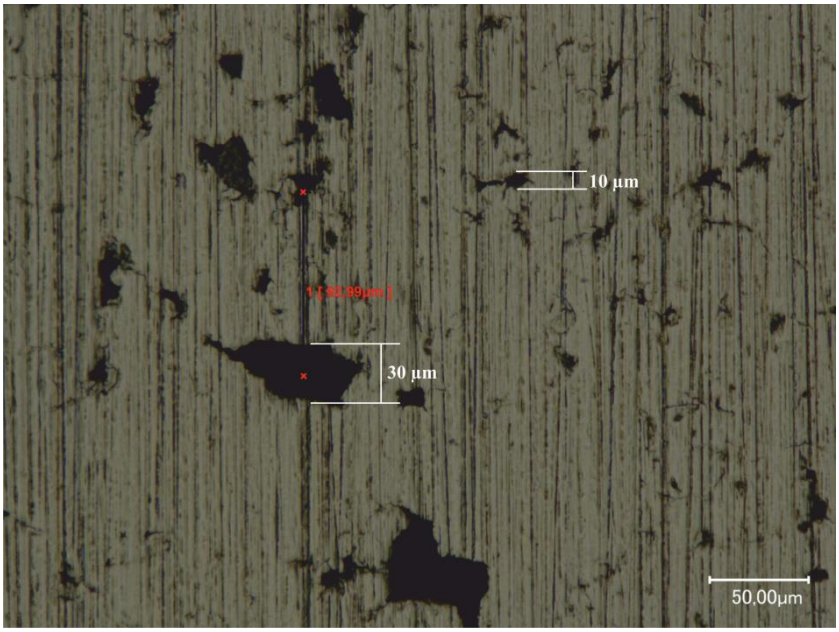

Figure 107: Optical image of M2 substrate.

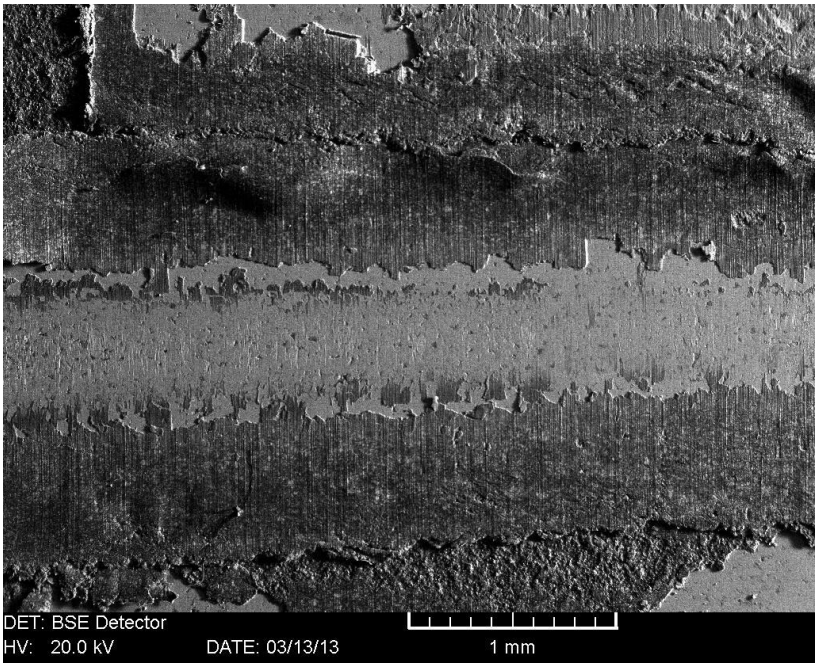

Figure 108: SEM for coated M2 at 17000 cycles under normal force 400 N.

According to the above analysis of effect of variables, it can be seen that M2 can the most effectively prolong the lifetime of coating by a factor of 3, followed by the effect of contact configuration and displacement amplitude. Thickness is not important for the change of lifetime.

IV.4.2.2 Parametric analysis

- **Log normal distribution**

For the survival analysis, it is interesting to predict the reliability of materials under the certain conditions. It is necessary to do a parametric analysis for the distribution of coating lifetime. According to the Box-transformation, the transformed lifetime (ln (*N*c)) is distributed normally

so that the distribution of lifetime can be expressed by the log normal probability density function, as Eq. (IV-3):

$$f(ln(Nc)) = \frac{1}{1.46\sqrt{2\pi}} exp(-\frac{(ln(Nc)-7.55)^2}{2\times 1.46^2}) \quad (IV\text{-}3)$$

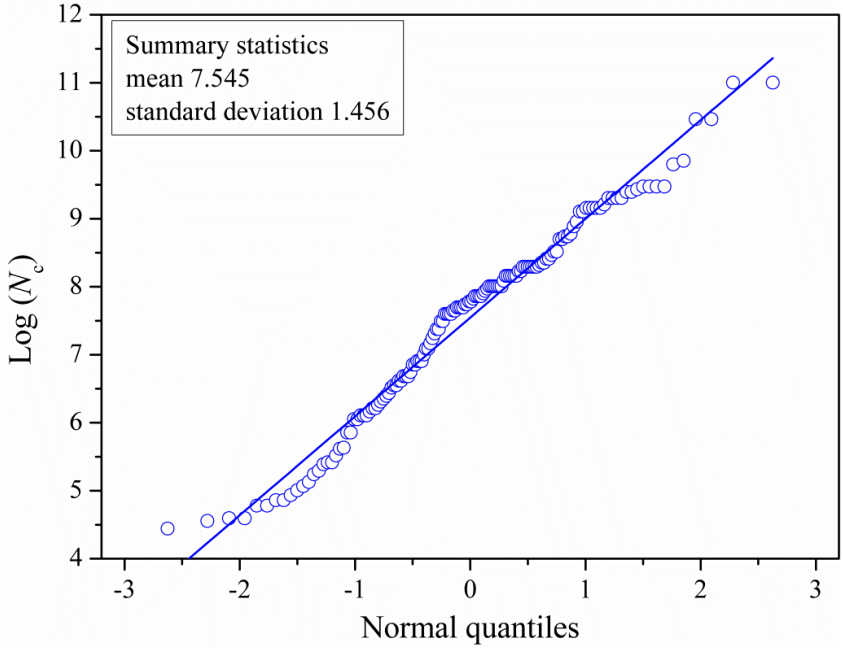

Figure 109: Probability plot for ln(lifetime).

- **Competing failure analysis**

In Chapter III, we have proved that the mixed Weibull distribution can be used as an effective way to distinct the failure modes, because it can model data that do not fall on a straight line on a Weibull probability plot (Figure 110), but life data of each failure mode may follow a distinct Weibull distribution for individual wear mode. In addition, the shape value should be larger than 1 according to the Weibull distribution for wear-out process. Therefore, the overall life data does not follow the Weibull distribution, because the value of shape factor (0.72) is less than 1. In addition, the value of scale factor reaches an agreement with Chapter III that long durability of coatings is related to the large value of scale factor when the shape factor is larger than 1.

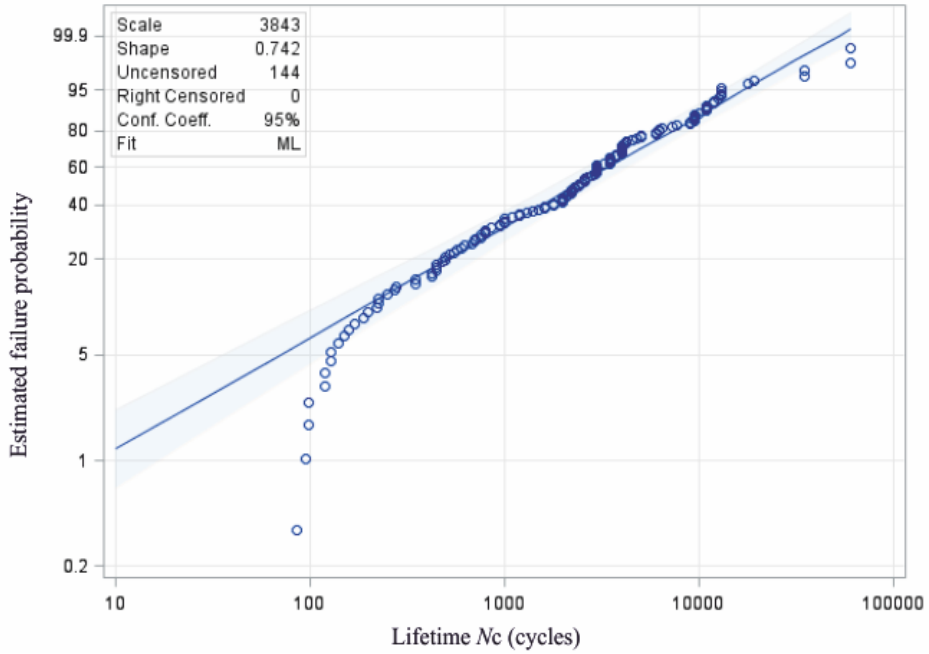

Figure 110: Weibull distribution for lifetime data (the blue points are the distribution of lifetime, the blue line is referred to the reference line for Weibull distribution, and the blue shadow is the 95% confidence limits).

In the above discussion, it has been seen that the failure modes are generally separated into 4: abrasive wear, adhesive wear, abrasive wear + coating embedding, adhesive wear + coating embedding. Figure 111 describes the Weibull distribution for each wear mode. It can be seen the life data falls on a straight line on a Weibull probability plot according to each wear mode. In addition, the scale factor of each wear mechanism is higher than 1 and the scale factor of wear mechanism involved with embedding coating (M2 substrate)is always higher than that without embedding coating (SS 304 substrate).

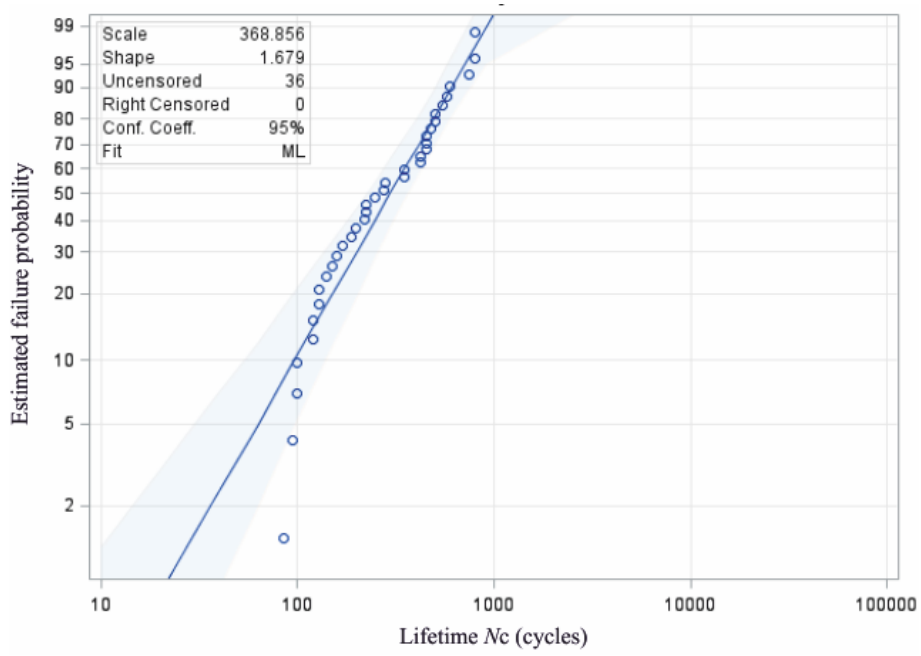

(a) abrasive wear for SS 304 substrate

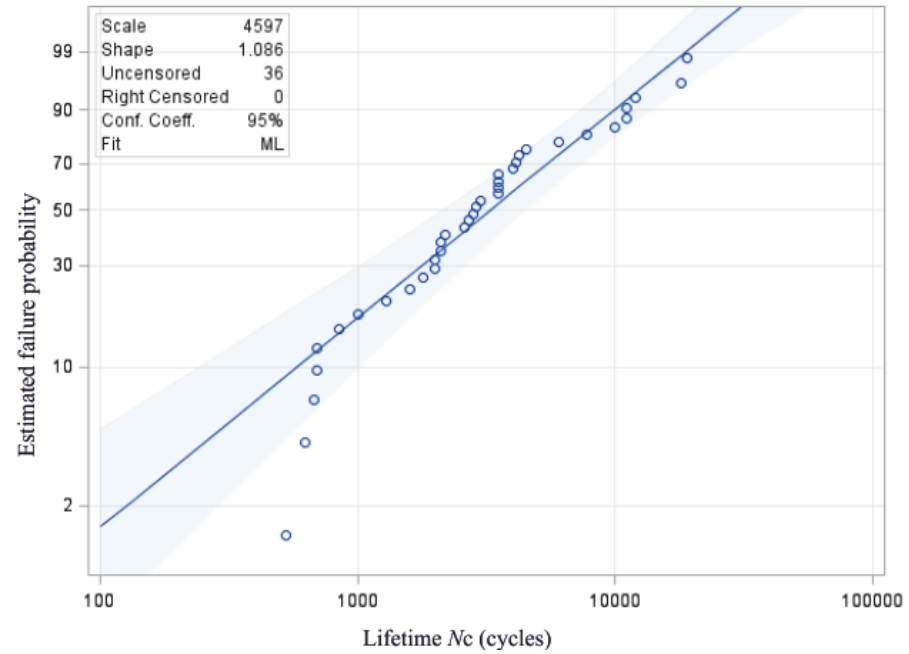

(b) adhesive wear for SS 304 substrate

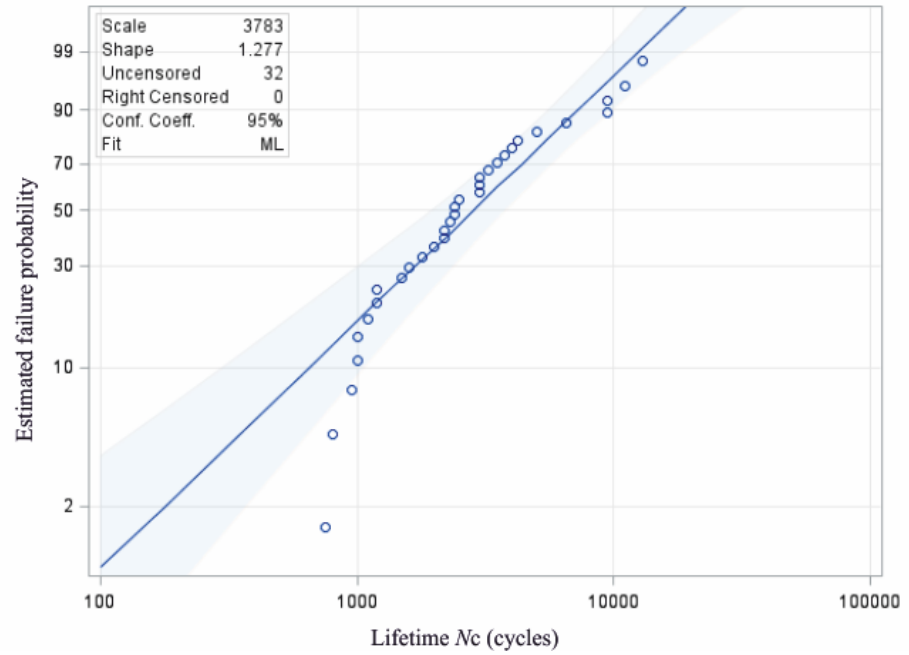

(c) abrasive wear for M2 substrate

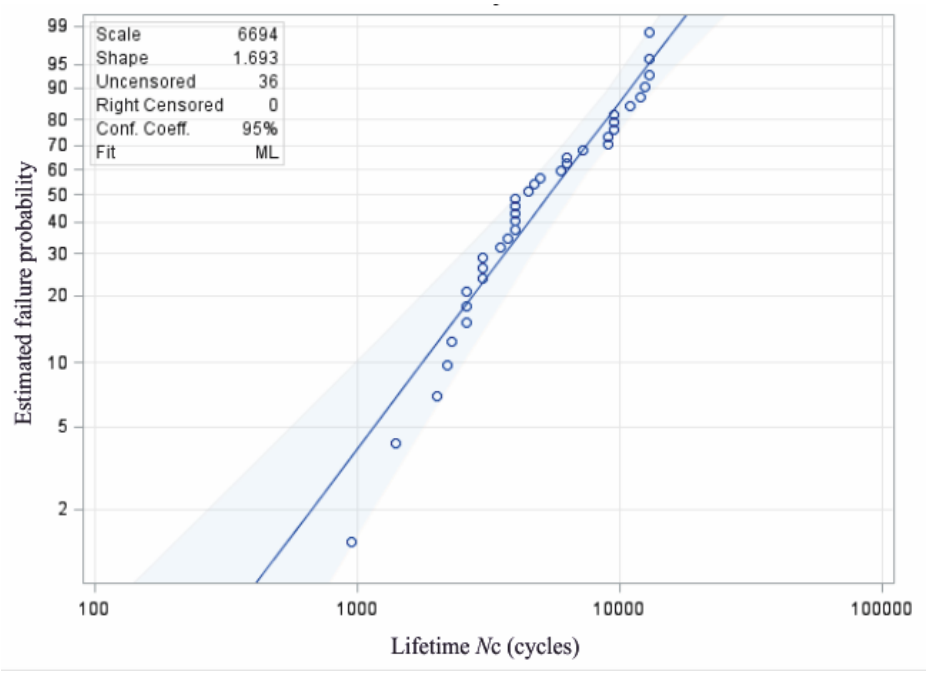

(d) adhesive wear for M2 substrate

Figure 111: Weibull distribution for different wear modes (the blue points are the distribution of lifetime, the blue line is referred to the reference line for Weibull distribution, and the blue shadow is the 95% confidence limits).

According to the Weibull distribution, the reliability for each wear mode can be calculated according to the Eq. (IV-4)

$$R(t) = \exp(-(\frac{t}{\eta})^{\beta}) \qquad (IV\text{-}4)$$

η refers to scale factor and β refers to shape factor.

For example, the reliability of 1000 cycles in different contact configurations and substrates can be calculated in Table 32. If the fretting is running on the coating on SS 304 substrate under cylinder-on-flat configuration, the coating should not be used, because its reliability for 1000 cycles is about 0.

Table 32 : Reliability for 1000 cycles.

Contact configuration	Substrate	Reliability
Cylinder-on-flat	SS 304	0.004
	M2	0.83
Ball-on-flat	SS 304	0.95
	M2	0.96

IV.4.3 Summary

The lifetime of MoS_2 based varnish coating depends on the test conditions, because the test conditions affect the wear mechanism and ejection debris. In this study, coating on the M2 substrate always have higher coating durability than SS 304 substrate and it can improve the reliability of coating from 0 to 0.83 under cylinder-on-flat. It is because the porosity of the M2

substrate can hold some coating and thus it is difficult for coating in the porosity to be squeezed from the porosity. During the fretting movement of coating on M2 substrate, the embedded coating plays a great role in keeping low friction coefficient and extending the lifetime. The thickness of coating only plays a very ignorable role in durability of coating, because it does not change the plastic deformation of coating or wear mechanism.

IV.5 Conclusions

In this chapter, based on the investigation of MoS_2 base varnish coating under different contact configurations, contact force, displacement amplitude, coating position, thickness and substrates, the following conclusions can be drawn:

-The friction coefficient depends on the contact configuration and contact force, because both of them determine the contact pressure. This is in agreement with the results of Chapter III. The evolution of friction coefficient is inversely proportional to contact pressure. Thickness can change a little the friction coefficient, because the increase of thickness can increase the ploughing component of friction coefficient and thus it leads to an increase of friction coefficient. Some porosity in the substrate such as M2 can effectively increase shear strength of coating, resulting in an increase of friction coefficient.

-Nature of substrate is the most important variables for coating durability, because it can change the wear mechanism by adding the function of embedded coatings. It overrides the importance of contact configuration and displacement amplitude, which are the important variables for coating lifetime in Chapter III. The porosity can hold the coating and thus keep the low friction coefficient and prolong the coating durability. Thickness seems to be affectless to the durability, because it does not change the wear mechanism or ejection rate of wear particles.

CHAPTER V

DURABILITY OF A VARNISH COATING FOR VARIABLE DISPLACEMENT AMPLITUDES CONDITIONS

CHAPTER V: DURABILITY OF A VARNISH COATING FOR VARIABLE DISPLACEMENT AMPLITUDES CONDITIONS

This chapter investigates the effects of variable amplitudes on the friction coefficient and coating lifetime. The comparison between lifetime of variable displacement amplitudes and mean of value of that from several constant displacement amplitudes is made.

V.1 Introduction

According to the analysis presented in Chapter III and Chapter IV, we have seen that the displacement amplitude is a very important factor for the coating lifetime, following the nature of substrate and contact configuration. For the nature of substrate and contact configuration, they are related to the wear mechanism, but the displacement amplitude is controlling the debris flow of wear debris (Figure 112). If the displacement is large, the coating lifetime will be reduced, because the ejection rate of debris is accelerated due to the large displacement amplitude.

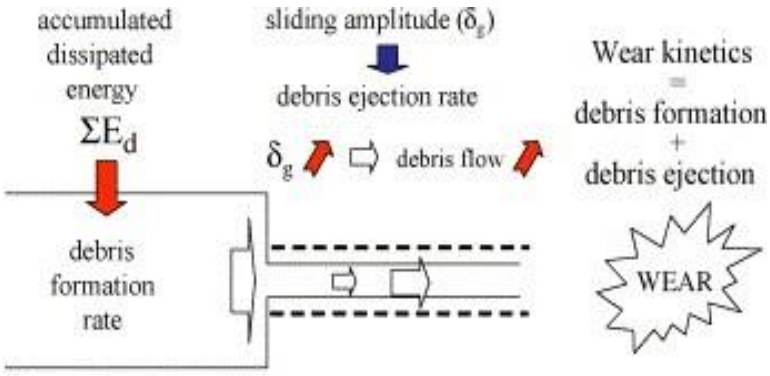

Figure 112: Debris chart illustrating the fretting wear parameters, by which the wear kinetics of adhesive materials submitted to gross slip fretting wear sliding can be quantified. δ_g: imposed sliding amplitude [142].

However, the above analysis is limited to constant displacement amplitude conditions, which occurs in the modeling tests. Real industrial applications are in fact subjected to the variable sliding displacement (Figure 113). Hence, the purpose of this chapter is to extend the model to take into account the effect of variable sliding conditions on the friction coefficient and durability of coatings, thereby better understanding the flow of third body. In addition, the lifetime of variable displacement amplitude will be compared with the lifetime of constant displacement amplitude. It is aimed to that whether the linear wear mode can be used to predict the wear of variable displacement amplitude.

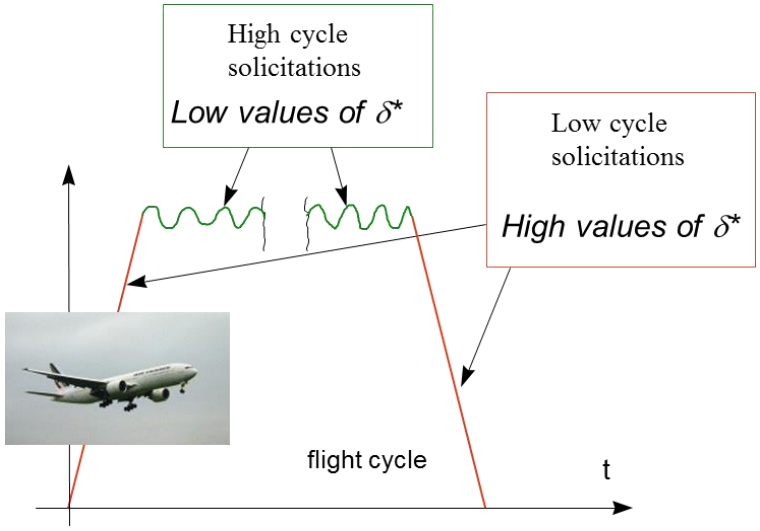

Figure 113: Illustration of variable sliding conditions imposed on a blade disk contact during a single commercial flight [127].

V.2 Evolution of friction coefficient

All tests are carried out with a constant normal force F_n = 400 N and F_n = 100 N. The thickness of coating is 2 layers (20 µm). The coating is only deposited on the SS 304 substrate. The description methods of experiments follow the test nomenclature, proposed by Paulin *et al* [142], but it changes a little due to different test materials. According to this study, the normal force is changed so that it is necessary to show the value of contact force in the test nomenclature. In this new test nomenclature, the value of contact force will replace the value of durability of materials shown in the nomenclature (Figure 114). To guarantee the accuracy of the test, each test was repeated four times.

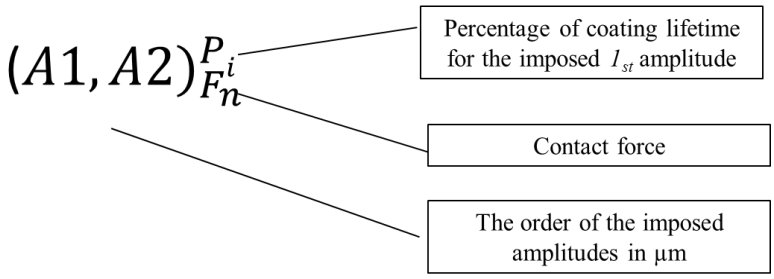

(a) Definition of the nomenclature

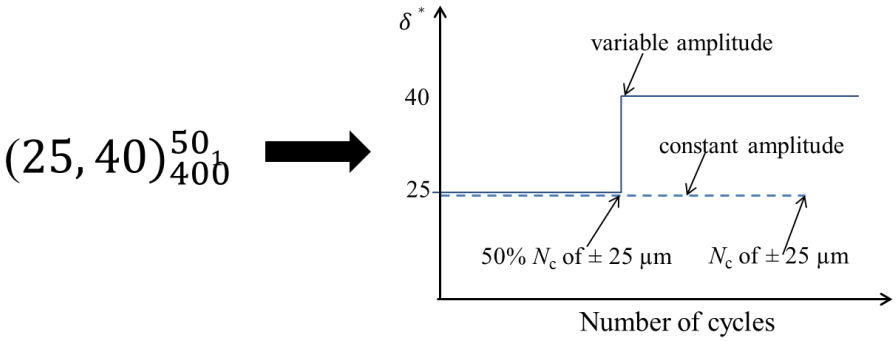

(b) Illustration of variable and non-symmetrical sliding condition test

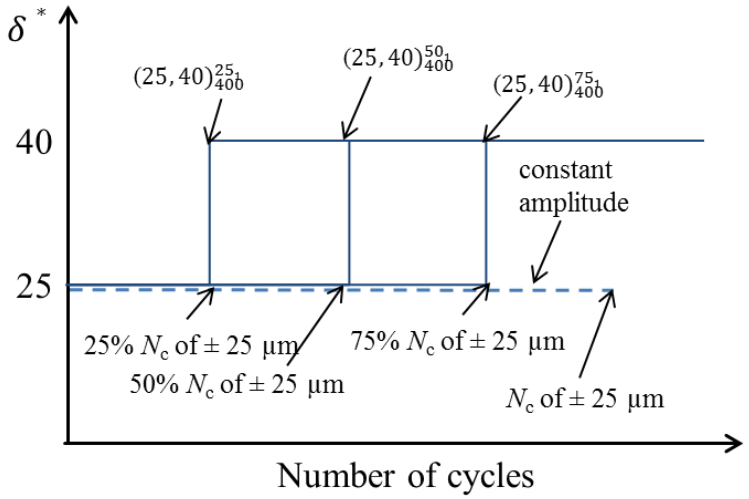

(c) Illustration of different sliding condition tests

Figure 114: Test nomenclature: (a) Definition of the nomenclature; (b) Illustration of variable and non-symmetrical sliding condition test; (c) Illustration of different sliding condition tests.

V.2.1 50% of the lifetime of first amplitude

The friction behavior of coating under variable displacement is studied for imposed amplitudes equal to ±25 µm and ±40 µm, as shown in Figure 115. The number of cycles of first amplitude is identical to 50% of durability for coatings under the imposed 1st constant displacement amplitude.

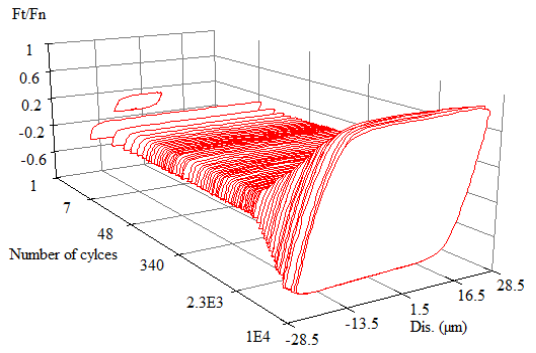

(a) Constant amplitude δ^* = ±25 µm

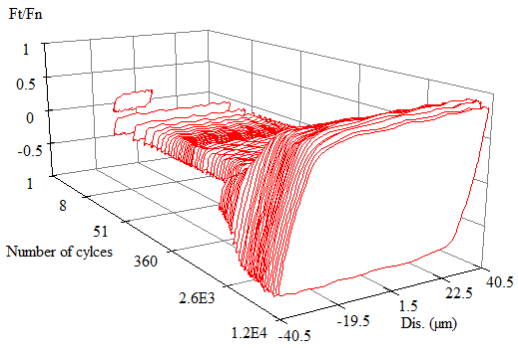

(b) $(25,40)^{50_1}_{400}$

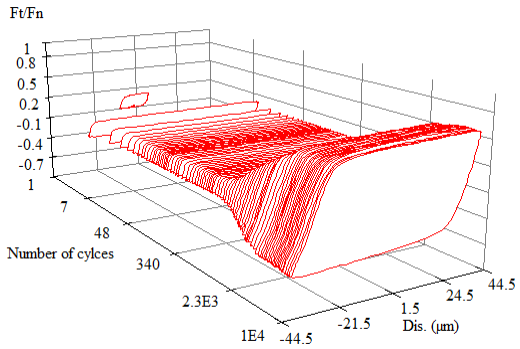

(c) Constant amplitude δ^* = ±40 µm

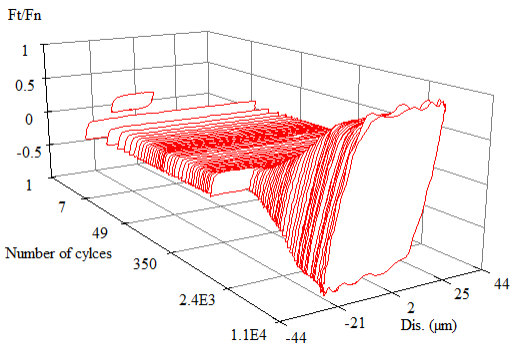

(d) $(40,25)^{50_1}_{400}$

Figure 115: Examples of fretting logs for fretting tests.

- **Contact force = 400 N**

Figure 116 describes the variation of displacement amplitude can lead to the increase of friction coefficient when it occurs at the moment that the coating is almost removed and the friction coefficient begins to increase.

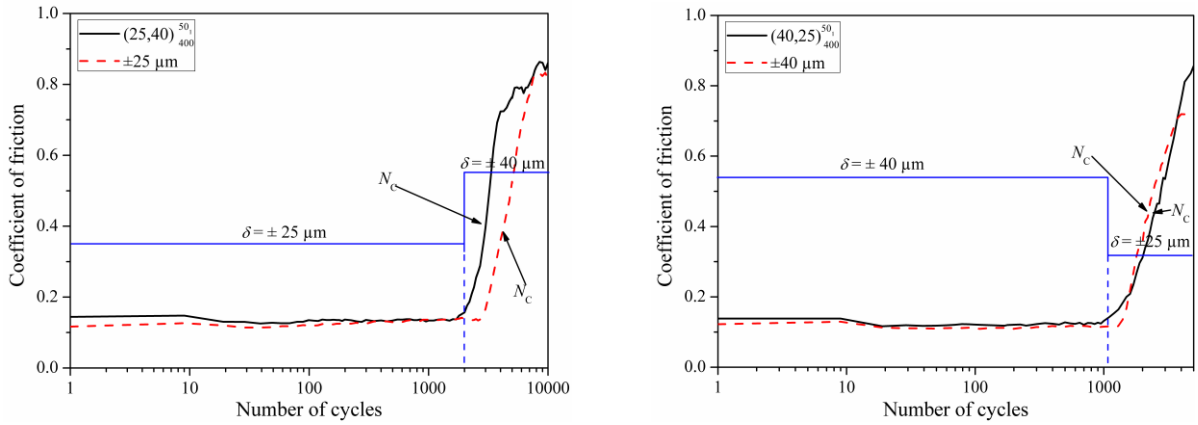

Figure 116: Comparison of friction coefficient for stable and variable displacement amplitude when the variation of displacement amplitude occurs at the 50% of durability of 1st amplitude (F_n= 400 N).

Figure 117 and Figure 118 describe the wear scar at the moment of 50% of durability for constant displacement amplitude of ±25 µm and ±40 µm, respectively. It shows that the most coating debris have been ejected from the contact area. Significant materials transfer is observed on the ball. In addition, fewer coatings are left on the wear track for the case of ±40 µm than the case of ±25 µm. It indicates that the larger displacement amplitude may accelerate the third body flow, leading to more coating ejected from contact area. At the same time, increasing displacement amplitude can decrease mean contact pressure for a given moment force (because of larger contact area), leading to the increase of friction coefficient.

Figure 117: Optical observation for wear scar under F_n = 400 N, δ^* = ± 25 µm, cycle = 50% of durability (2000th cycle).

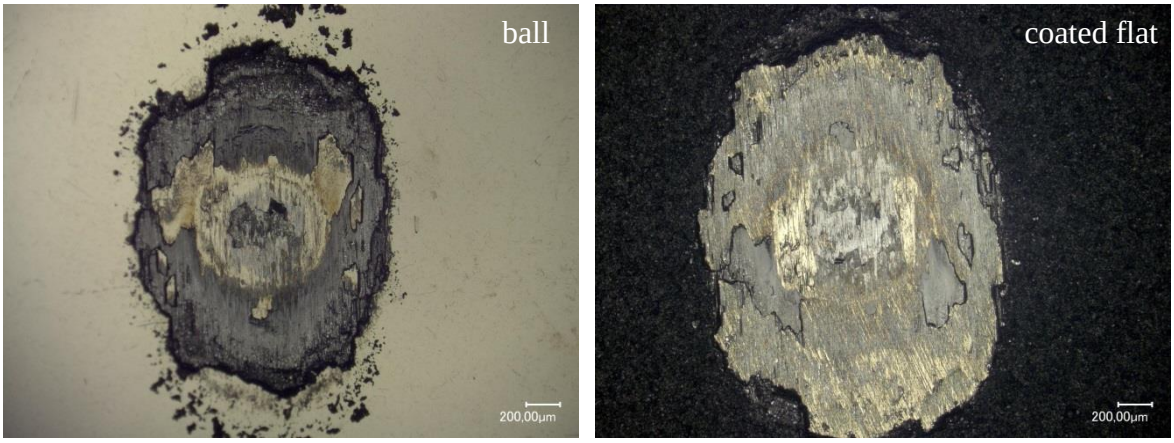

Figure 118: Optical observation for wear scar under F_n = 400 N, δ^* = ± 40 µm, cycle = 50% of durability (1150th cycle).

- **Contact force = 100 N**

Figure 119 describes the evolution of friction coefficient for constant and various displacement amplitudes under 100 N. The increase of displacement amplitude can decrease friction coefficient a little bit. Generally, the friction coefficient depends on three factors: adhesion between flat surfaces, ploughing by wear particles and asperity deformation. In this case, the increase of displacement amplitude can introduce some new coating into contact area. Adhesion between flat surfaces can be explained by that the junction growth comes from plastic flow between the asperities, as they are loaded with local contact force and local tangential displacement. These junctions are stuck locally and the resulting tangential force occurs as plastic flow which resists local sliding [143]. As a result of increased displacement amplitude, more coatings present at the contact area. These coatings have a characteristic of low-shearing strength so that the junctions between two contacts are reduced. The adhesion force is reduced. Therefore, the friction coefficient decreases a little bit.

When the displacement amplitude is decreased from ±40 µm to ±25 µm, the friction coefficient is also decreased a little bit (Figure 119). Figure 120 shows that almost all the coating has been ejected from the contact center at the 50% of the lifetime of ±40 µm for 100 N. The decreased displacement amplitude can decrease the contact area. Therefore, the coating debris at the small contact area can accommodate the fretting behavior. In other words, the junctions between two substrate asperities are decreased. The decreased junctions between two substrates can give less resistance to local sliding. Therefore, the friction coefficient is decreased a little bit.

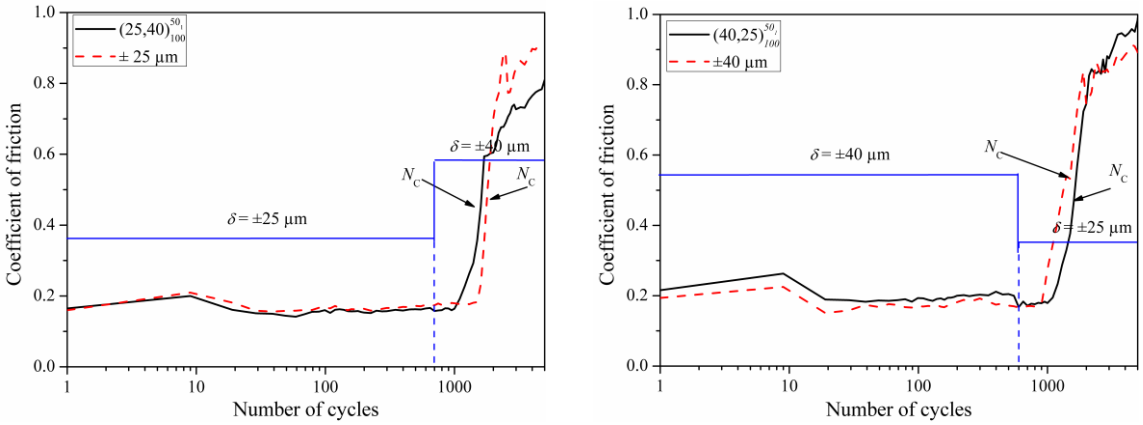

Figure 119: Comparison of friction coefficient for stable and variable displacement amplitude when the variation of displacement amplitude occurs at the 50% of durability of 1st amplitude (F_n= 100 N).

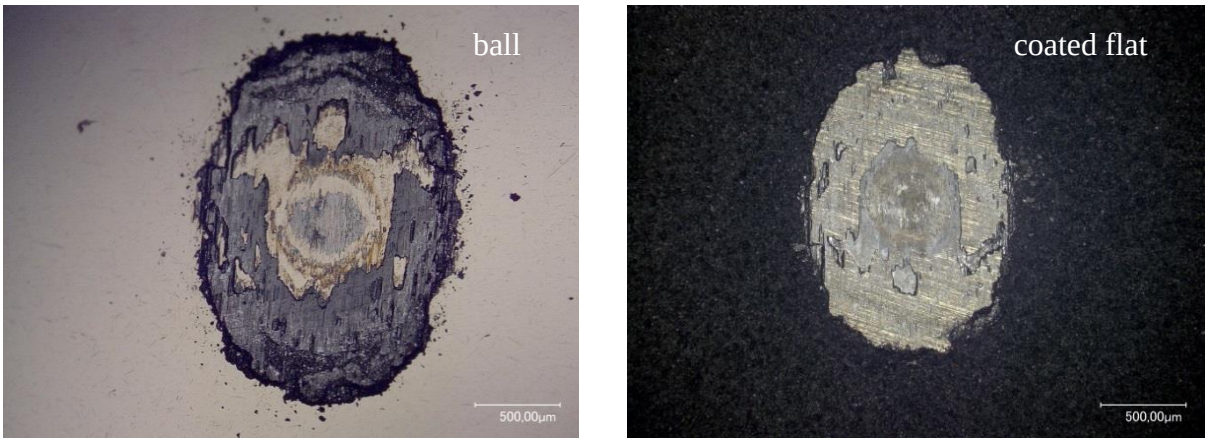

Figure 120: Optical observation for wear scar under F_n = 100 N, δ^* = ± 40 µm, cycle = 50% of durability (600th cycle).

- **Summary**

The decrease or increase of displacement amplitude can change the friction coefficient a little bit, but it depends on the contact force. When the contact force is 400 N, the change of displacement amplitude can lead to the increase of friction coefficient, but the change of displacement amplitude under 100 N can decrease friction coefficient a little bit. This can be explained by the model of Descartes *et al.* [120]. She explained the third body flow for MoSx based coating. It was dependent on the internal flow and recirculation of recycle particles (Figure 121). Some ejected coating can recirculate in the fretting movement and accommodate the fretting, providing the lower friction coefficient for the friction system. For contact force of 400 N, the large contact pressure can give a better isolate space for fretting at contact area than that of contact force 100 N. In other words, the external coating debris under 400 N is difficult to recirculate into the contact area. However, it is easier for the case 100 N. This recirculated coating debris can cover some exposure substrate and lower the adhering force, thereby lowering friction coefficient.

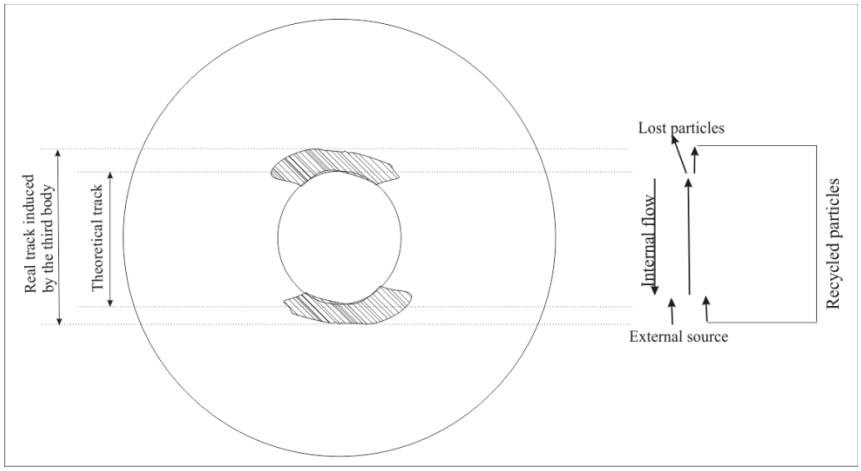

Figure 121: Flow of third body viewed from the ball [120].

V.2.2 25% of the lifetime of first amplitude

Figure 122 and Figure 123 present the variation of the friction coefficient versus the number of cycles of the tests for 25% lifetime of first constant displacement amplitude. In both cases, the increase or decrease of displacement amplitude does not change the value of friction coefficient significantly when the coating is working very well. For contact force of 400 N, the friction coefficient is decreased a little when the displacement amplitude is changed from ±40 µm to ±25 µm. The decrease of displacement amplitude may result in the decrease of contact area so that the contact pressure may be increased under the same contact force. The contact pressure is inversely proportional to the friction coefficient. However, the increase of contact area is so little because the increase of displacement amplitude is only 15 µm. Therefore, the change of contact pressure is a little bit, leading to a very little decrease of friction coefficient. Similar phenomenon can also be observed for the 100 N when the displacement amplitude is changed from the ±40 µm to ±25 µm, but the deviance of value (0.01) is less than the case of 400 N (0.02).

However, the increase of displacement amplitude seems to have no effect on the friction coefficient. New coating parts can be involved in the fretting movement due to the increase of displacement amplitude. At this time, the new involved coating cannot change the friction coefficient significantly, because there are many coating debris at the contact area. There are no junctions between two substrates asperities. This is different from the case of 50% of lifetime of coating. When the coating lifetime arrives 50%, the most coating has been removed from the contact center. Some junctions between two substrate asperities begin to appear. If some coatings are added at this moment, they can work as a third layer between two substrate asperities, thereby decreasing the friction coefficient a little bit. In this case of 25% of lifetime, more coatings are present at the contact area so that increase of displacement amplitude has no effect on the friction coefficient.

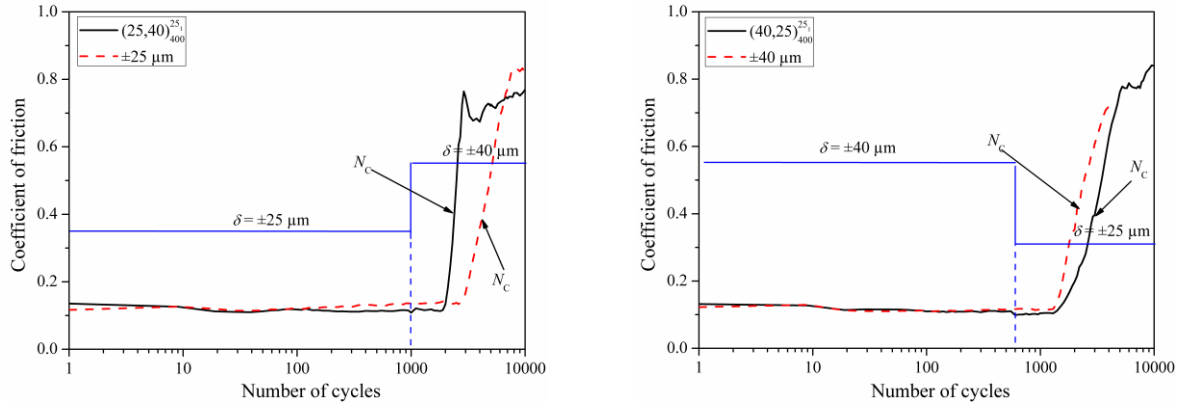

Figure 122: Comparison of friction coefficient for stable and variable displacement amplitude (25% of durability for coatings under the imposed 1st displacement amplitude, contact force = 400 N).

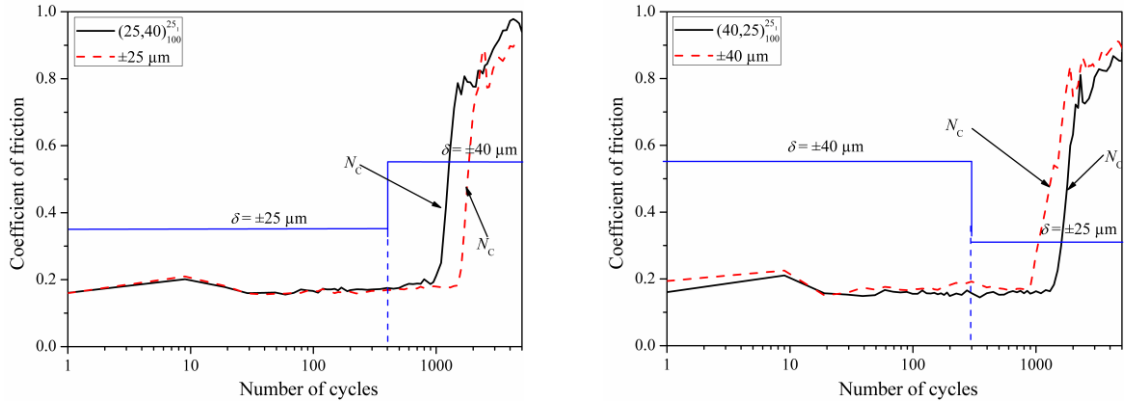

Figure 123: Comparison of friction coefficient for stable and variable displacement amplitude (25% of durability for coatings under the imposed 1st displacement amplitude, contact force = 100 N).

V.2.3 75% of the lifetime of first amplitude

Figure 124 and Figure 125 present the friction coefficient versus the number of cycles of the tests for 75% lifetime of first amplitude. For contact force F_n = 400 N, the variation of displacement amplitude occurs when the friction coefficient is increasing so that the increased displacement can increase the growth rate of friction coefficient. For the case of F_n = 100N, the variation of displacement can prolong the duration of low friction coefficient. For the displacement increased from ±25 µm to ±40 µm, the increased displacement can introduce more coating to be involved in the fretting process. Therefore, the adhesion between contact parts is decreased, leading to the decrease of friction coefficient. When the displacement is decreased from ±40 µm to ±25 µm, the contact area is decreased. At the same time, the junctions between two substrate asperities are decreased. The friction coefficient is decreased a little bit.

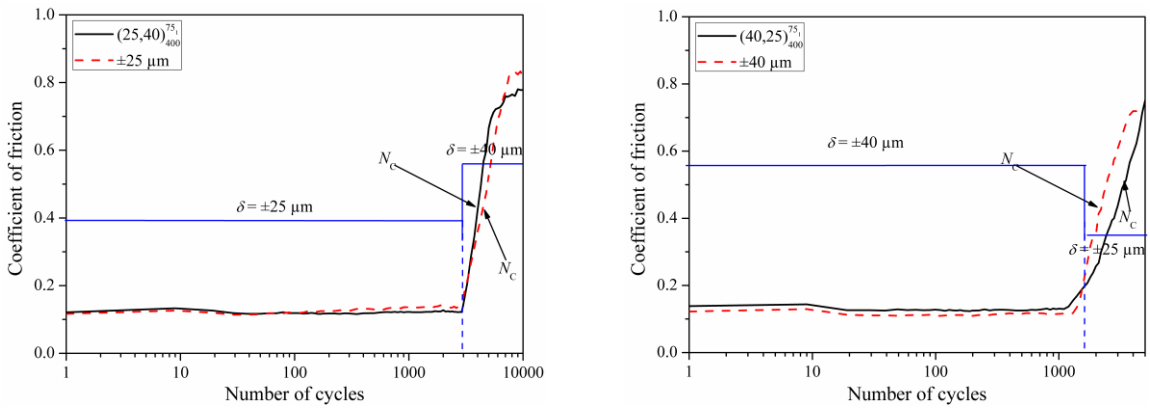

Figure 124: Comparison of friction coefficient for stable and variable displacement amplitude (75% of durability for coatings under the imposed 1st displacement amplitude, contact force = 400 N)

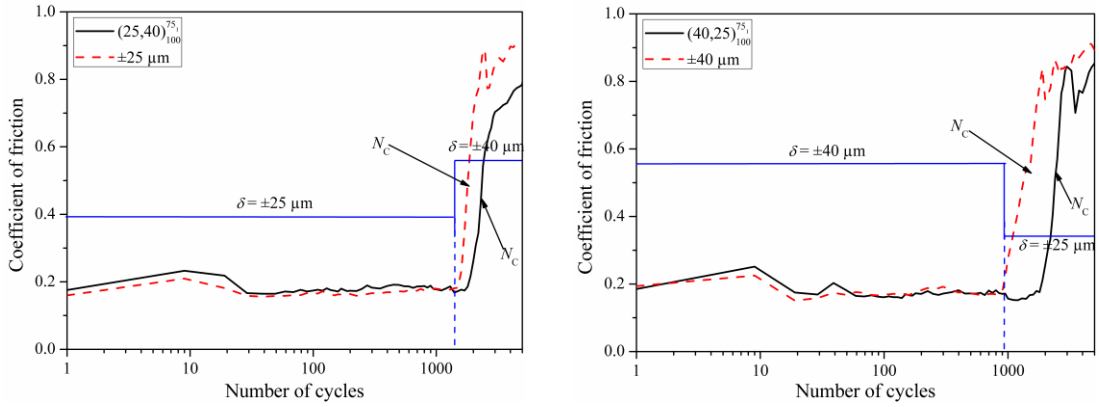

Figure 125: Comparison of friction coefficient for stable and variable displacement amplitude (75% of durability for coatings under the imposed 1st displacement amplitude, contact force = 100 N)

V.2.4 Summary

When the coating is almost removed (coating lifetime is about 50% and 75% of lifetime of constant displacement amplitude) for 400 N, the change of displacement amplitude can lead to the increase of friction coefficient. When most coatings are still on the substrate (coating lifetime is about 25% of lifetime of constant displacement amplitude), the change of displacement amplitude from ±25 µm to ±40 µm seems to have no effect on the friction coefficient for both contact force. However, the friction coefficient is decreased a little bit for both contact forces (100 N and 400 N) when the displacement amplitude is decreased from ±40 µm to ±25 µm. In the case of 100 N, the change of displacement amplitude at the 50% or 75% of lifetime of constant displacement amplitude can decrease the friction coefficient a little bit.

V.3 Evolution of coating lifetime

In the study of Paulin *et al.* [142], he confirmed that at given total number of fretting cycles, the wear volume of a variable displacement test is close to the mean value of that from the two constant displacement amplitude. However, in the case of coating, the result is a little different due to the complicate flow of third body.

To evaluate the influence of various displacement amplitudes on coating lifetime compared with the stable displacement friction coefficient, the relative lifetime is displayed as Eq.(V-1):

$$\left(\frac{M1}{N_{1ori}}+\frac{M2}{N_{2ori}}\right)\times 100\% = relative\ lifetime$$

$M1$ refers to the imposed cycles for 1st amplitude, $M2$ refers to the lifetime minus $M1$ (i.e. the number of cycles for the 2nd lifetime), N_{1ori} is the lifetime of constant 1st amplitude, N_{2ori} is the lifetime of constant 2nd amplitude. If the value of relative lifetime = 100%, it means the lifetime of a variable displacement is the mean of value of that from the two constant displacement amplitude and it means that the wear damage follows a linear rule.

V.3.1 50% of the lifetime of first amplitude

Figure 126 describes the relationship between the variable displacement and the mean value of that from the two. Generally, the relative lifetime is around 100%. With the increase of contact force, the relative lifetime is decreased. Under 400 N, the value of variable displacement is almost the mean value of that from two, but the value for 100 N is a little higher. The fretting movement under 400 N is mainly dependent of the internal flow rather than recirculation of recycle debris so that the lifetime of a variable displacement almost equals to the mean of value of that from the two. For the case of 100 N, it depends on the external flow so that increasing amplitude will give a result that the lifetime of variable displacement is larger than the mean of value of that from the two.

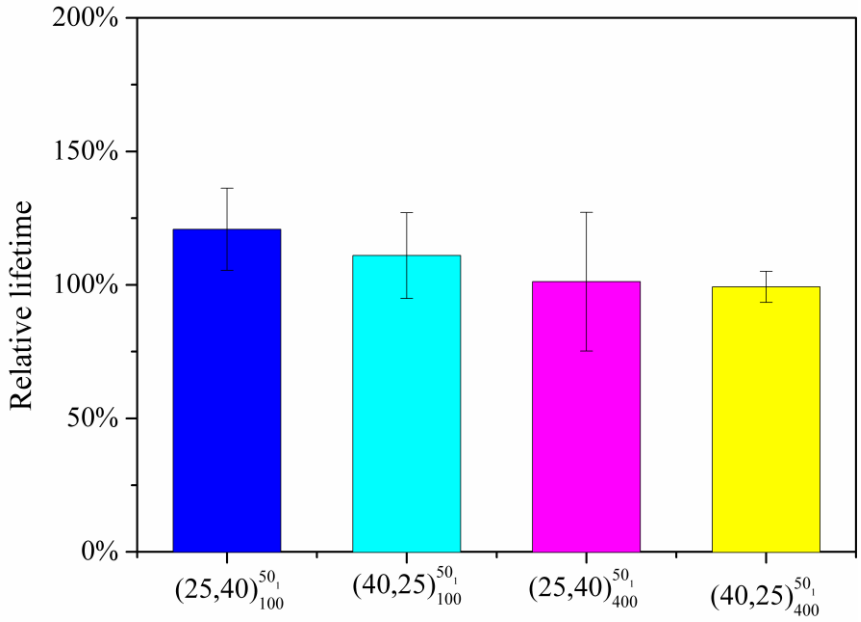

Figure 126: Comparison of lifetime for coating under 50% of durability for coatings under the imposed 1st displacement amplitude.

V.3.2 25% and 75% of the lifetime of first amplitude

Similar to the results in 3.1, the 25% and 75% of the lifetime of first amplitude for 400 N seems to have no effect on the relative lifetime (Figure 127). The value of relative lifetime is around 100%.

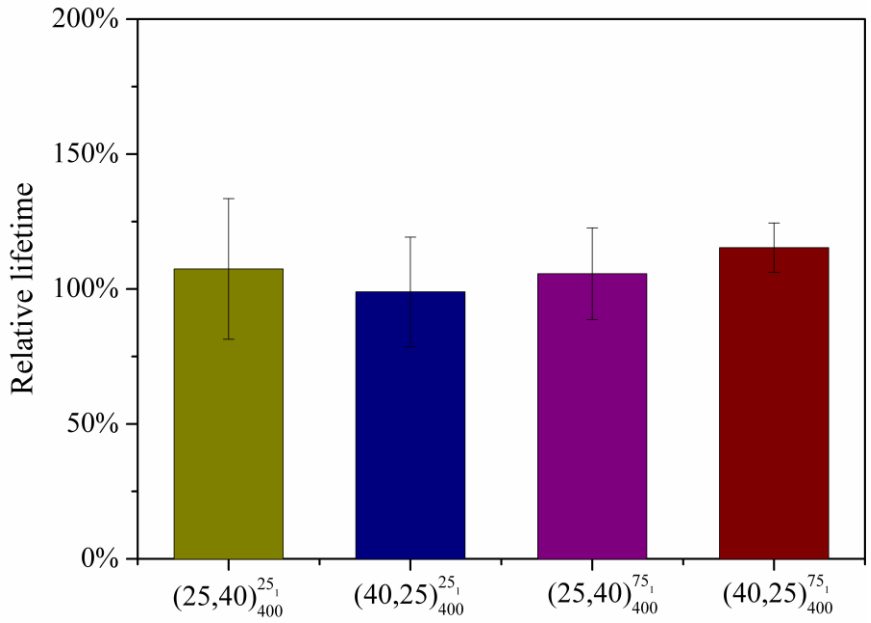

Figure 127: Comparison of coating lifetime for heterogeneous distribution (F_n= 400 N).

However, the results of 100 N show a significant difference from the 3.1 (Figure 126). When imposed cycles are 75% lifetime of 1st constant amplitude, the value of relative lifetime is higher than 100% (Figure 128). The value almost equals to 100% when the imposed cycle is 25% durability of 1st constant amplitude, because the variation of displacement occurs in the earlier time of coating lifetime and it does not affect a lot third body flow and friction coefficient. However, the variation of displacement amplitude can have a significant effect on the relative lifetime when the change of displacement amplitude occurs at the 75% of the constant coating lifetime. It is as a result of recirculation of recycle coating debris (Figure 121). When the contact force is 100 N, the recirculation is easy to occur. Therefore, some coating debris can easily recirculate into the contact center and provide the lubricating function. With the decrease of displacement amplitude, the ejection rate of particles is slowed. Therefore, the change of displacement amplitude from ±40 µm to ±25 µm can lead to a long durability.

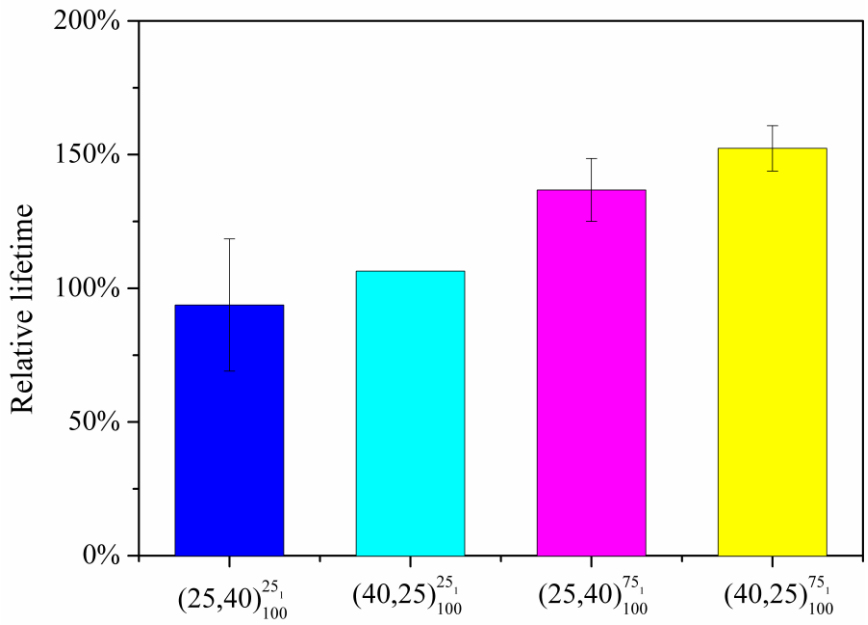

Figure 128: Comparison of coating lifetime for heterogeneous distribution (F_n= 100 N).

V.4 Conclusions

In this chapter, based on the investigation of variable displacement amplitude, the following conclusions can be drawn:

- The evolution of friction coefficient as a function of variable displacement amplitude depends on the contact force. When the contact force is 400 N, the change of displacement amplitude after 50% of lifetime of constant displacement amplitude can lead to the increase of friction coefficient. When the change of displacement amplitude occurs at 25% of lifetime of constant displacement amplitude, there is no change of friction coefficient when the displacement amplitude is changed from ±25 µm to ±40 µm. When the displacement amplitude is changed from ±40 µm to ±25 µm, the friction coefficient can be decrease a little bit. When the contact force is 100 N, the change of displacement amplitude at 25% of lifetime of constant displacement amplitude have no effect on the friction coefficient. If this change occurs at 50% and 75% of lifetime of constant displacement amplitude, the friction coefficient can be decreased a little bit.
- The relative lifetime is near to 100% for 400 N whenever the displacement amplitude is changed. The relative lifetime is near to 100% for 100 N when the change of displacement amplitude occurs at 25% and 50% of lifetime of 1st constant displacement amplitude. When the change occurs at 75% of lifetime of 1st constant displacement amplitude, the lifetime of coating will be long due to the effect of recycled coating debris.

GENERAL CONCLUSIONS

Fretting wear is considered as a complex phenomenon related to wear between two sliding bodies under very low displacement amplitude, which limits the lifetime of elements significantly. In industrial applications, coatings have been widely used to protect the surface from fretting wear. The evaluation of coating has become an important subject in the research. The selection of coating is involved with many factors such as properties of substrate, adhesion of coatings to the substrate and various test conditions. However, there are no general rules to evaluate the coating according to these factors. The objectives of the thesis were to study the friction and wear behavior of a varnish coating, in order to evaluate the effect of factors on the tribological behavior of coating.

To evaluate the properties of coatings, several methods have been used: experimental method and modeling method. Experimental method uses different tests rig to model the real industrial running conditions. According to results of experimental methods, modeling method can deduce some equation to predict the friction and wear behavior of coating in the industrial applications. At present, some statistical methods (including factorial analysis and regression analysis) have also been used in the tribological analysis. Factorial analysis is aimed to describe the effect of test parameters on the tribological behavior of coatings. Regression analysis is used to predict the tribological behavior in the industrial applications according to the experimental results. Finally, the reliability method has also been used in the research. It can describe and predict the failure rate or survival rate of coatings under certain running conditions.

In order to investigate the tribological behaviors of a solid lubricant, fretting test studies were performed with different coating positions (on the flat substrate, on the ball or cylinder substrate and both counterbodies) and different substrates (304 stainless steel, AISI M2 steel) with the objective to understand the effect of running conditions on the tribological performance of a varnish coating and to analyze the effects of test conditions on the tribological behavior of the coating.

In order to **understand the effect of test conditions on tribological behavior of a MoS_2 based varnish coating**, the tests were firstly performed on the one layer coating (thickness of about 10 µm) on 304 stainless steel under different contact forces (100 N, 400 N and 700 N), different displacement amplitudes (±10 µm, ±25 µm and ±40 µm), different contact configurations (ball-on-flat and cylinder-on-flat) and different coating positions (flat, ball or cylinder, both counterbodies).

- A MoS_2 based varnish coating could effectively reduce the friction coefficient to 0.09-0.20 under fretting conditions, and the specific value of friction coefficient depended on test parameters.

- Friction coefficient was mainly dependent on the contact configuration and contact force. The value of friction coefficient of ball-on-flat (around 0.1) was significantly lower than that of cylinder-on-flat (around 0.2). With the increase of contact force, the friction coefficient was decreased in both contact configurations. For this MoS_2 based varnish coating, the friction coefficient was inversely proportional to the contact pressure (the contact pressure is a consequence of contact force and contact configuration), which is quite usual for friction in Hertzian contacts. Coating on only one counterpart failed to change the value of friction coefficient, but coating on both counterbodies could decrease the friction coefficient a little. Variation of displacement amplitude can change the value of friction coefficient a little, but the effect of displacement amplitude was not so significant as the effect of contact configuration and contact force.

- Coating lifetime was mainly dependent on the contact configuration and displacement amplitude. The effect of contact configuration was ranked at first place, because it accounts for 71% variation of coating lifetime. The lifetime of ball-on-flat was about 10 times as many as that of cylinder-on-flat. In this study, the contact configuration of cylinder-on-flat was related to abrasive wear and the contact configuration of ball-on-flat was related to adhesive wear. Therefore, the coating lifetime of cylinder-on-flat configuration was significantly lower than that of ball-on-flat. This was explained by the fact that the transfer film in ball-on-flat configuration was made of coating debris, which can provide a good lubrication between the two contacting bodies. Displacement amplitude is ranked at the second place. Larger displacement amplitude can lead to lower coating lifetime, because it influenced the third body flow between two contacts. Coating on the curved substrate (such as ball and cylinder) can have longer durability than that on the flat substrate, because curved substrate can accelerate the recirculation of coating debris into the contact area and thus prolong the coating lifetime.

- Two predictive equations have been made by regression analysis to describe the relationship between test parameters and friction coefficient or lifetime.

- Survival or Reliability analysis was used to describe the survival rate of the coating under certain running conditions. Weibull distribution was proven as an effective way to distinct the wear modes under different running conditions, because the lifetime data of same wear modes should be distributed randomly around the center line of Weibull distribution.

In order to **identify the relationships between the nature of substrate and the thickness of coating, and the tribological performance of the coated system,** an orthogonal design of experiments was made to study the effects of the nature of substrate and the thickness of coatings with other running conditions (contact force, displacement amplitude, contact configuration and coating position).

- The effect of nature of substrate on the friction coefficient was not so significant as the effects of contact configuration and contact force. The coating on the M2 substrate had a little higher friction coefficient (0.16) than that on the SS 304 substrate (0.15), because the porosities on the M2 substrate could hold the coating, thereby increasing the shear stress a little bit. The effect of thickness was not as significant as contact configuration and contact force. The relative thick coating (20 µm) could increase the friction coefficient a little compared with the thin coating (10 µm). It was because the relative thick coating could lead to a little lower contact pressure than the thin coating.

- The nature of substrate replaced the contact configuration and became the most important factor on the coating lifetime, because it changed the wear mechanism of coatings. The coatings on the M2 substrate had a significant higher lifetime (7153 cycles) than that of SS 304 substrate (2382 cycles), because the porosity in M2 substrate can hold the coating and thus keep the low friction coefficient and prolong the coating durability. Thickness seems to be affectless to the durability, because it does not change the wear mechanism.

- The friction coefficient of coating was mainly dependent on the contact pressure. If a factor can change the contact pressure significantly, then the friction coefficient of the coating will be changed significantly. The lifetime of the coating was mainly dependent on the wear mechanism and the third body flow. If a factor can significantly change the wear mechanism or third body flow, this factor will have a significant effect on the coating lifetime.

In order to **identify whether a linear wear model based on the results of tests in constant displacement amplitude can be used effectively to predict the wear behavior of the coating under variable displacement amplitude** (which occurs in industrial applications), some fretting tests were carried out on the one layer coating on SS 304 substrate with variable displacement amplitude.

- The evolution of friction coefficient as a function of variable displacement amplitude depended on the contact force. When the contact force was 400 N, the change of displacement amplitude after 50% of lifetime of constant displacement amplitude could lead to an increase of friction coefficient. When the change of displacement amplitude occurred at 25% of lifetime of constant displacement amplitude, there was no change of friction coefficient when the displacement amplitude was changed from ±25 µm to ±40 µm. When the displacement amplitude was changed from ±40 µm to ±25 µm, the friction coefficient could decrease a little bit. When the contact force was 100 N, the change of displacement amplitude at 25% of lifetime of constant displacement amplitude had no effect on the friction coefficient. If this change occurred at 50% and 75% of lifetime of constant displacement amplitude, the friction coefficient could decrease a little.

- The relative lifetime determine with the linear wear model was near to 100% for 400 N whenever the displacement amplitude is changed. The relative lifetime was near to 100% for

100 N when the change of displacement amplitude occurred at 25% and 50% of lifetime of 1st constant displacement amplitude. When the change occurred at 75% of lifetime of 1st constant displacement amplitude, the lifetime of coating was longer due to the effect of recycled coating debris.

In brief, the MoS_2 based varnish coating can be used to effectively protect the substrates from the fretting wear. To have a higher lifetime of the coating, it will be better to deposit the coating on a substrate with optimized porosity. The MoS_2 based coating is preferred to be used under high contact pressure and low displacement amplitude.

Finally, the objective of this research can be realized by proposing a method of evaluating coatings according to tribological behavior of coatings. Therefore, several steps can be done as following:

- Analyze the tribological application, find out the requirements;
- According to the requirements, test the coatings under relevant tribological conditions to investigate the test parameters on tribological performance;
- Apply the analysis of variance to rank the effect of test conditions on the coating performance and find out the controlling factor(s) for the coating performance and irrelevant factors for the coating performance. Give the limits of the controlling factor(s) for the coatings;
- Employ the reliability analysis to predict the reliability of the coating under certain running conditions.

REFERENCES

[1] A.K. Ray, S.C. Bose, P.K. De, D.K. Das, Lifetime evaluation of a thick thermal barrier coated superalloy used in turbine blade, Materials Science and Engineering: A, 527 (2010) 5474-5483.
[2] T. Lampe, S. Eisenberg, E. Rodrıguez Cabeo, Plasma surface engineering in the automotive industry—trends and future prospectives, Surf. Coat. Technol., 174–175 (2003) 1-7.
[3] G.E. Totten, Hankbook of lubrication and tribology, second ed., CRC Press, Taylor & Francis Group, Boca Raton, FL, 2006.
[4] K.B. Theo Mang, and Thorsten Bartels, Industrial tribology: tribosystems, friction, wear and surface engineering, lubrication, Wiley-VCH Verlag & Co. KGaA, Weinheim, 2011.
[5] A. Gosalia, Emerging trends and opportunities for the base oil and lubricant industry, The 5th ICIS Middle Eastern Base Oils and Lubricants Conference, Dubai, 2008.
[6] K. Miyoshi, Considerations in vacuum tribology (adhesion, friction, wear, and solid lubrication in vacuum), Tribol. Int., 32 (1999) 605-616.
[7] S. Hogmark, S. Jacobson, M. Larsson, Design and evaluation of tribological coatings, Wear, 246 (2000) 20-33.
[8] J. Zhang, A. Polycarpou, J. Economy, An improved tribological polymer-coating system for metal surfaces, Tribol. Lett., 38 (2010) 355-365.
[9] H. Holleck, Material selection for hard coatings, Journal of Vacuum Science & Technology A: Vacuum, Surfaces, and Films, 4 (1986) 2661-2669.
[10] B.Podgornik, S.Hogmark, O.Sandberg, Hard PVD coatings and their perspectives in forming tool applications, 6th International Tooling Conference, Karlstad (Sweden) 2002, pp. 1053-1066.
[11] S.Y. Zhang, W.G. Zhu, TiN coating of tool steels: a review, J. Mater. Process. Technol., 39 (1993) 165-177.
[12] M. Scholl, Abrasive wear of titanium nitride coatings, Wear, 203-204 (1997) 57-64.
[13] S.-Y. Yoon, M.-C. Kang, S.-C. Kwon, K.H. Kim, The influence of counterface materials and humidity on the tribological behavior of arc ion plated TiN films, Surf. Coat. Technol., 157 (2002) 144-150.
[14] S.E.P. M. Kamal Akhtar, Gas phase synthesis processes—thermal aerosol processes, in: A. Weimer (Ed.) Carbide, Nitride and Boride Materials Synthesis and Processing, Chapman & Hall, Cambridge, 1997, pp. 333-334.
[15] A. Savan, H.J. Boving, E. Fluehmann, H.E. Hintermann, Increased performance of bearing using TiC-coated balls, Journal de Physique IV, 3 (1993) 943-948.
[16] H. Boving, H.E. Hintermann, W. Hanni, Ball bearing with CVD-TiC coated component, 3rd European Space Mechanism & Tribology Symposium Madrd, Spain, 1987, pp. 155-159.
[17] K. Holmberg, A. Matthews, Coatings tribology-properties, techniques and applications in surface engineering, Elsevier Science, Amsterdam, 1994.
[18] K.-H. Habig, Friction and wear of sliding couples coated with TiC, TiN or TiB_2, Surf. Coat. Technol., 42 (1990) 133-147.
[19] K.G. Nickel, Y.G. Gogotsi, Corrosion of hard materials, in: R. Riedel (Ed.) Handbook of Ceramic Hard Materials, Wiley-VCH Verlag GmbH, 2008, pp. 140-182.
[20] S. PalDey, S.C. Deevi, Single layer and multilayer wear resistant coatings of (Ti,Al)N: a review, Materials Science and Engineering: A, 342 (2003) 58-79.
[21] D. Vallauri, I.C. Atias Adrian, A. Chrysanthou, TiC-TiB_2 composites: A review of phase relationships, processing and properties, Journal of the European Ceramic Society, 28 (2008) 1697-1713.

[22] Y.G. Tkachenko, B.L. Grabchuk, N.I. Bodnaruk, V.V. Sychev, Friction and wear of boron carbide at temperatures in the range 20-1500°C, Soviet Powder Metallurgy and Metal Ceramics, 16 (1977) 541-543.
[23] K.A. Schwetz, L.S. Sigl, L. Pfau, Mechanical properties of injection molded B_4C-C ceramics, Journal of Solid State Chemistry, 133 (1997) 68-76.
[24] P.D. Cuong, H.-S. Ahn, E.-S. Yoon, K.-H. Shin, Effects of relative humidity on tribological properties of boron carbide coating against steel, Surf. Coat. Technol., 201 (2006) 4230-4235.
[25] P. Larsson, N. Axén, S. Hogmark, Tribofilm formation on boron carbide in sliding wear, Wear, 236 (1999) 73-80.
[26] G.I. Kalandadze, S.O. Shalamberidze, A.B. Peikrishvili, Sintering of boron and boron carbide, Journal of Solid State Chemistry, 154 (2000) 194-198.
[27] I. Sigalas, R.J. Caveney, M.W. Bailey, Diamond materials and their applications, Handbook of Ceramic Hard Materials, Wiley-VCH Verlag GmbH, 2008, pp. 478-572.
[28] O. Wanstrand, M. Larsson, P. Hedenqvist, Mechanical and tribological evaluation of PVD WC/C coatings, Surf. Coat. Technol., 111 (1999) 247-254.
[29] M. Ham, K.A. Lou, Diamond-like carbon films grown by a large-scale direct current plasma chemical vapor deposition reactor: System design, film characteristics, and applications, Journal of Vacuum Science & Technology A: Vacuum, Surfaces, and Films, 8 (1990) 2143-2149.
[30] X. He, W. Li, H. Li, Diamond-like carbon film synthesized by ion beam assisted deposition and its tribological properties, Journal of Vacuum Science and Technology A: Vacuum, Surfaces and Films, 14 (1996) 2039-2047.
[31] G. Dearnaley, J.H. Arps, Biomedical applications of diamond-like carbon (DLC) coatings: A review, Surf. Coat. Technol., 200 (2005) 2518-2524.
[32] C.P. Klages, K. Bewilogua, Diamond-Like Carbon Films, Handbook of Ceramic Hard Materials, Wiley-VCH Verlag GmbH, 2008, pp. 623-647.
[33] J.E. Field, Natural Diamond: The Standard, in: R. Clausing, L. Horton, J. Angus, P. Koidl (Eds.) Diamond and Diamond-like Films and Coatings, Springer US, 1991, pp. 17-35.
[34] E. Liu, Y.F. Ding, L. Li, B. Blanpain, J.P. Celis, Influence of humidity on the friction of diamond and diamond-like carbon materials, Tribol. Int., 40 (2007) 216-219.
[35] H. Holleck, V. Schier, Multilayer PVD coatings for wear protection, Surf. Coat. Technol., 76-77, Part 1 (1995) 328-336.
[36] X. Nie, E.I. Meletis, J.C. Jiang, A. Leyland, A.L. Yerokhin, A. Matthews, Abrasive wear/corrosion properties and TEM analysis of Al_2O_3 coatings fabricated using plasma electrolysis, Surf. Coat. Technol., 149 (2002) 245-251.
[37] C. Subramanian, K.N. Strafford, Review of multicomponent and multilayer coatings for tribological applications, Wear, 165 (1993) 85-95.
[38] E.F. Rico, I. Minondo, D.G. Cuervo, The effectiveness of PTFE nanoparticle powder as an EP additive to mineral base oils, Wear, 262 (2007) 1399-1406.
[39] K. Tanaka, Y. Uchiyama, S. Toyooka, The mechanism of wear of polytetrafluoroethylene, Wear, 23 (1973) 153-172.
[40] J.A. Williams, Engineering tribology Oxford University Press, New York, 1994.
[41] H. Unal, A. Mimaroglu, U. Kadioglu, H. Ekiz, Sliding friction and wear behaviour of polytetrafluoroethylene and its composites under dry conditions, Mater. Des., 25 (2004) 239-245.
[42] C. Kang, N.S. Eiss Jr, Fretting wear of polysiloxane-polyimide copolymer coatings as a function of varying humidity, Wear, 158 (1992) 29-40.
[43] R.L. Fusaro, Mechanisms of lubrication and wear of a bonded solid-lubricant film, ASLE Transactions, 24 (1981) 191-204.

[44] C. Mary, S. Fouvry, J.M. Martin, B. Bonnet, Pressure and temperature effects on fretting wear damage of a Cu-Ni-In plasma coating versus Ti17 titanium alloy contact, Wear, 272 (2011) 18-37.
[45] J.-I. Moon, Y.-H. Lee, H.-J. Kim, S.-M. Noh, J.-H. Nam, Synthesis of elastomeric polyester and physical properties of polyester coating for automotive pre-primed system, Progress in Organic Coatings, 75 65-71.
[46] A. Shankara, P.L. Menezes, K.R.Y. Shimha, S.V. Kailas, Study of solid lubrication with MoS_2 coating in the presence of additives using reciprocating ball-on-flat scrach tester, Sadhana, 33 (2008) 207-220.
[47] Solid Lubricants / Dry Lubrication, http://www.tribology-abc.com
[48] S.C. Sharma, B.M. Girish, R. Kamath, B.M. Satish, Graphite particles reinforced ZA-27 alloy composite materials for journal bearing applications, Wear, 219 (1998) 162-168.
[49] M. Babic, M. Slobodan, D. Dzunic, B. Jeremic, B. Ilija, Tribological behavior of composites based on ZA-27 alloy reinforced with graphite particles, Tribol. Lett., 37 (2010) 401-410.
[50] J.K. Lancaster, Solid lubricants, in: E.R. Booser (Ed.) CRC Handbook of Lubrication (Theory and practice of tribology), CRC Press, Boca Raton, 1983, pp. 269-290.
[51] L.E. Pope, J.K.G. Panitz, The effects of hertzian stress and test atmosphere on the friction coefficients of MoS_2 coatings, Surf. Coat. Technol., 36 (1988) 341-350.
[52] A. Mesgarnejad, M.M. Khonsari, On the tribological behavior of MoS_2-coated thrust ball bearings operating under oscillating motion, Wear, 269 547-556.
[53] T. Spalvins, A review of recent advances in solid film lubrication, Journal of Vacuum Science and Technology A: Vacuum, Surfaces and Films, 5 (1986) 212–219.
[54] I.L. Singer, S. Fayeulle, P.D. Ehni, Wear behavior of triode-sputtered MoS2 coatings in dry sliding contact with steel and ceramics, Wear, 195 (1996) 7-20.
[55] S. Fayeulle, P.D. Ehni, I.L. Singer, Analysis of transfer films formed on steel and Co-WC during sliding against MoS_2-coated steel in argon, Surf. Coat. Technol., 41 (1990) 93-101.
[56] C. Donnet, A. Erdemir, Historical developments and new trends in tribological and solid lubricant coatings, Surf. Coat. Technol., 180–181 (2004) 76-84.
[57] S. Jahanmir, E.P. Abrahamson Ii, N.P. Suh, Sliding wear resistance of metallic coated surfaces, Wear, 40 (1976) 75-84.
[58] Z. Deng, M.R. Lovell, Effects of lubrication and die radius on the friction behavior of Pb-coated sheet steels, Wear, 244 (2000) 41-51.
[59] M.A. Sherbiney, J. Halling, Friction and wear of ion-plated soft metallic films, Wear, 45 (1977) 211-220.
[60] J. Gerkema, Lead thin film lubrication, Wear, 102 (1985) 241-252.
[61] S. Harold E, The role of silver in self-lubricating coatings for use as extreme temperatures, Annual meeting of the american society of lubrication engineers Las Vegas, 1986.
[62] J.J. Liu, X.H. Zhang, B.L. Zhu, The effect of soft metallic plateled layer on the tribological behavior of steels under boundary lubrification, Tribol. Trans., 34 (1991) 17-22.
[63] S. Fouvry, P. Jedrzejczyk, P. Chalandon, Introduction of an exponential formulation to quantify the electrical endurance of micro-contacts enduring fretting wear: Application to Sn, Ag and Au coatings, Wear, 271 1524-1534.
[64] P. Cosemans, X. Zhu, J.P. Celis, M. Van Stappen, Development of low friction wear-resistant coatings, Surf. Coat. Technol., 174–175 (2003) 416-420.
[65] O. Knotek, F. Loffler, G. Kramer, Cutting performance of multicomponent and multilayer coatings on cemented carbides and cermets for interrupted cut machining, International Journal of Refractory Metals and Hard Materials, 14 (1996) 195-202.
[66] R. Zhang, Z. Lin, Z. Cui, Q. Song, Studies on multilayer wear of CVD TiC-TiN multilayer composite coating, Wear, 147 (1991) 227-251.

[67] V.V. Uglov, V.M. Anishchik, S.V. Zlotski, G. Abadias, S.N. Dub, Stress and mechanical properties of Ti–Cr–N gradient coatings deposited by vacuum arc, Surf. Coat. Technol., 200 (2005) 178-181.
[68] H.A. Jehn, Multicomponent and multiphase hard coatings for tribological applications, Surf. Coat. Technol., 131 (2000) 433-440.
[69] Q. Yang, L.R. Zhao, Dry sliding wear of magnetron sputtered TiN/CrN superlattice coatings, Surf. Coat. Technol., 173 (2003) 58-66.
[70] M. Chhowalla, G.A.J. Amaratunga, Thin films of fullerene-like MoS_2 nanoparticles with ultra-low friction and wear, Nature, 407 (2000) 164-167.
[71] K.H. Hu, J. Wang, S. Schraube, Y.F. Xu, X.G. Hu, R. Stengler, Tribological properties of MoS_2 nano-balls as filler in polyoxymethylene-based composite layer of three-layer self-lubrication bearing materials, Wear, 266 (2009) 1198-1207.
[72] J.F. Li, H. Liao, X.Y. Wang, B. Normand, V. Ji, C.X. Ding, C. Coddet, Improvement in wear resistance of plasma sprayed yttria stabilized zirconia coating using nanostructured powder, Tribol. Int., 37 (2004) 77-84.
[73] P.M. Martin, Chapter 3 - Surface preparation for film and coating deposition processes, in: P.M. Martin (Ed.) Handbook of deposition technologies for films and coatings (third edition), William Andrew Publishing, Boston, 2010, pp. 93-134.
[74] B. North, Six issues for the hard coatings community, Surf. Coat. Technol., 106 (1998) 129-134.
[75] J.-O. Carlsson, P.M. Martin, Chapter 7 - Chemical vapor deposition, in: P.M. Martin (Ed.) Handbook of Deposition Technologies for Films and Coatings (Third Edition), William Andrew Publishing, Boston, 2010, pp. 314-363.
[76] W. Jeitschko, R. Pottgen, R.D. Hoffmann, Structural chemistry of hard materials, in: R. Riedel (Ed.) Handbook of Ceramic Hard Materials, Wiley-VCH Verlag GmbH, 2008, pp. 2-40.
[77] Titanium Nitride Chemical Vapor Deposition, TimeDomain CVD Inc.
[78] S. Kamiya, H. Nagasawa, K. Yamanobe, M. Saka, A comparative study of the mechanical strength of chemical vapor-deposited diamond and physical vapor-deposited hard coatings, Thin Solid Films, 473 (2005) 123-131.
[79] S.I. Shah, G.H. Jaffari, E. Yassitepe, B. Ali, Chapter 4 - Evaporation: processes, bulk microstructures, and mechanical properties, in: P.M. Martin (Ed.) Handbook of Deposition Technologies for Films and Coatings (Third Edition), William Andrew Publishing, Boston, 2010, pp. 135-252.
[80] P.M. Martin, Chapter 1 - Deposition technologies: an overview, Handbook of Deposition Technologies for Films and Coatings (Third Edition), William Andrew Publishing, Boston, 2010, pp. 1-31.
[81] J. Gansheimer, Optimerung von Schraubenverbindungen durch festschemierstoffe., Tribologie + Schmierungstechnik, 38 (1991) 16-23.
[82] R. Gadow, D. Scherer, Composite coatings with dry lubrication ability on light metal substrates, Surf. Coat. Technol., 151–152 (2002) 471-477.
[83] K. Holmberg, A. Laukkanen, H. Ronkainen, K. Wallin, Tribological analysis of fracture conditions in thin surface coatings by 3D FEM modelling and stress simulations, Tribol. Int., 38 (2005) 1035-1049.
[84] H. Jiang, R. Browning, J.D. Whitcomb, M. Ito, M. Shimouse, T.A. Chang, H.J. Sue, Mechanical Modeling of Scratch Behavior of Polymeric Coatings on Hard and Soft Substrates, Tribol. Lett., 37 (2010) 159-167.
[85] S.J. Bull, E.G. Berasetegui, An overview of the potential of quantitative coating adhesion measurement by scratch testing, Tribol. Int., 39 (2006) 99-114.
[86] D.T. F.P. Bowden, The Friction and Lubrication of Solids, Oxford University Press, Oxford, 1950.

[87] J.H.W. Siu, L.K.Y. Li, An investigation of the effect of surface roughness and coating thickness on the friction and wear behaviour of a commercial MoS_2-metal coating on AISI 400C steel, Wear, 237 (2000) 283-287.
[88] I.P. Hayward, I.L. Singer, L.E. Seitzman, Effect of roughness on the friction of diamond on cvd diamond coatings, Wear, 157 (1992) 215-227.
[89] D.Tabor, in: J.E. Field (Ed.) Properties of Diamond, Academic Press, Oxford, 1979.
[90] F. Svahn, Å. Kassman-Rudolphi, E. Wallén, The influence of surface roughness on friction and wear of machine element coatings, Wear, 254 (2003) 1092-1098.
[91] E.W. Roberts, B.J. Williams, J.A. Ogilvy, The effect of substrate surface roughness on the friction and wear of sputtered MoS_2 films, Journal of Physics D: Applied Physics, 25 (1992) A65.
[92] Evaluating polymer wear and particulation for semiconductors and data storage, http://www.gslb.cleanrooms.com/index/display/article-display/0723054128/articles/solid-state-technology/semiconductors/subsystems/2010/11/evaluating-polymer-wear-and-particulation-for-semiconductors-and.html, 2010.
[93] P. Kapsa, S. Fouvry, L. Vincent, Basic principles of fretting, in: G. Stackowiack (Ed.) Wear-materials, mechanisms and practice, John Wiley & Sons, Ltd, West Sussex, 2005, pp. 317-338.
[94] A. Matthews, S. Franklin, K. Holmberg, Tribological coatings: contact mechanisms and selection, Journal of Physics D-Applied Physics, 40 (2007) 5463-5475.
[95] M.F. Buchely, J.C. Gutierrez, L.M. León, A. Toro, The effect of microstructure on abrasive wear of hardfacing alloys, Wear, 259 (2005) 52-61.
[96] J.F. Archard, Contact and rubbing of flat surfaces, Journal of Applied Physics, 24 (1953) 981-988.
[97] H. Mohrbacher, J.P. Celis, J.R. Roos, Laboratory testing of displacement and load induced fretting, Tribol. Int., 28 (1995) 269-278.
[98] S. Fouvry, P. Kapsa, H. Zahouani, L. Vincent, Wear analysis in fretting of hard coatings through a dissipated energy concept Wear, 203 (1997) 393-403.
[99] V. Fridrici, S. Fouvry, P. Kapsa, P. Perruchaut, Impact of contact size and geometry on the lifetime of a solid lubricant, Wear, 255 (2003) 875-882.
[100] I.L. Singer, R.N. Bolster, J. Wegand, S. Fayeulle, B.C. Stupp, Hertzian stress contribution to low friction behavior of thin MoS_2 coatings, Appl. Phys. Lett., 57 (1990) 995-997.
[101] S.D. Dvorak, K.J. Wahl, I.L. Singer, In Situ Analysis of Third Body Contributions to Sliding Friction of a Pb-Mo-S Coating in Dry and Humid Air, Tribol. Lett., 28 (2007) 263-274.
[102] D.P. Mondal, S. Das, A.K. Jha, A.H. Yegneswaran, Abrasive wear of Al alloy–Al_2O_3 particle composite: a study on the combined effect of load and size of abrasive, Wear, 223 (1998) 131-138.
[103] S. Chinchanikar, S.K. Choudhury, Effect of work material hardness and cutting parameters on performance of coated carbide tool when turning hardened steel: An optimization approach, Measurement, 46 (2013) 1572-1584.
[104] S.S. Rajahram, T.J. Harvey, R.J.K. Wood, Full factorial investigation on the erosion–corrosion resistance of UNS S31603, Tribol. Int., 43 (2010) 2072-2083.
[105] J. Esteban Fernández, M. del Rocío Fernández, R. Vijande Diaz, R. Tucho Navarro, Abrasive wear analysis using factorial experiment design, Wear, 255 (2003) 38-43.
[106] T. Bučar, M. Nagode, M. Fajdiga, Reliability approximation using finite Weibull mixture distributions, Reliab. Eng. Syst. Saf., 84 (2004) 241-251.
[107] L.A. Escobar, W.Q. Meeker, A review of accelerated test models, Stat. Sci., 21 (2006) 552-577.
[108] Competing failure anlysis, Life data analysis reference book, http://www.reliasoft.com, 2013.

[109] M. Sivapragash, P.R. Lakshminarayanan, R. Karthikeyan, K. Raghukandan, M. Hanumantha, Fatigue life prediction of ZE41A magnesium alloy using Weibull distribution, Mater. Des., 29 (2008) 1549-1553.
[110] O. Guseva, S. Brunner, P. Richner, Service life prediction for aircraft coatings, Polymer Degradation and Stability, 82 (2003) 1-13.
[111] M. Evans, A statistical degradation model for the service life prediction of aircraft coatings: With a comparison to an existing methodology, Polymer Test., 31 (2012) 46-55.
[112] K. Rajkumar, K. Kundu, S. Aravindan, M.S. Kulkarni, Accelerated wear testing for evaluating the life characteristics of copper–graphite tribological composite, Mater. Des., 32 (2011) 3029-3035.
[113] R. Sakin, İ. Ay, Statistical analysis of bending fatigue life data using Weibull distribution in glass-fiber reinforced polyester composites, Mater. Des., 29 (2008) 1170-1181.
[114] G.J.H.a.W.Q.M. Necip Doganaksoy, Reliability analysis by failure mode, Quality Progress, (2002) 47-52.
[115] X.C. Zhang, B.S. Xu, F.Z. Xuan, S.T. Tu, H.D. Wang, Y.X. Wu, Fatigue resistance of plasma-sprayed CrC–NiCr cermet coatings in rolling contact, Appl. Suf. Sci., 254 (2008) 3734-3744.
[116] J.E.B. B.A. Robert, C.H. Medlin, G.L. Reinman, Weibull analysis handbook, Prepared for the Aero Propulsion and Power Laboratory,Wright-Patterson AFB, OH 1983, pp. 222.
[117] I.s.s. forum, The stainless steel family.
[118] J.R. Davis, Tool materials, ASM International, Chigago, 1995.
[119] S. Bec, A. Tonck, J.M. Georges, E. Georges, J.L. Loubet, Improvements in the indentation method with a surface force apparatus, Philos. Mag. A, 74 (1996) 1061-1072.
[120] S. Descartes, M. Cassard, Y.Berthier, A. Ginet, A. Aubert, MoSx, a solid lubricant : yes, but which scales of tribological interpretation should be used ? The consequences on the friction of mechanisms, in: W.R. Burke (Ed.) Sixth European Space Mechanisms and Tribology Symposium, Switzerland, 1995, pp. 29-34.
[121] D.B. Luo, V. Fridrici, P. Kapsa, Relationships between the fretting wear behavior and the ball cratering resistance of solid lubricant coatings, Surf. Coat. Technol., 204 (2010) 1259-1269.
[122] D.B. Luo, V. Fridrici, P. Kapsa, Selecting solid lubricant coatings under fretting conditions, Wear, 268 (2010) 816-827.
[123] D.B. Luo, V. Fridrici, P. Kapsa, A systematic approach for the selection of tribological coatings, Wear, 271 (2011) 2132-2143.
[124] D.B. Luo, V. Fridrici, P. Kapsa, Evaluating and predicting durability of bonded solid lubricant coatings under fretting conditions, Tribol. Int., 44 (2011) 1577-1582.
[125] W.F. Kuhfeld, R.D. Tobias, M. Garratt, Efficient experimental design with marketing research applications, J. Market. Res., 31 (1994) 545-557.
[126] T. Jamal, R. Nimmagadda, R.F. Bunshah, Friction and adhesive wear of titanium carbide and titanium nitride overlay coatings, Thin Solid Films, 73 (1980) 245-254.
[127] V. Fridrici, Fretting d'un alliage de titane revêtu et lubrifié : application au contact aube/disque, Thèse, Ecole Centrale de Lyon, Ecully, 2002, pp. 200.
[128] E-Handbook of Statistical Methods, NIST/SEMATECH http://www.itl.nist.gov/div898/handbook/.
[129] Determining polynomial contrast coeffcients, Biometrics information, 1988.
[130] C. Langlade, B. Vannes, M. Taillandier, M. Pierantoni, Fretting behavior of low-friction coatings: contribution to industrial selection, Tribol. Int., 34 (2001) 49–56.
[131] H. Bagheri, M. Saraji, M. Chitsazan, S.R. Mousavi, M. Naderi, Mixed-level orthogonal array design for the optimization of solid-phase extraction of some pesticides from surface water, Journal of Chromatography A, 888 (2000) 197-208.

[132] M.K. Goel, Pardeep Khanna, J. Kishore, Understanding survival analysis: Kaplan-Meier estimate, International Journal of Anurveda Research, 4 (2010) 274-278.
[133] A. Iwabuchi, K. Hori, Y. Sugawara, Effects of temperature and ambient pressure on fretting properties of polyimide, Wear, 125 (1988) 67-81.
[134] K. Elleuch, S. Fouvry, Experimental and modeling aspects of abrasive wear of a 357 aluminum alloy under gross slip fretting conditions, Wear, 258 (2005) 40-49.
[135] E. Sauger, S. Fouvry, L. Ponsonnet, P. Kapsa, J.M. Martin, L. Vincent, Tribologically transformed structure in fretting, Wear, 245 (2000) 39-52.
[136] W.F. Kuhfeld, Marketing Research Methods in SAS, SAS Institute Inc., Cary, NC, USA, 2010, pp. 53–241.
[137] S.N. Deming, S.L. Morgan, Experimental design: A chemometric approach, Elsevier, Amsterdam, 1987.
[138] P. Menezes, Kishore, S. Kailas, M. Lovell, Role of Surface Texture, Roughness, and Hardness on Friction During Unidirectional Sliding Tribol. Lett., 41 (2011) 1-15.
[139] Y. Wang, E.J. Terrell, Influence of coating thickness and substrate elasticity on the tribological performance of PEEK coatings, Wear, 303 (2013) 255-261.
[140] M. Shima, J.i. Sato, H. Koguchi, Contact stresses of an elastic surface layer bonded to a half-space ealstic body Nippon Kikai Gakkai Ronbunshu, A Hen/Transactions of the Japan Society of Mechanical Engineers, Part A, 51 (1985) 1983-1989.
[141] M. Shima, J. Okado, I.R. McColl, R.B. Waterhouse, T. Hasegawa, M. Kasaya, The influence of substrate material and hardness on the fretting behaviour of TiN, Wear, 225–229, Part 1 (1999) 38-45.
[142] C. Paulin, S. Fouvry, S. Deyber, Wear kinetics of Ti–6Al–4V under constant and variable fretting sliding conditions, Wear, 259 (2005) 292-299.
[143] J. Hintikka, A. Lehtovaara, C. Lönnqvist, Effect of start-up schemes and amplitude of tangential motion on friction behavior in fretting point contact, Tribol. Int., 44 (2011) 1535-1543.

ANNEX

1. Transformation

To meet the requirement of analysis of variance, two assumptions should be complemented. One is the normal distribution of data for each treatment (the combination of one group of test parameters) and the other is the homogeneity of variance across the treatment. Due to the fact that only two tests have been performed for each condition, these two assumptions can be completed automatically. Some scholars [128] suggested doing other assumptions prior to analysis of variance: 1) a run sequence plot of the residuals; 2) a normal probability plot of the residuals; 3) a scatter plot of the predicted values against the residuals. If the distribution of residuals fails to meet the requirement, some transformation should be done, which has been explained in Chapter III and Chapter IV.

In Chapter III, only coating lifetime needs to be transformed as Eq. (III-3)

$$Trans(Nc) = \ln(Nc)$$

In Chapter IV, two values (friction coefficient and coating lifetime) are transformed as Eq. (IV-2) and (IV-3):

$$Trans(\mu) = (\mu^{-0.5} - 1)/(-0.5) \qquad \textit{(IV-2)}$$

$$Trans(Nc) = (Nc^{-0.25} - 1)/(-0.25) \qquad \textit{(IV-3)}$$

2. Coding method

Prior to regression analysis, it is necessary to code the value of each factor, because coding can reduce range of each factor to a common scale regardless of its relative magnitude and scaling establishes factor levels that can be orthogonal (or nearly). Generally, the coded value for numeric value can be calculated according to Eq. (III -1).

$$coded\ value = \frac{x_i - \frac{x_n + x_1}{2}}{\frac{x_n - x_1}{2}} \quad i = 1, 2, \cdots n \qquad \textit{(III-1)}$$

Therefore, the coded value of each numeric factor is shown in Table 20. In this study, the evolution of friction coefficient or coating lifetime as a function of normal force is not linear so that we should consider the quadratic part for coded value. The array of linear part and quadratic part should be orthogonal. In addition, the normalization should be calculated according to that the coded value is divided by the square root of summer of square of coded value for each factor. Therefore, all independent values (value of factor) can have the same scale (-1 ~ 1), as shown in Table 33. Then, the coefficient in the equation can be used to describe the variation of dependent value as a function of factors.

Table 20: Coded value for contact force and displacement amplitude.

	Real value	Coded value	
		linear part	quadratic part
Contact force	100 N	-1	1
	400 N	0	-2
	700 N	1	1
	Real value	Coded value	
		linear part	quadratic part
Displacement amplitude	± 10 µm	-1	1
	± 25 µm	0	-2
	± 40 µm	1	1

Table 33: Standardized value for contact force and displacement amplitude.

	Real value	Standardized value	
		linear part	quadratic part
Contact force	100 N	$-1/\sqrt{2}$	$1/\sqrt{6}$
	400 N	0	$-2/\sqrt{6}$
	700 N	$1/\sqrt{2}$	$1/\sqrt{6}$
	Real value	Standardized value	
		linear part	quadratic part
Displacement amplitude	± 10 µm	$-1/\sqrt{2}$	$1/\sqrt{6}$
	± 25 µm	0	$-2/\sqrt{6}$
	± 40 µm	$1/\sqrt{2}$	$1/\sqrt{6}$

To get the value of contact configuration and coatings position, dummy values can be used because they are categorical values. Dummy coding uses only one and zero to convey all of the necessary information on group membership, as shown in Table 21. In addition, the ball-on-flat configuration is coded as $CON = 1$ and cylinder-on-flat configuration is $CON = 0$. For the dummy case, the standardized values are same to the coded value.

Table 21: Dummy values of coating position.

Coating position	C_1	C_2
Coating on the flat	0	0
Coating on the ball or cylinder	1	0
Coating on both counterbodies	0	1

3. Summary

Table 34 summarizes all the nomenclatures used in this thesis for the regression analysis.

Table 34: Nomenclatures used in thesis for the regression analysis.

(a) Standardized value for contact force and displacement amplitude

	Real value	Standardized value	
		linear part	quadratic part
Contact force	100 N	$-1/\sqrt{2}$	$1/\sqrt{6}$
	400 N	0	$-2/\sqrt{6}$
	700 N	$1/\sqrt{2}$	$1/\sqrt{6}$
	Real value	Standardized value	
		linear part	quadratic part
Displacement amplitude	± 10 µm	$-1/\sqrt{2}$	$1/\sqrt{6}$
	± 25 µm	0	$-2/\sqrt{6}$
	± 40 µm	$1/\sqrt{2}$	$1/\sqrt{6}$

(b) Standardized value for contact configuration

Contact configuration	*CON*
Ball-on-flat	1
Cylinder-on-flat	0

(c) Standardized value for coating positions

Coating position	C_1	C_2
Coating on the flat	0	0
Coating on the ball or cylinder	1	0
Coating on both counterbodies	0	1

Abstract

Fretting wear is considered as a complex wear phenomenon related to interaction between two sliding bodies under very low displacement amplitude, which limits the lifetime of elements significantly. Solid lubricant is more and more applied in tribological applications to reduce friction and protect the substrate surface from fretting wear. The performance of coating depends on many factors such as running conditions, properties of substrate, counterbody and coating, and adhesion between coating and substrate. The objectives of this thesis are to discuss the friction and wear behavior of the coating under different running conditions, and to analyze the effect of test parameters on the friction coefficient and lifetime of the coating, which can be effectively helpful for the evaluation of quality of the coating. Fretting experiments are carried out to understand the relationships between the tribological behavior of a MoS_2 based varnish coating and running conditions. The coating is investigated under different contact forces, different displacement amplitudes, different contact configurations, different coating positions, different substrates and different thicknesses. The rank of effect of factors is evaluated by the analysis of variance. Regression analysis is used to predict the performance of coatings under certain running conditions. The observation of evolution of wear scar is applied to explain the rank of factor and coefficients in the prediction equations. Furthermore, the reliability analysis is used to describe and predict the survival rate of coatings under certain running conditions. Finally, a linear model for lifetime is assessed in order to take into account variable displacement amplitude.

Keywords: friction, wear, fretting, lifetime, bonded coating, solid lubricant, analysis of variance, regression analysis, reliability analysis.

Résumé:

La dégradation des contacts tribologiques sous une sollicitation de fretting est un phénomène complexe lié à l'interaction entre deux corps sous une faible amplitude de débattement, ce qui limite la durée de vie des pièces de manière significative. La lubrification solide est de plus en plus utilisée dans les applications tribologiques pour réduire les frottements et protéger la surface du substrat contre l'usure par fretting. La performance du revêtement dépend de nombreux facteurs tels que les conditions de sollicitation, les propriétés du substrat, du contre-corps et du revêtement et l'adhérence entre le revêtement et le substrat. Les objectifs de cette thèse sont de discuter le frottement et le comportement en usure du revêtement sous différentes conditions et d'analyser l'effet des paramètres d'essai sur le coefficient de frottement et la durée de vie du revêtement, ce qui peut être effectivement utile pour l'évaluation de la qualité des revêtements. Les tests de fretting sont menés pour comprendre les relations entre le comportement tribologique d'un vernis à base de MoS_2 et les conditions d'essai. Le revêtement est étudié pour différentes valeurs de force de contact, amplitude de déplacement, configuration de contact, position du revêtement, nature du substrat et épaisseur. L'effet de chaque facteur est évalué par l'analyse de variance. L'analyse de régression est utilisée pour prévoir la performance du revêtement. L'observation de l'évolution de la trace d'usure est réalisée pour expliquer l'importance des facteurs et les coefficients dans les équations de prédiction. En outre, l'analyse de fiabilité est utilisée pour décrire et prévoir le taux de survie du revêtement sous certaines conditions d'essai. Enfin, un modèle linéaire de durée de vie est évalué afin de prendre en compte l'amplitude de déplacement variable.

Mots-clés: frottement, usure, fretting, durée de vie, vernis de glissement, lubrifiant solide, analyse de la variance, analyse de régression, analyse de fiabilité.

dernière page de la thèse

AUTORISATION DE SOUTENANCE

Vu les dispositions de l'arrêté du 7 août 2006,

Vu la demande du Directeur de Thèse

Monsieur P. KAPSA

et les rapports de

Monsieur C. LANGLADE
Professeur - LERMPS-UTBM - Sites de Sévenans et de Montbéliard - 90010 BELFORT

Et de

Monsieur H. ZAIDI
Professeur - Institut P' - Dept D2 - 211 bd Marie et Pierre Curie
86962 FUTUROSCOPE CHASSENEUIL cedex

Mademoiselle YANG Jiao

est autorisée à soutenir une thèse pour l'obtention du grade de **DOCTEUR**

Ecole doctorale MATERIAUX

Fait à Ecully, le 10 octobre 2013

P/Le directeur de l'E.C.L.
La directrice des Etudes

ECOLE CENTRALE DE LYON
Service Vie Sociale
ECULLY

M-A. GALLAND